Polymeric vesicles for drug delivery over the blood-brain barrier and *in vivo* Imaging

René Pascal Brinkhuis

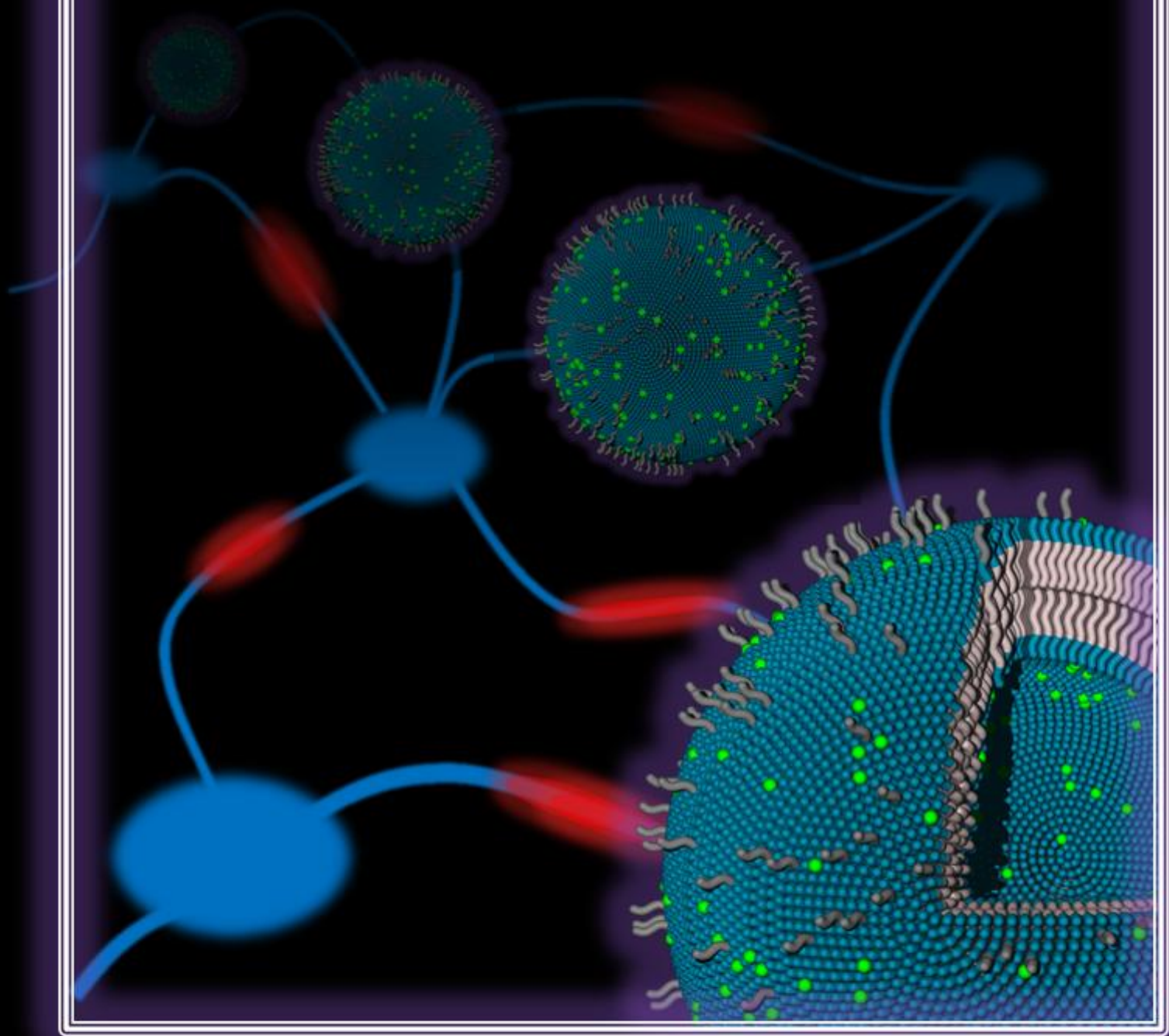

Polymeric vesicles for drug delivery over the blood-brain barrier and *in vivo* imaging

Een wetenschappelijke proeve op het gebied van de Natuurwetenschappen, Wiskunde en Informatica

Proefschrift

ter verkrijging van de graad van doctor aan de Radboud Universiteit Nijmegen op gezag van de rector magnificus prof. mr. S.C.J.J. Kortmann, volgens besluit van het college van decanen in het openbaar te verdedigen op maandag 10 december 2012 om 13.30 uur precies

door

René Pascal Brinkhuis

geboren op 11 april 1981 te Deventer

Promotoren:

Prof. dr. ir. J.C.M. van Hest

Prof. dr. F.P.J.T. Rutjes

Manusscriptcommissie:

Prof. dr. R.J.M. Nolte

Prof. dr. D. Hoekstra (UMC Groningen)

Prof. dr. O.C. Boerman (UMC Nijmegen)

Druk: Ipskamp drukkers B.V., Enschede

ISBN: 978-90-9027254-2

Preface

One of the main hurdles in medicinal chemistry is the presence of the blood-brain barrier. This mono-layer of cerebral endothelial cells prevents passage of basically all molecules into the brain parenchyma, except for a few low molecular weight lipophilic molecules. Small polar molecules and proteins can only cross the blood-brain barrier via receptor mediated transcytosis (Figure 1). Most potent drugs, developed for brain and central nervous system related diseases, lack the ability to cross the blood-brain barrier. Furthermore, since most drugs are hydrophobic they also suffer from low bioavailability[1]. Both hurdles might be tackled by the development of drug formulations in the form of nano-carriers. A specific group of *nano-carriers* are *polymeric vesicles* or *polymersomes* which have gained much attention over the past 10 years.

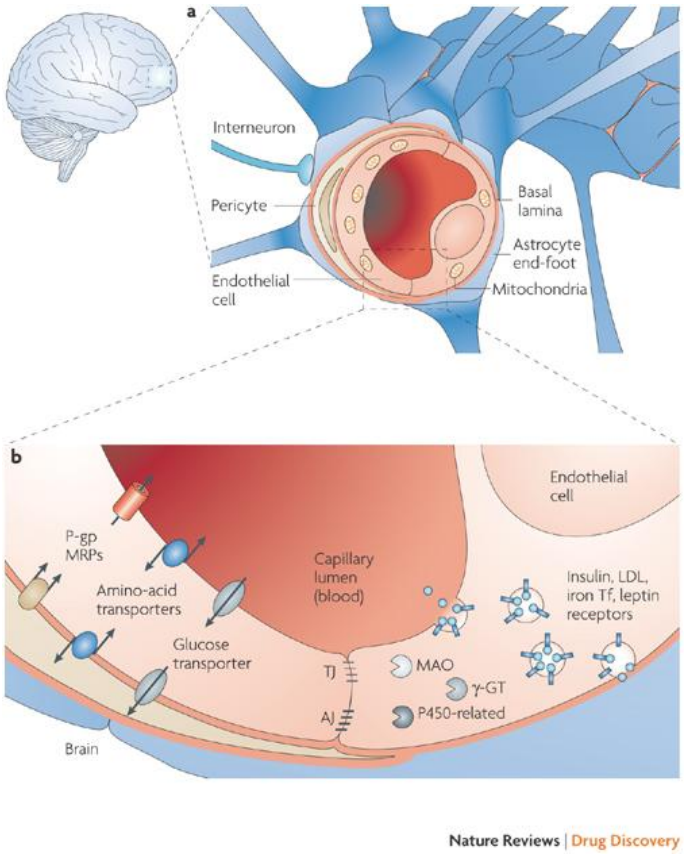

Figure 1. a) The blood brain barrier is formed by a monolayer of cerebral endothelial cells, forming a barrier that physically separates the blood stream from the brain parenchyma. **b)** Cerebral endothelial cells are connected via tight junctions that effectively seal the paracellular pathway. Small polar molecules and larger proteins can only enter the brain by receptor mediated transport, specifically designed to regulate the microenvironment of the brain. Reprinted with permission (Ref. 1)

Polymersomes are spherical vesicles that are composed of amphiphilic block copolymers. The amphiphilic polymers form a bilayered structure, enclosing a aqueous lumen, while the bilayered membrane forms a hydrophobic compartment of 10 – 20 nm in thickness[2,3] (Figure 2). When the overall structure is regarded the resemblance with

liposomes is clear, yet there are also some major differences. Polymersomes are formed from amphiphilic block copolymers with a molecular weight of 5-100 kDa, whereas liposomes are assembled from phospholipids with an average weight of 500-800 Da. The higher molecular weight of the building blocks establishes itself in a lower critical micelle concentration, resulting in a more robust and stable membrane. Furthermore, the membrane is thicker, which allows for a more efficient storage and transport of hydrophobic drugs. These features render polymersomes as potent nonocariers for biomedical applications, like (targeted) drug delivery[4] and *in vivo* imaging[5].

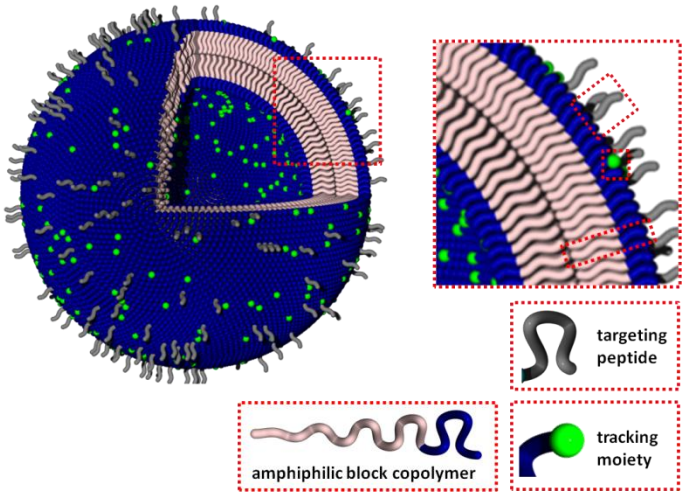

Figure 2. Schematic presentation of polymersomes formed from a bilayer of amphiphilic block copolymers. The surface is tagged with peptides as which mediate transport over the blood-brain barrier. Furthermore, tracking moieties are included for visualization and radio-isotope labelling.

The research described herein aims at the development of polymersomes as smart nano-carriers to target and accommodate transport over the blood-brain barrier (Figure 2). In order to design such a carrier we need to develop a good understanding of factors like size, stability and stealth character that will influence *in vivo* behaviour. Furthermore, a reliable synthetic platform is needed to be able to synthesize biocompatible amphiphilic polymers that self-assemble in polymersomes of controlled size. These arguments form the basic design criteria of polymersome for biomedical applications. In order to target the vesicles to the brain, or any tissue of interest, there is also a need to introduce targeting and/or tracking moieties at the periphery. Therefore reliable chemistry is essential to modify the periphery of vesicles, while keeping good control over the overall stability. Finally, with the chemistry available there is a need for efficient and specific targeting moieties, which are still active after they have been coupled to the periphery of polymersomes.

In ***Chapter 1***[6] recent literature on the design and use of polymeric vesicles in biomedical application was reviewed. Next, in ***Chapter 2*** the platform chemistry to synthesise block copolymers, self-assemble polymersomes of well defined size and functionalize the periphery with peptides and fluorescent tracers was developed. In ***Chapter 3***[7] the effect of polymersome size on *in vivo* circulation was evaluated via the quantitative method of radio-isotope labelling. Furthermore these polymersomes were applied in SPECT/CT imaging. In ***Chapter 4***[8], polymersomes tagged with a small peptide (G23) that recognizes gangliosides GM1 and GT1b were developed. These vesicles were shown to accommodate blood-brain barrier transport both *in vitro* and *in vivo*. Next, in ***Chapter 5***[9] a more quantitative study after the biodistribution of G23 tagged polymersomes was performed. For that purpose, polymersomes were both targeted and labelled with a radio-isotope.

In the final two chapters a more fundamental study after the controlled modification of the surface topology of polymersomes was performed. In ***Chapter 6***[10] block copolymer analogues were prepared of which the blocks were connected via a hydrazone bond. By mixing in this polymer, and applying acidic conditions, it was shown that the degree of surface PEGylation can be controlled from 100 to 5 percent. Below 5 percent PEGylation the colloidal stability was lost in a pH dependent rate. Finally, in ***Chapter 7***[11] polymersomes from hydrazone-coupled block copolymers were shown to exchange surface PEG chains between vesicles and the enviroment via the aniline catalyzed transimination equilibrium. This method allowed to modify the polymersome-periphery to form complex (asymmetrically)-functionalized vesicles.

(1) Cecchelli, R.; Berezowski, V.; Lundquist, S.; Culot, M.; Renftel, M.; Dehouck, M. P.; Fenart, L. *Nat Rev Drug Discov* **2007**, *6*, 650.
(2) Discher, B. M.; Won, Y. Y.; Ege, D. S.; Lee, J. C. M.; Bates, F. S.; Discher, D. E.; Hammer, D. A. *Science* **1999**, *284*, 1143.
(3) Discher, D. E.; Eisenberg, A. *Science* **2002**, *297*, 967.
(4) Ahmed, F.; Pakunlu, R. I.; Srinivas, G.; Brannan, A.; Bates, F.; Klein, M. L.; Minko, T.; Discher, D. E. *Mol Pharmaceut* **2006**, *3*, 340.
(5) Christian, D. A.; Garbuzenko, O. B.; Minko, T.; Discher, D. E. *Macromol Rapid Comm* **2010**, *31*, 135.
(6) Brinkhuis, R. P.; Rutjes, F. P. J. T.; van Hest, J. C. M. *Polym Chem-Uk* **2011**, *2*, 1449.
(7) Brinkhuis, R. P.; Stojanov, K.; Laverman, P.; Eilander, J.; Zuhorn, I. S.; Rutjes, F. P. J. T.; van Hest, J. C. M. *Bioconjugate Chemistry* **2012**, 23, 958.
(8) Georgieva, J.; Brinkhuis, R. P.; Stojanov, K.; Weijers, C. A. G. M.; Zuilhof, H.; Rutjes, F. P. J. T.; Hoekstra, D.; van Hest, J. C. M.; Zuhorn, I. S. *Angewandte Chemie int. ed.* **2012**, 51, 8339.
(9) Stojanov, K.; Georgieva, J.; Brinkhuis, R. P.; van Hest, J. C. M.; Rutjes, F. P. J. T.; Dierckx, R. A. J. O.; de Vries, E. F. J., *Mol. Pharm*. **2012**, 9, 1620.
(10) Brinkhuis, R. P.; Visser, T. R.; Rutjes, F. P. J. T.; van Hest, J. C. M. *Polym Chem-Uk* **2011**, *2*, 550.
(11) Brinkhuis, R. P.; de Graaf, F.; Borre Hansen, M.; visser, T. R.; Rutjes, F. P. J. T.; van Hest, J. C. M., Polym Chem-UK, accepted.

1

Polymeric Vesicles in Biomedical Applications

Polymeric vesicles, or polymersomes, are nano- to micrometer sized polymeric capsules with a bilayered membrane. Applications of these vesicles are foreseen in nano medicine, in vivo imaging and drug delivery. Such applications put many restrictions on the choice of polymer, the size and the surface of the vesicle. In this respect much can be learned and translated to polymersome science from lines of research with a longer history of practical knowledge such as liposomal formulation and polymer drug conjugation. The dimensions of a vesicle, such as size and shape can be controlled for polymersomes and will influence the in vivo circulation time. The surface can be adjusted to induce stealth character, or chemically modified to introduce targeting moieties. And last but not least the choice of block copolymers - the building blocks of a polymersome - can introduce features like biocompatibility, inherent or induced permeability and triggered release. In this Chapter we will discuss the recent advances in polymersome science with regard to biomedical applications and will specifically address the abovementioned features which affect their biological behaviour

René P. Brinkhuis, Floris P.J.T. Rutjes and Jan C.M. van Hest, Polymer Chemistry **2011**, 2, 1449-1462

1.1 Introduction

Polymeric vesicles, or polymersomes, are nano- to micro- meter-sized polymeric capsules with a bilayered membrane which is comprised of amphiphilic block copolymers. Although the aggregation behaviour of amphiphilic polymers was noticed before[1-4], the first systematic study after the formation of polymersomes was reported by Discher *et al*.[5]. In this paper the name polymersomes was coined, in analogy to liposomes. With regard to the bilayer membrane architecture, the similarity between polymersomes and liposomes is obvious in the sense that both species are composed of a bilayer of amphiphiles enclosing an aqueous compartment. There are however also major differences. The building blocks of liposomes are in most cases naturally occurring phospholipids with a molecular weight well below 1 kDa; a polymersome is constructed of amphiphilic block copolymers with a molecular weight of up to 100 kDa. This higher molecular weight of the building blocks manifests itself in a tougher, less permeable and less fluidic membrane and as a result superior physical and chemical stability. With regard to the use of high molecular weight building blocks and the resulting robustness of the capsule structure one can argue that polymersomes resemble to a certain extent viral capsids[6-7] and therefore can be interesting candidates for *in vivo* and cellular delivery.

Amphiphilic block copolymers have not only been found to form vesicular structures; in fact, the formation of a bilayered vesicular structure puts quite some restrictions on the overall block copolymer composition. Depending on the ratio between the hydrophobic and hydrophilic part of the polymer, spherical micelles, rods and vesicles have been found to form spontaneously[8]. The morphology that is observed is dependent on the geometry of the amphiphile, which can vary between cylindrical and conical depending on the ratio of the hydrophobic and hydrophilic segments. For small molecular weight amphiphiles this geometry is captured in the dimensionless packing parameter[9-10] - depicted in Figure 1 - which to some extent can also be translated to polymeric amphiphiles. More intuitively, however, the hydrophilic fraction (f) is better suited to predict the expected morphology[6-8].

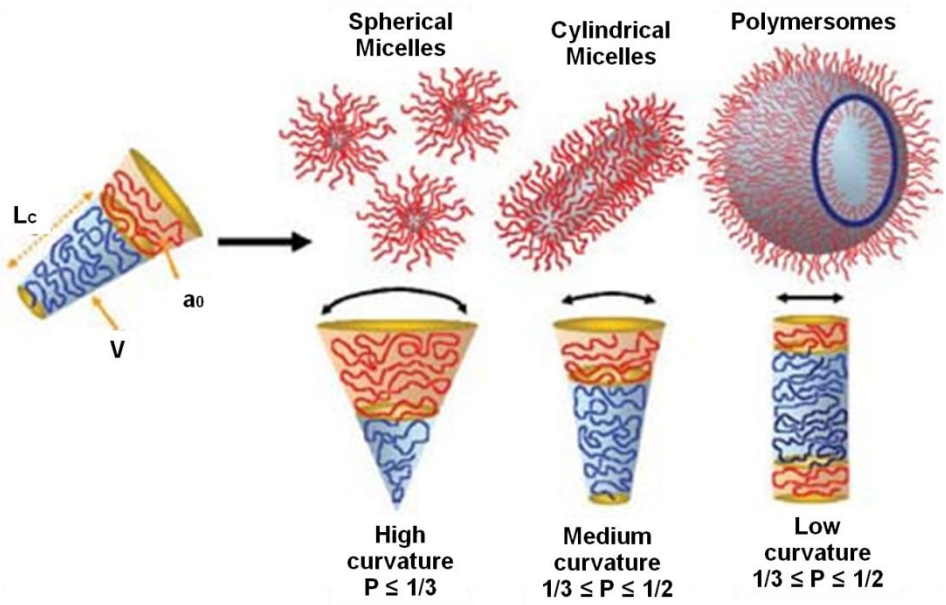

Figure 1. Several structures formed by the self assembly of amphiphilic block copolymers as determined by the geometry of the amphiphile. The geometry is captured by the dimensionless packing parameter $p=V/(a_0 l_c)$. Reprinted with permission (ref. 10)[10].

Block copolymers with a hydrophilic fraction of more than 45 – 50 percent will mostly yield micelles. In the region where f is around 35 ± 10% in many cases polymersomes are observed and in case the hydrophilic fraction is less than 25 percent, inverted structures can be expected. Finally, there is a small region where worm-like micelles have been reported, when the hydrophilic fraction is around 50 percent. Although this basic empirical rule holds quite well in most cases, the exact aggregation behaviour can depend strongly on the type of block copolymer and the conditions applied.

Polymersomes have been prepared in a variety of ways. Among them two methods seem to be favoured. First of all the "solvent switch" method is broadly applied[11-12]. The block copolymer is dissolved in an organic solvent which is a good solvent for both blocks. The organic solvent is diluted with or injected in a non-solvent of one of the blocks, mostly water or a buffered solution, until the desired aggregates are formed. Residual organic solvents are removed by dialysis or are allowed to evaporate. One of the major drawbacks is the need of an organic solvent which is not always compatible with applications in which bioactive compounds have to be encapsulated. Furthermore, traces of the organic solvents tend to stay behind which is not desirable for *in vivo* applications. The second general method is a

technique based on rehydration[12]. A polymer film is cast on a substrate and an aqueous solution is used to rehydrate the polymer to form vesicles. Furthermore, methods like electro formation, bulk rehydration and rehydration from pre-treated substrates have been applied. The choice of the method of formation has a big influence on the properties such as size of the obtained vesicles.

Vesicles are thought to form in a two-step procedure. In an early stage of formation a flat bilayer is formed from micelles or polymer clusters, as depicted in Figures 2a-b. Thereafter under the influence of a curvature change, and therefore a change in packing parameter, this sheet will form a closed structure or a vesicle[13-14]. This mechanism is depicted in the cartoon presented in Figure 3. This sequence of events leads to statistical encapsulation of compounds dissolved in the water layer, but does not provide an explanation for the many fascinating shapes found experimentally[13]. More recent simulation studies show the possibility of an alternative, more complex, mechanism in which vesicles do not evolve from the closing of a bilayer membrane, but evolve from micelles that grow and change morphology[14-15]. It should be noted that for the second pathway the loading efficiency of hydrophilic compounds would be lower compared to the former one since there is no closure, and hence encapsulation step involved. Experimentally, polymersome formation along path I is supported by Du *et al*.[16] (Figure 2). They were able to trap and visualize transition states like micelles and lamellae that eventually formed polymersomes by systematically adjusting the solvent polarity and chemically locking the structure prior to transmission electron microscope (TEM) imaging. Experimental evidence for the second route was found by Adams *et al*.[17] They showed that indeed poor loading efficiencies for hydrophilic compounds were found. These two seemingly contradictive experimental results show that it is possible that multiple mechanisms of formation do exist, depending on the exact conditions applied[14].

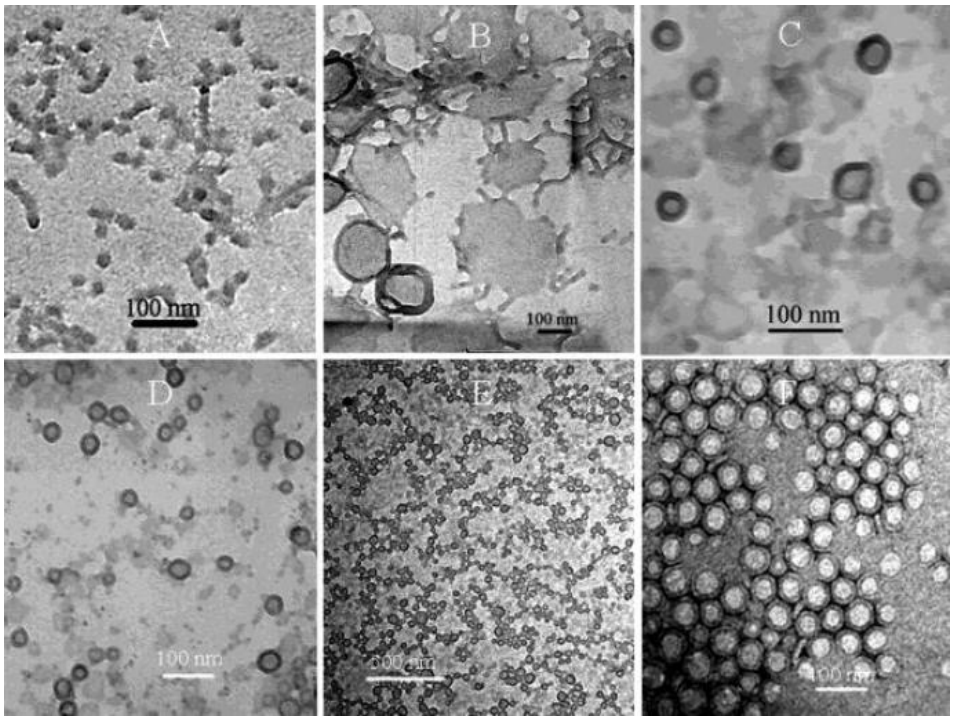

Figure 2. Several stages of polymersome formation captured by Du and co-workers[16] as a function of the water/organic solvent ratio. First spheres and rods are formed that transform into lamella which close to form polymersomes due to an increase in water content. Reprinted with permission (ref. 16).

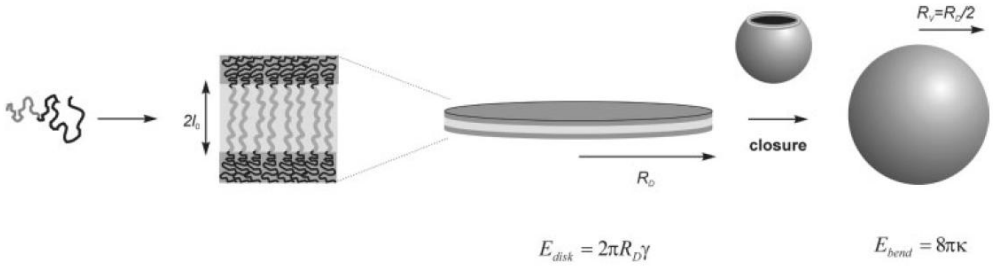

Figure 3. Cartoon of polymersome formation along path I as described by Antonietti *et al.*[13]. First spheres transforming into sheets are formed which close in a second step to form polymersomes. Reprinted with permission (ref. 13).

The field of polymersome research has been reviewed extensively in the past [6,10,12,18-25] and often the potential of polymersomes for biomedical applications such as smart drug delivery systems, *in vivo* imaging vehicles or artificial organelles is mentioned. Many of these applications involve cell specific interactions and/or require non-toxic and tuneable *in vivo* behaviour, and these criteria put quite some restrictions on e.g. the choice of polymer and the polymersome dimensions. In the remainder of this chapter we specifically address the factors that affect the use of polymersomes in biomedical applications. In the next sections we will focus on suitable components for the construction of polymeric vesicles for this specific field

of application. We will furthermore address the importance of size, topology, tuneable stability and permeability. Finally, a selection of functionalization methods will be discussed. In addition we will illustrate these topics with recent research and try to extrapolate facts from liposomal research to polymersomes.

1.2 Block Copolymers

The starting point of formation for any polymersome are the amphiphilic diblock or triblock copolymers that are the building blocks of the membrane. More than a decade of research into polymeric vesicles not only yielded some understanding underlying the formation of block copolymer nanostructures, but also allowed researchers to use their full creativity in the synthesis of new amphiphilic polymers. This resulted in an extensive library of block copolymers known today to form aggregates. For a comprehensive overview of polymers used for polymersome formation, one is referred to recent reviews on biohybrid amphiphiles[24] and synthetic amphiphilic block copolymers[10,26]. This section will focus on the most common types of polymers used in biomedical polymersome research.

For biomedical applications it is obligatory to use biodegradable or at least biocompatible polymers as building blocks. The field of polymer drug conjugates has already a long history of practical knowledge on suitable polymers that are in clinical use/evaluation nowadays[27-28]. These polymers include synthetic polymers such as poly(ethylene glycol) (PEG), poly(*N*-(2-hydroxypropyl)methacrylamide) (pHPMA), poly(vinyl pyrrolidone) (PVP) and poly(ethylene-imine) (PEI), but also natural polymers like dextran, dextrin and pseudosynthetic polymers such as poly L-glutamic acid (PGA) and poly(L-lysine) are commonly used. The translation from polymer drug conjugates to polymersome-forming amphiphilic block copolymers is not always straightforward, but many examples can be found in literature in which biocompatible and bio-inspired block copolymers have been employed to form polymeric vesicles.

1.2.1 Synthetic polymers

The first well-studied polymersome-forming system was based on the biocompatible block copolymer poly (ethylene-oxide)-b-poly (ethyl-ethylene) (PEO-b-PEE)[5]. Although the PEE block is highly biocompatible, it is the PEO block that gives these polymersomes useful *in vivo* characteristics. The water-soluble poly (ethylene-oxide) (PEO) or poly (ethylene-glycol) (PEG) is a polymer which is generally known for good biocompatibility and excellent *in vivo* behaviour. Application of a PEG mantle is used in liposome formulations to strongly reduce *in vivo* and *in vitro* non-specific protein adsorption, resulting in stealth behaviour and therefore prolonged circulation times[29-30]. PEG has been coupled to many hydrophobic blocks such as the non-degradable polystyrene (PS) and polybutadiene (PBd)[31], or biodegradable polymers such as polycaprolactone (PCL) or poly(lactic acid) (PLA)[32-34]. Each hydrophobic polymer introduces specifically desired characteristics in the polymersome. Polystyrene as an example has a relatively high glass transition temperature (T_g) and will yield after removal of the organic solvent a rigid semi-crystalline membrane. Polybutadiene on the other hand has a T_g well below room temperature which will result in a flexible and fluidic membrane allowing for extrusion and therefore size control after polymersome formation. Polymersomes of polybutadiene-b-polyethylene glycol (PBd-b-PEG) are generally considered as fully biocompatible and therefore popular in research towards *in vivo* applications like drug delivery. However, polybutadiene is not biodegradable, at least not on the timescale of days. PCL and PLA on the other hand are biodegradable and bio-compatible and are therefore also often encountered as the hydrophobic block[31-34].

Instead of using the neutral and inert PEG block as hydrophilic element, also some more functional moieties can be applied. The most straightforward way is to introduce ionic character in a block copolymer. In this way the water-soluble PEG block was replaced for poly acrylic acid (PAA) to introduce negatively charged acid residues[35], but also the zwitterionic, phospholipid mimic, poly(2-methacryloyloxy-ethyl phosphorylcholine) (PMPC) has been applied as the hydrophilic block by Armes and co-workers[36-38]. They furthermore showed that polymersomes with interesting pH-dependent properties are obtained if both blocks contain zwitter-ionic or ionisable monomers as is the case with vesicles prepared from poly(2-(diisopropylamino)ethyl methacrylate) (PDPA) as the hydrophobic and PMPC[36] as

the hydrophilic block. The PDPA block is hydrophobic at a pH above 6.4, but readily becomes hydrophilic and protonated below this pH. This results in a sharp transition from polymersomes to free dissolved block copolymers upon lowering the pH, which can be used as a drug release mechanism.

The previous example involved an external stimulus (pH change) to release content from the vesicle, but also amphiphilic block copolymers with inherently leaky properties have been reported. Polymersomes of polystyrene-b-poly 3-(isocyano-L-alanyl-aminoethyl) thiophene (PS-PIAT) turned out to be excellent candidates for nanoreactors, since these polymersomes are permeable for small molecules while large molecules such as enzymes stay trapped inside[3, 39]. Although not fully understood, this permeability is probably a result of the helical rodlike secondary structure of the hydrophilic PIAT block, which frustrates the packing of the polymers in a closed bilayer.

These selected examples already show a few of the many possibilities to alter and tune the characteristics of the polymersomes, like robustness, charge and permeability. One crucial property however remains biocompatibility and/or biodegradability. It is therefore a logical step that many researchers have developed amphiphilic block copolymers capable of forming polymersomes which are partly based on naturally occurring building blocks such as amino acids, nucleotides and carbohydrates.

1.2.2 Bio(hybrid) polymers

Oligo- and polypeptides are highly versatile and biodegradable polymersome building blocks, since their properties can be varied in many different ways. A wide variety of secondary structures can be created based on the primary sequence of amino acids. By selecting the correct amino acid residues stimulus-responsive behaviour is introduced, such as pH dependent charge and hence solubility[40]. One of the first reports on the formation of vesicular structures from peptide hybrids made use of an antibacterial hydrophobic helical peptide, Gramicidin A. By coupling Gramicidin A with PEG an amphiphilic block copolymer was obtained[41] which readily formed a variety of aggregated structures in aqueous solution. Among the obtained structures a vesicle-like aggregate was found, which was called a peptosome[2,42]. Since then the name peptosome has been more generally used for peptide-containing

polymersomes. This early example involved a hydrophobic peptide which was buried under a PEG mantle. However, in most other cases the peptide moiety is the hydrophilic part, forming the periphery of the vesicles. This was for example demonstrated by Dirks *et al.*[43] who coupled a tripeptide, Gly-Gly-Arg-AMC, via the copper-catalysed azide-alkyne Huisgen (3+2) cycloaddition to polystyrene. Even more common than the use of oligopeptides is the application of polypeptides as building blocks in polymersome-forming block copolymers. Peptides consisting of a repetition of the same amino acid, and block copolymers of homopolypeptides can nowadays be obtained in a controlled fashion by the polymerisation of *N*-carboxyanhydrides (NCA) with a nickel catalyst and an amine initiator[44-45]. In this way PBd was used as the amine functional initiator to polymerize for example PBd-poly(L-glutamate)[46-49] and PBd-poly(L-lysine)[50] which both have been extensively studied with respect to their aggregation behaviour. These examples involve a combination of synthetic polymers and polypeptides, but also block copolymers of which both the hydrophobic and the hydrophilic part are composed of polypeptides have been designed to form polymersomes.[40,51-52] In two recent examples Kimura *et al*. showed the usefulness of peptosomes for *in vivo* cancer imaging[53]. They constructed peptosomes out of a block copolymer composed of poly(N-methylglycine) and poly(γ-methyl-L-glutamate) (PMLG) in which a near infrared dye was encapsulated. These peptosomes showed good *in vivo* circulation times and low recognition by the reticuloendothelial system RES (blood clearance mostly by liver and spleen).

Another group of naturally occurring building blocks which have recently gained more attention are carbohydrates or polysaccharides[23,54-56]. In natural systems saccharides are conjugated to the surface of cells via lipids constituting the cell membrane (glycolipids), and they are also found conjugated to proteins (glycoproteins). These glycoconjugates play an important role in biological processes such as cellular recognition and pathogen infection. In many cases these processes are mediated via interactions between saccharides and receptor proteins, called lectins. In general lectins have only a low affinity for saccharides, so this needs to be compensated by multivalent interactions via the so-called cluster glycoside effect. Application of (poly)saccharides in polymersomes as hydrophilic part of block

copolymers or as the end group of block copolymer amphiphiles allows for the construction of highly functionalised and multivalent vesicle surfaces.

Although quite some research has focused on the synthesis of polysaccharide block copolymers not many examples have been reported that actually form polymersomes[23]. An example which also demonstrates specific recognition is a fairly simple rod-coil amphiphile, tetra(*p*-phenylene)-block-PEG_{12}-α-D-mannopyranoside[57] This molecule formed small polymersomes which specifically interacted with the pili of a specific *Escherichia coli* bacterial strain as depicted in Figure 4. When the head group was replaced for galactose, polymersomes were still formed, but without the binding properties. Another example involved a β-cyclodextrin head group coupled to PS which also formed vesicles[58]. The hydrophobic interior of β-cyclodextrin was used to attach hydrophobic fluorescent dyes and the adamantane-coupled enzyme horse radish peroxidise (HRP) to the surface.

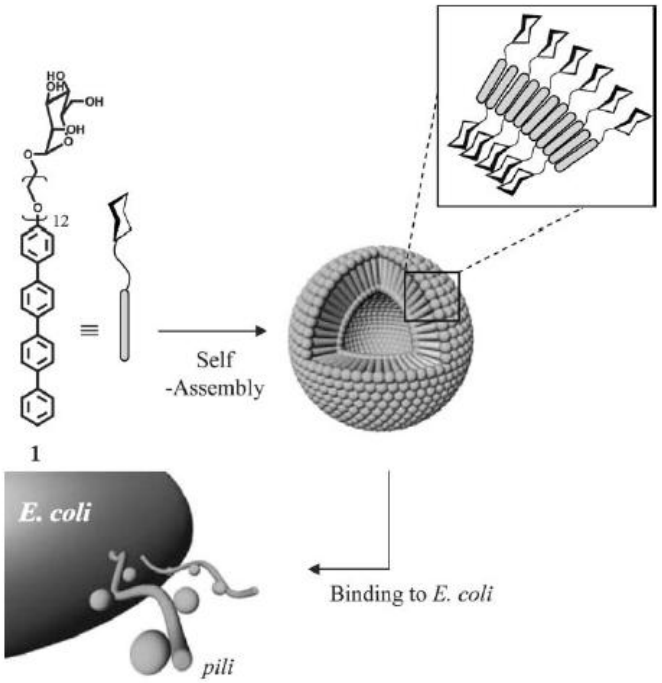

Figure 4. Rod coil amphiphile which forms small vesicles. The manno-pyranoside head group induces recognition and binding to the pili of *Escherichia coli*. Replacing this moiety for galactose had no influence on the aggregate formation, but resulted in loss of recognition[57]. Reprinted with permission (ref. 57).

Block copolymers comprising polysaccharides such as dextran-b-poly(benzyl-L-glutamate) (PBLG)[54] dextran-b-PS and hyaluronan-b-PBLG[59] have also been used for vesicle formation. Dextran-b-PS was found to form both micelles and vesicles, depending on the PS length. The usefulness of these peptide-carbohydrate hybrid polymersomes in drug delivery was nicely demonstrated in a series of recent papers

by Lecommandoux *et al.*[60-62] They prepared docetaxel loaded hyaluronan-b-PBLG polymersomes and showed both *in vivo* and *in vitro* (tumour-) targeting by the hyaluronan periphery as well as release and shrinkage of the tumours in animal models. Finally, an elegant first example of a thermoresponsive saccharide-containing block copolymer was reported by Otsuka *et al.*[63]. They coupled maltoheptaose (mal7) to poly(*N*-isopropylacrylamide) (PNIPAM) via click chemistry to obtain polymersomes. They showed that above the lower critical solution temperature (LCST) of PNIPAM polymersomes were spontaneously formed whereas below the LCST the assemblies were dissolved again.

1.2.3 Polymeric vesicles with non-bilayer structures

A group of vesicle-forming polymers exists which don't yield a bilayer structure. An interesting example is the self-assembly into vesicles of ABA or ABC triblock copolymers[64]. Although the overall composition is similar to a vesicle bilayer, namely two hydrophilic outer blocks separated by a hydrophobic inner domain, the entire structure is a single layered vesicle. By changing the blocks A, B or C one can even direct the orientation of the polymers in the membrane, thereby obtaining asymmetric membranes that display different functional groups on the inside and outside as was elegantly demonstrated by Wolfgang Meier and co-workers. Very recently Percec *et al.*[65] reported an in depth investigation into a variety of amphiphilic, or Janus dendrimers that formed a variety of aggregates, among them a vesicular structure that was named dendrimersomes. A peptidic-dendron polymersome was also reported to form polymersome-like structures[66]. Another interesting system comprises the so-called polyion polymer complexes or PICsomes[67-71]. They are based on two polymers with opposite charges that self-assemble and phase separate into vesicular structures This is an example of a series of polymers that recognize each other and form recognition-induced aggregates, so-called RIP's[72-74]. A final example of vesicles that do not exhibit a bilayered membrane was developed by Caruso and Möhwald[75]. They showed that enzymes can be entrapped in vesicles that were formed by a layer-by-layer deposition of anionic and cationic polymers.

1.3 Structural Factors

For *in vivo* and biomedical applications of polymersomes it is important to ascertain that particles circulate sufficiently long to reach the desired place. This can be achieved by protecting the particle from interactions with the immune system. We have already mentioned examples of polymers that exhibit such stealth-like behaviour which was attributed to the PEG surface of the particles. It should be noted however that although PEGylation is a good start to rule out non-specific interactions, it is by itself not enough to escape clearance by the RES. Not all factors influencing *in vivo* circulation times have been fully investigated yet, but in case of polymersomes, the analogy between polymersomes and liposomes allows for some extrapolation.

From liposome research it is known that factors like stealth-like behaviour, size and shape play an important role[76-77]. Therefore this section will review how these parameters can be controlled. Furthermore, we will highlight research where these effects have been observed.

1.3.1 Stealth-like behaviour

To prolong blood circulation times and prevent recognition by the RES a PEG mantle is applied in liposomal formulations by introducing up to ten percent PEGylated phospholipids. PEG has very useful characteristics in the sense that it blocks (almost all) non-specific protein adsorption and induces no immune response, basically giving a vessel stealth characteristics[29-30]. These stealth liposomes have blood circulation half times in the order of 15 hours and will circulate in traceable amounts for many days. Discher and co-workers investigated the *in vivo* fate of polymersomes formed from PBd-b-PEG by preparing polymersomes with a fluorescent dye entrapped[78-79]. These polymersomes were inherently hundred percent PEGylated. The blood circulation half life was determined by counting fluorescent dots in blood samples derived at different time points. Compared to PEGylated liposomes the circulation half life appeared even longer and polymersomes could still be found after several days. These results show that PEGylated polymersomes also display stealth-like behaviour. It should be noted that not only PEG has the useful characteristics of reducing interactions with opsonins and preventing clearance by

the reticuloendothelial system (RES). Also the zwitterionic polymer PMPC has been recognized to reduce the adsorption of opsonins[80]. Other possibilities include use of pHPMA, and oligosaccharides such as cyclodextrin, which might be used since these polymers are already under investigation as polymer-conjugated therapeutics[27]. Finally in liposomal formulations poly(oxazoline) conjugates also showed prolonged circulation times[81]. The non-adsorptive character and hydration shell of the hydrophilic mantle is obligatory to create stealth-like particles, but it is certainly not enough.

1.3.2 Size

Although not fully investigated for polymeric vesicles it is known from liposome science that size has a big influence on blood circulation times, RES recognition, biodistribution and the mechanism of cell uptake[76,82]. Figure 5 shows a literature compilation by Harashima *et al.* on the influence of the size of liposomes on the circulation time. What is not clear from this picture is that there is also a lower limit for prolonged circulation times. The junctions in vascular endothelium of healthy tissue vary depending on the tissue type. In most tissues these openings are below 2-6 nm, so too small for liposomes and polymersomes to enter. Organs and tissue with discontinuous endothelium like the fenestrated endothelium of kidney glomerulus or sinusoidal endothelium of the liver and spleen can have pores of 40-60 and up to 150 nm[83]. Particles with a size below these values will therefore be excreted or trapped within the tissue resulting in clearance from the circulation. It is notable that tumours can have discontinuous microvasculature with pore sizes above 100 nm. In fact, this is the basis for non targeted delivery to tumours since particles that are small enough to enter will accumulate in the tumour. Taking these mechanisms into account the optimum size for circulation in the blood stream is expected to be around 80-150 nm. It might be expected that a similar trend is valid for polymersomes and the polymersome size should be controlled to achieve optimal blood circulation half lives.

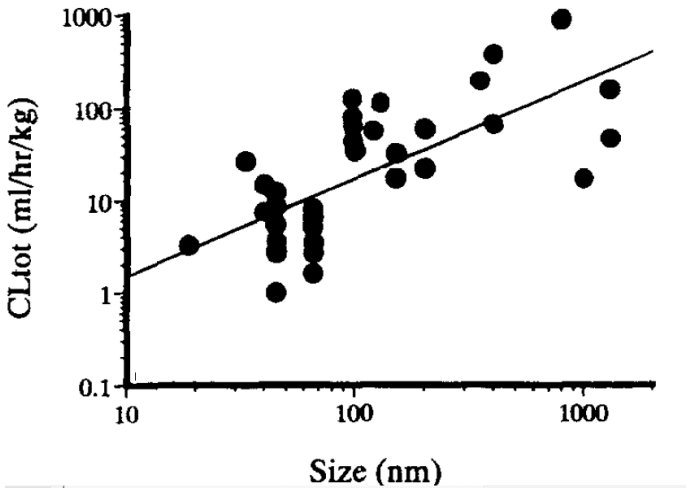

Figure 5. Compilation of literature by Harashima *et al.*[76] on the effect of particle size on the blood clearance of liposomes. Reprinted with permission (ref. 76).

For polymersomes the eventual vesicle size can be influenced at different points in the process of preparation. The first level to exert influence is on the polymer level. For example, it has been shown that there is correlation between amphiphile molecular weight and aggregate size[84]. Furthermore, the polydispersity[11] of the block copolymer and the ratio between blocks can have an influence on the size distribution.

One stage further, one can influence the size using different methods of vesicle formation[85]. Rehydration methods and solvent displacement[86] or injection[87] methods have been applied and mostly yield 50 to 800 nanometre-sized polymersomes. On the other hand electroformation will yield micrometre-sized giant polymersomes. Howse *et al.*[85] recently showed that they were able to use surface-directed templating with different mesh surfaces to influence the size of PEO-PBO vesicles. They were able to deposit block copolymer domains of predefined size on a grid and showed that rehydration from these grids yielded control over polymersome size as depicted in Figure 6. Smaller polymer domains yielded smaller polymersomes (5-10 μm) with in all cases small size distributions. The presence of pH-responsive, ionizable groups can also allow control over size during vesicle formation by changing the pH or ionic strength[49]. A certain amount of control over polymersome size was shown by Shen *et al.*[88] They were able to influence the vesicle size by changing the solvent nature and composition during solvent displacement formation of PS-PAA polymersomes. Luo *et al.*[86] showed also that binary organic solvent systems can be used to influence size. Furthermore the presence of additives like dendrimers[89], (homo)polymers[11] and surfactants[90] have been shown to influence the average polymersome size and polydispersity[11].

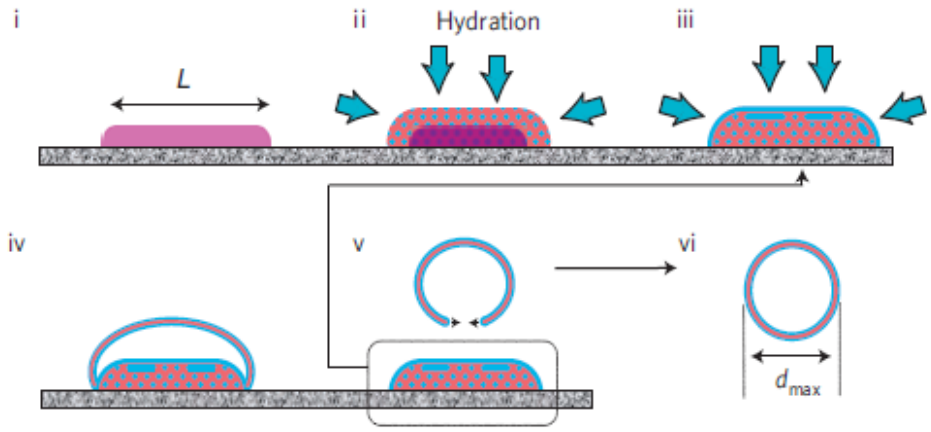

Figure 6. Rehydration of amphiphilic block copolymers from a surface template. The dimensions of the polymer domain (L) dictate the eventual polymersome size (d_{max})[85]. i) block copolymer domain of predefined dimensions, ii) hydration and phase separation, iii) further hydration and lamellae formation, iv) expansion, v) detachment, vi) energy minimisation resulting in polymersome formation. Reprinted with permission (ref. 85)

Finally polymersomes can be resized after they have been formed. In this respect the most straightforward way to obtain polymersomes of a predefined size is by extrusion. This basically means that a preformed sample of polymersomes is pressed through a filter with nanopores[79]. This procedure has also been proven to be applicable on larger scale by the use of hollow nano-fibers[91]. The only restriction is that the polymeric membrane should remain fluidic till the end of the procedure, therefore polymers with a low T_g are needed. In the stage after formation it is also possible to exert influence on the size via more sophisticated methods than extrusion. Eisenberg and co-workers reported that membrane fusion and fission driven by a change in dioxane/water content (change of interfacial energy) allowed vesicles to grow and shrink reversibly[86,88].

Another example involves the swelling of the membrane by an external stimulus. In this way pH-responsive blocks have been introduced in the corona to trigger size change, but also a change in secondary structure of polypeptides has been employed[46]. In a recent example by Yu and Eisenberg[92] the formation of so-called "breathing vesicles" from PEO-PS-PDEAEMA was reported. By variation of the pH they were able to swell and shrink the polymersome (membrane) with a factor of ~1.9 changing simultaneously the membrane permeability as depicted in Figure 7. This approach shows that a well-chosen balance between solubility and hydration will keep the aggregate together, but still allows considerable changes. If this balance is not carefully chosen, the polymersome will disassemble into its constituents.

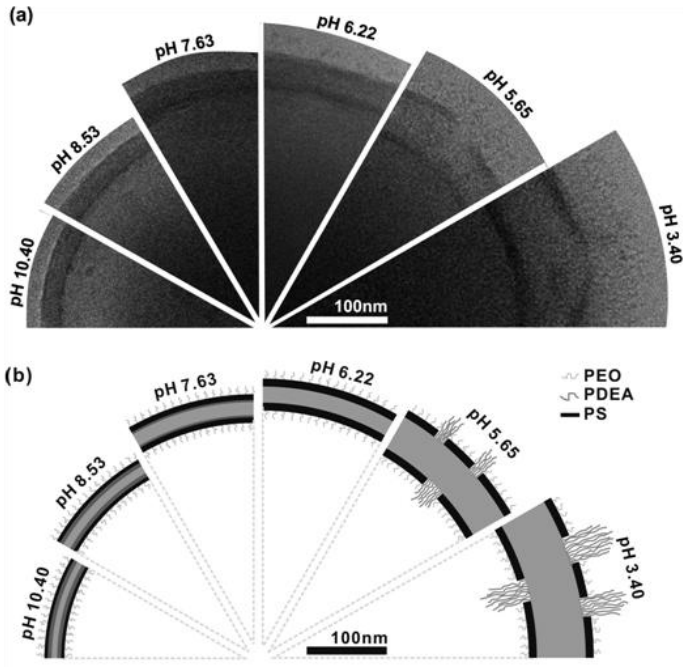

Figure 7. Reversible change of the PEG-b-PS-b-PDEAEMA membrane upon pH change. (A) Cryo-TEM images of the vesicle wall structure at several pH values. (B) Schematic illustration of the presumed membrane structure at corresponding pH values. Reprinted with permission (ref 92)

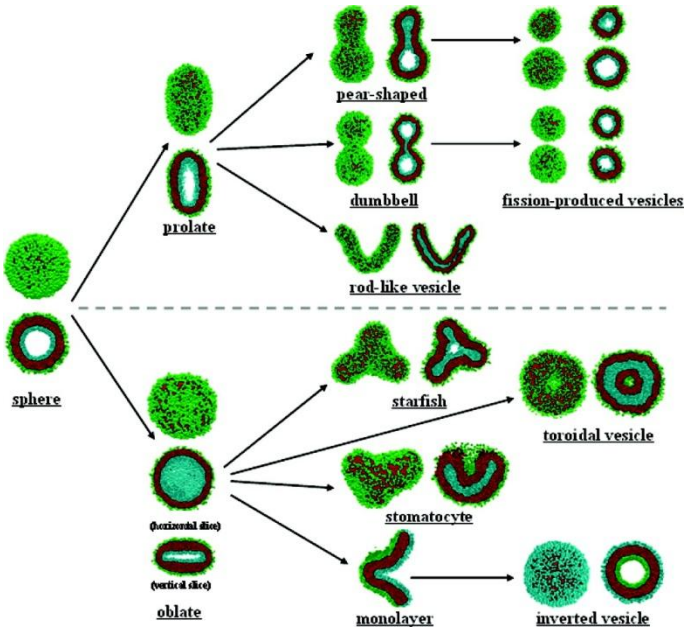

Figure 8. Morphologies possible for triblock copolymers as determined theoretically by Li *et al.*[93] Reprinted with permission (ref. 93).

1.3.3 Shape

The influence of shape and topology on *in vivo* behaviour is not so well studied for liposomes and polymersomes. In fact, probably the most illustrative example for the

influence of shape in amphiphilic assemblies for *in vivo* behaviour comes from rod like micelles as studied by Geng *et al*.[94] They showed that worm-like micelles, which are non spherical in nature, have blood circulation times exceeding those of spherical particles like liposomes and polymersomes by far; even if the persistence length at the moment of injection is several microns. Micelles or worm-like micelles[95-97] do not have an aqueous lumen and therefore do not allow for delivery of hydrophilic compounds, but also worm-like polymersomes have been observed and described[98-99] that do enable the encapsulation of hydrophilic compounds, and which should have similar behaviour.

These cylindrical shapes are not the only non-spherical shaped vesicles that have been reported. In fact, a realm of non-spherical aggregates is possible[13]. This has already been demonstrated for giant phospholipid vesicles (10-50 um) of which it is known that they can transform shape from spherical into a variety of nonspherical shapes upon a change in environment[100-101]. Theoretical studies on triblock copolymers by Li *et al*.[93] showed that this transformation should also be possible for polymersomes as depicted in the phase diagram in Figure 8.

Recently, experiments have been performed in which non-spherical polymeric assemblies were created chemically[16] or via kinetic entrapment.[102] It should therefore be possible in the near future to investigate the effect of shapes other than rodlike or spherical on *in vivo* behaviour

1.4 Release and Permeabilisation Mechanisms

One of the advantages of polymersomes over liposomes is their more robust and therefore less leaky membrane, which is very useful for improved circulation times and the prevention of uncontrolled release of drugs. However, at one point almost each *in vivo* application involves a disruption step to release the vesicle content or make the content accessible. Despite the fact that polymersomes display improved stability, many successful examples exist of stimuli-responsive vesicles, which release their contents upon action of an external trigger[9,20,24]. It is also possible to achieve permeability control, i.e. controlled pore formation, without complete disruption of the vesicular structure. In the next section we will highlight a few recent and illustrative examples.

1.4.1 Triggered Disruption

The most straightforward example of a release mechanism is actually degradation of the biodegradable polymers of which the vesicle is composed. Polymersomes of PCL-b-PEG released their cargo due to biodegradation based on (pH driven) hydrolysis of the polymers. During this process a transformation change from polymersomes to rods and eventually micelles was in some cases observed due to the change in hydrophilic fraction (f). By mixing in a stable PBd-b-PEG block copolymer it was possible to tune the speed of degradation[6,31]. Besides hydrolysis disruption based on chemical alteration of the block copolymer by oxidation[99], or reduction have been reported[20].

pH-Triggered release mechanisms which in principle are reversible have also been reported. A nice example of a polymersome that can disassemble upon a pH change was already encountered in Section 1.2.1. Armes and co-workers used the biocompatible zwitterionic PMPC-b-PDPA block copolymer to form polymersomes at pH above six. By lowering the pH a sharp transition was observed from vesicles to molecularly dissolved polymers due to protonation of the PDPA block. The polymersome content was thereby instantaneously released. The driving force for polymersome formation is in most cases based on phase separation due to the amphiphilic character of the block copolymer. By switching the character of the hydrophobic block to hydrophilic it is possible to dissolve the whole polymersome and release the content. Recently Kim *et al*.[103] reported a system based on this principle. They developed a stimulus-responsive amphiphilic polymer containing boronic acid moieties in the hydrophobic domain that, upon increase of pH and in the presence of monosaccharides such as D-glucose, became soluble in an aqueous environment. Another interesting example was reported by Lecommandoux. They prepared polymersomes of a block copolymer comprising two polypeptides, poly-L-glutamate-b-poly-L-lysine (PGA-b-PLys). By changing the pH they were able to switch the solubility of *both* blocks, effectively flopping the whole membrane[104]. Those examples all involve a change in pH as the trigger, but there are more stimuli explored.

Also changes in temperature can be used for altering the hydrophilicity of a block copolymer[20]. From literature there are quite some polymers, peptides and proteins which demonstrate LCST behaviour as was mentioned before in Section 1.2.2 with

the example by Otsuka *et al.*[63]. Figure 9 shows another very versatile example based on P(DEAEMA$_{98}$-b-NIPAM$_{392}$), a so-called "schizophrenic" polymer[105-106]. This system was shown to reversibly dissolve and assemble into polymersomes, as well as transform micelles to polymersomes based on either a pH and/or a temperature trigger[105]. Based on a pH-induced conformational change Bellomo *et al.*[40] reported a release mechanism for polymersomes composed of a dipeptide block copolymer which contained a stable hydrophilic α-helix of PEGylated poly-L-lysine and a hydrophobic α-helix of poly(L-leucine$_{0.3}$-co-L-lysine$_{0.7}$). Upon lowering the pH the alpha-helix of the hydrophobic block transformed into a random coil due to protonation of the lysine residues. This conformational change was found to disrupt the vesicle, allowing the transport of calcium ions and dyes in and out of the polymersome.

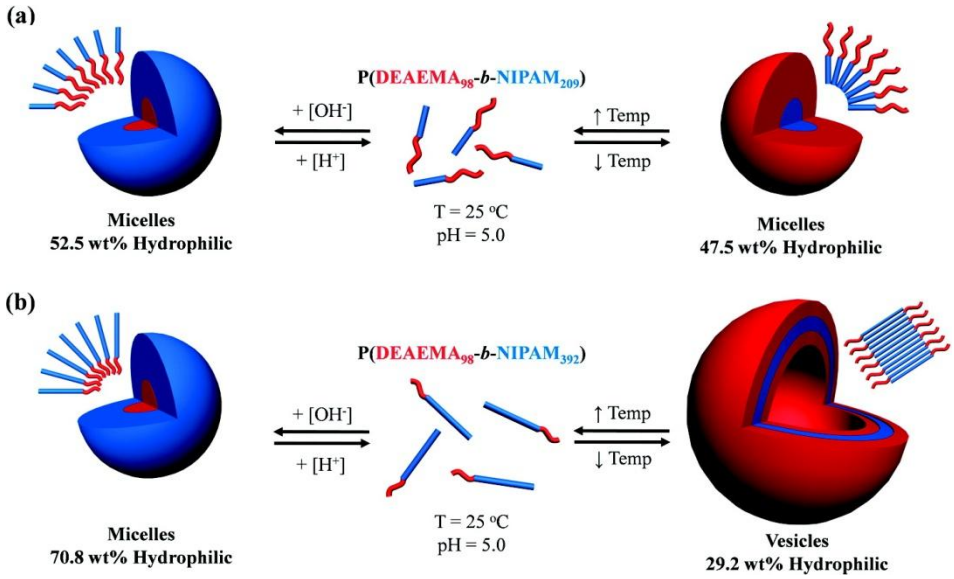

Figure 9. Mechanism of aggregation and dissolution of schizophrenic vesicles as described by Smith *et al.*[105] Reprinted with permission (ref. 105)

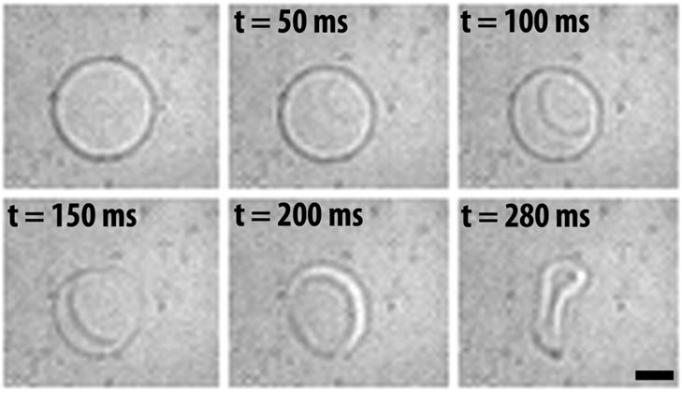

Figure 10. Polymersome disruption by illuminating with UV light. A fraction of the polymeric building blocks is functionalized with azobenzene moieties. Illumination with light induced a conformational change, disrupting the polymersome and releasing its content[107]. Reprinted with permission (ref 107)

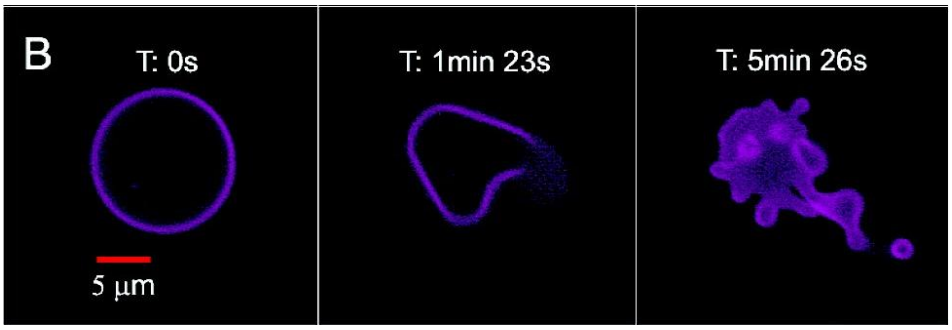

Figure 11. Polymersomes loaded with enzymes in the lumen and porphyrins in the membrane respond to light by a morphology change and eventually release of content[108]. Reprinted with permission (ref. 108)

Researchers also have developed methods of disruption, based on external stimuli such as ultrasound and light. An interesting system was reported by Mabrouk *et al.*[107] as depicted in Figure 10. They described how the incorporation of azobenzene moieties allowed for a conformational change in the membrane upon illumination with UV light. Their polymersomes were disrupted within a second. Figure 11 shows another example of a light-driven vesicle shape transformation and release. Robbins *et al*[108] reported that polymersomes formed from PBd-b-PEG with porphyrins entrapped in the membrane and proteins in the lumen disrupted in response to light. When either the protein or the porphyrin was left out this effect was negligible, indicating a synergy between the fluorophore and the encapsulated enzyme.

1.4.2 Controlled Permeability

For some applications a complete disruption of the vesicle is not desired. Rather, the polymersome should be semi-permeable. This is for example the case in enzyme therapeutics or artificial organelles, in which enzymes are encapsulated in the vesicle. The polymersome functions as a protective cage, i.e keeping the enzymes in and allowing substrate and products to diffuse in and out of the polymersome. Different strategies have been reported to create in a controlled fashion these semi-permeable or leaky polymersomes.

An example of an inherently leaky polymersome is based on the earlier mentioned PS-b-PIAT block copolymer system. These polymersomes have been used as biocatalytic reactors, by encapsulating enzymes in the lumen. It was shown that substrate diffused through pores in the membrane, and the encapsulated enzyme

was not able to escape, essentially making it a nano reactor with a semi permeable membrane[39]. This line of research was developed further by creating a nano reactor[109] capable of performing a three-enzyme cascade reaction. The cascade scheme is depicted in Figure 12. and shows that one enzyme is entrapped in the lumen, a second is captured in the hydrophobic membrane and finally a third enzyme is coupled covalently to the surface via clickable anchors. Another system that has been reported by Kataoka to assemble a semi-permeable membrane is based on oppositely charged block copolypeptides which yield PICsomes[71]. These PICsomes have also been used as biocatalytic nanoreactors. Although these two examples show the usefulness of semi-permeable vesicles, in both cases the permeability was not tuneable.

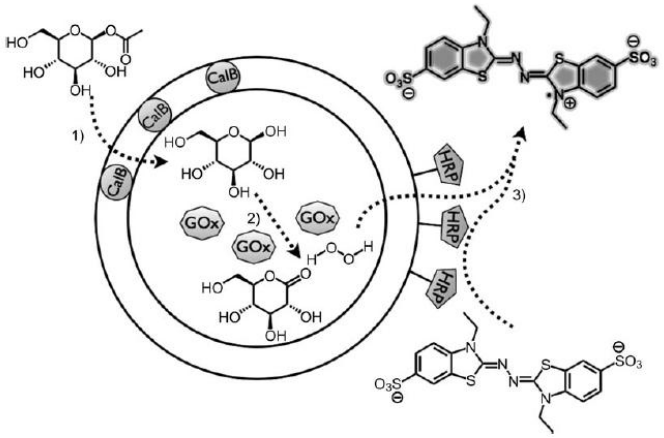

Figure 12. Polymersome nano-reactor performing a three enzyme cascade reaction. All three enzymes are associated with the PS-PIAT vesicle and leaving out one will stop the whole cascade[109]. Reprinted with permission (ref. 109)

Meier and co-workers followed a bio-inspired approach for the construction of semi-permeable vesicles.[110] They nicely showed that bacterial transmembrane channel proteins OmpF and aquaporin[111,112] could be successfully reconstituted into the membrane of polymersomes composed of the triblock copolymer poly(2-methyl oxazoline)-b-poly(dimethylsiloxane)-b-poly(2-methyloxazoline) (PMOXA-PDMS-PMOXA), which made these vesicles selectively porous. In nature many transmembrane pores have a directed orientation, but upon reconstitution into liposomes or polymersomes they tend to adopt a random orientation, basically blocking out fifty percent of the channels. By using an asymmetric ABC type of triblock copolymer it is possible to form vesicles with either the A or the C block on the outside[112], effectively constructing an asymmetric membrane as depicted in Figure 13. Meier and co-workers reconstituted aquaporin 0 in these membranes and

were able to tune the direction of insertion. An elegant approach towards the construction of semi-permeable polymersomes[113] was the reconstitution of LamB protein in PDMS-b-PMOXA polymersomes. This protein was recognized by Bacteriophage lambda and used to dock the phage, after which it injected its DNA into the polymersome, as nicely captured by TEM imaging in Figure 14.

In another example Choi *et al*.[114] showed that it is also possible to reconstitute two different proteins, bacteriorhodopsin and F1-ATP-ase, in a polymeric vesicle membrane, as depicted in Figure 15. ATP-ase can be regarded as a proton gradient driven motor that, while rotating, converts ADP into ATP. The required proton gradient is supplied by bacteriorhodopisin, which is activated by a light source. Choi and co-workers nicely showed that the enzymes worked together. If no light was applied there was no production of ATP. This research is one of the first systems reported where a complex biocatalytic process is performed in a polymersome nanoreactor.

Only few examples of synthetic approaches towards controlled semi-permeable polymersomes have been reported. One of the first of these approaches was reported by Tsourkas and co-workers[115]. They designed polymersomes based on PBd-b-PEG and mixed in phospholipids, 1-palmitoyl-2-oleoyl-*sn*-glycero-3-phospho-choline (POPC). After they crosslinked the PBd membrane, POPC was extracted leaving a porous vesicle. The same method was applied by exchanging POPC for the biodegradable block copolymer poly(caprolactone)-PEG. After crosslinking and hydrolysis a highly permeable polymersome was obtained[116]. Recently, another fully synthetic approach to controlled permeable polymersomes was reported by Kim *et al*.[117] They used the boronic acid based block copolymers described in Section 1.4.1 and mixed it in with PS-PEG, which forms a semi-crystalline membrane. Upon washing away the boronic acid polymer by applying sugar and base they were able to form pores in the membrane of which the size was tuneable by the ratio of boronic acid block copolymer and PS-PEG. This procedure could be used in combination with the encapsulation of CalB, allowing the substrate to pass the membrane while keeping CalB enclosed. They also showed that bigger pores allowed faster diffusion of substrate, as determined by the reaction rate.

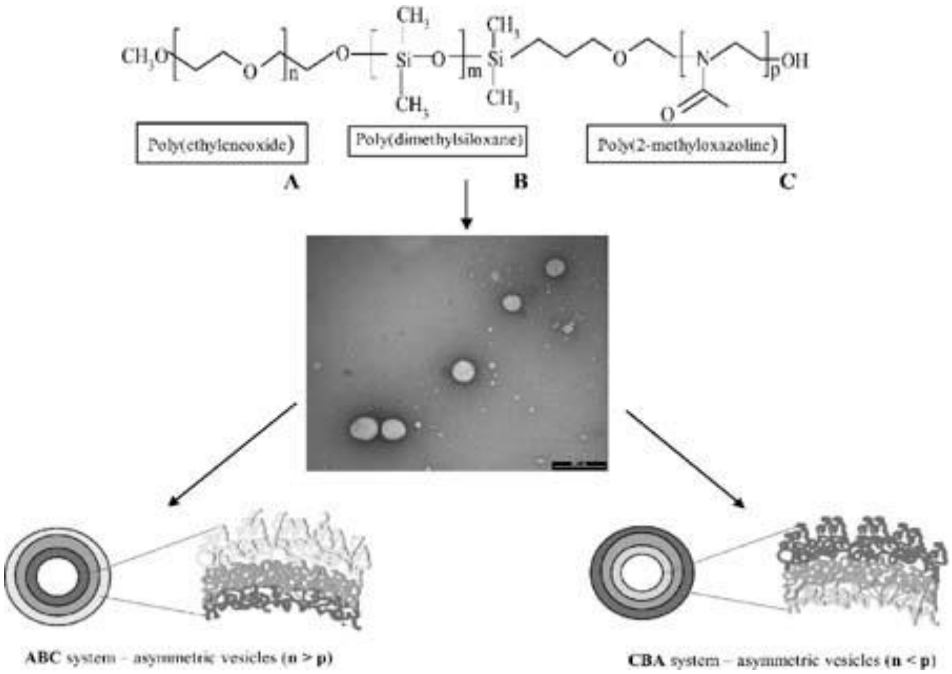

Figure 13. Asymmetric polymersome membranes obtained from ABC triblock copolymers allow for the directed reconstitution of transmembrane channels.[112] By changing the molecular weight of the A and C block either the A or the C block is directed outwards. Reprinted with permission (Ref. 112)

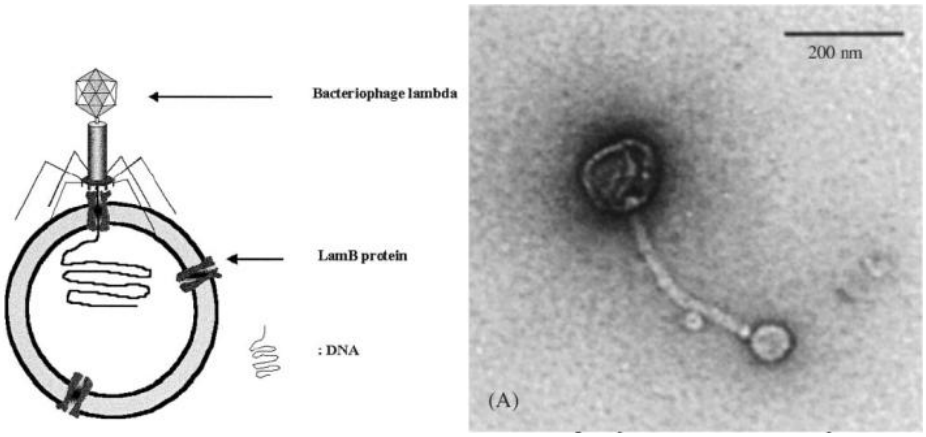

Figure 14. Schematic and TEM image of a polymersome in which membrane protein LambB is reconstituted.[113] This membrane protein is recognized by bacteriophage lambda which is shown to dock on the polymersome to inject its RNA. Reprinted with permission (ref. 113)

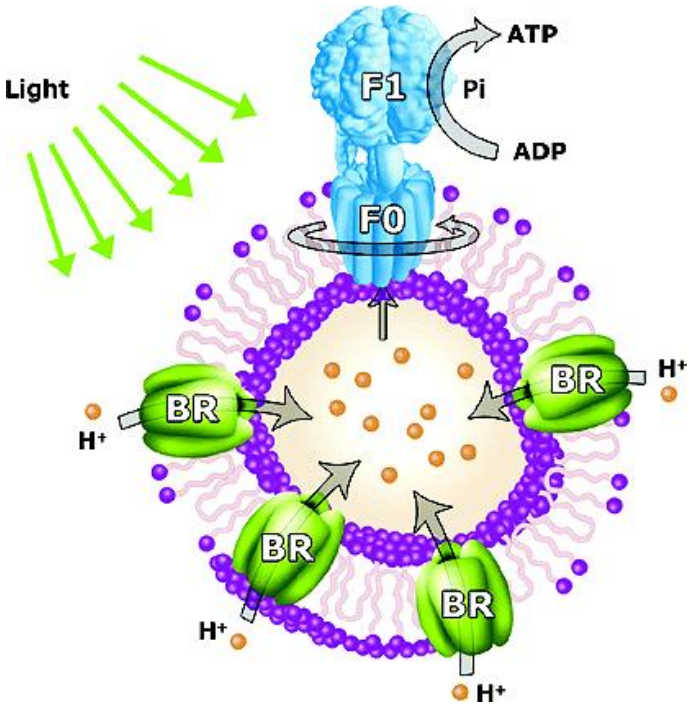

Figure 15. Light driven nano reactor. Under the influence of light bacteriorhodopisin (BR) establishes a proton gradient, which is used by ATP-ase to produce ATP from ADP [114]. Reprinted with permission (ref. 114).

1.5 Surface Functionality

PEGylated liposomes are neutral and are considered to be long circulating vesicles, with circulation times up to days. When compared to natural systems there is however room for improvement. Red blood cells for example circulate up till 100 days. Their cell surface has an overall negative charge due to the external glycocalyx moieties. The effect of surface charge of liposomes has therefore been studied, but the general trend is not so obvious and seems to be influenced by the size of the liposome, especially in rat and mice studies.[76] In rabbits a clear trend was observed which was in favour of neutral PEGylated liposomes ($t_{1/2}$ = 19.3h.), while negative and PEGylated negatively charged liposomes showed circulation half times of only 9.6 and 16.5 hours respectively[118]. Charge is only one of the possible functionalities which affect the interaction of polymersomes with biological systems. Another aspect is surface topology. Research on both will be discussed in the next sections

1.5.1 Surface topology

Christan *et al.*[119] recently reported on the synthesis and *in vivo* evaluation of polymersomes with a red blood cell like surface (i.e. negatively charged surface). They prepared polymersomes of PBd-b-PEG with a near infrared dye entrapped, and

compared them with polymersomes where a fraction of PBd-b-PAA was introduced to obtain a negative surface charge. After 24 hours they showed that polymersomes with negative surfaces predominantly accumulated in the liver. Liposomes often are covered with up to ten percent of PEG chains that induce stealth character. In general it is thought that the conformation of the surface PEG chains has an influence on the stealth effect. PEG chains can either adopt a mushroom conformation to cover the full surface or a fully stretched conformation depending on the available space. Smart *et al*.[120] studied these conformations for polymersomes both theoretically and experimentally. For polymersomes it is not so straightforward to reduce the number of PEG chains in the corona. Often PEG is a part of the block copolymer, covalently linked to the hydrophobic block and needed to form and stabilize the polymersome in solution. By the introduction of a hydrazone bond between PS and PEG (PS-Hz-PEG) He *et al*.[121] showed that polymersomes constructed of this polymer were able to shed off their PEG mantle by adjusting the pH. Brinkhuis *et al*.[122] (Chapter 6) used this concept on PBd-Hz-PEG vesicles and systematically mixed in a non-hydrolysable analogue. They showed that after vesicle formation the number of PEG chains could be reduced to five percent without losing colloidal stability. This is already an example where the surface structure is adapted, but more complex surface topologies have also been reported, involving domain formation.

In liposomes it is possible to create surface domains via micro-phase separation either assisted or not assisted by the addition of ions[123]. This domain formation was recently also described in polymersomes[124]. The effect of more complex surface topologies on cell interactions was shown by Battaglia *et al.*[125]. They were able to create domains within the polymersome surface by mixing different ratios of two triblock copolymers based on PMPC. They nicely showed how the ratio of polymers influenced the size and number of domains present in their polymersomes as depicted in Figure 16. Furthermore, this figure indicates how the cellular uptake is influenced by the surface topology and size of these patchy polymersomes, pointing out the importance of surface topology.

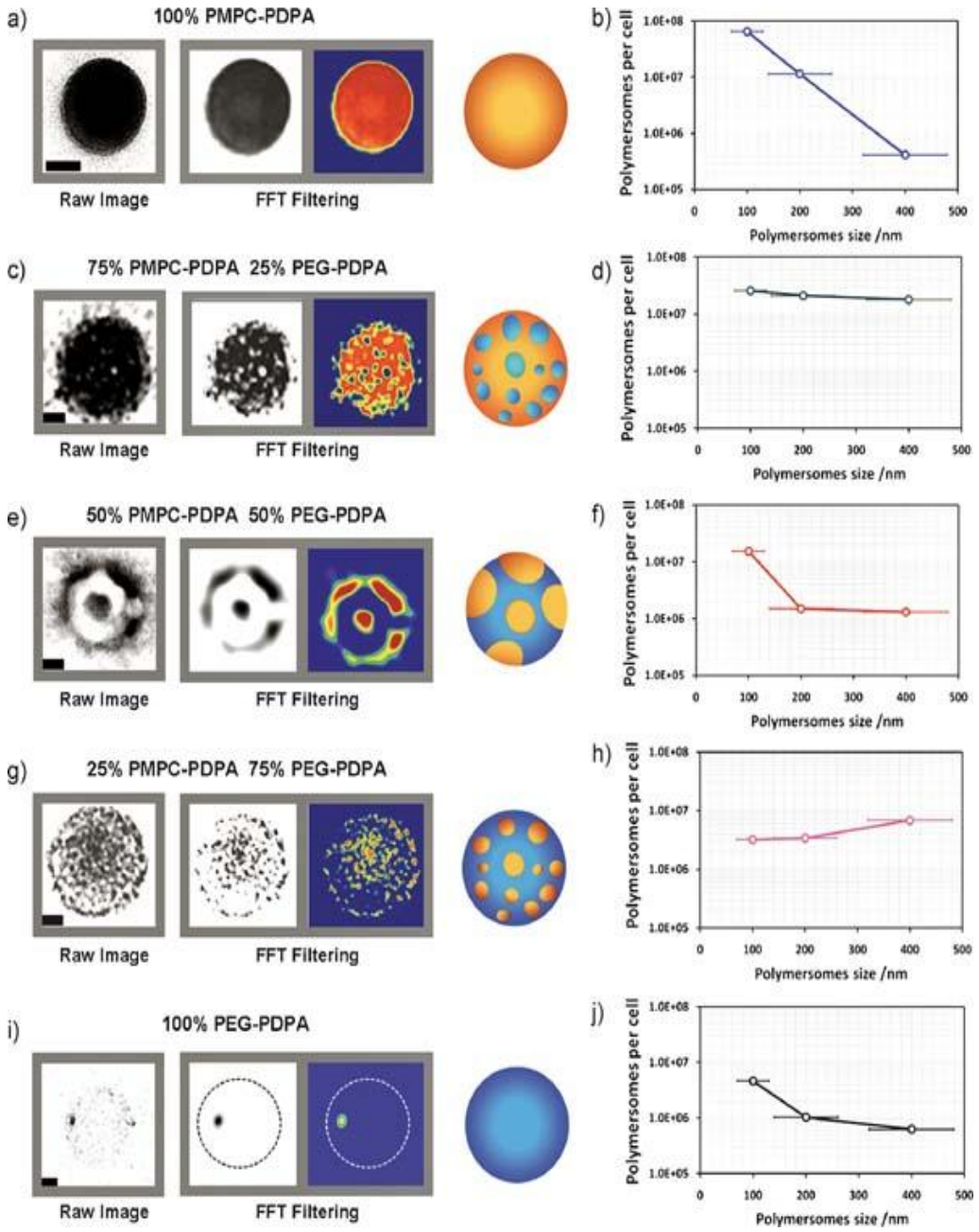

Figure 16. a)Effect of the ratio of PMPC-PDPA and PEG-PDPA on the domain size of patchy polymersomes. b) the number and size of domains influence the cell binding and uptake of patchy polymersomes[125]. Reprinted with permission (ref 125).

1.5.2 Surface functionalization

In many biomedical applications reported thus far, such as *in vivo* imaging, polymersomes have been used which contained a functional content, e.g. near infrared fluorescent dyes[53,119,126] and MRI contrast agents[115-116], but which did not have any surface functionality. In fact, they were mostly designed for prolonged *in vivo* circulation times, which means that they were predominantly PEGylated. However, for imaging and drug delivery it might be desirable to functionalize the

periphery with ligands or moieties that allow (specific) recognition. In principle two approaches can be followed for this purpose. In the first method the functional group is attached to the polymer prior to vesicle formation. One of the first examples of this approach was the preparation of a functionalized polymersome for cellular delivery via the conjugation of the cell penetrating peptide Tat to PBd-b-PEG. After the polymersomes were formed they showed good cellular uptake and were able to deliver a near infrared dye loaded polymersome to dendritic cells[126]. However this approach is not always trivial. If the functionality that needs to be introduced is too hydrophobic, the moiety might fold back in the membrane upon polymersome formation, reducing its availability. Furthermore, if bigger moieties need to be introduced, this will put quite some restrictions on the preparation methods and also the expected behaviour of the amphiphiles. Therefore researchers have also developed a second approach which entails post functionalization of polymersomes either via covalent or via strong non-covalent interactions, as recently reviewed by Meier and co-workers.[25]

In many cases non-covalent interactions are reversible and this can be useful, but also makes the system less robust. A non-covalent interaction that is almost as strong as a chemical bond is the interaction between biotin and streptavidin[127]. Hammer and co-workers[128] used polymersomes of PBD-B-PEG end-functionalized with biotin (actually biocytin) to study the adhesiveness of these polymersomes to streptavidin, both surface immobilized and free in solution. They showed that when biotin was attached to a longer PEG chain than the non-functionalized membrane polymers there was a difference in adhesive properties. When biotin sticks out of the membrane the adhesion to immobilized streptavidin increased whereas in solution no difference was found. The group of Meier published a series of papers where they used biotin-functional polymers to adhere polymersomes to streptavidin[129-130]. In one example[131] they used a double biotinylated triblock copolymer PMOXA-PDMS-PMOXA to adhere biotinylated ligands to the surface. In this case streptavidin with four binding sites fulfilled the function of effectively connecting the polymersome and targeting ligand. The fact that streptavidin has four binding sites also puts some restrictions on its applicability. If the concentration of streptavidin becomes too high crosslinking of polymersomes will become dominant and bigger aggregates will form. The interaction of cyclodextrin and adamantane is another example of a host-guest

pair that strongly interacts and of which one of the binding partners can be easily immobilized on the surface of a polymeric membrane[58,132]

An interesting, strong, metal ion complexation that is often used in protein science to purify proteins from a cell lysate is the nickel–NTA interaction with histidine-tags. The group of Meier showed two[133-134] examples where they immobilized the NTA ligand on the surface of PBD-B-PEG polymersomes. They demonstrated to be able to complex both green fluorescent protein (GFP) and bone morphogenetic protein (BMP) via their His-tags on the polymersome surface.

Functional moieties have also been attached covalently to premade polymersomes. However, there are some restrictions to the chemistry involved. In most cases polymersomes are formed and used in an aqueous environment, so the chemistry should be applicable in water and be selective. A recent report[135] on the immobilisation of polymersomes on a substrate exploited peripheral aldehydes to form an imine bond, which is in principle reversible. An irreversible bond that can be formed and is common in bio-conjugation techniques is the amide bond. Carboxylic acids present on the periphery of polymersomes were activated as NHS esters[33] which allowed the attachment of several proteins via available amine residues. Another coupling strategy adopted from bioconjugation is the use of the maleimide functionality. Maleimides readily react with thiols which can be made available in a controlled fashion in both peptides and proteins by the introduction of a cysteine residue. In this way Pang *et al*. [136] showed how they were able to couple mouse-anti-rat monoclonal antibodies for brain delivery in rats to the surface of polymersomes.

As depicted in Figure 17 Opsteen *et al.*[137] reported the use of the copper-catalysed (2+3) Huisgen cycloaddition to immobilise fluorescent dansyl, GFP and biotin on the surface of azide end-functional PS-PAA vesicles. PS-PAA was easily synthesised via ATRP and the introduction of the azide moiety was achieved by substitution of the bromine end group present after ATRP. However, not all block copolymers allow for easy modification. Therefore, van Dongen *et al*. [138] adopted a strategy in which they mixed in up to ten percent of an acetylene-functional PS-PEG in their PS-PIAT polymersomes. These so-called anchors allowed for the immobilisation of enzymes on the vesicle surface. In order to steer away from the toxic Cu catalyst, in recent years also strain-promoted copper-free click reactions

have been developed[139]. Other click strategies have also been adopted. Very recently Petersen *et al.*[140] introduced the vinyl sulfone moiety in polymersomes. This moiety also reacts fast and selective with thiols. They showed how via this method RGD peptides could be coupled on the periphery of their poly(methyl caprolactone)-b-PEG polymersomes.

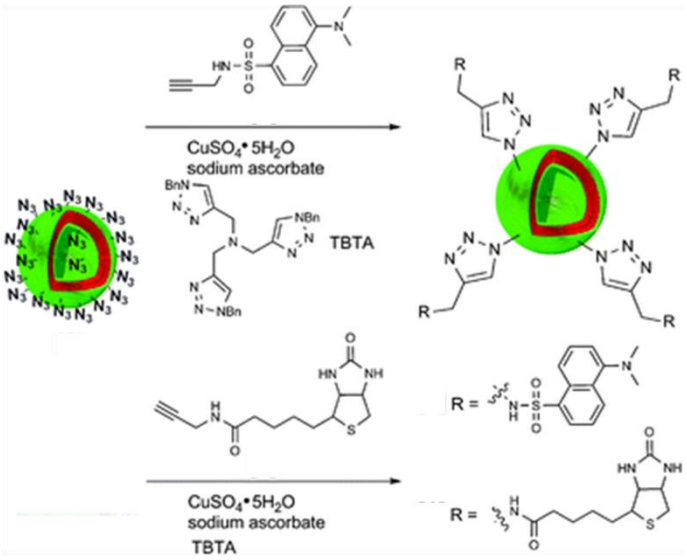

Figure 17. Surface functionalization of polymersomes assembled from PS-PAA-N_3 with molecular probes via click chemistry. The same methodology has been applied to immobilize proteins, e.g. green fluorescent protein[137]. Reprinted with permission (ref 137)

Besides the use of surface functionalization to improve drug delivery or *in vivo* imaging, it has been employed to improve on the cellular uptake of the polymersome nanoreactors as discussed in section 4.2.

A first report of such an artificial organelle inside a cell was provided by Ben-Haim *et al.*[141]. They showed how PMOXA-PDMS-PMOXA polymersomes functionalized with oligonucleotide polyguanylic acid (polyG) are efficiently recognized by macrophages and engulfed. A selection of other cell types did not show significant cell uptake, underlining the specificity for macrophages. After assessing the fate and distribution of the polymersomes inside the macrophages they loaded the newly constructed organelle with trypsin, an intestinal protease, and delivered it to the cell. As a traceable substrate they chose the hydrophobic tripeptide serine protease specific substrate BZiPAR (bis-(CBZ-Ile-Pro-Arg)-R110), which can diffuse passively through both cell membranes and the polymeric membrane. First they blocked the cell's own protease to prevent false positives. After the substrate reached the

polymersome loaded trypsin in the cell, the substrate was converted to release the coupled Rhodamine effectively making the cells fluorescent.

In a more recent example van Dongen, Verdurmen *et al.*[139] used the inherently semi-permeable polymersome based on PS-PIAT to construct an artificial organelle. They ligated the cell penetrating peptide Tat to the surface of their polymersomes to induce cellular uptake by HeLa cells. The enzyme horseradish peroxidase (HRP), which was encapsulated in the polymersome, subsequently catalysed the oxidation of compound 3,3',5,5'-tetramethylbenzidine (TMB) by hydrogen peroxide. The oxidation product of TMB was easily detected and showed good conversion inside the cell. This model reaction was used to demonstrate that the artificial organelle was capable of neutralizing oxidative species in a cellular environment.

1.6 Conclusion

Polymersomes are new versatile carriers that have high potential for *in vivo* imaging and nano therapeutics. Although quite different from liposomes general aspects known from liposomal science can be used to design polymersomes with specific functions. Control can be exerted over size, shape, surface function and topology, which will influence the *in vivo* circulation time and therefore the applicability of these nano-carriers. A large variety of examples can nowadays be found in literature that show how polymersome research has caught up with liposomal science in the past decade and in many cases adds extra dimensions to what is possible.

1.7 References

(1) Vanhest, J. C. M.; Delnoye, D. A. P.; Baars, M. W. P. L.; Vangenderen, M. H. P.; Meijer, E. W. *Science* **1995**, *268*, 1592.
(2) Fujita, K.; Kimura, S.; Imanishi, Y. *Langmuir* **1999**, *15*, 4377.
(3) Cornelissen, J. J. L. M.; Fischer, M.; Sommerdijk, N. A. J. M.; Nolte, R. J. M. *Science* **1998**, *280*, 1427.
(4) Zhang, L. F.; Yu, K.; Eisenberg, A. *Science* **1996**, *272*, 1777.
(5) Discher, B. M.; Won, Y. Y.; Ege, D. S.; Lee, J. C. M.; Bates, F. S.; Discher, D. E.; Hammer, D. A. *Science* **1999**, *284*, 1143.
(6) Ahmed, F.; Pakunlu, R. I.; Brannan, A.; Bates, F.; Minko, T.; Discher, D. E. *J Control Release* **2006**, *116*, 150.
(7) Discher, D.; Ahmed, F. *Abstr Pap Am Chem S* **2006**, *232*, 148.
(8) Discher, D. E.; Eisenberg, A. *Science* **2002**, *297*, 967.
(9) Du, J. Z.; O'Reilly, R. K. *Soft Matter* **2009**, *5*, 3544.
(10) Blanazs, A.; Armes, S. P.; Ryan, A. J. *Macromol Rapid Comm* **2009**, *30*, 267.
(11) Soo, P. L.; Eisenberg, A. *J Polym Sci Pol Phys* **2004**, *42*, 923.
(12) Kita-Tokarczyk, K.; Grumelard, J.; Haefele, T.; Meier, W. *Polymer* **2005**, *46*, 3540.

(13) Antonietti, M.; Forster, S. *Adv Mater* **2003**, *15*, 1323.

(14) Uneyama, T. *J Chem Phys* **2007**, *126*.

(15) He, X. H.; Schmid, F. *Macromolecules* **2006**, *39*, 2654.

(16) Du, J. Z.; Chen, Y. M. *Macromolecules* **2004**, *37*, 5710.

(17) Adams, D. J.; Adams, S.; Atkins, D.; Butler, M. F.; Furzeland, S. *J Control Release* **2008**, *128*, 165.

(18) Letchford, K.; Burt, H. *Eur J Pharm Biopharm* **2007**, *65*, 259.

(19) Rijcken, C. J. F.; Soga, O.; Hennink, W. E.; van Nostrum, C. F. *J Control Release* **2007**, *120*, 131.

(20) Onaca, O.; Enea, R.; Hughes, D. W.; Meier, W. *Macromol Biosci* **2009**, *9*, 129.

(21) Kim, K. T.; Meeuwissen, S. A.; Nolte, R. J. M.; van Hest, J. C. M. *Nanoscale* **2010**, *2*, 844.

(22) Discher, D. E.; Ortiz, V.; Srinivas, G.; Klein, M. L.; Kim, Y.; David, C. A.; Cai, S. S.; Photos, P.; Ahmed, F. *Prog Polym Sci* **2007**, *32*, 838.

(23) Schatz, C.; Lecommandoux, S. *Macromol Rapid Comm* **2010**, *31*, 1664.

(24) van Dongen, S. F. M.; de Hoog, H. P. M.; Peters, R. J. R. W.; Nallani, M.; Nolte, R. J. M.; van Hest, J. C. M. *Chem Rev* **2009**, *109*, 6212.

(25) Egli, S.; Schlaad, H.; Briuns, N.; Meier, W. *Polymers* **2011**, *3*, 28.

(26) Opsteen, J. A.; Cornelissen, J. J. L. M.; van Hest, J. C. M. *Pure Appl Chem* **2004**, *76*, 1309.

(27) Duncan, R. *Nat Rev Drug Discov* **2003**, *2*, 347.

(28) Satchi-Fainaro, R.; Duncan, R.; Barnes, C. M. *Polymer Therapeutics Ii: Polymers as Drugs, Conjugates and Gene Delivery Systems* **2006**, *193*, 1.

(29) Klibanov, A. L.; Maruyama, K.; Torchilin, V. P.; Huang, L. *Febs Lett* **1990**, *268*, 235.

(30) Woodle, M. C. *Chem Phys Lipids* **1993**, *64*, 249.

(31) Ahmed, F.; Hategan, A.; Discher, D. E.; Discher, B. M. *Langmuir* **2003**, *19*, 6505.

(32) Ahmed, F.; Pakunlu, R. I.; Srinivas, G.; Brannan, A.; Bates, F.; Klein, M. L.; Minko, T.; Discher, D. E. *Mol Pharmaceut* **2006**, *3*, 340.

(33) Meng, F. H.; Engbers, G. H. M.; Feijen, J. *J Control Release* **2005**, *101*, 187.

(34) Meng, F. H.; Hiemstra, C.; Engbers, G. H. M.; Feijen, J. *Macromolecules* **2003**, *36*, 3004.

(35) Choucair, A.; Lavigueur, C.; Eisenberg, A. *Langmuir* **2004**, *20*, 3894.

(36) Du, J. Z.; Armes, S. P. *J Am Chem Soc* **2005**, *127*, 12800.

(37) Lomas, H.; Du, J. Z.; Canton, I.; Madsen, J.; Warren, N.; Armes, S. P.; Lewis, A. L.; Battaglia, G. *Macromol Biosci* **2010**, *10*, 513.

(38) Lomas, H.; Canton, I.; MacNeil, S.; Du, J.; Armes, S. P.; Ryan, A. J.; Lewis, A. L.; Battaglia, G. *Adv Mater* **2007**, *19*, 4238.

(39) Vriezema, D. M.; Hoogboom, J.; Velonia, K.; Takazawa, K.; Christianen, P. C. M.; Maan, J. C.; Rowan, A. E.; Nolte, R. J. M. *Angew Chem Int Edit* **2003**, *42*, 772.

(40) Bellomo, E. G.; Wyrsta, M. D.; Pakstis, L.; Pochan, D. J.; Deming, T. J. *Nat Mater* **2004**, *3*, 244.

(41) Kimura, S.; Kim, D. H.; Sugiyama, J.; Imanishi, Y. *Langmuir* **1999**, *15*, 4461.

(42) Kimura, S.; Muraji, Y.; Sugiyama, J.; Fujita, K.; Imanishi, Y. *J Colloid Interf Sci* **2000**, *222*, 265.

(43) Dirks, A. J. T.; van Berkel, S. S.; Hatzakis, N. S.; Opsteen, J. A.; van Delft, F. L.; Cornelissen, J. J. L. M.; Rowan, A. E.; van Hest, J. C. M.; Rutjes, F. P. J. T.; Nolte, R. J. M. *Chem Commun* **2005**, 4172.

(44) Deming, T. J. *Nature* **1997**, *390*, 386.

(45) Deming, T. J. *Adv Polym Sci* **2006**, *202*, 1.

(46) Checot, F.; Lecommandoux, S.; Gnanou, Y.; Klok, H. A. *Angew Chem Int Edit* **2002**, *41*, 1339.

(47) Kukula, H.; Schlaad, H.; Antonietti, M.; Forster, S. *J Am Chem Soc* **2002**, *124*, 1658.

(48) Checot, F.; Lecommandoux, S.; Klok, H. A.; Gnanou, Y. *Eur Phys J E* **2003**, *10*, 25.

(49) Checot, F.; Brulet, A.; Oberdisse, J.; Gnanou, Y.; Mondain-Monval, O.; Lecommandoux, S. *Langmuir* **2005**, *21*, 4308.
(50) Gebhardt, K. E.; Ahn, S.; Venkatachalam, G.; Savin, D. A. *J Colloid Interf Sci* **2008**, *317*, 70.
(51) Holowka, E. P.; Pochan, D. J.; Deming, T. J. *J Am Chem Soc* **2005**, *127*, 12423.
(52) Gaspard, J.; Silas, J. A.; Shantz, D. F.; Jan, J. S. *Supramol Chem* **2010**, *22*, 178.
(53) Tanisaka, H.; Kizaka-Kondoh, S.; Makino, A.; Tanaka, S.; Hiraoka, M.; Kimura, S. *Bioconjugate Chem* **2008**, *19*, 109.
(54) Schatz, C.; Louguet, S.; Le Meins, J. F.; Lecommandoux, S. *Angew Chem Int Edit* **2009**, *48*, 2572.
(55) Lundquist, J. J.; Toone, E. J. *Chem Rev* **2002**, *102*, 555.
(56) Seeberger, P. H.; Werz, D. B. *Nature* **2007**, *446*, 1046.
(57) Kim, B. S.; Yang, W. Y.; Ryu, J. H.; Yoo, Y. S.; Lee, M. *Chem Commun* **2005**, 2035.
(58) Felici, M.; Marza-Perez, M.; Hatzakis, N. S.; Nolte, R. J. M.; Feiters, M. C. *Chem-Eur J* **2008**, *14*, 9914.
(59) Upadhyay, K. K.; Le Meins, J. F.; Misra, A.; Voisin, P.; Bouchaud, V.; Ibarboure, E.; Schatz, C.; Lecommandoux, S. *Biomacromolecules* **2009**, *10*, 2802.
(60) Misra, A.; Upadhyay, K. K.; Bhatt, A. N.; Mishra, A. K.; Dwarakanath, B. S.; Jain, S.; Schatz, C.; Le Meins, J. F.; Farooque, A.; Chandraiah, G.; Jain, A. K.; Lecommandoux, S. *Biomaterials* **2010**, *31*, 2882.
(61) Mishra, A. K.; Upadhyay, K. K.; Bhatt, A. N.; Castro, E.; Chuttani, K.; Dwarakanath, B. S.; Schatz, C.; Le Meins, J. F.; Misra, A.; Lecommandoux, S. *Macromol Biosci* **2010**, *10*, 503.
(62) Lecommandoux, S.; Upadhyay, K. K.; Le Meins, J. F.; Misra, A.; Voisin, P.; Bouchaud, V.; Ibarboure, E.; Schatz, C. *Biomacromolecules* **2009**, *10*, 2802.
(63) Otsuka, I.; Fuchise, K.; Halila, S.; Fort, S.; Aissou, K.; Pignot-Paintrand, I.; Chen, Y. G.; Narumi, A.; Kakuchi, T.; Borsali, R. *Langmuir* **2010**, *26*, 2325.
(64) Iatrou, H.; Frielinghaus, H.; Hanski, S.; Ferderigos, N.; Ruokolainen, J.; Ikkala, O.; Richter, D.; Mays, J.; Hadjichristidis, N. *Biomacromolecules* **2007**, *8*, 2173.
(65) Percec, V.; Wilson, D. A.; Leowanawat, P.; Wilson, C. J.; Hughes, A. D.; Kaucher, M. S.; Hammer, D. A.; Levine, D. H.; Kim, A. J.; Bates, F. S.; Davis, K. P.; Lodge, T. P.; Klein, M. L.; DeVane, R. H.; Aqad, E.; Rosen, B. M.; Argintaru, A. O.; Sienkowska, M. J.; Rissanen, K.; Nummelin, S.; Ropponen, J. *Science* **2010**, *328*, 1009.
(66) Harada, A.; Nakanishi, K.; Ichimura, S.; Kojima, C.; Kono, K. *J Polym Sci Pol Chem* **2009**, *47*, 1217.
(67) McKenna, B. J.; Birkedal, H.; Bartl, M. H.; Deming, T. J.; Stucky, G. D. *Angew Chem Int Edit* **2004**, *43*, 5652.
(68) Koide, A.; Kishimura, A.; Osada, K.; Jang, W. D.; Yamasaki, Y.; Kataoka, K. *J Am Chem Soc* **2006**, *128*, 5988.
(69) Guo, B.; Shi, Z. Q.; Yao, Y.; Zhou, Y. F.; Yan, D. Y. *Langmuir* **2009**, *25*, 6622.
(70) Kishimura, A.; Liamsuwan, S.; Matsuda, H.; Dong, W. F.; Osada, K.; Yamasaki, Y.; Kataoka, K. *Soft Matter* **2009**, *5*, 529.
(71) Kishimura, A.; Koide, A.; Osada, K.; Yamasaki, Y.; Kataoka, K. *Angew Chem Int Edit* **2007**, *46*, 6085.
(72) Thibault, R. J.; Uzun, O.; Hong, R.; Rotello, V. M. *Adv Mater* **2006**, *18*, 2179.
(73) Thibault, R. J.; Hotchkiss, P. J.; Gray, M.; Rotello, V. M. *J Am Chem Soc* **2003**, *125*, 11249.
(74) Thibault, R. J.; Galow, T. H.; Turnberg, E. J.; Gray, M.; Hotchkiss, P. J.; Rotello, V. M. *J Am Chem Soc* **2002**, *124*, 15249.
(75) Caruso, F.; Trau, D.; Mohwald, H.; Renneberg, R. *Langmuir* **2000**, *16*, 1485.
(76) Harashima, H.; Kiwada, H. *Adv Drug Deliver Rev* **1996**, *19*, 425.
(77) Nagayasu, A.; Uchiyama, K.; Kiwada, H. *Adv Drug Deliver Rev* **1999**, *40*, 75.
(78) Photos, P. J.; Bacakova, L.; Discher, B.; Bates, F. S.; Discher, D. E. *J Control Release* **2003**, *90*, 323.
(79) Lee, J. C. M.; Bermudez, H.; Discher, B. M.; Sheehan, M. A.; Won, Y. Y.; Bates, F. S.; Discher, D. E. *Biotechnol Bioeng* **2001**, *73*, 135.
(80) Lam, J.; Ma, Y.; Armes, S.; Lewis, A.; Stolnik, S. *J Pharm Pharmacol* **2004**, *56*, S70.
(81) Woodle, M. C.; Engbers, C. M.; Zalipsky, S. *Bioconjugate Chem* **1994**, *5*, 493.

(82) Litzinger, D. C.; Buiting, A. M. J.; Vanrooijen, N.; Huang, L. *Bba-Biomembranes* **1994**, *1190*, 99.
(83) Drummond, D. C.; Meyer, O.; Hong, K. L.; Kirpotin, D. B.; Papahadjopoulos, D. *Pharmacol Rev* **1999**, *51*, 691.
(84) Wang, W.; McConaghy, A. M.; Tetley, L.; Uchegbu, I. F. *Langmuir* **2001**, *17*, 631.
(85) Howse, J. R.; Jones, R. A. L.; Battaglia, G.; Ducker, R. E.; Leggett, G. J.; Ryan, A. J. *Nat Mater* **2009**, *8*, 507.
(86) Luo, L. B.; Eisenberg, A. *Langmuir* **2001**, *17*, 6804.
(87) Sanson, C.; Schatz, C.; Le Meins, J. F.; Brulet, A.; Soum, A.; Lecommandoux, S. *Langmuir* **2010**, *26*, 2751.
(88) Shen, H. W.; Eisenberg, A. *J Phys Chem B* **1999**, *103*, 9473.
(89) Li, X. F.; Kroeger, A.; Azzam, T.; Eisenberg, A. *Langmuir* **2008**, *24*, 2705.
(90) Huang, J. B.; Zhu, Y.; Zhu, B. Y.; Li, R. K.; Fu, H. I. *J Colloid Interf Sci* **2001**, *236*, 201.
(91) Rameez, S.; Bamba, I.; Palmer, A. F. *Langmuir* **2010**, *26*, 5279.
(92) Yu, S. Y.; Azzam, T.; Rouiller, I.; Eisenberg, A. *J Am Chem Soc* **2009**, *131*, 10557.
(93) Li, X. J.; Pivkin, I. V.; Liang, H. J.; Karniadakis, G. E. *Macromolecules* **2009**, *42*, 3195.
(94) Geng, Y.; Dalhaimer, P.; Cai, S. S.; Tsai, R.; Tewari, M.; Minko, T.; Discher, D. E. *Nat Nanotechnol* **2007**, *2*, 249.
(95) Zhu, J. T.; Jiang, W. *Macromolecules* **2005**, *38*, 9315.
(96) Geng, Y.; Discher, D. E. *J Am Chem Soc* **2005**, *127*, 12780.
(97) Kim, Y.; Dalhaimer, P.; Christian, D. A.; Discher, D. E. *Nanotechnology* **2005**, *16*, S484.
(98) Yang, X. Q.; Grailer, J. J.; Rowland, I. J.; Javadi, A.; Hurley, S. A.; Steeber, D. A.; Gong, S. Q. *Biomaterials* **2010**, *31*, 9065.
(99) Napoli, A.; Valentini, M.; Tirelli, N.; Muller, M.; Hubbell, J. A. *Nat Mater* **2004**, *3*, 183.
(100) Lipowsky, R. *Nature* **1991**, *349*, 475.
(101) Yanagisawa, M.; Imai, M.; Taniguchi, T. *Phys Rev Lett* **2008**, *100*.
(102) Kim, K. T.; Zhu, J. H.; Meeuwissen, S. A.; Cornelissen, J. J. L. M.; Pochan, D. J.; Nolte, R. J. M.; van Hest, J. C. M. *J Am Chem Soc* **2010**, *132*, 12522.
(103) Kim, K. T.; Cornelissen, J. J. L. M.; Nolte, R. J. M.; van Hest, J. C. M. *J Am Chem Soc* **2009**, *131*, 13908.
(104) Rodriguez-Hernandez, J.; Lecommandoux, S. *J Am Chem Soc* **2005**, *127*, 2026.
(105) Smith, A. E.; Xu, X. W.; Kirkland-York, S. E.; Savin, D. A.; McCormick, C. L. *Macromolecules* **2010**, *43*, 1210.
(106) Butun, V.; Billingham, N. C.; Armes, S. P. *J Am Chem Soc* **1998**, *120*, 11818.
(107) Mabrouk, E.; Cuvelier, D.; Brochard-Wyart, F.; Nassoy, P.; Li, M. H. *P Natl Acad Sci USA* **2009**, *106*, 7294.
(108) Robbins, G. P.; Jimbo, M.; Swift, J.; Therien, M. J.; Hammer, D. A.; Dmochowski, I. J. *J Am Chem Soc* **2009**, *131*, 3872.
(109) van Dongen, S. F. M.; Nallani, M.; Cornelissen, J. L. L. M.; Nolte, R. J. M.; van Hest, J. C. M. *Chem-Eur J* **2009**, *15*, 1107.
(110) Ranquin, A.; Versees, W.; Meier, W.; Steyaert, J.; Van Gelder, P. *Nano Lett* **2005**, *5*, 2220.
(111) Kumar, M.; Grzelakowski, M.; Zilles, J.; Clark, M.; Meier, W. *P Natl Acad Sci USA* **2007**, *104*, 20719.
(112) Stoenescu, R.; Graff, A.; Meier, W. *Macromol Biosci* **2004**, *4*, 930.
(113) Graff, A.; Sauer, M.; Van Gelder, P.; Meier, W. *P Natl Acad Sci USA* **2002**, *99*, 5064.
(114) Choi, H. J.; Montemagno, C. D. *Nano Lett* **2005**, *5*, 2538.
(115) Cheng, Z. L.; Tsourkas, A. *Langmuir* **2008**, *24*, 8169.
(116) Cheng, Z. L.; Thorek, D. L. J.; Tsourkas, A. *Adv Funct Mater* **2009**, *19*, 3753.
(117) Kim, K. T.; Cornelissen, J. J. L. M.; Nolte, R. J. M.; van Hest, J. C. M. *Adv Mater* **2009**, *21*, 2787.
(118) Awasthi, V. D.; Garcia, D.; Klipper, R.; Goins, B. A.; Phillips, W. T. *J Pharmacol Exp Ther* **2004**, *309*, 241.
(119) Christian, D. A.; Garbuzenko, O. B.; Minko, T.; Discher, D. E. *Macromol Rapid Comm* **2010**, *31*, 135.
(120) Smart, T. P.; Mykhaylyk, O. O.; Ryan, A. J.; Battaglia, G. *Soft Matter* **2009**, *5*, 3607.
(121) He, L.; Jiang, Y.; Tu, C. L.; Li, G. L.; Zhu, B. S.; Jin, C. Y.; Zhu, Q.; Yan, D. Y.; Zhu, X. Y. *Chem Commun* **2010**, *46*, 7569.

(122) Brinkhuis, R. P.; Visser, T. R.; Rutjes, F. P. J. T.; Van Hest, J. C. M. *Polymer Chemistry* **201x**, *xx*, DOI: 10.1039/C0PY00316F

(123) Baumgart, T.; Hess, S. T.; Webb, W. W. *Nature* **2003**, *425*, 821.

(124) Christian, D. A.; Tian, A. W.; Ellenbroek, W. G.; Levental, I.; Rajagopal, K.; Janmey, P. A.; Liu, A. J.; Baumgart, T.; Discher, D. E. *Nat Mater* **2009**, *8*, 843.

(125) Massignani, M.; LoPresti, C.; Blanazs, A.; Madsen, J.; Armes, S. P.; Lewis, A. L.; Battaglia, G. *Small* **2009**, *5*, 2424.

(126) Christian, N. A.; Milone, M. C.; Ranka, S. S.; Li, G. Z.; Frail, P. R.; Davis, K. P.; Bates, F. S.; Therien, M. J.; Ghoroghchian, P. P.; June, C. H.; Hammer, D. A. *Bioconjugate Chem* **2007**, *18*, 31.

(127) Weber, P. C.; Ohlendorf, D. H.; Wendoloski, J. J.; Salemme, F. R. *Science* **1989**, *243*, 85.

(128) Lin, J. J.; Silas, J. A.; Bermudez, H.; Milam, V. T.; Bates, F. S.; Hammer, D. A. *Langmuir* **2004**, *20*, 5493.

(129) Grzelakowski, M.; Onaca, O.; Rigler, P.; Kumar, M.; Meier, W. *Small* **2009**, *5*, 2545.

(130) Rigler, P.; Meier, W. *J Am Chem Soc* **2006**, *128*, 367.

(131) Broz, P.; Benito, S. M.; Saw, C.; Burger, P.; Heider, H.; Pfisterer, M.; Marsch, S.; Meier, W.; Hunziker, P. *J Control Release* **2005**, *102*, 475.

(132) Guo, M. Y.; Jiang, M.; Zhang, G. Z. *Langmuir* **2008**, *24*, 10583.

(133) Nehring, R.; Palivan, C. G.; Casse, O.; Tanner, P.; Tuxen, J.; Meier, W. *Langmuir* **2009**, *25*, 1122.

(134) Nehring, R.; Palivan, C. G.; Moreno-Flores, S.; Mantion, A.; Tanner, P.; Toca-Herrera, J. L.; Thunemann, A.; Meier, W. *Soft Matter* **2010**, *6*, 2815.

(135) Domes, S.; Filiz, V.; Nitsche, J.; Fromsdorf, A.; Forster, S. *Langmuir* **2010**, *26*, 6927.

(136) Pang, Z. Q.; Lu, W.; Gao, H. L.; Hu, K. L.; Chen, J.; Zhang, C. L.; Gao, X. L.; Jiang, X. G.; Zhu, C. Q. *J Control Release* **2008**, *128*, 120.

(137) Opsteen, J. A.; Brinkhuis, R. P.; Teeuwen, R. L. M.; Lowik, D. W. P. M.; van Hest, J. C. M. *Chem Commun* **2007**, 3136.

(138) van Dongen, S. F. M.; Nallani, M.; Schoffelen, S.; Cornelissen, J. J. L. M.; Nolte, R. J. M.; van Hest, J. C. M. *Macromol Rapid Comm* **2008**, *29*, 321.

(139) van Dongen, S. F. M.; Verdurmen, W. P. R.; Peters, R. J. R. W.; Nolte, R. J. M.; Brock, R.; van Hest, J. C. M. *Angew Chem Int Edit* **2010**, *49*, 7213.

(140) Petersen, M. A.; Yin, L. G.; Kokkoli, E.; Hillmyer, M. A. *Polymer Chemistry* **2010**, *1*, 1281.

(141) Ben-Haim, N.; Broz, P.; Marsch, S.; Meier, W.; Hunziker, P. *Nano Lett* **2008**, *8*, 1368.

2

Functionalized Polymersomes Based on Poly-butadiene-b-poly(ethylene glycol)

In this chapter we describe the synthesis of block copolymers of polybutadiene-triazole-poly(ethylene glycol), which form the basis of Chapters 3, 4 and 5, via a copper catalyzed "click" approach. We introduce a variety of different end functionalities at the poly(ethylene glycol) block, while keeping the polybutadiene block constant. Secondly, we show in this chapter that polymersomes of polybutadiene-triazole-poly(ethylene glycol) are readily formed, and sized down, via either the solvent switch or rehydration method. The latter allows for straightforward loading of hydrophobic drugs in the membrane.

Finally, polymersomes were formed and tagged with a fluorescent dye and the cell penetrating Tat-peptide to illustrate the self assembly of polymeric vesicles and the surface functionalization with peptides. Bare polymersomes hardly showed binding to a monolayer of hCMEC/D3 cells, whereas polymersomes conjugated with Tat to the periphery showed good association with this cell line.

2.1 Introduction

Polymersomes, or polymeric vesicles, have large potential for use in biomedical applications[1] as was discussed in depth in Chapter 1. The basic building blocks of polymersomes are amphiphilic block copolymers[2]. In order to form a bilayer vesicular structure the hydrophilic block should constitute approximately 25 percent of the block copolymer amphiphile. For imaging and targeting applications, it is obligatory to introduce functional handles in the polymeric vesicles to attach tracers or targeting moieties[3]. Therefore a set of amphiphilic block copolymers is required with a variety of functionalities.

Throughout this thesis we chose to work with the amphiphilic block copolymer of 1,2-polybutadiene-*block*-poly(ethylene glycol) (PBd-b-PEG) to form polymeric vesicles. This choice was made mainly for three reasons. First of all, this block copolymer is generally considered to be biocompatible and has been reported to readily form polymersomes within a relatively large experimental window[4]. Secondly, the poly(ethylene glycol) block covering the periphery is known to introduce stealth characteristics and is therefore preventing all non-specific interactions with living cells and bio(macro)molecules[5]. Finally, 1,2-polybutadiene is a hydrophobic polymer with a glass transition temperature well below room temperature. Therefore the membrane forming the polymersome is relatively fluidic and dynamic in nature. This allows polymersomes to be resized to a desired average particle size by means of extrusion and ultrasound. A low glass transition temperature also allows polymersomes to be formed via rehydration in addition to the solvent switch method[6]. Formation of polymersomes via rehydration will yield relatively large polymersomes – which can be downsized - and is anticipated to allow the encapsulation of hydrophilic drugs in the lumen.

Synthetic approach

We chose to adopt a modular approach to synthesize block copolymers of PBd-b-PEG based on the copper catalyzed (2+3) cycloaddition[7] of azides and alkynes as depicted in Scheme 1. Both polymer blocks are connected via a triazole moiety, resulting in polybutadiene-*triazole*-poly(ethylene glycol). The main advantage of this approach is the possibility to synthesize a set of block copolymers with different end groups, starting from a single batch of polybutadiene. Thus only the poly(ethylene glycol) (PEG) block has to be modified in order to access end-functional or higher molecular weight

analogues. As shown in Scheme 1 we aimed for the synthesis of PBd_{66}-b-PEG_{22} in combination with a maleimide or amine functional PEG_{44} analogue.

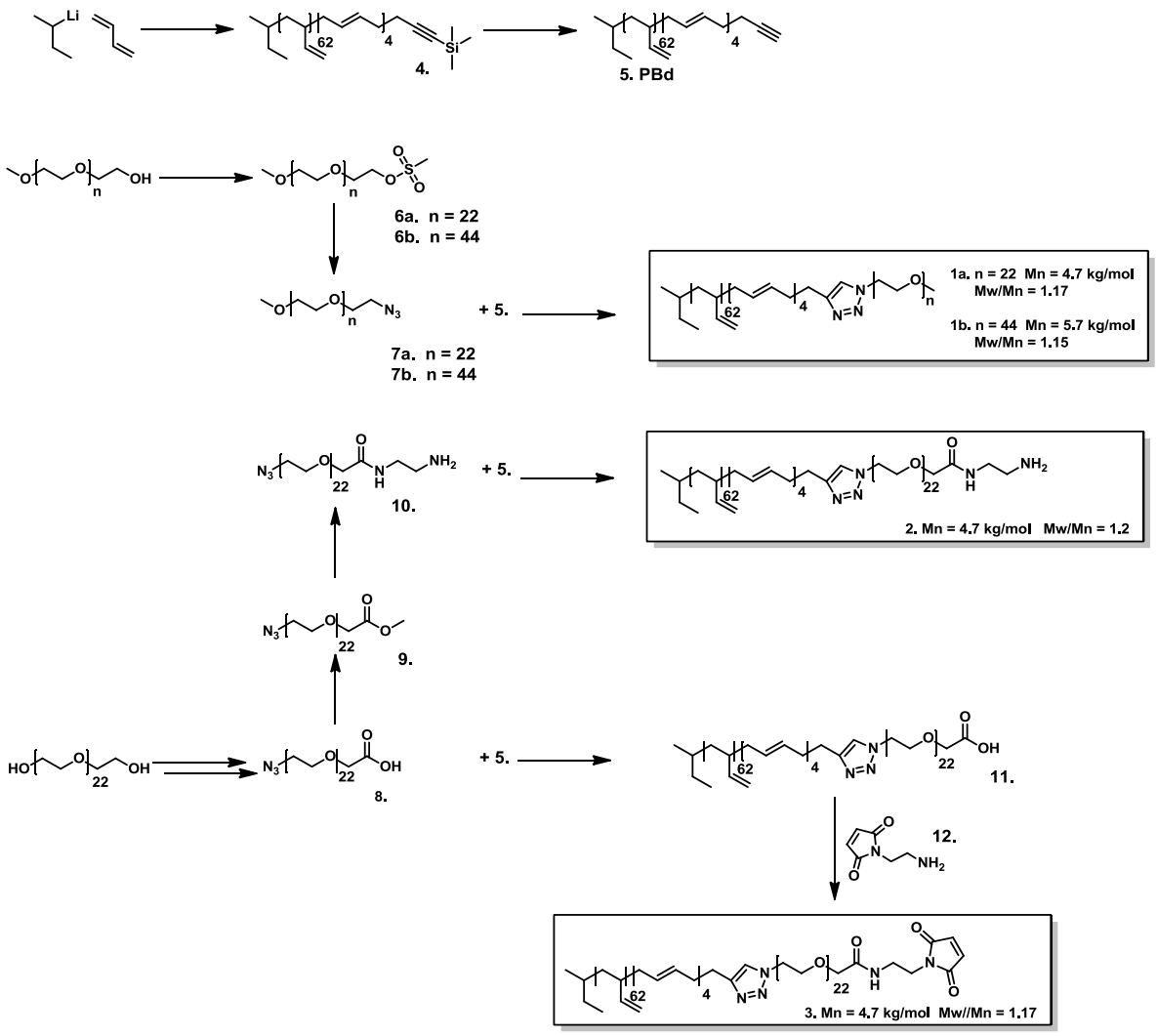

Scheme 1. Synthetic overview to amphiphilic block copolymers of PBd-b-PEG (**1**-**3**) with different end functionalities. Polymer **1** is inert and forms the basic building block for polymersome formation. Block copolymer **2** bears an amine end group to allow conjugation with isothiocyanate derivatives of e.g. fluorescein. Finally, polymer **3** is maleimide end-functionalized to allow for conjugation with cysteine containing peptides.

In this chapter we describe the synthesis of the amphiphilic block copolymer PBd-b-PEG, as well as the amine and maleimide end-functional analogues. We show that this block copolymer easily forms resizable polymersomes, either via the solvent switch method or via rehydration. Furthermore, we demonstrate that conjugation of peptides to the surface can be achieved and that in the case of Tat-peptides cell adhesion is induced. The experimental procedures also serve as an experimental platform for the biofunctional systems described in Chapters 3-5.

2.2 Results and Discussion

2.2.1 Block copolymer synthesis

Polybutadiene is synthesized via anionic polymerization of 1,3-butadiene[8]. The choice of solvent in the polymerization has a large influence on the reactivity of the monomers. Propagation in THF will mainly yield 1,2-polybutadiene, while propagation in e.g. hexane will yield mainly 1,4-polybutadiene as reported by Kalnin'sh and Panarin[9]. Since we chose to adopt a modular approach, we need to introduce a functional end-group. Three methods exist for the introduction of functional groups in anionic polymerizations as was summarized by Hirao and Hayashi[10]. One can either (i) start with a protected functional group as the initiator, (ii) polymerize monomers with a protected functional group, or the strategy we adopted (iii) terminate the living polymer with a protected functional group.

The polymerizations of 1,3-butadiene were straightforward and could be easily followed by the colour of the reaction mixture. After addition of butyllithium at -78 °C the colour changed from yellow to dark orange, and turned to pale yellow after all monomer was consumed. At that point, the polymerization was terminated with 1-(trimethylsilyl)propargyl bromide to obtain alkyne end-functional PBd. The product was analyzed by means of size exclusion chromatography (SEC) as depicted in Figure 1. The product showed a double molecular weight distribution which is a phenomenon previously observed and explained by Tohyama *et al.*[11] During termination fast halogen-metal exchange between the living polymer and terminating molecule occurs as a side reaction, after which the living polymer chain can react with the halogenated polymer chain via a S_N2' mechanism. The double molecular weight polymer therefore does not contain any functional group and is not reactive toward azides. Furthermore excess of PBd is easily removed via column chromatography after PBd-b-PEG is formed as shown in the SEC traces in Figures 1 and 2 for the formation of polymer **1a**.

Poly(ethylene glycol) is a frequently used hydrophilic polymer and commercially available in a variety of different lengths. We purchased poly(ethylene glycol) (PEG) with a molecular weight of 1 kg/mol and poly(ethylene glycol) monomethyl ether (mPEG) with molecular weights of 1 and 2 kg/mol. The synthesis of the mono-azide functionalized polymers **7a-b** proceeded straightforward using mesylation and

subsequent nucleophilic substitution by azides following previously reported procedures[12].

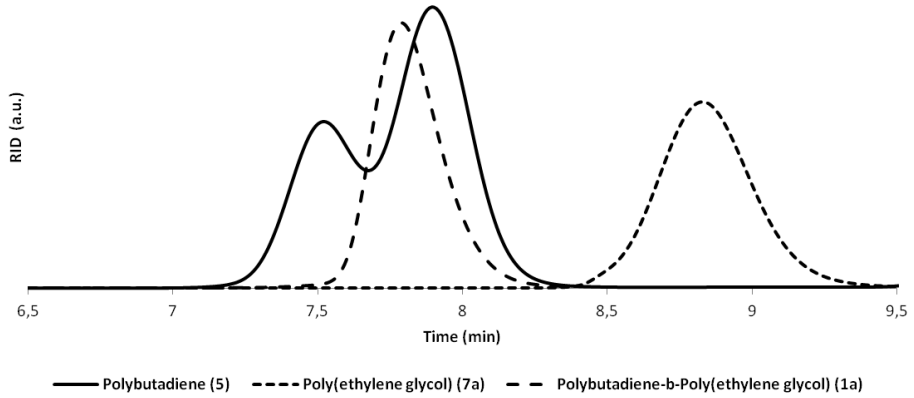

Figure 1. SEC traces for the synthesis of **1a** starting from polybutadiene (**5**) and PEG derivative **7a**. As can be seen polybutadiene shows a bimodal distribution after polymerization, which does however not interfere in the synthesis of **1a**

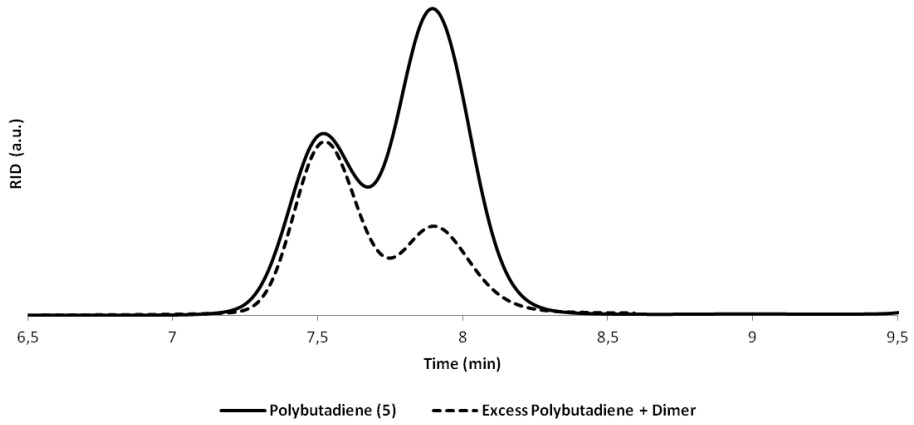

Figure 2. The non reactivity of the dimeric polybutadiene polymerization by-product was further illustrated by analyzing the silica column waste fraction (dashed line). It mainly contains the higher molecular weight polybutadiene, while the lower molecular weight polybutadiene in **5** (solid line) is consumed to form the desired block copolymers.

Starting from PEG with a molecular weight of 1 kg/mol we synthesized the hetero bifunctional derivative **8**, which formed the precursor for compounds **9** and **10**. First, an azide and carboxylic acid were introduced to obtain a statistical mixture of the diacid (25%), diazide (25%) and desired compound **8** (50%). The three products were separated on a silica column to isolate α-azido ω-carboxy poly(ethylene glycol) (**8)**. In the infrared spectrum of **8** (Figure 3), the presence of an azide is clearly visible as shown by the absorption around 2100 cm^{-1}. The carbonyl stretch of the carboxylic acid residue

shows an absorption around 1650 cm^{-1}. In addition, in the ^{1}H-NMR spectrum the two protons next to the azide (triplet at 3.39 ppm) and the two protons next to the carboxylic acid (singlet at 3.98 ppm) are clearly visible and integrate in a 2:2 ratio.

The amine functionality of **10** was introduced in a two step procedure. First, the methyl ester derivative **19** was formed, after which 1,2 diaminoethane was coupled via a nucleophilic acyl substitution. These two conversions were quantitative and can be visualized by analyzing the ^{1}H-NMR spectrum showing a clear shift of the singlet of the methylene group adjacent to the carbonyl.

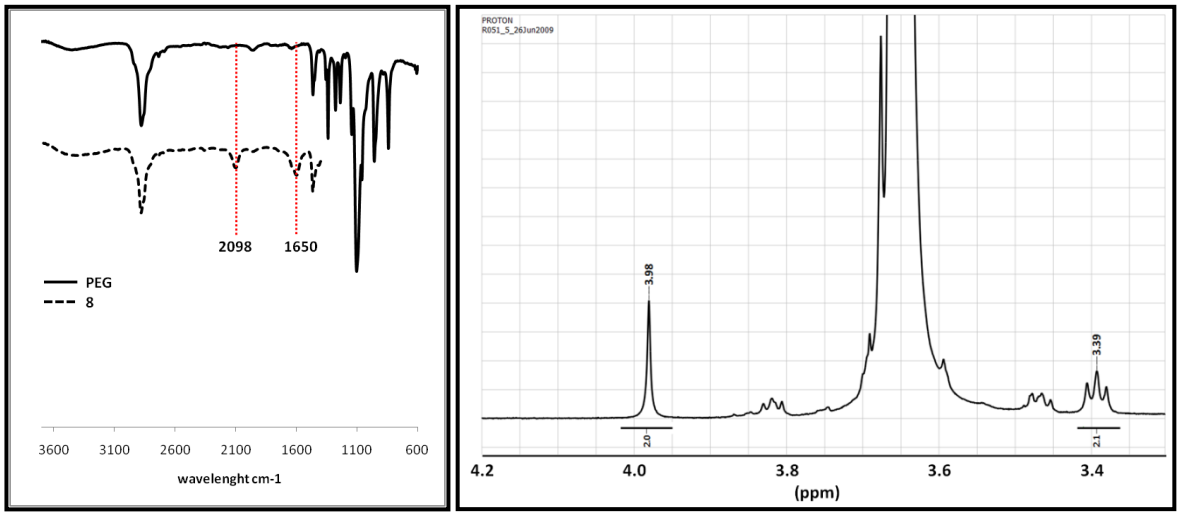

Figure 3. Left) Indicative infrared absorptions of **8** (dashed) compared to PEG (solid) PEG derivative **8** contains both an azide (2100 cm^{-1}) signal as well as the carbonyl stretch of the carboxylic acid (1650 cm^{-1}). Right) Indicative proton NMR shifts ($CDCl_3$) of **8** contains a triplet at 3.38 ppm originating from the methylene next to the azide moiety, a broad signal originating from the backbone and finally a singlet at 3.98 ppm originating from the methylene next to the carboxylic acid function.

The PBd and PEG blocks were coupled via the copper catalyzed azide/alkyne (3+2) cycloaddition, which is often referred to as "click reaction"[7]. The use of this click reaction to form block copolymers has been described in detail by Opsteen *et al.*[12-13] The reaction was performed under argon with a twofold excess of polybutadiene to ensure that all PEG was coupled to PBd. After the coupling reaction, the excess of PBd – along with the double molecular weight by-product - was removed via silica gel column chromatography. Eluting with dichloromethane, polymers **1, 2** and **11** had an R_f value of 0 compared to 1 for PBd (**5**). After the excess of PBd had been eluted, polymers **1, 2** and **11** were eluted with 8% methanol in dichloromethane. The SEC traces associated with the standard block copolymer **1a** are shown in Figures 1 and 2.

Via this methodology three types of block copolymers were obtained. One without a functional handle (**1a-b**), which served as a basic building block for polymersome formation, a second one with an amine end function (**2**) allowing for fast labelling with isothiocyanate probes to visualize polymersomes. Finally, a carboxylic acid end functional block copolymer (**11**) was synthesized. Next, polymer **11** was coupled to maleimide derivative **12**[14] via a carbodiimide mediated coupling to obtain the maleimide end functional block copolymer **3**. This maleimide functional polymer served as scaffold to conjugate peptides, enzymes and antibodies to the polymersome periphery by means of thiol-maleimide coupling[15].

2.2.2 Polymersome formation and functionalization

Polymersomes have been reported to form in a variety of ways. Of all reported methods, the solvent switch method (and variations thereof) and the rehydration method are most often applied[6]. In the solvent switch method the amphiphilic block copolymer is dissolved in a solvent suitable for both blocks, after which aggregation is induced by dilution of the polymer solution with a poor solvent for one of the blocks, in most cases an aqueous buffer. The rehydration method generally yields relatively large polymersomes of up to several micrometers. In this technique first a thin, thoroughly dried block copolymer film is formed by coating a block copolymer solution onto a glass or Teflon substrate. Polymeric vesicles are formed by rehydrating the film in aqueous buffer, which allows polymeric vesicles to bubble off the polymer film into the solution.

First the rehydration method was used to form polymersomes of polymer **1a** without any additional surface functionalities. To visualize the polymersome membrane, 0.01 weight% of the hydrophobic and fluorescent dye Nile-Red was dissolved in 1 mL chloroform along with 1 mg of polymer **1a**. While fast rotating the chloroform was removed under reduced pressure to obtain a thin polymer film on the inside of a glass vial, which was dried thoroughly for an additional hour under reduced pressure (5 mbar). Polymeric vesicles were formed by the addition of 3 mL THF:MilliQ (1:3), while the sample was rotated at atmospheric pressure. After 15 minutes the THF was removed to obtain polymersomes in MilliQ. The membranes of the vesicles were visualized by means of confocal laser scanning microscopy (CLSM) as depicted in Figure 4.

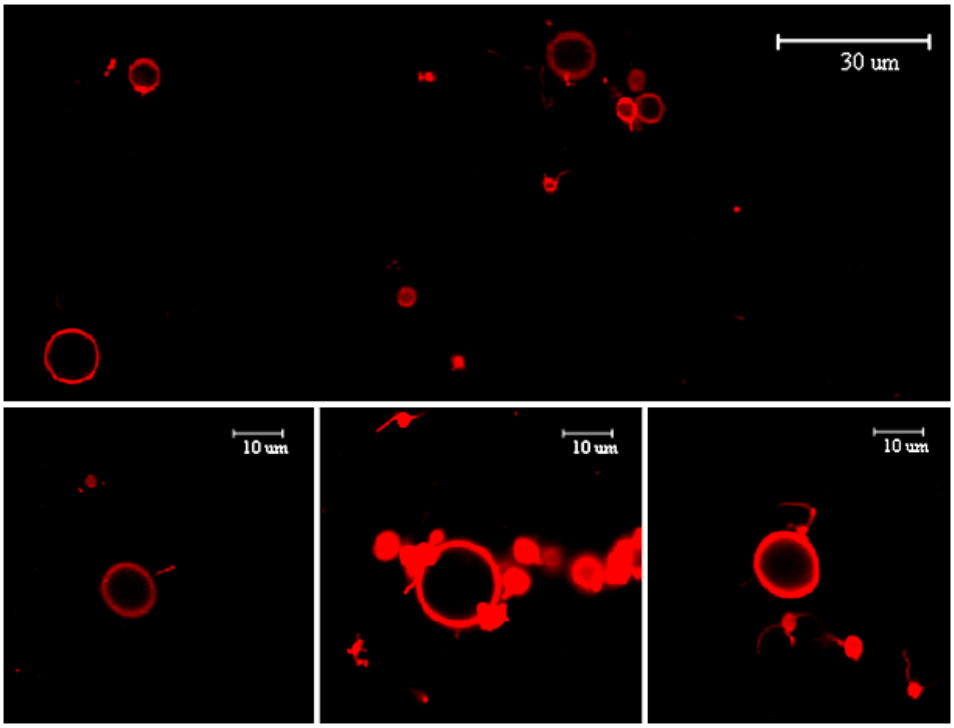

Figure 4. Several CLSM pictures of giant polymersomes prepared via the rehydration method. The membrane was loaded with 1 w% of the hydrophobic fluorescent dye Nile-Red.

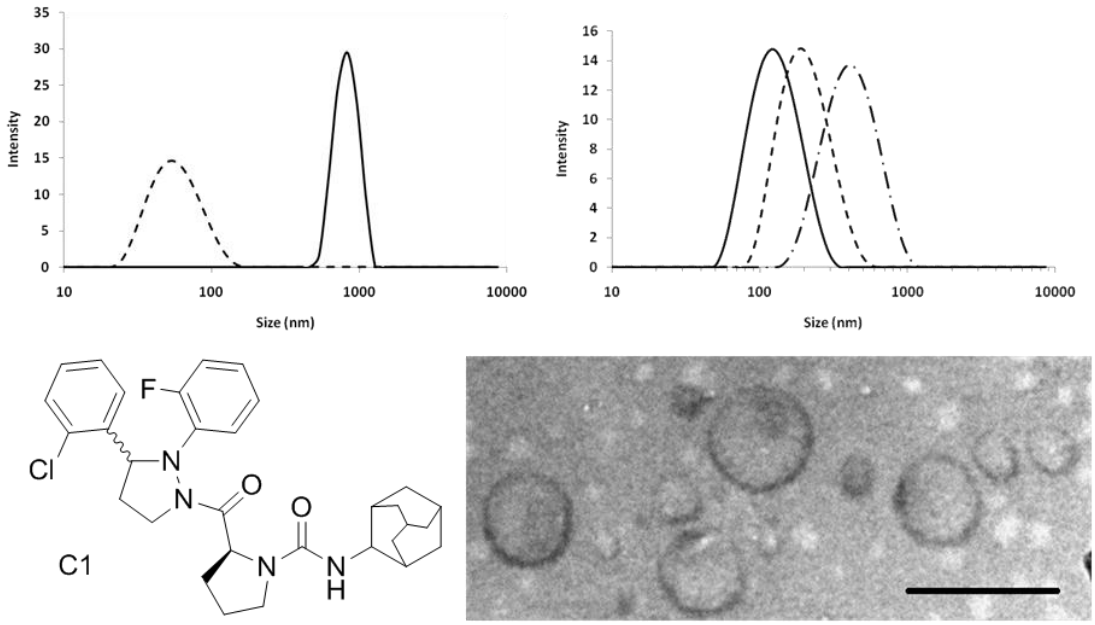

Figure 5. Top left) DLS results of polymersomes formed via rehydration with the drug C1 encapsulated both before (solid) and after (dashed) the sample was resized by ultrasound treatment. Top right) DLS analysis of polymersomes formed via the solvent switch method (long dashed), which were downsized by means of extrusion; 200 nm (dash-dotted) and 100 nm (solid). Bottom left) molecular structure of hydrophobic model drug C1. Bottom right) TEM image of a dried polymersome sample formed via solvent switch of **1a** and extruded through 200 nm membranes (bar is 200 nm).

Analogous to the encapsulation of Nile-Red, we also encapsulated 1 w% of the hydrophobic model drug C1 in the membrane (Figure 5). The polymersome size distribution was analyzed directly after rehydration by means of dynamic light scattering (DLS) as depicted in Figure 5. Since for most biomedical applications vesicles in the micrometer size regime are too large, we reduced the size of these drug loaded vesicles by treating them with ultrasound, prior to removal of THF. The resulting vesicles showed a particle size distribution around 90 nm. The encapsulation efficiency of C1 was 90 percent and stable for at least 5 days as was measured by means of HPLC analogous to the procedure reported by van Rooy *et al*.[16] for this compound.

Intrinsically smaller polymeric vesicles were obtained upon forming polymersomes via the solvent switch method as was deduced from the DLS measurements depicted in Figure 5 (right panel). Polymersomes were formed by dissolving 10 mg of polymer **1a** in 1 mL THF, after which 3 mL of MilliQ was added slowly to form the polymersomes. The initial size was around 500 nm and was downsized to 200 and 100 nm by means of extrusion through membranes with predefined sizes as depicted in Figure 5. Transmission electron microscope (TEM) pictures were obtained from the 200 nm samples (Figure 5, bottom) and showed polymersomes characterized by a single membrane of approximately 12-18 nm[17].

2.2.3 Surface functionalization and cell adhesion

In the preceding paragraphs, the synthesis of polymers and the methods to form polymersomes were described and illustrated. All polymersome samples described thus far, however, did not contain any functionalities coupled to the periphery. As noted in the first section, we chose PEG as the hydrophilic polymer since it is known to prevent all interactions with the environment. Therefore polymersomes consisting of polymers **1a-b** were not expected to show any interactions both *in vitro* and *in vivo*. In order to induce (specific) interactions of polymersomes the periphery should be functionalized with a suitable ligand.

To illustrate that interactions with living cells can be induced *in vitro*, we prepared a set of polymersomes according to the solvent switch procedure. This time, however, we partially labelled the amine end functional polymer **2** with fluorescein isothiocyanate (FITC) and mixed it in for 10 percent. The maleimide end functional polymer **3** was also mixed in for 10 percent, so that the standard polymer **1a** made up 80 percent of the

polymer (10 mg polymer in total in 1 mL of THF). Polymersomes were formed by the addition of 3 mL phosphate buffered saline (1xPBS) and extruded through a 200 nm membrane to obtain polymersomes of 200 nm and a PDI of 0.12. The remainder of THF was removed by running the sample over a Sephadex G200 column after which the combined opaque polymersome fractions were diluted to 10 mL (1 mg polymer/mL PBS).

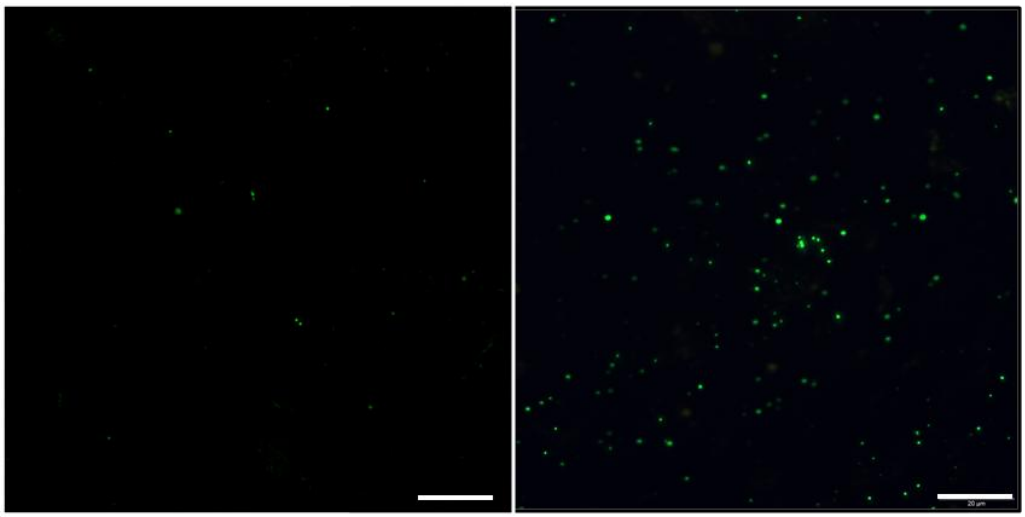

Figure 6. CLSM images of a monolayer of hCMEC/D3 cells, incubated with fluorescent polymersomes (bar is 20 μm). Polymeric vesicles which are not functionalized with peptides only show limited association with the cell monolayer (left), whereas polymersomes with Tat-peptide on the surface show high association with these cells.

Tat-peptide[18] was synthesized by standard Fmoc chemistry[19] with an additional cysteine added to the C-terminus to allow conjugation to the peripheral maleimide of polymersomes. To reduce possible Cys-Cys dimmers of the peptide, 1 mg of peptide (excess) was dissolved in 0.25 mL PBS together with 0.5 mg of (tris(2-carboxyethyl)phosphine (TCEP). After 15 minutes the peptide solution was added to 1.5 mL of the polymersome solution and allowed to couple for 1 hour. The excess of TCEP and Tat-peptide were removed by dialysis against PBS for 24 hours, after which both the polymersomes without and with Tat-peptide were separately added to the medium of a monolayer of hCMEC/D3[20] cells grown on a transwell filter (for details on this specific cell type and assay, see Chapter 4). The cells were fixed and visualized by CLSM, selectively exciting the fluorescein label on the polymersomes. Comparison of the fluorescent images (Figure 6) shows that the polymersomes without any targeting moiety do not interact with the cell layer, whereas the Tat-functionalized polymersomes

strongly interact with the cells. This experiment therefore clearly demonstrates that polymersomes of **1** indeed display stealth characteristics toward these cells and that the chemistry developed in this chapter allows for labelling of polymersomes with fluorescent markers and peptides.

2.3 Conclusion

In this chapter we have shown the modular synthesis of the amphipilic block copolymer of PBd-b-PEG (**1a-b**) along with its amine (**2**) and maleimide (**3**) analogues. These polymers readily formed polymersomes via rehydration techniques and allowed the encapsulation of the hydrophobic dye Nile-Red and the hydrophobic drug C1 in the membrane. The drug loaded polymersomes could be resized by ultrasound treatment to 90 nm with a PDI of 0.15. Intrinsically smaller polymersomes were formed via the solvent switch method and sized down by extrusion. Upon mixing in 10 percent of fluorescently labelled polymer **2** and 10 percent of maleimide functional polymer **3** we were able to visualize polymersomes by CLSM and conjugate the cell penetrating Tat-peptide to the periphery. Polymersomes without Tat-peptide showed limited association with a monolayer of hCMEC/D3 cells, while Tat-polymersomes showed a strong association with the cells. Thus, we showed that we gained access to PBd-b-PEG block copolymers and were able to form polymersomes with controlled size, membrane loading and surface functionalization forming an experimental platform for the polymersomes and experiments described in Chapters 3-5.

2.4 Acknowledgements

The work described in this chapter has been carried out jointly with several Bachelor's and Master's students, who are greatly acknowledged for their input. Without the efforts of Berry Bögels, Kelly van Helden, Sanne Bakker, Sander Dik, Jos Eilander and Ruoyu Xing this platform chemistry would not have been developed.

2.5 Experimental Procedures

General Notes Compound **12** was synthesized according to the literature procedure published by van der Venken *et al*.[14]

Materials Sec-butyllithium (ALDRICH 1.4M in hexane), tetrabutylammonium fluoride (TBAF) (ALDRICH, 1.0M in THF), sodium hydride (ALDRICH, 60% dispersion in mineral oil, Chelex resin (ALDRICH), were used as received. Tetrahydrofuran (THF) (ACROS ORGANICS, 99+% extra pure, stabilized with BHT) was distilled under argon from sodium/benzophenone, and triethyl amine (TEA) (BAKER) was distilled from calcium hydride under an argon atmosphere prior to use. Polymersome extrusions were performed using 200 nm filters (Acrodisc 13 mm Syringe Filter, 0.2 μm Nylon membrane) and 0.1 μm PC membrane (WHATMAN). Column chromatography was carried out using silica gel (Acros, 0.035-0.070 mm, pore diameter ca. 6 nm)) Note that silica gel from other suppliers gave less satisfactory results for α- azido ω- carboxy poly(ethylene glycol).

Instrumentation Infrared (IR) spectra were obtained using a Thermo Matson IR 300 FTIR spectrometer. Data are presented as the frequency of absorption (cm^{-1}). Proton nuclear magnetic resonance (^{1}H NMR) spectra were recorded on a Varian Unity Inova 400 FTNMR spectrometer. Chemical shifts are expressed in parts per million (δ scale) relative to the internal standard tetramethylsilane (δ=0.00 ppm). Molecular weight distributions were measured using size exclusion chromatography (SEC) on a Shimadzu (CTO-20A) system equipped with a guard column and a PL gel 5 μm mixed D column (Polymer Laboratories) with differential refractive index and UV (λ=254 nm and λ=345nm) detection, using tetrahydrofuran (SIGMA ALDRICH chromasolv 99.9%) as an eluent at 1 mL/min and T = 35 °C. Particle size distributions were measured on a Malvern instruments Zetasizer Nano-S.

Polybutadiene-block-poly(ethylene glycol) general procedure (1a/b, 2 and 11) Poly(ethylene glycol) **7a**, **7b** or **10** (**7a, 10**: 80 mg 0.08mmol, **7b**: 160 mg 0.08 mmol) and **5** (800 mg, 2.6 equiv. 0.21mmol) were dissolved in dry tetrahydrofuran (10 mL) under an argon atmosphere. The general procedure is further described for the coupling of **7a** and **5**. The temperature was raised to 55 °C and CuBr (30 mg, 0,2 mmol) and PMDETA (70 mg, 0,3 mmol) were added. The reaction was allowed to proceed for 12 hours after which all solvents were removed. The crude product was redissolved in 50 mL dichloromethane and washed with 0.33 M EDTA (3 × 25 mL). The organic layer was dried over $MgSO_4$ and poured on a short silica column, which was eluted with dichloromethane. After all non-reacted polybutadiene (**5**) was flushed off, the product was eluted with 8 v% methanol in dichloromethane. After removal of all solvents the product was obtained (250 mg, 60%, **1a**). The product was analyzed by size exclusion chromatography, showing a single size distribution (PDI = 1.14) with a shift toward higher hydrodynamic volume compared to polybutadiene. ^{1}HNMR: δ 1.16 (m, 134H, CH_2CH), 2.11 (m, 67H, CH_2CH), 3.37 (s, 3H, CH_3O), 3.64 (m, 90H, CH_2CH_2O), 4.94 (m, 134H, $CHCH_2$), 5.45 (m, 67H, $CHCH_2$). Mn was determined by NMR (**1a.** 4.7 kg/mol, **1b.** 5.7 kg/mol, **3.** 4.7

kg/mol and **11.** 4.7 kg/mol) The SEC traces are shown in Figures 1 (**1a**) Figure 7 (**1b**).

maleimide end functional polybutadiene-b-poly(ethylene glycol) (3) Polymer **11** (100 mg, 21 µmol) was dissolved in 6 mL dichloromethane. Next, N,N'-diisopropylcarbodiimide (DIPCDI, 400 µL, 1M in DMF) and N-hydroxybenzotriazole (HOBt, 450 µL, 1M in DMF) were added. After ten minutes, **12** (20 mg, 0.14 mmol) was added and the solution was stirred overnight. All dichloromethane was removed and ice cold methanol (10 mL) was added at once. The precipitate was gently shaken to dissolve side products and excess of **12**. After 1 hour the suspension was centrifuged at 5000 rpm for 30 minutes. Methanol was decanted and a new aliquot was added to repeat the centrifuge step (3x). The product was dried under vacuum to yield the product (60 mg, 60%). ^{1}HNMR ($CDCl_3$): δ 1.16 (m, 134H, CH_2CH), 2.11 (m, 67H, CH_2CH), 3.65 (m, 90H, CH_2CH_2O), 4.08 (s, 2H, OCH_2CON), 4.94 (m, 134H, CHCH_2), 5.45 (m, 67H, CHCH_2), 6.96 (s, 2H, maleimide); SEC (THF): M_w/M_n 1.17, M_n = 4.7 kg/mol.

propyne- endcapped polybutadiene (5) A Schlenk tube was thoroughly cleaned, rinsed with butyllithium, flushed with MilliQ and oven dried over night. The Schlenk tube was evacuated and an argon atmosphere was applied, after which 1,3-butadiene (7.1 g, 131 mmol) was condensed at -78 °C. THF was distilled under argon over sodium/benzophenone and was added to the flask (10 mL). The polymerisation was initiated by the addition of sec-butyllithium (1,4 mL, 2 mmol, 1.4M in hexane). The mixture was allowed to heat up to -35 °C as the colour changed from pale yellow to orange. After the colour changed back to yellow the reaction was terminated by the addition of dry THF (10 mL) containing trimethylsilyl propargylbromide (400 mg, 2.1 mmol). After all colour had disappeared tetrabutyl ammonium fluoride (4 mL, 4 mmol,1M in THF) was added and the mixture was stirred for 1 hour. All solvents were removed and the product was dissolved in dichloromethane, after which it was filtered over a slab of silica, eluting with dichloromethane. The final product was obtained by coevaporation with toluene (4x 50 mL) to remove any traces of propargyl bromide. The product contained two molecular weight distributions as determined by size exclusion chromatography (THF): 3.7 kg/mol (60%) and 7.4 kg/mol (40%). The higher molecular weight, a polymer dimer as reported and explained by Tohyama *et al.*[21], is not reactive toward azides and was easily removed by silica column chromatography, after the block copolymers were formed as shown in Figures 4-6. ^{1}HNMR: δ 5.45 (m, 67H, CHCH_2), 4.94 (m, 134H, CHCH_2), 2.11 (m, 67H, CH_2CH), 1.16 (m, 134H, CH_2CH).

α- azido ω-methoxy poly(ethylene glycol) (7a/b) Poly(ethylene glycol) monomethyl ether (5 mmol, 1 or 2 kg/mol to obtain respectively **7a** or **7b**) was coevaporated with benzene (3x) and dissolved in dry and under argon distilled THF (250 mL). The general procedure is further described for the preparation of **7a**. The flask was cooled on an ice bath and air was replaced by argon before freshly distilled triethyl amine was added (5 mL). The mixture was stirred for 3 hours, after which mesyl chloride (1.14 gram 2 equiv. 10mmol) in THF (10 mL) was added. The mixture was allowed to warm to room temperature and was stirred for 6 hours. All THF was removed and methanol (100 mL) containing sodium azide (3.25 g, 10 equiv., 50mmol) was added. The mixture was refluxed overnight

after which methanol was removed and water (100 mL) was added. The product was extracted with dichloromethane (5x 100 mL). The combined organic layers were dried over magnesium sulfate and DCM was removed, yielding 4.5 gram (90%) product **7a.** The SEC traces of both **7a** and **7b** are depicted in Figures 1 and 7 respectively. ^{1}HNMR (**7a**): δ 3.37 (s, 3H, CH_3O), 3.39 (t, 2H, CH_2N$_3$), 3.64 (m, 90H, CH_2CH_2O). FTIR: 2098 cm^{-1} (azide). SEC (THF): Mn (**7a**) = 1 kg/mol, Mw/Mn = 1.19.

α- azido ω- carboxy poly(ethylene glycol) (8) Poly(ethylene glycol) (5 g, 5 mmol, 1 kg/mol) was coevaporated with benzene (3x) and dissolved in dry and under argon distilled THF (250 mL). The flask was cooled on ice and air was replaced by argon, followed by the addition of distilled triethyl amine (5 mL). The mixture was stirred for 3 hours, after which mesyl chloride (0.6 gram, 1.1 equiv., 5.1mmol) in THF (10 mL) was added over 1 hour. The reaction was allowed to warm to room temperature and stirred for 6 hours. THF was removed. Next, methanol (100 mL) and sodium azide (3.25 g, 10 equiv. 50 mmol) were added. The reaction was heated to reflux overnight, whereafter methanol was removed and water (100 mL) was added. The mixture of statistical products was extracted with dichloromethane (5x 100 mL). The combined organic layers were dried over $MgSO_4$, and dichloromethane was removed.

The products were coevaporated with benzene (3x), dissolved in freshly distilled THF (250 mL) and cooled on an ice bath. An argon atmosphere was applied and sodium hydride (400 mg, 60% in oil, 2 equiv.) was added. After three hours t-butyl bromoacetate (2.9 g, 3equiv. 14mmol) in THF (10 mL) was added and the temperature was raised to 50 °C. The reaction was allowed to proceed overnight, after which all solids were filtered off and THF was removed. The products were dissolved in 2M HCl (100 mL) and heated to reflux for 5 hours. The final product was extracted with dichloromethane (5x 100 mL). The combined organic layers were dried over $MgSO_4$ and all solvents were removed. The product (R_f = 0.5) was purified using silica column chromatography (eluent MeOH:DCM:NH_3 =15:85:5) yielding 1.5 gram (30%) of product. TLC: R_f = 0.5, permanganate staining, eluent DCM:MeOH = 92:8. ^{1}HNMR: δ 3.39 (t, 2H, CH_2N$_3$), 3.64 (m, 90H, CH_2CH_2O), 4.00 (s, 2H, OCH_2COOH). FTIR: 2098 cm^{-1} (azide), 1570 (C=O of carboxylic acid salt). SEC (THF): Mn = 1 kg/mol, Mw/Mn = 1.19

α- azido ω- amino poly(ethylene glycol) (10) α- azido ω- carboxy poly(ethylene glycol) (**8**, 1 g, 1 mmol) was dissolved in methanol (50 mL) Next, concentrated sulphuric acid (5 drops) was added. The mixture was heated under reflux overnight, after which methanol was removed. The product was dissolved in water (50 mL) and extracted with dichloromethane (5x 50 mL). The organic layer was dried over $MgSO_4$ and all solvents were removed. TLC: R_f = 0.65, permanganate staining, eluent DCM:MeOH = 92:8. Indicative ^{1}HNMR shifts: δ 4.17 (s, 2H, OCH_2COOMe), 3.75 (s, 3H, COOCH_3) and IR: 1748 cm^{-1} (carbonyl/ester)

The product was dissolved in methanol (50 mL) and 1,2-diamino ethane (0.5 mL, excess) was added. The mixture was heated under reflux for 48 hours, after which all methanol was removed. The product was dissolved in 1M hydrochloric acid (50 mL) and extracted with dichloromethane (5x 50 mL). The combined organic layers were dried over $MgSO_4$ and all solvents were removed to yield 800 mg product (80%). TLC: R_f = 0.55, permanganate and nynhydrin staining, eluent DCM:MeOH = 92:8.

^{1}HNMR: δ 2.99 (t, 2H $CH_2CH_2NH_2$), 3.39 (t, 2H, CH_2N_3), 3.64 (m, 90H, CH_2CH_2O), 4.01 (s, 2H, OCH_2CONH). FTIR: 2098 cm^{-1} (azide), 1696 cm^{-1} (amide). SEC (THF): Mn = 1 kg/mol, Mw/Mn = 1.24.

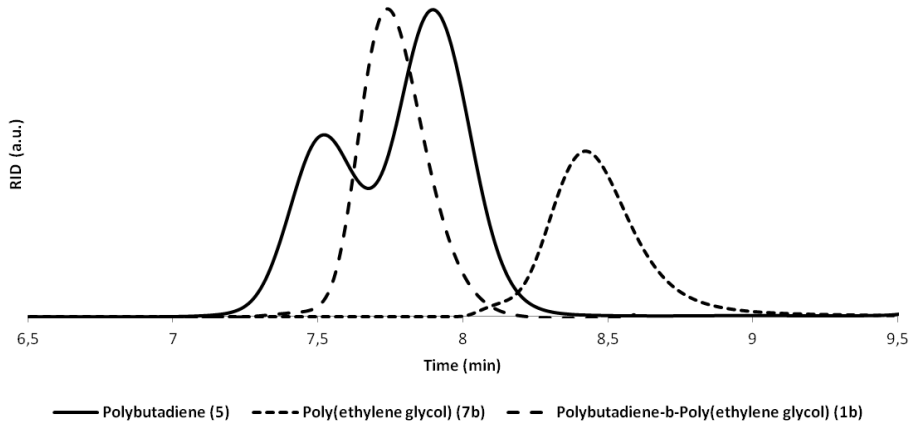

Figure 7. SEC (THF) traces of alkyne –endcapped polybutadiene after anionic polymerization (solid line, **5**), α-azido ω-methoxy poly(ethylene glycol) (short dashed line, **7b**) and the block copolymer polybutadiene-b-poly(ethylene glycol) (long dashed line, **1b**).

Partial Fluorescein labelling of polymer 2 Polymer **2** (50 mg, 10 μmol) was dissolved in THF (10 mL) and Et_3N (1 mL) was added. Next, fluorescein isothiocyanate (1 mg, 0.2 equiv.) was added and allowed to react for 48 hours. Solvents were removed and the labelled polymer was purified by preparative SEC (THF) to yield 25 mg product (50 %). The product was a single spot on TLC (8 percent methanol in DCM; UV and permanganate stain) which appeared brightly fluorescent and in contrast to the starting material showed good absorption @ 340 nm in the UV detector of SEC.

Tat-peptide Tat-peptide was synthesized by means of standard Fmoc chemistry. The purity was more than 95 percent as analyzed by means of HPLC eluting in water/acetonitrile containing 0.1% v/v trifluoroacetic acid. The volume fraction of acetonitrile was increased from zero to hundred percent over 30 minutes. Maldi-TOF (cyano-4-hydroxycinnamic acid): [M+H] calc: 1719.0 g/mol and [M+H] found: 1718.7 g/mol.

Polymersome formation via rehydration Polymer **1** (1 mg) and the drug or dye (1w%, 0.1 mg) was dissolved in chloroform (1 mL) and added to a 5 mL glass vial. While fast rotating the chloroform was removed under reduced pressure to obtain a thin polymer film on the inside of the glass vial, which was dried thoroughly for an additional hour under reduced pressure (5 mbar). Polymeric vesicles were formed by the addition of 3 mL THF:MilliQ (1:4), while the sample was rotated at atmospheric pressure. After 15 minutes the polymersomes were reduced in size by treating them for 60 minutes with ultrasound (35 °C, 48 kHz, 200W). Finally THF was removed to obtain polymersomes in 3 mL MilliQ.

Determination of drug encapsulation Polymersomes were formed via the rehydration method as described above, containing 1 w% of C1. The free drug was spun down in an eppendorf tube to pellet the free drug and the top 1.00 mL of the polymersomes was freeze-dried. The drug was extracted into 500 µL acetonitrile and analyzed on HPLC. The amount of encapsulated drug was back calculated. To validate this method we also added free drug to empty polymersomes and repeated the procedure to find no drug encapsulated (negative control). A calibration curve (0.01 – 0.1 mg C1/mL) was measured on a analytical HPLC, eluting over 30 minutes in a gradient of 0 to 100% acetonitrile in water (both containing 0.1 v% TFA, 0.7 mL/min). C1 was dissolved in MeCN and the UV detector was set to measure absorbtion at 333 nm.

Polymersome formation via solvent switch the desired ratio of block copolymer **1:2:3** (10 mg total) was dissolved in THF (1 mL) and slowly diluted with MilliQ or 1x PBS buffer (3 mL). The opaque solution was extruded subsequently trough 400 nm, 200 nm and 100 nm filters (WHATMAN, extrusion kit) and purified over a Sephadex G200 column. The opaque fractions were combined and diluted to 10 mL (1 mg polymer/mL) The average size and polydispersity was determined by DLS.

Conjugation of peptides to polymersomes TCEP (0.5 mg) was dissolved in 300 µL PBS pH 7.4 and added to peptide (1 mg, excess to maleimides). The solution was allowed to stand for 15 minutes, after which it was added to the polymersomes (1.5 mL). The coupling was allowed to proceed for three hours, after which the solution was transferred into a dialysis bag (Spectrapore MWCO 12-14 kDa) and dialyzed against PBS buffer for 24 hours (replacing PBS every 5-10 hours).

2.6 References

(1) Brinkhuis, R. P.; Rutjes, F. P. J. T.; van Hest, J. C. M. *Polym Chem-Uk* **2011**, *2*, 1449.
(2) Discher, B. M.; Won, Y. Y.; Ege, D. S.; Lee, J. C. M.; Bates, F. S.; Discher, D. E.; Hammer, D. A. *Science* **1999**, *284*, 1143.
(3) Egli, S.; Schlaad, H.; Bruns, N.; Meier, W. *Polymers* **2011**, *3*, 252.
(4) Photos, P. J.; Bacakova, L.; Discher, B.; Bates, F. S.; Discher, D. E. *J Control Release* **2003**, *90*, 323.
(5) Duncan, R. *Nat Rev Drug Discov* **2003**, *2*, 347.
(6) Kita-Tokarczyk, K.; Grumelard, J.; Haefele, T.; Meier, W. *Polymer* **2005**, *46*, 3540.
(7) Rostovtsev, V. V.; Green, L. G.; Fokin, V. V.; Sharpless, K. B. *Angew Chem Int Edit* **2002**, *41*, 2596.
(8) Webster, O. W. *Science* **1991**, *251*, 887.
(9) Kalnin'sh, K. K.; Panarin, E. F. *Dokl Phys Chem* **2001**, *377*, 112.
(10) Hirao, A.; Hayashi, M. *Acta Polym* **1999**, *50*, 219.
(11) Tohyama, M.; Hirao, A.; Nakahama, S.; Takenaka, K. *Macromol Chem Physic* **1996**, *197*, 3135.
(12) Opsteen, J. A.; van Hest, J. C. M. *Chem Commun* **2005**, 57.
(13) Opsteen, J. A.; Van Hest, J. C. M. *J Polym Sci Pol Chem* **2007**, *45*, 2913.
(14) van der Veken, P.; Dirksen, E. H. C.; Ruijter, E.; Elgersma, R. C.; Heck, A. J. R.; Rijkers, D. T. S.; Slijper, M.; Liskamp, R. M. J. *Chembiochem* **2005**, *6*, 2271.
(15) Pang, Z. Q.; Lu, W.; Gao, H. L.; Hu, K. L.; Chen, J.; Zhang, C. L.; Gao, X. L.; Jiang, X. G.; Zhu, C. Q. *J Control Release* **2008**, *128*, 120.

(16) van Rooy, I.; Wu, S. Y.; Storm, G.; Hennink, W. E.; Dinter-Heidorn, H.; Schiffelers, R. M.; Mastrobattista, E. *Int J Pharmaceut* **2011**, *416*, 448.

(17) Discher, D. E.; Eisenberg, A. *Science* **2002**, *297*, 967.

(18) Green, M.; Loewenstein, P. M. *Cell* **1988**, *55*, 1179.

(19) Merrifield, R. B. *J Am Chem Soc* **1963**, *85*, 2149.

(20) Weksler, B. B.; Subileau, E. A.; Perriere, N.; Charneau, P.; Holloway, K.; Leveque, M.; Tricoire-Leignel, H.; Nicotra, A.; Bourdoulous, S.; Turowski, P.; Male, D. K.; Roux, F.; Greenwood, J.; Romero, I. A.; Couraud, P. O. *Faseb J* **2005**, *19*, 1872.

(21) Tohyama, M.; Hirao, A.; Nakahama, S. *Macromolecular Chemistry and Physics* **1996**, *197*, 3135.

3

Size Dependent Biodistribution and SPECT Imaging of ^{111}In-labelled Polymersomes

Polymersomes, self assembled from the block copolymer polybutadiene-block-poly(ethylene glycol), were prepared with well-defined diameters between 90 and 250 nm. The presence of ~1% of diethylene triamine penta acetic acid on the polymersome periphery allowed to chelate radioactive ^{111}In onto the surface and determine the biodistribution in mice as a function of both the polymersome size and poly(ethylene glycol) corona thickness (i.e. PEG molecular weight). Doubling the PEG molecular weight from 1 kg/mol to 2 kg/mol did not change the blood circulation half-life significantly. However, the size of the different polymersome samples did have a drastic effect on the blood circulation times. It was found that polymersomes of 120 nm and larger become mostly cleared from the blood within 4 hours, presumably due to recognition by the reticuloendothelial system. In contrast, smaller polymersomes of around 90 nm circulated much longer. After 24 hours more than 30 percent of the injected dose was still present in the blood pool. This sharp transition in blood circulation kinetics due to size is much more abrupt than observed for liposomes and was additionally visualized by SPECT/CT imaging. These findings should be considered in the formulation and design of polymersomes for biomedical applications. Size, much more than for liposomes, will influence the pharmacokinetics and therefore long circulating preparations should be well below 100 nm.

René P. Brinkhuis†, Katica Stojanova†, Peter Laverman, Jos Eilander, Inge S. Zuhorn, Floris P.J.T. Rutjes and Jan C. M. van Hest, Bioconjugate Chem. **2012**, 23, 958-965

† Equal contribution

3.1 Introduction

Polymersomes, or polymer vesicles, are a relatively new class of nanocapsules that are formed by the self assembly of amphiphilic block copolymers in aqueous media[1]. Polymersomes can be regarded as the polymeric analogues of liposomes with a thicker, more stable and less leaky membrane. These characteristics make polymersomes an interesting class of nanocarriers for the delivery of diagnostic and therapeutic agents. For these applications it is generally desired to have long circulating particles which are not readily cleared from the blood stream by the reticuloendothelial system (RES)[2]. From liposomal *in vivo* studies it is known that size, next to PEGylation and charge, is a major factor that influences the blood circulation kinetics and biodistribution. Liposomes of more than 200 nm have been shown to accumulate in the spleen and liver, whereas liposomes of less than 70 nm tend to accumulate predominantly in the liver[3,4]. Liposomes with a size between 90 and 150 nm have the longest blood circulation times. The blood circulation times of liposomes can be further enhanced by the introduction of up to ten percent PEGylated phospholipids[5,6]. Polyethylene glycol (PEG) prevents the opsonisation by blood proteins and the subsequent recognition and degradation by macrophages of the reticuloendothelial system. PEGylated liposomes may exhibit blood circulation half-lives (t½) of more than 15 hours, depending on the PEG chain length, charge and size of liposomes[3,4,7]. Finally, the effect of surface charge in liposomal formulations[8] and nanocarriers[9] has been studied. Both a slightly negative and positive surface charge was reported to have a positive effect on the blood circulation kinetics.

The number of reports on biodistribution of neutral polymersomes is limited and is basically restricted to the work of Discher[10,11] who used fluorescently labelled polymersomes to determine the effect of longer PEG chains and surface charge on t½ values, the work of Lee *et al*.[12] and the recent work by Kataoka *et al*. who studied the size dependence of fluorescently labelled polyelectrolyte vesicles (PICsomes) for the preferred accumulation in tumour tissue compared to healthy tissue[13]. Also near infrared dyes have been encapsulated in order to visualize tumours in mice[14,15]. Discher *et al.* reported that polymersomes exhibit blood circulation half-lives up to 28 hours. These high t½ values are partly due to the fact that polymersomes are fully PEGylated upon choosing PEG as the hydrophilic part of the block copolymer that constitutes the polymersome bilayer. It was furthermore shown that neutral

polymersomes circulate with the highest t½ values. Finally Tsourkas *et al.*[16] encapsulated a Gd-based magnetic resonance imaging (MRI) contrast agent for enhanced MRI imaging. By measuring the concentration of Gd in blood, they were also able to determine a concentration time profile.

One of the most quantitative methods to determine the biodistribution of drug delivery vehicles *in vivo* is by radio isotope labelling. This technique is often used for liposomal formulations, but has until now been hardly explored for polymersomes. There is one report on the biodistribution and radiolabelling (^{14}C/^{3}H) of negatively charged polymersomes[12] and one study that shows data on the encapsulation and biodistribution of a radio-labelled model drug encapsulated in polymersomes[17]. However, the effect of polymersome size on biodistribution has not been analysed before with this technique. If radiolabelling of polymersomes with a suitable isotope such as ^{111}In would be developed, this would not only allow quantitative determination of organ distribution but also visualisation with SPECT/CT imaging, as has previously been demonstrated for 50 nm polymer micelles [18,19].

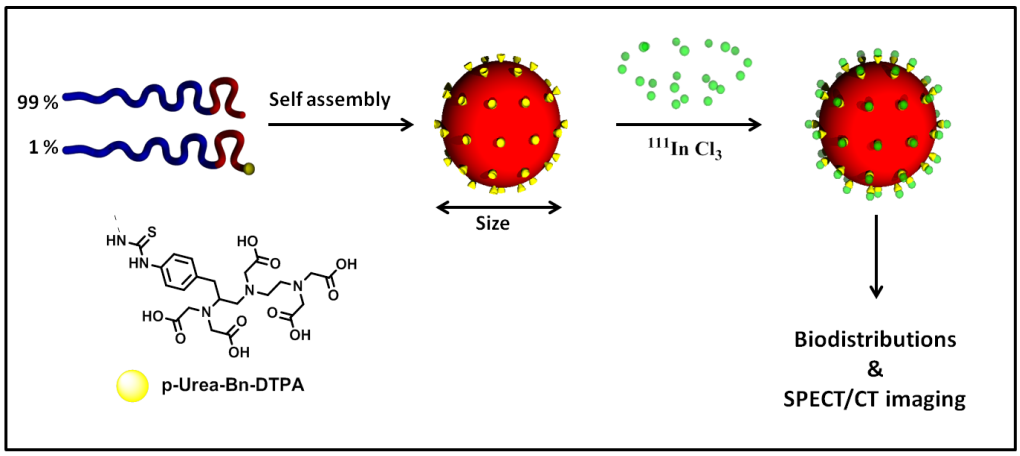

Figure 1. Schematic presentation of polymersome formation, ^{111}In labelling and *in vivo* SPECT/CT imaging.

In this chapter we present a systematic study into the effect of size on the biodistribution of polymersomes via the quantitative technique of ^{111}In radiolabelling, in combination with SPECT/CT imaging as depicted schematically in Figure 1. It is shown that polymersomes of around 90 nm in diameter have long circulation times in male Balb/C mice. Upon increasing the diameter to 120 nm and above the long circulating properties are lost and polymersomes are cleared from the

blood stream within a few hours by mainly the liver and spleen. The effect on circulation time upon changing the size from 90 to 120 nm is also clearly visualized by SPECT/CT imaging.

3.2 Results and Discussion

The amphiphilic block copolymer used in this study was polybutadiene-*block*-poly(ethylene glycol) (PBd-b-PEG) because of its well-known biocompatibility and glass transition temperature (T_g) well below room temperature. Because of this low T_g the membrane of polymersomes formed from PBd-b-PEG remains fluidic which allows good control over the size via standard sizing techniques such as extrusion.

The general synthetic route towards the three block copolymers used in this study is depicted in Scheme 1 (see also Chapter 2). As can be seen from this scheme we adopted a modular approach based on the copper-catalyzed (2+3) cycloaddition reaction[20]. One of the main advantages of this modular approach is the possibility to vary the molecular weight of PEG between 1 and 2 kg/mol, while keeping the molecular weight (distribution) of PBd exactly constant at 3.7 kg/mol. Polybutadiene was synthesised by means of anionic polymerisation. The reaction was initiated with sec-butyllithium at -78 °C. After all monomer was consumed, the living polymer was endcapped with 3-bromo-1-(trimethylsilyl)-1-propyne[21]. Deprotection with tetrabutyl ammonium fluoride yielded the alkyne-functional polybutadiene **1**. Poly(ethylene glycol) monomethyl ether was purchased with a molecular weight of either 1 or 2 kg/mol. The introduction of an azide was straight forward by mesylation and azidation as published elsewhere[22]. PBd and PEG were coupled in THF at 60 °C by the addition of copper bromide and PMDETA as ligand. This reaction yielded the non functional block copolymers PBd-b-PEG with a molecular weight of approximately 4.7 kg/mol (**4a**) and 5.7 kg/mol (**4b**) depending on the PEG molecular weight. These inert block copolymers served as the basic building blocks for polymersome formation.

To allow radiolabelling of polymersomes with ^{111}In a third block copolymer was synthesised with diethylene triamine penta acetic acid (DTPA) as chelating end group. Polybutadiene was coupled to α-amino-ω-azido-poly(ethylene glycol) via the same click approach as described above to obtain amine end-functional PBd-b-PEG (**5**) with a molecular weight of 4.7 kg/mol (PEG molecular weight of 1 kg/mol). DTPA

is a metal chelating agent that coordinates well to bi- and tri-valent metals. Copper, as used in the coupling reaction of PBd and PEG, can also coordinate strongly to DTPA. To prevent undesired occupation of DTPA by copper, all traces of copper in the different PBd-b-PEG analogues were removed by treating the polymers with Chelex resin in THF (as confirmed by ICP-MS). Finally p-benzyl-isothiocyanate DTPA was introduced in block copolymer **5** by reacting the amine end group and isothiocyanate in THF with triethylamine as base to form polymer **6**.

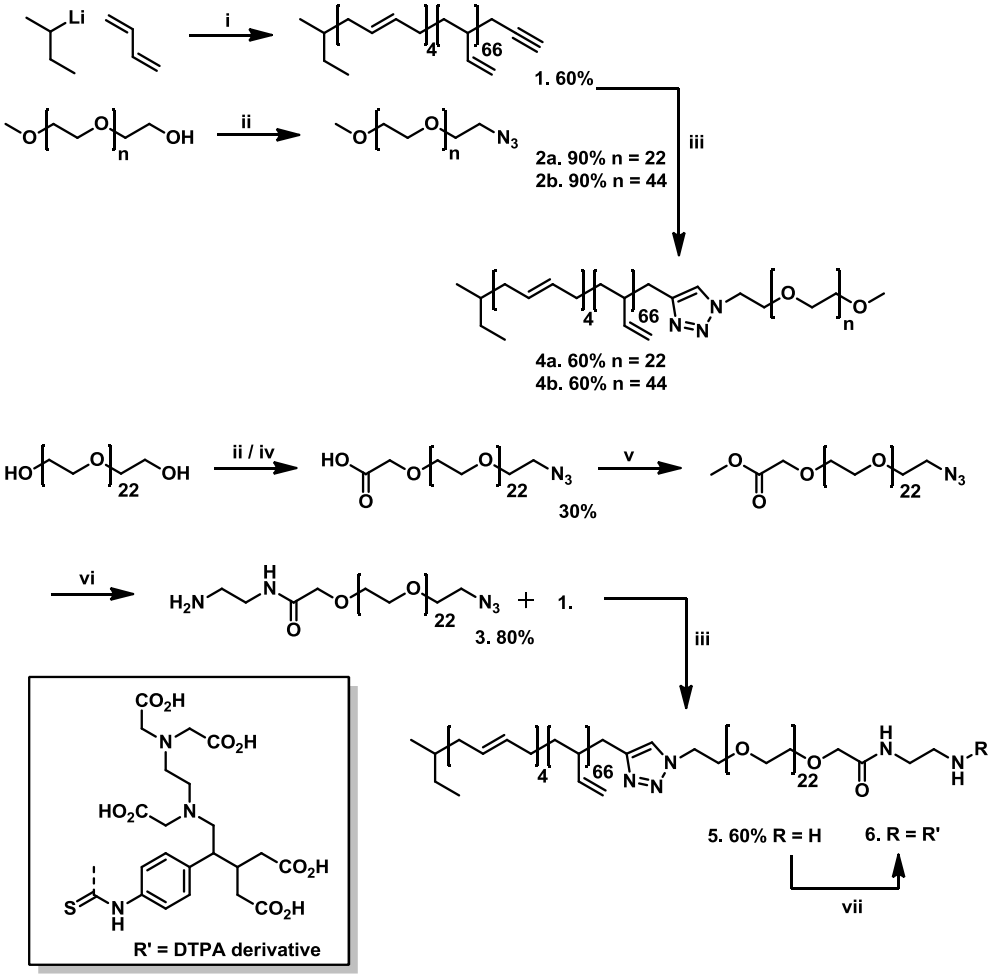

Scheme 1. Overview of polymers and the reaction path towards these compounds. Exact details on the synthesis can be found in the experimental section at the end of this Chapter and in Chapter 2. i) anionic polymerisation of 1,3 butadiene followed by endcapping and deprotection ii) azidation with MsCl followed by NaN_3 iii) coupling of polymers via copper catalysed (2+3) cycloaddition iv) NaH, t-butyl bromoacetate in THF, followed by deprotection in 1M HCl v) esterification in $MeOH/H_2SO_4$ vi) nucleophilic acyl substitution by 1,2 diamino ethane in MeOH vii) amine coupling of p-SCN-Bn-DTPA.

Polymersomes were formed by slowly diluting a solution of **4a**:**6** or **4b:6** = 99:1 (w:w) in THF with 2-(*N*-morpholino)ethanesulfonic acid (MES) buffer with a pH of 5.5. After the addition of MES buffer the samples were extruded through 0.2 μm

syringe filters to yield polymersomes of around 250 nm diameter. To size the polymersomes even further down the samples were either extruded through 100 nm filters (to yield ~120 nm polymersomes) or treated with ultrasonic sound waves at 35 °C (to yield ~90 nm polymersomes). After resizing, the samples were washed with MES buffer and concentrated. It should be noted that extrusion through 100 nm membranes yielded the narrowest particle size distribution, whereas ultrasound waves and extrusion through syringe filters gave broader distributions. All particle polydispersities were found to be below 0.15, which is comparable to results often encountered for liposomal formulations (see Figures 4 and 5 for the full DLS curves). The characteristics of the polymersomes are summarized in Table 1, as is the ^{111}In labelling efficiency and blood plasma stability of the different samples which will be discussed next.

Table 1. Overview of polymersome characteristics.

ID	size (nm)	PDI	M_w PEG (kg/mol)	ζ potential[a]	^{111}In labelling efficiency	specific activity (MBq/mg)	4 h plasma	24 h plasma
1k90	94	0.15	1	-14.76	97%	10	85%	79%
1k120	115	0.05	1	-13.11	95%	10	84%	78%
1k250	259	0.14	1	-12.42	94%	10	87%	80%
2k90	87	0.13	2	-9.96	60%	6	77%	73%

a) Zeta potentials were measured on a NanoSight NS500 in tap-water with an applied potential of 24V. Polymersomes (250 nm) formed from only polymer **4a,** i.e no DTPA chelated to the surface, have a zeta potential of -6.32 mV.

^{111}In labelling was performed by adding 15 MBq $^{111}InCl_3$ to 30 µL of polymersome solution. Samples that labelled with an efficiency of more than 95 percent were used without further purification, and were diluted with PBS to 1.25 MBq per mL. The one sample that had a labelling efficiency of only 60 percent (2k90) was purified over a PD10 desalting column after which it was also diluted with PBS. The stability of the ^{111}In-labelled preparations was tested by adding 20 µL of each sample to 500 µL human blood serum. After 24 hours about 80 percent of the Indium-111 radioactivity was still associated with the polymersomes as summarized in Table 1. These results show that these polymersomes of well-defined size allow for stable radio isotope labelling for *in vivo* applications.

After establishing polymersome synthesis and evaluation of the radiolabelling stability we studied the biodistribution as function of size and peripheral PEG thickness. As might be expected from similar studies based on liposomes, larger particles will influence the circulation kinetics negatively. In order to study if a similar trend is also valid for polymersomes, we injected male Balb/c mice (6 weeks old, 20-23 g/animal) with 250 kBq (0.2 mL or 0.42 mg/kg) of ^{111}In-labelled polymersome solution in the tail vein. Each group contained four animals which were sacrificed after 4 or 24 h. Tissues of interest were collected, weighed and counted for radioactivity as summarized in Figure 2.

Upon looking at the blood levels a clear effect of polymersome size can be recognized immediately. Vesicles of 90 nm circulate much longer than vesicles of 120 nm and larger. After 4 hours more than 50 percent of the 90 nm polymersomes were still present in the blood pool, which after 24 hours was reduced to 25 percent (based on a blood volume assumption of 1.5 g per animal). This allows us to estimate the blood half live of these 90 nm polymersomes to be around 20 hours, a number comparable to blood circulation half lives as reported by Photos *et al*[10]. Upon increasing the particle size both the liver and spleen accumulation became higher, an effect that is more abrupt for the liver than for the spleen. The abundance of 90 nm polymersomes in lungs was relatively high, which most likely is caused by high blood levels in lung tissue. These data show that – similarly to liposomes – smaller polymersomes circulate longer. However there is a major difference in the correlation between size and blood circulation kinetics of these polymersomes and liposomes. For polymersomes the transition from long-circulating to short-circulating , upon increasing the size, is much more abrupt than for liposomes. A possible explanation might be found in the more rigid[1] structure of polymersomes which results in less flexibility. This feature could be of practical use since it could have a beneficial effect on tumour accumulation via the enhanced permeability and retention (EPR) effect[13,23].

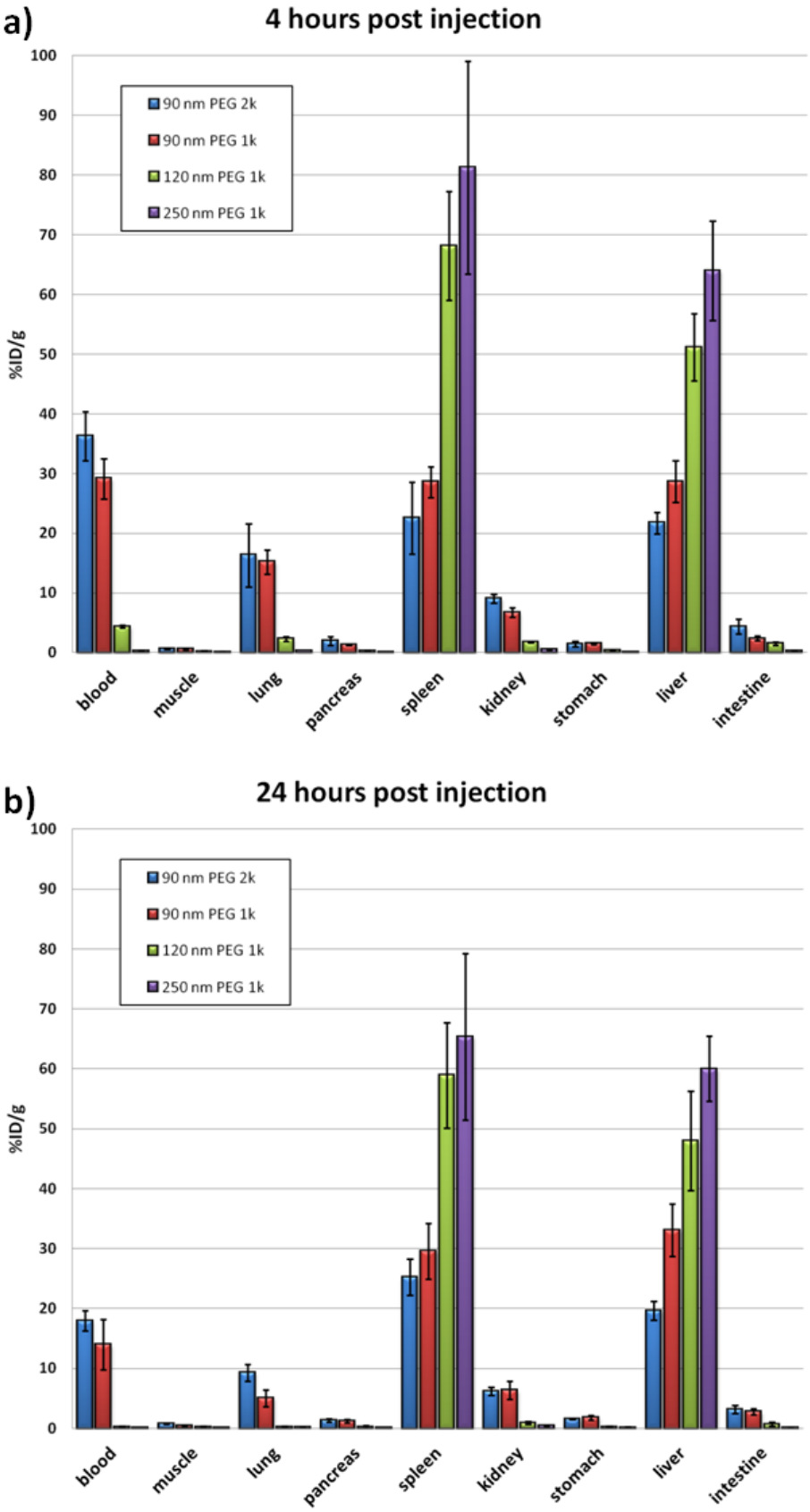

Figure 2. Biodistribution of differently sized ^{111}In-labelled polymersomes in Balb/C mice (n=4/group). **a)** 4 hours post injection and **b)** 24 hours post injection.

In order to investigate the effect of the PEG corona on biodistribution two polymersome samples were included in these experiments with an average diameter of ~90 nm, but with different PEG lengths of 1 and 2 kg/mol (Table 1 and Figure 2). Although the sample with the thicker PEG corona seemed to circulate longer in the blood stream and showed lower liver and spleen accumulation this effect is not significant, especially because there is also a small size difference between both samples.

A powerful method of imaging organs/tissue particle distributions in living animals (and humans) is by Single Photon Emission Computed Tomography (SPECT) imaging. SPECT/CT imaging is a tool often used in nuclear medicine to obtain three dimensional images in a non-invasive manner. The polymersomes as described in this chapter have a high enough specific activity to image them by this technique. Typically for imaging of mice 15 MBq of activity is needed, an amount easily accessible via the route described herein.

In order to illustrate by SPECT/CT the abrupt transition from long circulating to fast clearance upon increasing the polymersome size, we prepared samples of 90 nm polymersomes and 120 nm polymersomes with 15 MBq of ^{111}In. The procedure was analogous as described above, only the dilution factor with PBS was adjusted to end up with a sample of 75 MBq per mL. Each animal was injected intravenously with 15 MBq (0.2 mL, 25.2 mg/kg) ^{111}In-polymersomes in the tail vein and was scanned after 4 hours. The resulting images are depicted in Figure 3. The top panel of Figure 3 (a-c) shows the results for the long circulating polymersomes of 90 nm with a PEG molecular weight of 1 kg/mol. As visualized by radioactivity in the heart and lungs, the polymersomes are still present in the blood circulation. The lower panel of Figure 3 (d-f) shows 4 h post-injection scans of the 120 nm polymersomes. All the radioactivity is present in liver and spleen. This is in agreement with the biodistribution data as discussed above. These scans again show the strong size dependence of polymersomes with regard to blood circulation kinetics.

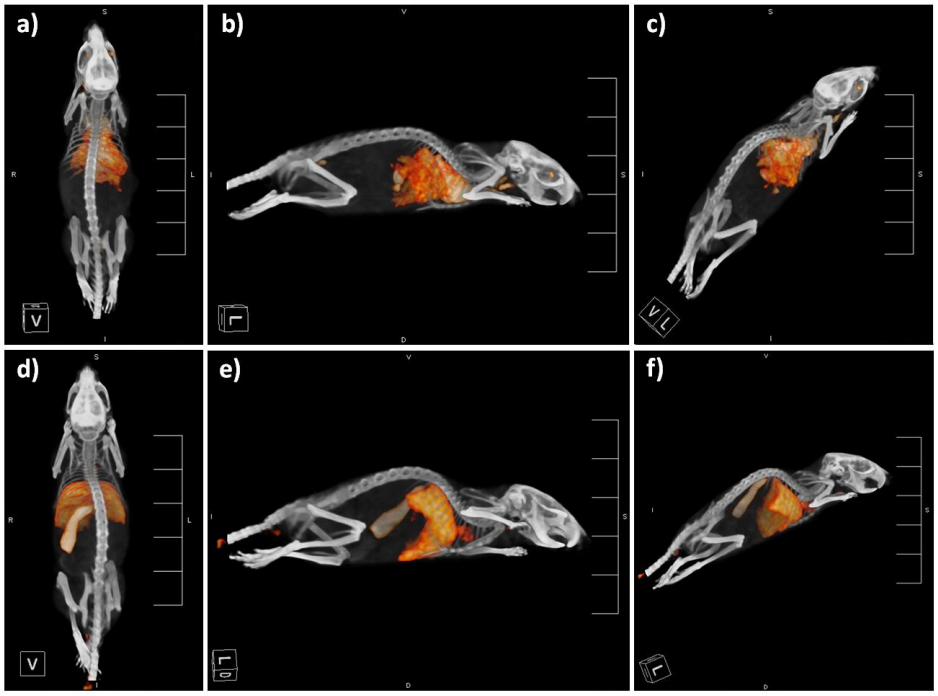

Figure 3. SPECT/CT images (4 h p.i.) of polymersomes injected in male BalB/c mice. Top (a-c) long circulating 90 nm polymersomes clearly show circulation through the liver, lungs and carotid artery. Bottom (d-f), 120 nm polymersomes show fast accumulation in the liver and the spleen.

3.3 Conclusion

We have demonstrated that for polymersomes, size is an important factor in the blood circulation kinetics. Polymersomes of 120 nm and larger are readily cleared from the blood, whereas smaller polymersomes of approximately 90 nm are long circulating with an estimated blood half life of 20 hours. We have shown that polymersomes containing 1 percent of a DTPA end-functional amphiphilic block copolymer of polybutadiene-block-poly(ethylene glycol) can be prepared with a sufficient specific activity for SPECT/CT imaging. The effect of size on the biodistribution could therefore also be illustrated by this technique to confirm that 90 nm polymersomes are long circulating whereas 120 nm polymersomes readily accumulate in the liver and spleen. The effect of increasing the PEG molecular weight from 1 to 2 kg/mol was not found to be significant in this case. These findings should be taken into account upon designing polymersome formulations for imaging or drug delivery purposes. Polymersome size, much more than for liposomes, will influence the circulation kinetics of polymersomes.

3.4 Acknowledgment

Jos Eilander and Peter Laverman are acknowledged for their help in the animal studies and development of ^{111}In labelled polymersomes.

3.5 Experimental Procedures

General note The synthesis of polymers **1**-**5** was described in detail in Chapter 2. Animal experiments were approved by the local animal welfare committee and carried out according to national regulations.

Materials p-isothiocyanate-benzyl diethylenetriamine penta-acetic acid (MACROCYCLICS >94%), Chelex resin (ALDRICH), were used as received. Tetrahydrofuran (THF) (ACROS ORGANICS, 99+% extra pure, stabilized with BHT) was distilled under argon from sodium/benzophenone, and triethyl amine (TEA) (BAKER) was distilled from calcium hydride under an argon atmosphere prior to use. Polymersome extrusions were performed using 200 nm filters (Acrodisc 13 mm Syringe Filter, 0.2 µm Nylon membrane) and 0.1 µm PC membrane (WHATMAN). $^{111}InCl_3$ was purchased from Covidien, Petten, The Netherlands. Instant Thin-Layer Chromatography Silica Gel impregnated glass fibre (ITLC-SG) strips were purchased from Varian.

Instrumentation Infrared (IR) spectra were obtained using a Thermo Matson IR 300 FTIR spectrometer. Data are presented as the frequency of absorption (cm^{-1}). Molecular weight distributions were measured using size exclusion chromatography (SEC) on a Shimadzu (CTO-20A) system equipped with a guard column and a PL gel 5 µm mixed D column (Polymer Laboratories) with differential refractive index and UV (λ=254 nm and λ=345nm) detection, using tetrahydrofuran (SIGMA ALDRICH chromasolv 99.9%) as an eluent at 1 mL/min and T = 35 ^{o}C. Particle size distributions were measured on a Malvern instruments Zetasizer Nano-S and zeta potentials were measured on a NanoSight NS 500 instrument.

Conjugation of Diethylene Triamine Penta Acetic acid (DTPA) (6) amine end-functional polybutadiene-*block*-poly(ethylene glycol) (**5**, 110 mg, 23 µmol) was dissolved in THF (10 mL). To the solution, p-isothiocyanate-benzyl diethylene-triamine-penta-acetic-acid (14 mg, 0.95 equiv. 22 µmol) and triethylamine (5 mL) were added. The mixture was stirred at room temperature for 48 hours, after which all solvents were removed. The products were dissolved in THF (5 mL) and cooled on ice for 6 hours, after which the solution was filtered through a 200 nm syringe filter. The product was obtained by removing all THF. The DTPA end groups were not quantified, yet their presence was confirmed by FTIR and ^{111}In test labelling. FTIR: 1730 cm^{-1} (carboxylic acid). SEC (THF): Mw/Mn = 1.26, Mw (theoretical) = 5.3 kg/mol.

Polymersome formation (general) Polymer **4a** (9.9 mg, 2.1 μmol) or **4b** (9.9 mg, 1.7 μmol) and diethylene-triamine-penta-acetic-acid functional polybutadiene-*block*-poly(ethylene glycol) **6** (0.1 mg, 0.02 μmol)were dissolved in THF (200 μL). Polymersomes were formed by the slow addition of 0.1 M. 2-(N-morpholino)ethanesulfonic acid buffer of pH 5.5 (0.6 mL, MES). The samples were passed three times through a 200 nm syringe filter to yield polymersomes of ~250 nm. Polymersomes of ~120 nm were obtained by multiple extrusion through 100 nm filters (one pass will yield ~160 nm polymersomes) and polymersomes of less than 100 nm were obtained by treating the sample with ultrasonic sound waves (48 kHz, 200W) for 30 minutes at 35 °C. Samples were washed and concentrated to 200 μL by means of a spin column (100 kDa MWCO, 3000 rpm). Note that for the biodistribution samples a stock solution containing 9.9 mg **4a** and 0.1 mg **6** per 200 μL THF was prepared to prevent variation in concentration and ratio of polymers. The DLS results of all samples are depicted in Figures 4 and 5.

^{111}In labelling To 30 μL polymersomes, 150 μL 0.1 M. 2-(N-morpholino)ethanesulfonic acid (MES) buffer (pH 5.5) and 15 MBq $^{111}InCl_3$ were added. The labelling mixture was incubated at room temperature for 30 minutes. Labelling efficiency was analyzed by Instant Thin-Layer Chromatography Silica Gel impregnated glass fibre (ITLC-SG), developed in 0.1 M NH_4Ac (pH 5.5)/0.1 M EDTA (1:1, v/v). Samples with a labelling efficiency of more than 95 percent were used without purification and diluted with PBS buffer prior injection. Samples with a coupling efficiency of less than 95 percent were purified over a PD10 desalting column and diluted with PBS.

Blood Plasma stability To study the stability of polymersome preparations, 20 μL of radio-labelled polymersomes was incubated in 500 μL blood serum for 4 and 24 hours at 37 °C. Association of ^{111}In with the polymersomes was analyzed by ITLC-SG, developed in 0.1 M NH_4Ac (pH 5.5)/0.1 M EDTA (1:1, v/v).

Biodistribution studies Biodistribution was analyzed in male BALB/c mice (6 weeks of age, 20-23 g per animal). The animals were divided in 8 groups of 4 animals and injected in their tail vein with 250 kBq (0.2 mL or 0.42 mg/kg) of ^{111}In-labelled polymersome preparation. Mice were sacrificed by CO_2 inhalation 4 or 24 h postinjection (p.i.), a blood sample was drawn, and tissues of interest were dissected, weighed, and counted in a gamma-counter along with a standard of the injected activity to allow calculation of the injected dose per gram tissue (% ID/g).

SPECT/CT imaging Two animals were selected for SPECT/CT imaging and injected with 15 MBq (0.2 mL, 25.2 mg/kg) ^{111}In-polymersomes in the tail vein. The animals were sacrificed by CO_2 inhalation and scanned with the U-SPECT-II (MILabs) 4 hours postinjection.

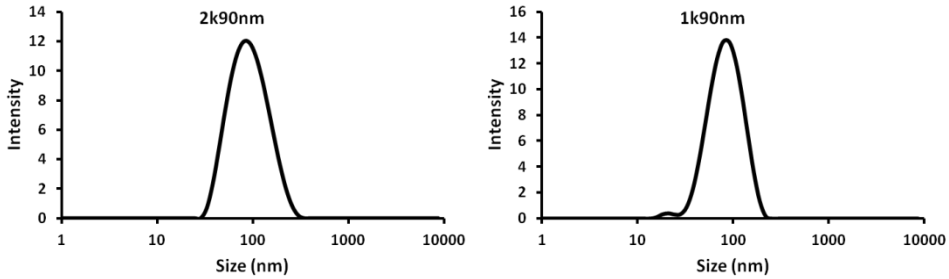

Figure 4. DLS *intensity* size distributions of sample 2k90nm (top) and 1k 90nm (bottom) as measured on a Malvern Nano S machine. Both samples were resized by treatment with ultrasound (48 kHz, 200 W, 35 degrees Celsius).

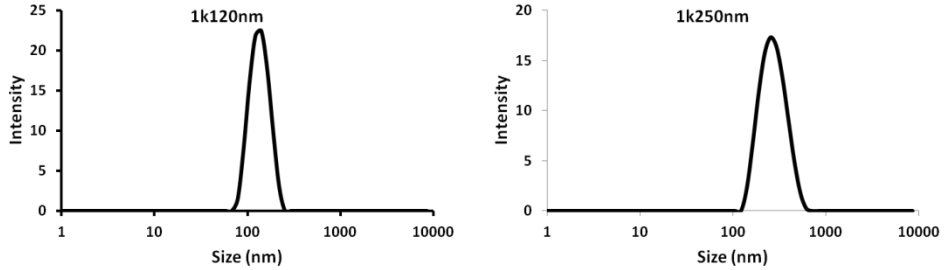

Figure 5. DLS *intensity* size distributions of sample 1k120nm (top) and 1k 250nm (bottom) as measured on a Malvern Nano S machine. Both samples were resized by means of extrusion through respectively 200 and 100 nm membranes.

3.6 Notes and References

(1) Discher, B. M.; Won, Y. Y.; Ege, D. S.; Lee, J. C. M.; Bates, F. S.; Discher, D. E.; Hammer, D. A. *Science* **1999**, *284*, 1143.

(2) Brinkhuis, R. P.; Rutjes, F. P. J. T.; van Hest, J. C. M. *Polymer Chemistry* **2011**, *2*, 13.

(3) Harashima, H.; Kiwada, H. *Adv Drug Deliver Rev* **1996**, *19*, 425.

(4) Litzinger, D. C.; Buiting, A. M. J.; Vanrooijen, N.; Huang, L. *Bba-Biomembranes* **1994**, *1190*, 99.

(5) Klibanov, A. L.; Maruyama, K.; Torchilin, V. P.; Huang, L. *Febs Lett* **1990**, *268*, 235.

(6) Allen, T. M.; Hansen, C.; Martin, F.; Redemann, C.; Yauyoung, A. *Biochim Biophys Acta* **1991**, *1066*, 29.

(7) Lian, T.; Ho, R. J. Y. *J Pharm Sci* **2001**, *90*, 667.

(8) Gabizon, A.; Papahadjopoulos, D. *Biochim Biophys Acta* **1992**, *1103*, 94.

(9) Yamamoto, Y.; Nagasaki, Y.; Kato, Y.; Sugiyama, Y.; Kataoka, K. *J Control Release* **2001**, *77*, 27.

(10) Photos, P. J.; Bacakova, L.; Discher, B.; Bates, F. S.; Discher, D. E. *J Control Release* **2003**, *90*, 323.

(11) Christian, D. A.; Garbuzenko, O. B.; Minko, T.; Discher, D. E. *Macromol Rapid Comm* **2010**, *31*, 135.

(12) Lee, J. S.; Ankone, M.; Pieters, E.; Schiffelers, R. M.; Hennink, W. E.; Feijen, J. *J Control Release* **2011**, *155*, 282.

(13) Anraku, Y.; Kishimura, A.; Kobayashi, A.; Oba, M.; Kataoka, K. *Chem Commun* **2011**, *47*, 6054.

(14) Ghoroghchian, P. P.; Frail, P. R.; Susumu, K.; Blessington, D.; Brannan, A. K.; Bates, F. S.; Chance, B.; Hammer, D. A.; Therien, M. J. *P Natl Acad Sci USA* **2005**, *102*, 2922.

(15) Tanisaka, H.; Kizaka-Kondoh, S.; Makino, A.; Tanaka, S.; Hiraoka, M.; Kimura, S. *Bioconjugate Chem* **2008**, *19*, 109.

(16) Cheng, Z. L.; Thorek, D. L. J.; Tsourkas, A. *Adv Funct Mater* **2009**, *19*, 3753.

(17) Upadhyay, K. K.; Bhatt, A. N.; Castro, E.; Mishra, A. K.; Chuttani, K.; Dwarakanath, B. S.; Schatz, C.; Le Meins, J. F.; Misra, A.; Lecommandoux, S. *Macromol Biosci* **2010**, *10*, 503.

(18) Damen, D. M. *EP 2 161 020 A1* **2008**.

(19) Allen, C.; Hoang, B.; Lee, H.; Reilly, R. M. *Mol Pharmaceut* **2009**, *6*, 581.

(20) Opsteen, J. A.; van Hest, J. C. M. *Chem Commun* **2005**, 57.

(21) Hirao, A.; Hayashi, M. *Acta Polym* **1999**, *50*, 219.

(22) Brinkhuis, R. P.; Visser, T. R.; Rutjes, F. P. J. T.; van Hest, J. C. M. *Polymer Chemistry* **2011**, *2*, 550.

(23) Maeda, H.; Wu, J.; Sawa, T.; Matsumura, Y.; Hori, K. *J Control Release* **2000**, *65*, 271.

4

Peptide-Mediated Blood-Brain Barrier Transport of Polymersomes

In this chapter we report the design of polymersomes tagged with a dodecamer peptide, G23, that are able to cross the blood-brain barrier both in vitro and in vivo. Transport over the blood-brain barrier was induced by recognition of G23 to the gangliosides GM1 and GT1b to accommodate transcytosis of 220 nm polymersomes in an in vitro model and 166 nm polymersomes in vivo. These findings open new opportunities for the development and formulation of medicines against brain related diseases.

Julia Georgieva†, René P. Brinkhuis†, Katica Stojanov, Carel A. G. M. Weijers, Han Zuilhof, Floris P. J. T. Rutjes, Dick Hoekstra, Jan C. M. van Hest and Inge S. Zuhorn, *Angewandte Chemie Int. Ed.* **2012**,*51, 8339-8342*

† Equal contribution

4.1 Introduction

The effective treatment of brain-related diseases is severely hampered by the presence of the blood-brain barrier (BBB), a polarized layer of endothelial cells that physically separate blood from brain tissue[1]. Besides being able to cross the BBB, drugs must display sufficient stability and bioavailability[2]. Once drugs have reached the brain side, they are exposed to multidrug receptors on the endothelial cell surface to rapidly clear them from the brain[3]. Of these challenges, both bioavailability and crossing the BBB may be overcome by the application of nanocarriers that effectively target the endothelial cell layer and induce transcytosis across the BBB.

The best studied nanocarriers for drug delivery over the BBB are liposomes. To target them over the BBB, liposomes have been decorated[4-7] with antibodies, proteins[8] or peptide[9-10] parts of protein binding domains[11]. However, most targeted liposomes showed only a limited association with the BBB *in vivo* as was recently shown by van Rooy *et al*. in a comparative study[8]. Only liposomes conjugated to transferrin antibody RI7217 – having a molecular weight of 90 kg/mol – were able to significantly enhance brain uptake.

A relatively new class of nanocarriers consist of polymeric vesicles, or polymersomes[12-13], which spontaneously self-assemble in aqueous media from amphiphilic block copolymers. They resemble liposomes in their basic morphology, but have as a clear difference a thicker bilayer membrane. This renders them considerably more stable than liposomes, and improves the blood circulation ability[14]. Furthermore, the large apolar compartment allows a more efficient transport of hydrophobic drugs. Since the majority of CNS drugs are hydrophobic, there is a large added value in preparing polymeric carriers for efficient transport over the BBB into the brain parenchyma. Until now, only one group has reported the conjugation of transferrin[15] or transferrin antibody RI7217[16] to polymersomes, for targeted transport over the BBB. Clearly, to develop an efficient nanocarrier system, a broader choice in selective targeting units is required. Moreover these targeting units should still be active when conjugated to the polymersome surface and preferential have a low molecular weight for easy synthesis and conjugation.

In this chapter we report the design and synthesis of a polymersome nanocarrier, tagged with a dodecamer peptide of only 1645 g/mol, that is able to efficiently cross the BBB, both *in vitro* and *in vivo*. The peptide G23 was identified by means of phage display

with ganglioside GM1 as target. Although the G23 peptide has previously been reported for binding to gangliosides[17], it has now been employed for the first time to accommodate transport of nanocarriers over the BBB.

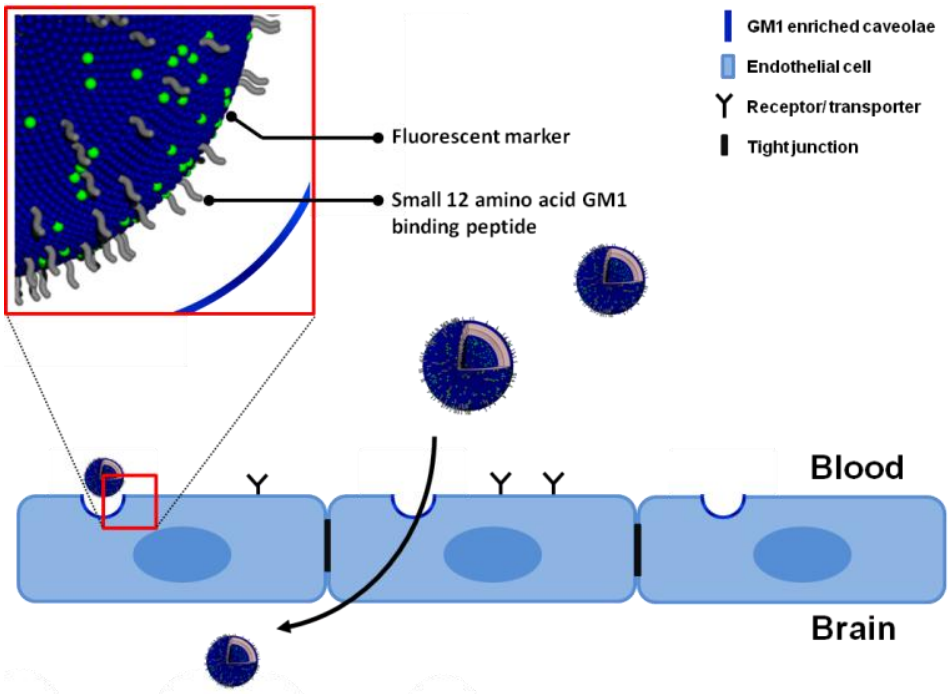

Figure 1. Cartoon of polymeric vesicles tagged with a small GM1 binding peptide. The polymersome formulations are able to efficiently cross the BBB into the brain parenchyma, opening new routes toward effective treatment of brain-related diseases.

4.2 Results and Discussion

The block copolymers for the formation of polymersomes are depicted in Scheme 1. Details on the synthetic procedures can be found in Section 4.5 and Chapter 2. We chose to work with amphiphilic block copolymers (**1**) consisting of polybutadiene and poly(ethylene glycol) (PEG) mainly for two reasons. First of all, this block copolymer is generally considered to be biocompatible, and secondly the low glass transition temperature of polybutadiene allows for extrusion – and therefore resizing – of the resulting polymersomes. This has been shown to be of great importance for long *in vivo* circulation[18-19]. Furthermore, PEG induces stealth behaviour of the vesicles and therefore prevents cell adhesion as well as opsonisation and thereby recognition by the reticulo endothelial system (RES). To functionalize the polymersomes with targeting peptides, maleimide end groups were introduced (**2**). As a tracing moiety, either

fluorescein (**4**), rhodamine (**5**) or diethylenetriamine pentaacetate (**6**) (DTPA, for radio-isotope labelling) was introduced in **3** via isothiocyanate derivatives of the tracer.

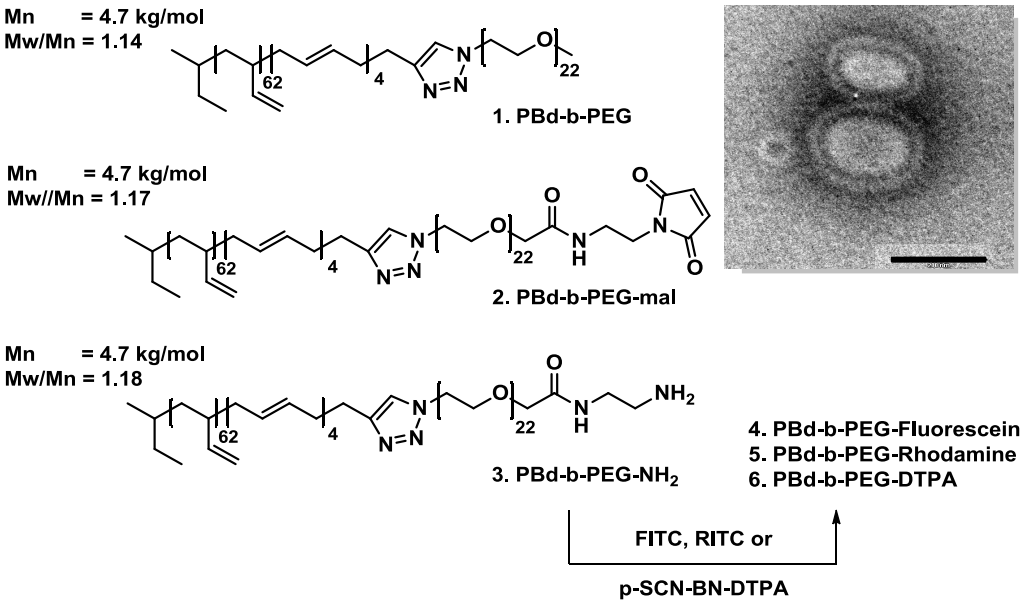

Scheme 1. Left) Amphiphilic block copolymers used in this study. Polymer **1** is the main building block of the polymersomes. Polymer **2** is a maleimide-functionalized analogue to couple peptides. Starting from polymer **3**, fluorescein, rhodamine and DTPA end-functionalized analogues were obtained. Right) TEM picture of polymersomes formed from **1**, **2** and **4** in a ratio of 8:1:1. The black bar represents 200 nm.

The peptides that were known before this study to target the BBB were limited to Tat-peptide[9-10], opioid-derived peptides[20] and the bigger RVG-9R peptide[11], which all showed limited *in vivo* delivery into the brain parenchyma. In order to identify more potent peptides, we recognized that caveolae, which are present on the luminal surface of endothelial cells, are well known as cellular entry portals for transcytotic transport[21]. Since caveolae are enriched in GM1, we reasoned that this could be an appropriate target to mediate transport into the brain. A phage library selection was performed, using the Ph.D-12 library from BioLabs with immobilized GM1 as target[22]. After three panning rounds 20 plaques were selected of which 10 shared a known carbon nanotube binding sequence[23]. Three plaques shared the sequence defined as G23. The other seven plaques showed unique sequences. We selected the peptides defined as G23 and G88 based on their efficient binding and homogeneous patterning upon interaction of the phages with human Cerebral Microvascular Endothelial Cells (hCMEC/D3)[24] as shown in Figure 9. The selected peptides were synthesized via standard Fmoc chemistry with an additional C-terminal cysteine as a functional handle.

Polymersomes were prepared by mixing block copolymers **1**, **2** and **4** in a ratio of 8:1:1 for all *in vitro* studies (Table 1). The polymeric vesicles were formed via the solvent switch method, after which they were extruded to an average size of 220 nm with a polydispersity index (PDI) of 0.11. The selected peptides were coupled via cysteine/maleimide chemistry, starting from the same batch of maleimide-functionalized polymersomes. To check whether the peptide coupling was successful, zeta potentials were measured. The zeta potentials showed in all cases a clear change in surface charge after coupling of the peptides (table 1). For *in vivo* experiments polymersomes were prepared with rhodamine as tracer, thus combining polymers **1**, **2** and **5** in a ratio of 8:1:1. The polymersomes were reduced in size to 160 nm, to allow sufficiently long blood circulation to pass the brain endothelial cells, yet short enough to prevent false comparison of targeted and non-targeted particles due to a big difference in blood clearance[19].

Table 1. Characteristics of polymersome samples used for *in vivo* and *in vitro* studies.

ID/Peptide[a]	Sequence[b]	Size (PDI)	Charge[c]	Zeta[d]
Non_{fluor}	–	220 (0.11)	–	–6.32
$G88_{fluor}$	NPAGPSPAHIISC	220 (0.11)	0	–14.59
$G23_{fluor}$	HLNILSTLWKYRC	220 (0.11)	+2	–1.70
Scr_{fluor}	KISHLLNYRTWLC	228 (0.10)	+2	–2.83
$G23(5\%)_{fluor}$	HLNILSTLWKYRC	227 (0.12)	+2	–3.21
Non_{rhod}	–	164 (0.10)	–	–2.64
$G23_{rhod}$	HLNILSTLWKYRC	165 (0.12)	+2	–8.42

[a] Samples contain 10 mol% fluorescently labelled polymer (fluor = fluorescein, rhod = rhodamine), 10% of the surface is covered with peptides. [b] Peptide sequences with C-terminal cysteine for coupling to the polymersome surface. [c] Formal charge at pH 7. [d] Measured in water with an applied potential of 24 V.

First the transcytosis capacity of targeted and non-targeted polymersomes was determined in hCMEC/D3 cells, cultured on transwell filters. The hCMEC/D3 cell line is a good model for the human blood-brain barrier, as developed and verified by Weksler *et al.*[24-25]. Recently this assay was used and validated by Ragnaill *et al.*[26] to study the transcytosis of SiO_2 nanoparticles. An overview of the experimental setup is provided in Figure 2c. The polymersomes were added to the apical side of the model and incubated for 18 hours at 37 °C, after which the percentages of applied dose in the apical chamber (AP), basolateral chamber (BA) and cell monolayer (FIL) were determined by means of fluorescence spectroscopy.

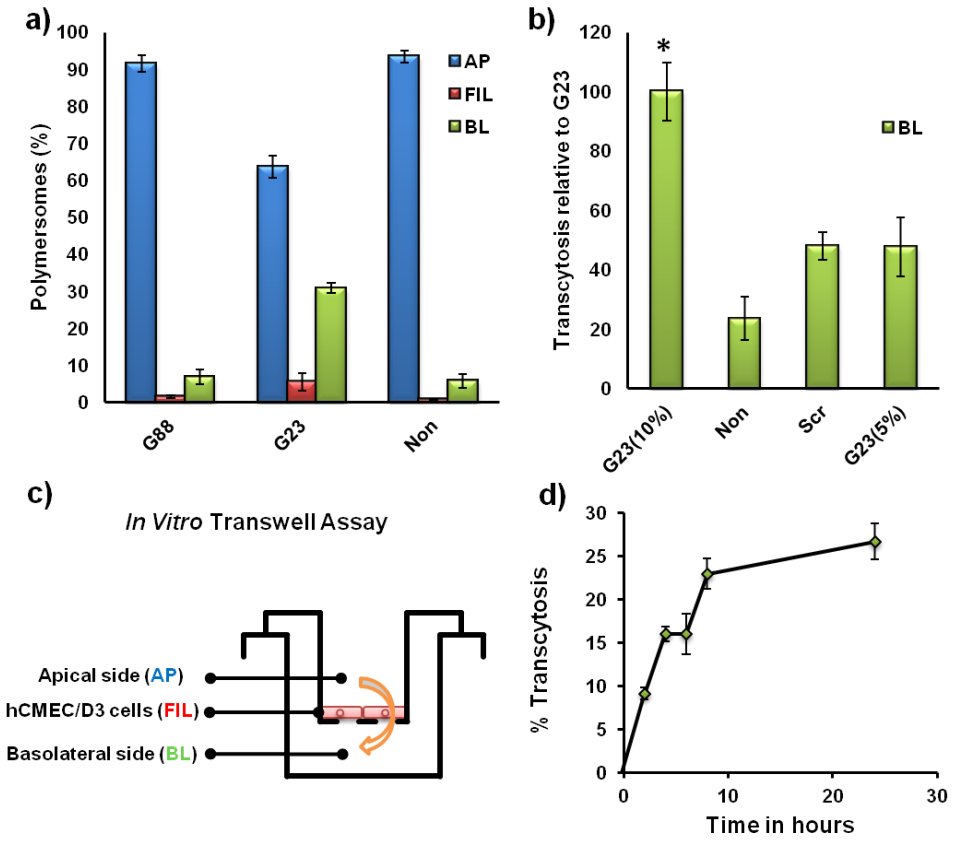

Figure 2. a) *In vitro* transcytosis capacity of polymersomes functionalized with the selected peptides. b) Scrambling of the G23 sequence and lowering the surface functionalization with G23 both resulted in reduced *in* vitro transcytosis. c) Schematic overview of the *in vitro* hCMEC/D3 cell transwell assay. d) Kinetic plot of *in vitro* G23/mediated transcytosis of polymersomes.

As evident from Figure 2a, the G23-polymersomes showed the most prominent transcytotic capacity. Specifically, 30.8 ± 1.4% of the G23-polymersomes were recovered at the basolateral side. This implies on average a more than four-fold increase in transcytotic capacity, compared to the basolateral recovery of non-targeted polymersomes (5.7 ± 0.8%), or polymersomes tagged with G88 (6.8 ± 1.9%). In addition to a highly efficient appearance in the basolateral medium, the G23-polymersomes showed an enhanced association with the cells (Figure 2a; G23; FIL). Thus, 5.5 ± 2.3% of the added dose remained cell-associated, representing 2-3 times as much as the cellular association of the other polymersome preparations tested, i.e. non-targeted (1.5% ± 0.8%) and those tagged with G88 (1.5 ± 0.4%). These data thus emphasize the specific role of G23 in mediating the observed enhancement in transcytotic transport, and exclude potential leakiness of the cell monolayer, as this should have resulted in a non-specific appearance of polymersomes in the basolateral medium. The specificity of G23-mediated transport was further supported by determining the kinetics of transcytosis of

the G23-polymersomes across hCMEC/D3 cells. As shown in Figure 2d, typical saturation kinetics were obtained, supporting the involvement of an active, receptor-mediated transport pathway, possibly reflecting differences in the kinetics of transcytosis and recycling of the receptor(s).

To investigate a potential correlation between physicochemical properties (e.g. charge, hydrophobicity) and transcytotic capacity of the peptide, a scrambled version of the G23-peptide (Scr) was prepared and its ability in transport of polymersomes was compared to that of 'native' G23 and non-targeted polymersomes. As illustrated in Figure 2b a twofold reduction in transcytosis across the *in vitro* BBB model was observed between Scr-polymersomes and G23-targeted polymersomes. Secondly the peptide density was reduced to 5 mol%. Lowering the incorporation of G23 in polymersomes also led to a two-fold reduction in transcytosis (Figure 2b). Together, these data strongly support the view that the G23-peptide, when coated on the surface of polymersomes, displays a specific capacity in mediating their transport across polarized hCMEC/D3 cells.

Although in a different context, peptide G23 was reported to bind to a structurally similar ganglioside GT1b[17]. Furthermore the removal of tetanus toxin C from its ganglioside receptor GT1b by peptide G23 has been reported[27], together with this study clearly indicating that G23 recognizes at least two gangliosides. In nature additional gangliosides are encountered which are structural equivalents of GM1. We therefore investigated whether these gangliosides are present on the BBB model and secondly for which gangliosides G23 tagged polymersomes have affinity.

Using a set of specific antibodies against individual ganglosides, immuno analysis revealed the presence of GD1a and GT1b, but not GD1b at the cell surface of hCMEC/D3 cells as shown in Figure 3. Subsequently, we investigated whether the G23-polymersomes display binding capacity towards GD1a and GT1b, using related and unrelated gangliosides as controls. The gangliosides – spotted on a dot blot – were incubated with radioactively labelled G23-polymersomes, after which binding only occurred to GM1 and GT1b. Accordingly, we determined whether the binding of G23-polymersomes to GT1b also occurs in a cellular context by establishing the extent of colocalization between GT1b and fluorescently labelled G23-polymersomes. The colocalization of G23-polymersomes with GT1b was 16.2 ± 6.4%, while colocalization

with GD1a was less than 3% (Figure 4). Hence, these data support that both GM1 and GT1b may function as target sites for G23-polymersomes.

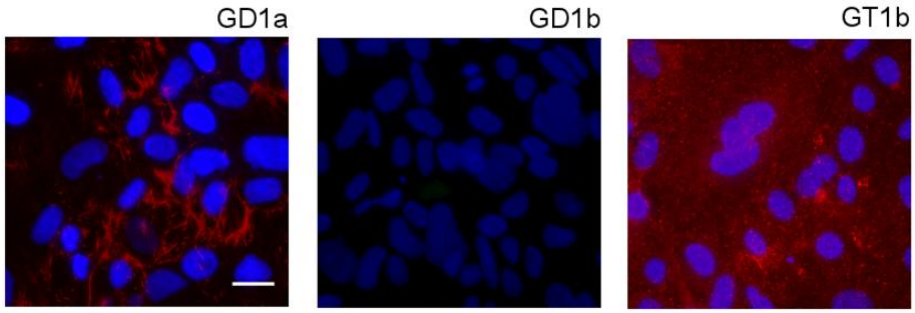

Figure 3. Distribution of gangliosides, GD1a, GD1b and GT1b in a monolayer of hCMEC/D3 cells. The nuclei are stained blue by DAPI and the gangliosides are stained red via the corresponding antibody.

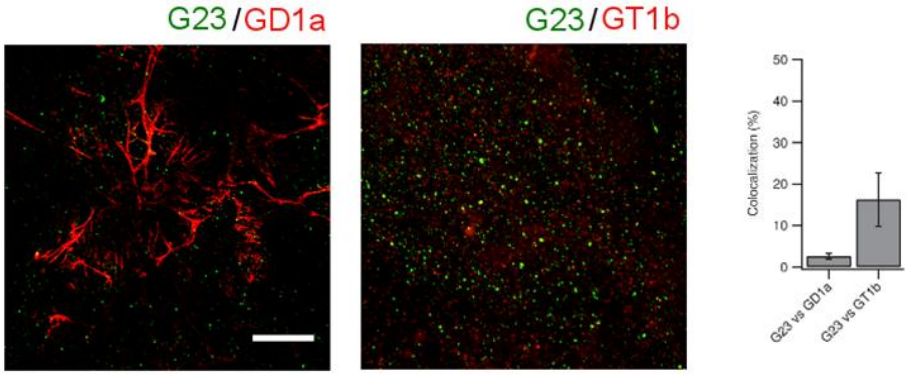

Figure 4. Colocalisation of G23 tagged polymersomes (green) with ganglioside GD1a (left, stained in red), ganglioside GT1b (middle, stained red) and the evaluation of the amount of colocalisation (right).

To reveal the potential of G23 to also mediate BBB passage *in vivo,* rhodamine-labelled G23-polymersomes and non-targeted polymersomes were administered by intracarotid artery injection in BALB/c mice. The brain distribution of both rhodamine-labelled polymersomes was then analyzed 24 h after injection by preparing thin brain slices as described in detail in the Section 4.5. The nuclei were stained green (CD31), the vessels were stained blue (DAPI) and polymersomes red (rhodamine). As demonstrated in Figure 5, next to their localization within the endothelial cells of the BBB (Figures 5a, b – upper panel), substantial amounts of the G23-polymersomes reached the brain parenchyma (Figures 5a, b – lower panel, c), indicating that they crossed the BBB and penetrated into the brain tissue. In marked contrast, non-targeted polymersomes were found mainly in the leaky vessels of the forth ventricle (Figure 5d) and ependymal cells of the aqueduct (Figures 5e, f – lower panel), and only occasionally in brain parenchyma

(Figures 5e, f – upper panel), further emphasizing the potency of G23 to mediate effective transfer of polymersomes across the BBB.

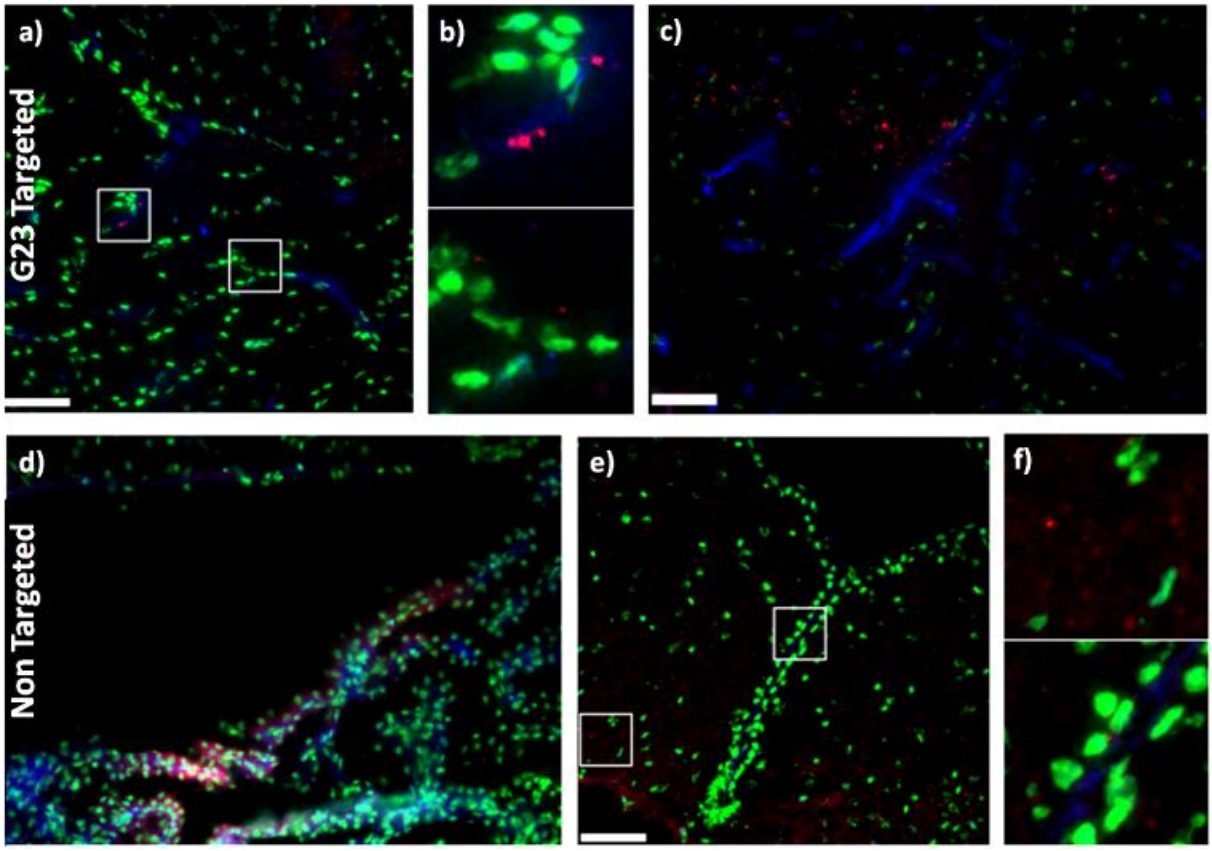

Figure 5. *In vivo* brain distribution of polymersomes after intracarotid artery injection in mice. BALB/c mice were injected with G23- and non-targeted polymersomes. 24 h after injection brains were isolated and processed as specified in methods. (a, magnification in (b) upper panel) G23-polymersomes are found in microvessels, visualized with CD31 (PECAM), and in (a, magnification in (b) lower panel, and c) brain parenchyma. (d) Non-targeted polymersomes are found in the leaky vessels of the forth ventricle, and in (e, magnification in (f) upper panel) in parenchyma, and (e, magnification in (f) lower panel) ependymal cells of the aqueduct. Polymersomes are pseudocolored in red, CD31 in blue, and nuclei in green. Scale bars, 50 μm.

4.3 Conclusion

In conclusion, we have identified the low molecular weight peptide, G23, which when coupled to polymeric vesicles, binds to cell surface localized gangliosides GM1 and GT1b. By doing so it is able to mediate the transport of nanocarriers over the blood brain barrier both in vitro and in vivo. The combination of the low molecular weight targeting peptide, GM1/GT1b as targeting receptor, the robust polymeric carrier and the efficient in vitro and in vivo transcytosis is unprecedented and therefore adds new possibilities to the development of efficient drug nanocarriers for the treatment of brain and central nervous system-related diseases

4.4 Acknowledgement

Sander Dik is acknowledged for his work on polymersome transport over the hCMEC/D3 cell line and forming a bridge between UMCG and RUN collaborators. Julia Georgieva is acknowledged for performing the phage display and analysing the transcytosis of polymersomes *in vitro* and Katica Stojanov is acknowledged for enabling animal studies.

4.5 Experimental procedures

4.5.1 Synthesis and characterisation

Notes The synthesis of compounds **1-3** and **7-14** were performed as discussed in Chapter 2.

Materials Chelex resin (ALDRICH), was used as received. Tetrahydrofuran (THF) (ACROS ORGANICS, 99+% extra pure, stabilized with BHT) was distilled under argon from sodium/benzophenone, and triethylamine (TEA) (BAKER) was distilled from calcium hydride under an argon atmosphere prior to use. $^{111}InCl_3$ was purchased from Covidien, Petten, The Netherlands. Instant Thin-Layer Chromatography Silica Gel impregnated glass fibre (ITLC-SG) strips were purchased from Varian. Thin layer chromatography (TLC) was performed on Merck precoated silica gel 60 F-254 plates (layer thickness 0.25 mm). Compounds were visualized by UV, ninhydrin and/or permanganate reagents. Column chromatography (CC) was carried out using silica gel, Acros (0.035-0.070 mm, pore diameter ca. 6 nm). Polymersome extrusions were performed using 200 nm filters (Acrodisc 13 mm Syringe Filter, 0.2 μm Nylon membrane) and 0.1 μm PC membrane (WHATMAN).

Instrumentation Infrared (IR) spectra were obtained using a Thermo Matson IR 300 FTIR spectrometer. Data are presented as the frequency of absorption (cm^{-1}). Molecular weight distributions were measured using size exclusion chromatography (SEC) on a Shimadzu (CTO-20A) system equipped with a guard column and a PL gel 5 μm mixed D column (Polymer Laboratories) with differential refractive index and UV (λ = 254 nm and λ = 340nm) detection, using tetrahydrofuran (SIGMA ALDRICH chromasolv 99.9%) as an eluent at 1 mL/min and T = 30 °C. Particle size distributions were measured on a Malvern instruments Zetasizer Nano-S. and zeta potentials were measured on a NanoSight NS500 system in water with an applied potential of 24 V. MilliQ water was obtained from a Labconco water pro PS system.

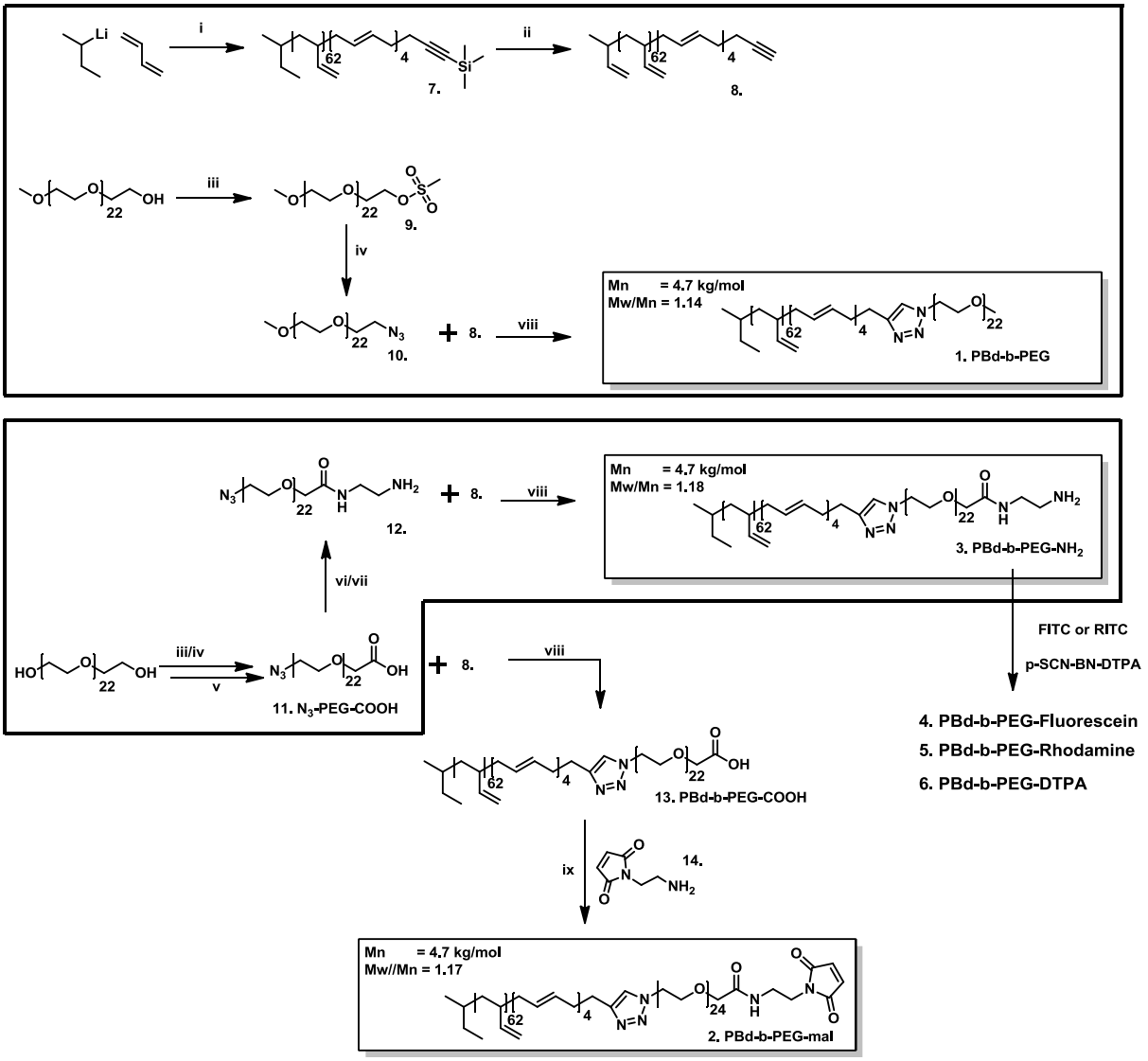

Scheme 2. Synthetic route to amphiphilic block copolymers of PBd-b-PEG (**1**-**3**) with different end functionalities as developed in Chapter 2. Polymer **1** is inert and forms the basic building block for polymersome formation. Block copolymer **2** bears an amine end group to allow conjugation with isothiocyanate derivatives of e.g. fluorescein. Finally, polymer **3** is maleimide end functionalized to allow for conjugation with cysteine bearing peptides. Prior to use, all polymers were extensively washed with Chelex 100 resin in THF to remove any traces of copper. The amount of residual copper was in all cases determined by ICP-MS and found to be equal or less than MilliQ references.

Fluorescent labelled polybutadiene-b-poly(ethylene glycol) (4 and 5) Compound **3** (50 mg, 10 µmol) was dissolved in THF (10 mL) and Et_3N (1 mL) was added. Rhodamine B isothiocyanate (7.5 mg, ca. 1.5 equiv.) or fluorescein isothiocyanate (7.5 mg, ca. 1.5 equiv.) was added and allowed to react for 48 hours. Solvents were removed and product **4** or **5** was purified by preparative SEC (THF) to yield 25 mg product. The product was a single spot on TLC (8 v% methanol in DCM; UV and permanganate stain) which appeared brightly fluorescent. Note that the isothiocyanate coupling of rhodamine B proceeded slowly as can be seen from the SEC traces (absorption @ 340 nm) in Figure 6. The elution volume that was collected in preparative SEC (THF) is depicted in the box (6.7 to 8.1 mL)

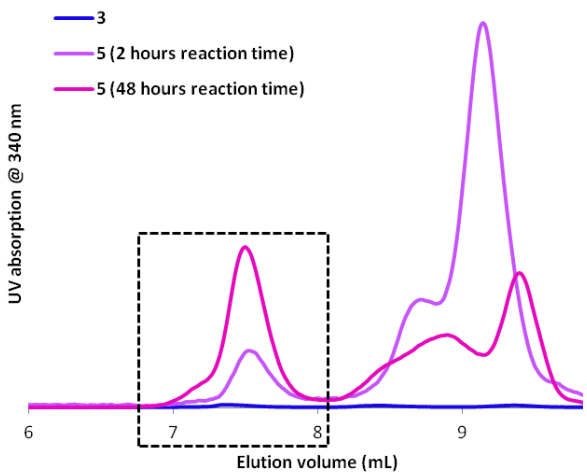

Figure 6. SEC (THF) analysis of block copolymer **3**, which does not absorb at 340 nm before the addition of rhodamine B isothiocyanate. After 2 hours the labelled polymer (top~7.5 mL) does absorb at 340 nm, which increases over the next 46 hours. The dashed box indicates the volume, containing product **5** (or **4** case of FITC), which was collected by preparative SEC in THF.

PBd-b-PEG-DTPA (6) This reaction was performed as described in Chapter 3. In short, the amine end functional polybutadiene-*b*-poly(ethylene glycol) **3** (110 mg, 23 µmol) was dissolved in THF (10 mL). To the solution, p-isothiocyanate-benzyl diethylene-triamine-penta-acetic-acid (14 mg , 0.95 equiv. 22 µmol) and triethylamine (5 mL) were added. The mixture was stirred at room temperature for 48 hours, after which all solvents were removed. The products were dissolved in THF (5 mL) and cooled on ice for 6 hours, after which the solution was filtered through a 200 nm syringe filter. The product was obtained by removing all THF. The DTPA end groups were not quantified, yet their presence was confirmed by FTIR and ^{111}In test labelling. FTIR: 1730 cm^{-1} (carboxylic acid). SEC (THF): Mw/Mn = 1.26, Mw (theoretical) = 5.3 kg/mol.

Peptide Synthesis All peptides were synthesised by means of standard Fmoc chemistry. To the C-terminus of all native peptide sequences (as determined in phage display) was an additional cysteine added to allow bioconjugation. All peptides were more than 90 percent pure as analyzed by means of HPLC (water/acetonitrile with 0.1% TFA; gradient acetonitrile from 0 to 100% in 30 minutes). Additionally in all cases the right mass was found by means of Maldi-TOF (Maldi-TOF (cyano-4-hydroxycinnamic acid), analyzed with m*overz* software:

G23: [M+H] calc: 1645.88 g/mol and [M+H] found:1645.6 g/mol.
SCR: [M+H] calc: 1645.88 g/mol and [M+H] found: 1645.6 g/mol.
G88: [M+H] calc: 1262.6 g/mol and [M+H] found: 1262.1 g/mol.

4.5.2 Polymersome formation and peptide conjugation

Fluorescent, maleimide displaying polymersomes Compounds **1** (8 mg, 1.7 µmol), **3** or **4** (1 mg, 0.2 µmol) and **2** (1 mg, 0.2 µmol) were dissolved in THF (200 µL). Polymersomes were formed by the slow addition of 0.8 mL of PBS buffer of pH 7.4. The samples were passed six times through a 200 nm syringe filter (Aerodisc) to yield polymersomes of approximately 220 nm. To obtain polymersomes of

around 160 nm the solution was extruded six times over a 100 nm filter (Lipex high pressure extruder, Northern Lipids). The resulting opaque suspension was purified over a Sephadex G200 column (1.5 x 8 cm). The opaque fractions were combined and PBS was added to a total volume of 10 mL, i.e. a polymersome suspension containing 1 mg polymer per mL. The final polymersome solution was analyzed by DLS to determine the mean size and polydispersity index.

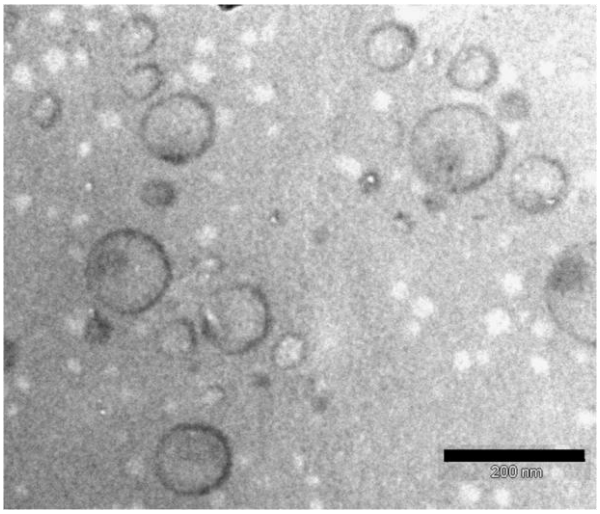

Figure 7. TEM image of polymersomes formed from block copolymer **1**. The black bar represents 200 nm.

Radio-labelled, maleimide displaying polymersomes Compounds **1** (9 mg, 1.9 µmol), **5** (0.1 mg, 0.02 µmol) and **2** (1 mg, 0.2 µmol) were dissolved in THF (200 µL). Polymersomes were formed by the slow addition of 0.6 mL of 0.1 M. 2-(*N*-morpholino)ethanesulfonic acid (MES) buffer of pH 5.5. The samples were passed three times through a 200 nm syringe filter to yield polymersomes of approximately 220 nm. The solution was extruded six times over a 100 nm filter (extrusion kit) to obtain polymersomes of around 160 nm. The resulting opaque suspension was purified over a Sephadex G200 column (1.5 x 8 cm), eluting with MES buffer. The opaque fractions were combined and the mean particle size was determined by DLS.

To 0.2 mL of polymersomes, 25 MBq of ^{111}InCl was added and allowed to chelate for 20 minutes, after which the coupling efficiency was analyzed by Instant Thin-Layer Chromatography Silica Gel impregnated glass fibre (ITLC-SG) strips, developed in 0.1 M NH_4Ac (pH 5.5)/0.1 M EDTA (1:1, v/v). The sample was purified over a PD10 desalting column, eluting with PBS buffer pH 7.4, and diluted with PBS to a total volume of 10 mL, i.e. a polymersome suspension containing 1 mg polymer per mL.

Conjugation of peptides to polymersomes Tris(2-carboxyethyl)phosphine (0.5 mg, TCEP) was dissolved in PBS of pH 7.4 (300 µL) and added to the peptide (1 mg). The solution was allowed to stand for 15 minutes, after which it was added to 1.5 mL of polymersomes . The coupling was allowed to proceed for three hours, after which the solution was transferred into a dialysis bag (Spectrapore MWCO 12-14 kD) and dialysed against PBS buffer for 24 hours (replacing PBS every 5-10 hours). The zeta potential of the polymersomes was determined by means of DLS (Table 1) and all preparations were tested for hCMEC/D3 cell binding as shown in Figure 8.

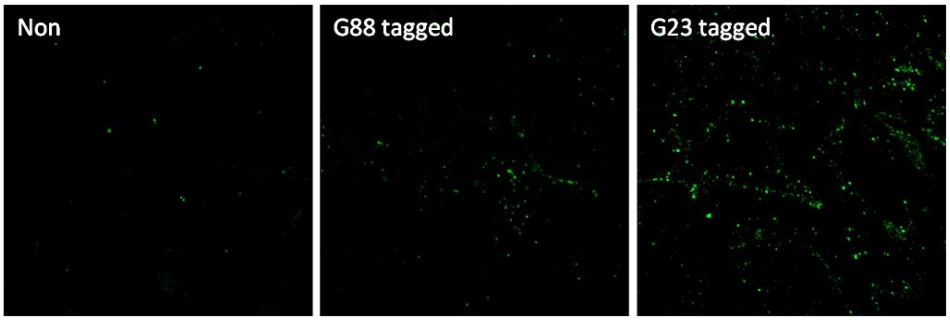

Figure 8. CLSM images revealing association of polymersomes (green fluorescent dots) with a monolayer of hCMEC/D3 cells. Left) Untargeted fluorescein labelled polymersomes. Middle) Polymersomes tagged with 10% G88 and labelled with fluorescein. Right) Polymersomes tagged with 10% G23 and labelled with fluorescein for visualization.

4.5.3 Phage display for selection of GM1-binding peptides

To perform a phage library selection on monosialotetrahexosylganglioside (GM1), GM1-C_{11}-N_3 was covalently coupled to a 96-wells plate via the Cu-catalyzed azide-alkyne cycloaddition, which assures a proper physiological orientation of the oligosaccharide chains[22]. A maleimide-functionalized plate (Thermo Scientific, Waltham, MA) was washed with phosphate buffered saline (3x, PBS (0.1 M Na_2HPO_4, 0.15 M NaCl pH 7.2) and incubated for 2 h at room temperature with 0.5 M propargylamine diluted in immobilization buffer (0.2 M $NaHCO_3$, 0.5 M NaCl, pH 8.0), with refreshing the solution after the first hour. Next, the plate was washed two times with ultrapure sterile water and GM1-C_{11}-N_3 (0.2 µg/well), sodium ascorbate (0.28 µg/well) and $CuSO_4$ (0.3 µg/well), all diluted in water, were sequentially added to the plate. After an overnight incubation at room temperature the plate was washed two times with ultrapure sterile water, followed by adding a small volume of PBS to cover the bottom of the plate, and stored at 4 °C. The coupling reaction was verified with Alexa Fluor 488 labelled cholera toxin B (CTxB-AF488). 0.43 nM CTxB-AF488 was added to the plate, followed by an incubation for 90 min at 37 °C Subsequently, the plate was washed 10 times with PBS and the fluorescence intensity was measured on a Perkin-Elmer LS 500 luminescence spectrometer. The fluorescence signal showed a 1.42-fold increase compared to a 5 mg/mL BSA-treated plate.

Three panning rounds with a premade phage library (Ph.D.-12, BioLabs) encoding peptide 12-mers, were performed according to the manufacturer's protocol. Briefly, each well was incubated with blocking buffer (5 mg/mL BSA in 0.1 M $NaHCO_3$ pH 8.6) for 1 h at 4 °C. After six times washing with Tris-Buffered Saline Tween-20 (TBST, 50 mM Tris-HCl pH=7.5, 0.1% [v/v] Tween-20), 10 µl of a 100-fold dilution of the original library in TBST (2 x 10^9 phage clones) was added to the wells and incubated for 1 h at room temperature with gentle shaking. The plate was washed 10 times with TBST, with an increase in the Tween-20 concentration to 0.5% [v/v] in the second and third panning round, to remove non-bound phages. Phages that were bound to the GM1-coated plate were eluted with 0.2 M Glycine-HCl containing 1 mg/mL BSA (pH 2.2) for 15 min at room temperature. Eluted phages were amplified in ER2738 E.coli, purified, precipitated in PEG/NaCl (20% [w/v] polyethylene glycol-8000, 2.5 M NaCl) or titered on IPTG/Xgal LB plates. After the third panning round, 20 out of the approximately 100 plaques present were randomly chosen and the DNA was isolated. The DNA was precipitated with ethanol from suspensions of

phage pellets in iodide buffer (10 mM Tris-HCl (pH 8.0), 1 mM EDTA, 4 M NaI), according to the manufacturer's protocol for single-stranded phage DNA isolation. The DNA samples were sequenced by BaseClear BV, Leiden, The Netherlands.

4.5.4 In vitro evaluation

hCMEC/D3 cell line maintenance and differentiation A human brain microvessel endothelial cell line, hCMEC/D3, was obtained from Dr. P.O. Couraud (Institut Cochin, Paris, France). Cells were maintained in 25 cm^2 flasks precoated with 100 µg/mL rat tail collagen type I (Cultrex, R&D Systems, Trevigen) in EBM-2 basal medium (Lonza Group, Basel, Switzerland), supplemented with EGM-2-MV bullet kit (Lonza Group, Basel, Switzerland) containing VEGF, R3-IGF-1, hEGF, hFGF-B, hydrocortisone, and 2.5% FBS and 100 µg/mL penicillin/streptomycin. For differentiation of the cells EBM-2 basal medium was supplemented with 1 µM dexamethasone (Sigma, St. Louis, MO) and 1 ng/mL bFGF (Invitrogen, Carlsbad, CA). Cells were maintained at 37 °C under an atmosphere of 5% CO_2.

Incubation of hCMEC/D3 cells with fluorescently labelled phage particles Individual phage clones were amplified according to manufacturer's protocol. Briefly, an overnight culture of ER2738 E. coli was diluted 1:100 and 10 µl of phage stock in glycerol was added to 1 mL of the diluted bacterial culture. The suspension was incubated for 4.5 h under shaking and subsequently centrifuged for 30 sec at 14 000 rpm., the supernatant transferred to a fresh tube and re-centrifuged. In a fresh tube, 1/6 volume of 20% PEG/2.5 M NaCl was added to the upper 80% of the supernatant. Phages were allowed to precipitate at 4°C for 2 hours. The PEG precipitate was spun down at 12,000 g for 15 minutes at 4°C, supernatant decanted, re-spun and residual supernatant removed with a pipette. The phage pellet was re-suspended in 100 µl 0.25 mg/mL FITC (Sigma, St. Louis, MO) in 0.3 M $NaHCO_3$ (pH 8.6). After 1 h of incubation under gentle shaking conditions, 20% PEG/2.5 M NaCl (1/5 of the original volume) was added. The resulting phage suspensions were kept for 30 min on ice and subsequently centrifuged for 10 min at 14 000 rpm at 4 °C. The supernatant, containing unbound FITC, was discarded and the pellet was resuspended in TBS. The precipitation and re-suspension of the phage particles was repeated twice more. The protein content in the final suspension was determined with a NanoDrop 1000 spectrometer (Thermo Scientific, Waltham, MA). Equal amounts of protein (phages) were added to hCMEC/D3 cells, grown on coverslips, and incubated for 2 h at 37°C. Cells were washed with prewarmed hank's buffered salt solution (HBSS) and fixed. Samples were analysed and representative images were acquired, using a Provis AX70 epifluorescence microscope (Olympus corporation, Center Valley, PA).

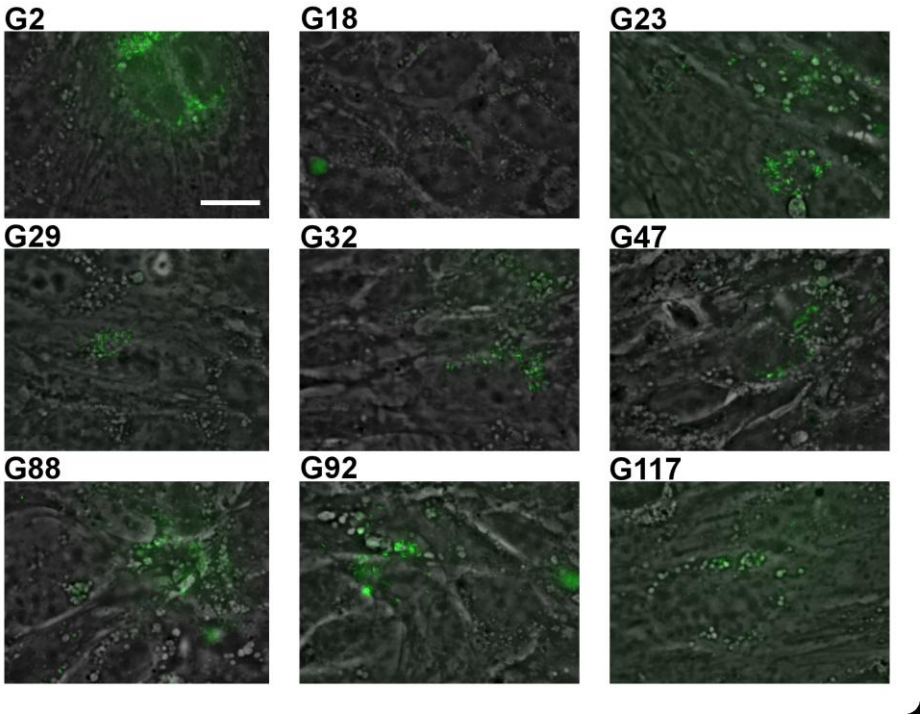

Figure 9. CLSM images of cell binding of fluorescein labelled plagues displaying the peptide sequences as selected in phage display. G88 and G23 were selected for further research based on their cell adhesion and homogeneous patterning.

Transcytosis assay 2 x 10^5 cells/cm^2 were seeded onto Transwell filters with a pore size of 0.4 μm (Corning Life Sciences B.V., Amsterdam, The Netherlands), precoated with collagen type I. Differentiation media was changed twice a week and the transendothelial electrical resistance (TEER) values were measured using a Millicell-ERS (Millipore, Billerica, MA). Experiments were performed in hCMEC/D3 monolayers, cultured for 14 days with TEER values of ~ 30 Ω/cm2. For further details see reference[25].

Fluorescein-labelled polymersomes (40 μg/mL) diluted in EBM-2 medium, were added to the apical compartment and incubated for 16-18 h at 37 °C. The media in the apical and basal compartments were collected and the filter membrane with the cells was separated from the support. Subsequently, the filter was soaked in water to osmotically rupture the cells, resulting in release of the polymersomes. The fluorescence intensity in the three compartments, i.e., apical, basal and filter with cells, was measured with a Perkin-Elmer spectrofluorometer LS500 at the corresponding wavelengths 495 nm (excitation) and 520 nm (emission).

Immunofluorescence detection of cell surface gangliosides in hCMEC/D3 cells, and their colocalization with G23-polymersomes hCMEC/D3 cells were seeded onto glass coverslips, precoated with 100 μg/mL collagen type I, and maintained in differentiation medium. The medium was refreshed when cells reached confluency and the experiments were performed the next day. To detect cell surface exposed glycosphingolipids, live cells were incubated with primary antibodies anti-GD1a 5 μg/mL, anti-GD1b 5 μg/mL, anti-GT1b 20 μg/mL (Seikagaku Corp., Japan) in 1% BSA (PBS) for 30 min, at 10 °C. Cells were fixed with 2.4% paraformaldehyde and incubated with secondary antibodies in the presence of DAPI

and mounted, or alternatively, the medium was aspirated and 40 μg/mL of G23-polymersomes were added for an additional 30 min at 10 °C prior to fixation. The coverslips were mounted onto microscopic slides with Faramount aqueous mounting medium (Dako). Images were acquired with a confocal microscope (Leica TCS SP2 (AOBS), 63x oil objective, NA = 1.4), and processed using ImageJ software (NIH, http://rsb.info.nih.gov/ij). After background correction, the colocalization analysis was performed according to the auto-threshold method. The extent of colocalization is presented as colocalizing pixels between particles and the lipid/protein of interest, divided by the total number of particles' pixels, i.e., percentage of colocalizing pixels.

Dot blot analysis of G23-polymersome binding to isolated gangliosides The binding of G23-polymersomes to isolated gangliosides was determined in a dot blot assay as described in reference[28] with minor modifications. Briefly, 10 μl of a 0.5 μM solution of GM1, and 5 μl of a 1 μM solution of GM2, GM3, GD3, GD1a, GD1b and GT1b gangliosides (Alexis Corporation, Läufelfingen, Switzerland) were spotted onto an immobulon-FL (PVDF) membrane (Millipore Corporation, Billerica, MA). The membrane was incubated with radio-labelled G23-polymersomes (5 μg/mL) in PBS containing 1% BSA for 3h. Upon extensive washing the membrane was air dried, covered with a multipurpose Cyclone phosphor imaging screen (Perkin-Elmer, Downers Grove, IL, USA), and placed in an X-ray film cassette overnight at room temperature. The screen was subsequently analyzed using a Perkin-Elmer Cyclone Storage Phosphor System (Downers Grove, IL, USA). The positions of gangliosides were visualized on the screen by spraying with Ehrlich's reagent (20 mL of 37% hydrochloric acid with 0.6 g of 4-(dimethylamino)-benzaldehyde (Sigma-Aldrich, Steinheim, Germany) solubilised in 80 mL ethanol), and heating at 120 °C for 10 min.

4.5.5 In vivo evaluation

Intracarotid artery injection of G23-polymersomes in mice Male 20–25 g BALB/c mice were obtained from Harlan (Horst, The Netherlands). The mice were kept in standard macrolon cages (26.2 x 42 x 15 cm) under controlled conditions (23 ± 1°C, 12-h light, 12-h dark cycle, pellets (Arie Blok, Woerden, The Netherlands) and water ad libidum). The experiments were approved by the Animal Ethics Committee of the University of Groningen, The Netherlands and performed by licensed investigators in accordance with the Law on Animal Experiments of The Netherlands. Mice were anaesthetized by isoflurane/oxygen. The neck was shaved and the mice were placed under a dissecting microscope. The neck was prepared for surgery with chlorhexidine and the skin was cut by a mediolateral incision. The muscles were separated to expose the right common carotid artery, which was then separated from the vagal nerve. The proximal end of the common carotid artery was clamped with a micro clamp. The tip of a 29 G needle connected to a 0.3 mL syringe was inserted into the carotid artery. The polymersomes were injected over 15 - 20 s (< 0.01 mL/s) in order not to open the blood brain barrier[29]. Following polymersomes administration the needle was retracted, the puncture hole was closed by suture and covered with collagen to prevent any leakage. The micro clamp was removed to establish the blood flow. The skin was closed with ~5 sutures. At the end of the procedure, 0.1 mg/kg buprenorfine (Temgesic) was injected subcutaneously for postoperative pain relief. The animal was kept warm during recovery. The surgical procedure took 15

min/animal. Rhodamine-labelled G23- polymersomes and non-targeted polymersomes were injected in 3 animals each. 24 h after polymersomes administration the mice were sacrificed by carbon dioxide asphyxiation, the brains were isolated, snap frozen in liquid nitrogen and stored at -80 °C until further processing. 8 and 10 µm brain sections were made on a Leica CM 3050 cryostat microtome and mounted onto polylysine microscopic slides (ThermoScientific, Waltham, MA). The sections were air dried for 1 h at room temperature and fixed for 15 min at -20 °C in acetone. After blocking with 10% goat serum in PBS for 1 h at room temperature, the sections were incubated with an antibody against PECAM- 1 (CD31) (MEC 13.3, BD Biosciences) overnight at 4 °C. Alexa Fluor 633 conjugated secondary antibody (Invitrogen Carlsbad, CA) was applied for 2 h at room temperature, together with DAPI. Samples were analyzed with a confocal microscope (BMBME Leica SP2) and a TissueFaxs fluorescence microscope (TissueGnostics, Vienna, Austria).

4.6 References

(1) Pardridge, W. M. *Drug Discov Today* **2007**, *12*, 54.

(2) Duncan, R. *Nat Rev Drug Discov* **2003**, *2*, 347.

(3) Cecchelli, R.; Berezowski, V.; Lundquist, S.; Culot, M.; Renftel, M.; Dehouck, M. P.; Fenart, L. *Nat Rev Drug Discov* **2007**, *6*, 650.

(4) Lee, H. J.; Engelhardt, B.; Lesley, J.; Bickel, U.; Pardridge, W. M. *J Pharmacol Exp Ther* **2000**, *292*, 1048.

(5) Boado, R. J.; Zhang, Y. F.; Zhang, Y.; Pardridge, W. M. *Biotechnol Bioeng* **2007**, *96*, 381.

(6) Ulbrich, K.; Knobloch, T.; Kreuter, J. *J Drug Target* **2011**, *19*, 125.

(7) Garcia-Garcia, E.; Andrieux, K.; Gil, S.; Couvreur, P. *Int J Pharmaceut* **2005**, *298*, 274.

(8) van Rooy, I.; Mastrobattista, E.; Storm, G.; Hennink, W. E.; Schiffelers, R. M. *J Control Release* **2011**, *150*, 30.

(9) Liu, L. H.; Venkatraman, S. S.; Yang, Y. Y.; Guo, K.; Lu, J.; He, B. P.; Moochhala, S.; Kan, L. J. *Biopolymers* **2008**, *90*, 617.

(10) Schwarze, S. R.; Ho, A.; Vocero-Akbani, A.; Dowdy, S. F. *Science* **1999**, *285*, 1569.

(11) Kumar, P.; Wu, H. Q.; McBride, J. L.; Jung, K. E.; Kim, M. H.; Davidson, B. L.; Lee, S. K.; Shankar, P.; Manjunath, N. *Nature* **2007**, *448*, 39.

(12) Discher, B. M.; Won, Y. Y.; Ege, D. S.; Lee, J. C. M.; Bates, F. S.; Discher, D. E.; Hammer, D. A. *Science* **1999**, *284*, 1143.

(13) Brinkhuis, R. P.; Rutjes, F. P. J. T.; van Hest, J. C. M. *Polym Chem-Uk* **2011**, *2*, 1449.

(14) Photos, P. J.; Bacakova, L.; Discher, B.; Bates, F. S.; Discher, D. E. *J Control Release* **2003**, *90*, 323.

(15) Pang, Z. Q.; Gao, H. L.; Yu, Y.; Chen, J.; Guo, L. R.; Ren, J. F.; Wen, Z. Y.; Su, J. H.; Jiang, X. G. *Int J Pharmaceut* **2011**, *415*, 284.

(16) Pang, Z. Q.; Lu, W.; Gao, H. L.; Hu, K. L.; Chen, J.; Zhang, C. L.; Gao, X. L.; Jiang, X. G.; Zhu, C. Q. *J Control Release* **2008**, *128*, 120.

(17) Liu, J. K.; Tenga, Q. S.; Garrity-Moses, M.; Federici, T.; Tanase, D.; Imperiale, M. J.; Boulis, N. M. *Neurobiol Dis* **2005**, *19*, 407.

(18) Anraku, Y.; Kishimura, A.; Kobayashi, A.; Oba, M.; Kataoka, K. *Chem Commun* **2011**, *47*, 6054.

(19) Brinkhuis, R. P.; Stojanov, K.; Laverman, P.; Eilander, J.; Zuhorn, I. S.; Rutjes, P. J. T.; Hest, J. C. M. *Bioconjugate Chemistry* **2012**, *xx*, xxx.

(20) Costantino, L.; Gandolfi, F.; Tosi, G.; Rivasi, F.; Vandelli, M. A.; Forni, F. *J Control Release* **2005**, *108*, 84.

(21) Sprenger, R. R.; Fontijn, R. D.; van Marle, J.; Pannekoek, H.; Horrevoets, A. J. G. *Biochem J* **2006**, *400*, 401.

(22) Pukin, A. V.; Weijers, C. A. G. M.; van Lagen, B.; Wechselberger, R.; Sun, B.; Gilbert, M.; Karwaski, M. F.; Florack, D. E. A.; Jacobs, B. C.; Tio-Gillen, A. P.; van Belkum, A.; Endtz, H. P.; Visser, G. M.; Zuilhof, H. *Carbohyd Res* **2008**, *343*, 636.

(23) Wang, S. Q.; Humphreys, E. S.; Chung, S. Y.; Delduco, D. F.; Lustig, S. R.; Wang, H.; Parker, K. N.; Rizzo, N. W.; Subramoney, S.; Chiang, Y. M.; Jagota, A. *Nat Mater* **2003**, *2*, 196.

(24) Weksler, B. B.; Subileau, E. A.; Perriere, N.; Charneau, P.; Holloway, K.; Leveque, M.; Tricoire-Leignel, H.; Nicotra, A.; Bourdoulous, S.; Turowski, P.; Male, D. K.; Roux, F.; Greenwood, J.; Romero, I. A.; Couraud, P. O. *Faseb J* **2005**, *19*, 1872.

(25) Georgieva, J. V.; Kalicharan, D.; Couraud, P. O.; Romero, I. A.; Weksler, B.; Hoekstra, D.; Zuhorn, I. S. *Mol Ther* **2011**, *19*, 318.

(26) Ragnaill, M. N.; Brown, M.; Ye, D.; Bramini, M.; Callanan, S.; Lynch, I.; Dawson, K. A. *Eur J Pharm Biopharm* **2011**, *77*, 360.

(27) Federici, T.; Liu, J. K.; Teng, Q.; Yang, J.; Boulis, N. M. *Neurosurgery* **2007**, *60*, 911.

(28) Chabraoui, F.; Derrington, E. A.; Malliedidier, F.; Confavreux, C.; Quincy, C.; Caudie, C. *J Immunol Methods* **1993**, *165*, 225.

(29) Fredericks, W. R.; Rapoport, S. I. *Stroke* **1988**, *19*, 266.

5

Brain and Organ Distribution of G23, Scrambled G23 and RI7217 Tagged Polymersomes

In the previous chapter we developed a small peptide (G23) tagged polymersome that is able to efficiently cross the blood brain barrier in an in vitro model by recognition of ganglioside GM1 and GT1b. Furthermore we showed that these polymersomes are able to cross the blood brain barrier into brain parenchyma in vivo. In vivo and in vitro transport was either analyzed by means of fluorescence spectroscopy or confocal laser scanning microscopy of fluorescently labelled polymersomes. A more quantitative method to analyze biodistributions proceeds by means of radiolabelling as employed in Chapter 3. In this chapter, we compare the biodistribution of G23, scrambled G23 and RI7217 tagged polymersomes in the most relevant organs and different regions of the brain via the method of radioisotope labelling. We demonstrate that G23 polymersomes indeed show enhanced accumulation in the brain, albeit that also in the lungs a 15 fold increase in accumulation was observed. These findings underline that G23 tagged polymersomes might be promising carriers for brain targeting, but also suggest that application in lung tissue targeting is feasible.

Katica Stojanov, Julia Georgieva†, René P. Brinkhuis†, Erik F. J. de Vries, Floris P. J. T. Rutjes, Jan C. M. van Hest and Inge S. Zuhorn *Molecular Pharmaceutics* **2012**, 9, 1620-1627

† Equal contribution

5.1 Introduction

One of the major challenges in medicinal chemistry is the development of drugs or drug-formulations that are able to cross the blood-brain barrier (BBB)[1]. The effective treatment of many brain-related diseases is hampered by the presence of this polarized layer of endothelial cells that physically separates blood from brain tissue[2]. Furthermore most conventional drug candidates lack stability and/or bioavailability[3], or once having reached the brain side are cleared by multidrug receptors on the endothelial cell surface[1]. The field of nanomedicine may offer solutions to overcome these obstacles by making devices available such as nanocarriers providing options for tissue-targeted delivery of therapeutics and local release of drugs.

Various targeting moieties and targeting sites have been employed to induce transport of liposomes over the BBB[4]. However, in a recent comparative study van Rooy *et al*.[5] showed that most peptides and proteins are rather ineffective in inducing this transport. The most widely applied targeting moiety in literature is transferrin antibody RI7217, which in combination with transferrin and insulin have also been employed to target polymersomes over the BBB[6-7].

In Chapter 4 we described the development of a dodecamer peptide tagged polymersome that is able to cross the blood brain barrier both *in vitro* and *in vivo*. This report was the first to describe transport of polymersomes over the BBB by a small, 1645 g/mol, peptide which recognizes ganglioside GM1 and GT1b as targeting site. The polymersomes were visualized either by fluorescence spectroscopy or by confocal laser scanning microscopy. Although this analysis method provides a good impression of the efficiency with which polymersomes can cross the BBB into the brain parenchyma, it does not allow for a quantitative determination. A method that does so for biodistribution is radioisotope labelling, as we showed in Chapter 3 for differently sized polymersomes.

In this chapter we analyze *in vivo* biodistributions of polymersomes conjugated with G23 peptide, scrambled G23 peptide (Scr) and RI7217 by means of ^{111}In radioisotope labelling. After 24 hours, G23 tagged polymersomes showed increased brain accumulation by a factor of 5.8 compared to polymersomes bearing the scrambled G23 sequence. Polymersomes tagged with the 90 kg/mol RI7217 antibody showed a 10.3 fold increase in brain accumulation. The most striking result was found in the

biodistribution over the organs. G23 polymersomes gave a 15 fold increase in lung accumulation compared to polymersomes tagged with the scrambled G23 sequence. These data underline that G23-functionalized polymersomes are promising for targeted delivery over the BBB, although application in lung tissue targeting might be another viable option.

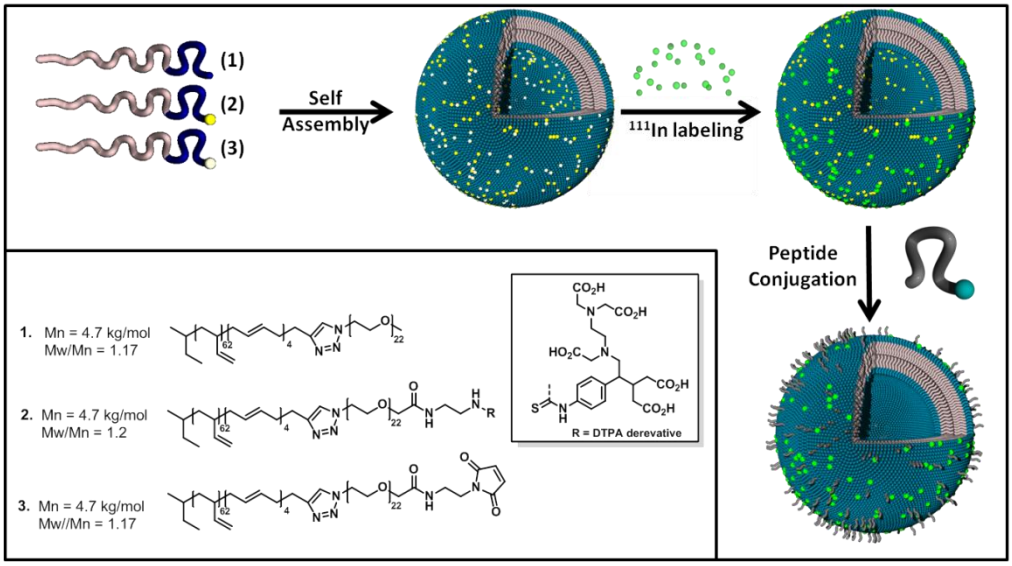

Figure 1. Polymersomes were self assembled from 89 w% (**1**), 1 w% (**2**) and 10 w% (**3**). After self assembly the polymersomes were labelled with radioactive ^{111}In and conjugated with peptide G23, Scr or transferrin antibody RI7217. Next, biodistributions were determined in male Balb/c mice.

5.2 Results and Discussion

The block copolymers used in this study are depicted in Figure 1 and are equal to the polymers described in Chapters 2 and 3. This Figure shows that polymersomes were formed from a mixture of polymers **1**, **2** and **3** in a ratio of 89:1:10 followed by ^{111}In labelling and finally peptide conjugation. It should be noted that switching the order of events led to a poor ^{111}In labelling efficiency.

Peptides G23 and Scr were synthesized via Fmoc chemistry[8] with a C-terminal cysteine for conjugation, only the monoclonal antibody RI7217 did not contain a free accessible cysteine. Therefore on average 3.1 thiols - as determined via Ellman's reagent - were introduced by means of a standard SATA modification[9]. The formation of polymersomes was accomplished via the solvent switch method, starting from a solution of 10 mg polymer in 0.2 mL THF. After the addition of 0.6 mL 2-(*N*-morpholino)ethanesulfonic acid MES buffer (0.1 M, pH 5.5, metal free) polymersomes

were formed as indicated by the opaque colour. The sample was extruded subsequently over 200 and 100 nm membranes to obtain polymersomes of 166 nm with a polydispersity index of 0.12 as determined by dynamic light scattering (DLS) before radiolabelling and conjugation of the targeting moieties. The polymersomes were purified over a Sephadex G200 column, labelled with 25 MBq ^{111}In and subsequently the MES buffer was switched for phosphate buffered saline (PBS, 20 mM, pH 7.4) over a PD10 desalting column. After switching buffers, the peptides or the antibody were coupled to the peripheral maleimide groups via the C-terminal cysteine or SATA moieties, respectively. Finally the samples were dialyzed over night to remove excess of peptide. The ^{111}In labelling efficiency was tested by means of IC-TLC after the initial indium labelling and subsequent dialysis. The radioisotope labelling efficiency was virtually quantitative and appeared stable towards dialysis. The polymersomes were diluted with PBS to 1 mg of polymer per mL (0.2 μmol polymer per mL, 2.5 MBq per mL)

After the successful formation of labelled polymersomes, the biodistribution in male Balb/c mice was evaluated by injecting 200 μL of polymersomes in the tail vain. The biodistribution over the main organs was determined as well as the distribution of polymersomes over different parts of the central nervous system (CNS). In Chapter 3 was shown that polymersomes of 120 nm and larger are readily cleared from the blood stream. The current research was performed using polymersomes with an average diameter of 166 nm, which are expected to circulate in the blood stream for less than 4 hours, excluding significant contributions of blood associated polymersomes in different organs to the counts (Table 1).

The observed distribution of polymersomes over the central nervous system is depicted in Figure 2. It shows that the G23 peptide is able to increase the transport of polymersomes into the total brain with a factor of 6.5 (4 hours) and 5.8 (24 hours) as compared to the scrambled sequence of G23. In the cerebellum, cortex and brain rest a similar increase as compared to scrambled G23 was observed, which in all cases was statistically relevant. This underlines the specificity of the native G23 sequence to enhance blood brain barrier transport. We also included RI7217 tagged polymersomes in this study, since RI7217 is the most widely employed targeting moiety in literature. Compared to the scrambled G23 sequence, polymersomes tagged with this antibody showed a 10 fold increase in total brain accumulation after 24 hours. Furthermore,

0.096 % ID/g was found to be associated with the total brain, a number that is in agreement with previous reports on polymersomes in male Balb/c mice[6].

Upon comparing G23 and RI7217 targeted polymersomes a clear trend becomes apparent from Figure 2. In all CNS domains, the RI7217 tagged polymersomes seem to perform better than the G23 tagged polymersomes. However, the difference in brain distribution is not statistically significant after 4 hours, while after 24 hours the accumulation in the cortex and brain rest is significantly lower for G23 polymersomes, but not for the total brain and cerebellum.

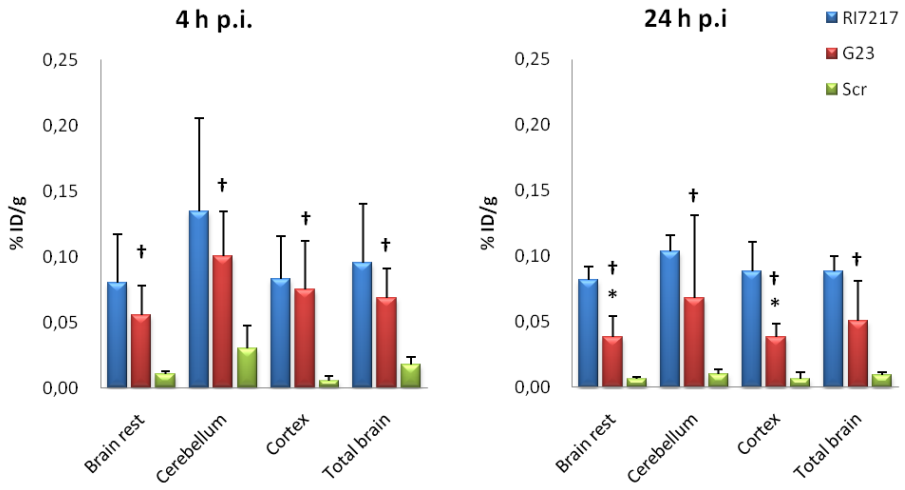

Figure 2. Biodistribution at 4 and 24 hours post injection (p.i.) of RI7217, G23 and Scr tagged polymersomes over different parts of the central nervous system in male Balb/c mice (n = 4, 9 weeks of age, 20-23 gram). †) Statistically significant difference as compared to Scr as calculated for G23, and *) statistically significant difference compared to RI7217 as calculated for G23.

	RI7217	scrG23	G23
Tissue		Tissue biodistribution at 4h	
Blood	1.695 + 0.749	0.347 + 0.029	1.324 + 0.336
Bone	1.567 + 0.552	1.338 + 0.110	2.209 + 0.973
Kidney	4.433 + 1.344	2.738 + 0.449	8.809 + 2.569
Liver	37.136 + 23.342	64.653 + 6.715	60.556 + 7.531
Lung	4.235 + 3.164	1.752 + 0.162	30.449 + 5.785
Muscle	0.315 + 0.146	0.157 + 0.115	0.360 + 0.119
Spleen	33.522 + 17.722	55.439 + 13.820	57.781 + 9.734
Total brain	0.074 + 0.036	0.013 + 0.006	0.052 + 0.019
		Tissue biodistribution at 24h	
Blood	0.402 + 0.061	0.088 + 0.020	0.299 + 0.078
Bone	3.770 + 1.002	1.626 + 0.336	2.922 + 0.507
Kidney	3.985 + 0.689	1.804 + 0.294	6.548 + 0.667
Liver	38.004 + 6.716	56.899 + 4.717	51.500 + 4.769
Lung	1.629 + 0.480	0.464 + 0.319	13.701 + 2.850
Muscle	0.516 + 0.107	0.103 + 0.036	0.279 + 0.063
Spleen	49.783 + 7.024	77.248 + 20.053	99.132 + 37.451
Total brain	0.083 + 0.011	0.008 + 0.002	0.047 + 0.031

Table 1. Biodistribution of polymersomes tagged with G23, Scr and RI7217 after blood volume correction as described in the experimental section.

Comparison of *in vivo* transport over the blood brain barrier with other targeted nanocarriers reported in literature is not straightforward, since the animal model,

method of administration and type/size of nanocarrier will influence the experimental outcome. However, in a recent literature study by van Rooy *et al.*[4], it was summarized that most targeted carriers show a 2 to 3 fold increase in BBB transport. Among the small peptides, Tat-peptide coupled to poly(lactic-co-glycolic acid) nanoparticles showed a most prominent (6.5 fold) increase in brain uptake in mice[10], followed by a 4.9 fold for the nine amino acid bradykinin agonist peptide RMP-7 targeted liposomes in rat[11]. This suggests that G23 targeted polymersomes are among the most efficient peptide targeted nanocarriers reported to date.

We also analyzed the biodistribution of targeted polymersomes over all main organs and corrected them for blood values[12] (Table 1). As anticipated – since we applied polymersomes of 166 nm – after 4 and 24 hours almost all polymersomes were cleared from the blood stream and accumulated in the liver and spleen. However, as depicted in Figure 3, the G23 tagged polymersomes revealed an interesting deviation from the expected distribution in the lung tissue. Compared to the scrambled sequence of G23, polymersomes tagged with native G23 showed a statistically significant 15 fold increase in lung association. This data again underlines the specificity of the sequence of G23 peptide in targeting, since the scrambled sequence did not show deviation from the expected biodistibution (Chapter 3). Interestingly, this finding opens up new opportunities for the application of G23 targeted polymersomes in lung tissue targeting.

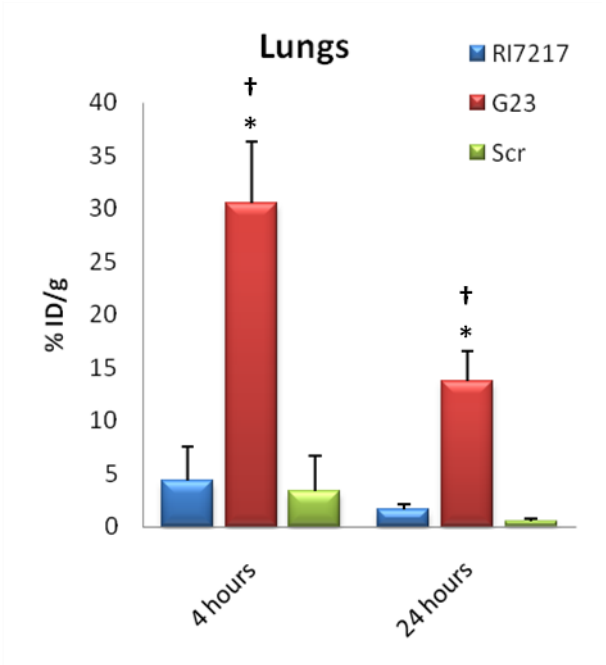

Figure 3. Biodistribution at 4 and 24 hours post injection (p.i.) of RI7217, G23 and Scr tagged polymersomes over lung tissue in male Balb/c mice (n = 4, 9 weeks of age, 20-23 gram). †) Statistically significant difference compared to Scr as calculated for G23, and *) statistically significant difference compared to RI7217 as calculated for G23.

The biodistribution of polymersomes tagged with RI7217 did not reveal any significant deviations. This is in agreement with considerations in literature behind the choice for RI7217 in BBB targeting research. Although other transferrin antibodies have been reported to cross the BBB more efficiently, RI7217 has the highest specificity,[5] i.e. does not target other tissues.

5.3 Conclusion and Perspective

G23 tagged and radio-labelled polymersomes were designed for GM1 (and GT1b) mediated brain targeting and indeed show a significant increase in brain accumulation. Compared to RI7217 tagged polymersomes, G23 labelled polymersomes accumulate to a slightly lower extent in the brain than RI7217 tagged polymersomes. Although no direct comparison could be made, G23 tagged polymersomes can cross the BBB rather efficiently compared to other small peptide targeted nanocarriers reported in literature. In addition, the lung association of G23 tagged polymersomes appeared substantial with a 15 fold increase compared to the scrambled sequence of G23. Hence, polymersomes tagged with G23 peptide may also have potential for targeted drug delivery to the lungs.

With respect to future experiments, it may be worthwhile to reconsider the size of the polymersomes applied. If the nanocarrier is circulating longer in the blood, the chances of transport either over the blood brain barrier or to the lungs might be higher. Furthermore it would be interesting to look beyond the design of G23 targeted polymersomes into the method of administration. Perhaps, it is possible to favour BBB transport over lung accumulation by injecting G23 targeted polymersomes into the intracarotid artery as was performed in Chapter 4.

5.4 Acknowledgement

Katica Stojanov is acknowledged for her work on the animal studies. Erik de Vries is acknowledged for allowing me to work 1-2 days a week for 2½ months in the labs of nuclear medicine at the University Medical Center Groningen.

5.5 Experimental Procedures

Radiolabelled, maleimide displaying polymersomes Polymers **1** (9 mg, 1.9 μmol), **2** (0.1 mg, 0.02 μmol) and **3** (1 mg, 0.2 μmol) were dissolved in THF (200 mL). Polymersomes were formed by slow addition of 0.6 mL 0.1 M 2-(*N*-morpholino)ethanesulfonic acid (MES) buffer of pH 5.5. The samples were passed three times through a 200 nm syringe filter to yield polymersomes of approximately 250 nm. The solution was extruded six times over a 100 nm filter (extrusion kit) to obtain polymersomes of around 160 nm. The resulting opaque suspension was purified over a Sephadex G200 column (1.5 x 8 cm), eluting with MES buffer. The opaque fractions were combined and the mean particle size was determined by DLS.

25 MBq of ^{111}InCl was added to the polymersomes and allowed to chelate for 20 minutes, after which the coupling efficiency was analyzed by Instant Thin-Layer Chromatography Silica Gel impregnated glass fibre (ITLC-SG) strips, developed in 0.1 M NH_4Ac (pH 5.5)/0.1 M EDTA (1:1, v/v). The sample was purified over a PD10 desalting column, eluted with PBS buffer pH 7.4, and diluted with PBS to a total volume of 10 mL, i.e. a polymersome suspension containing 1 mg of polymer per mL (2.5 MBq per mL).

Conjugation of peptides to polymersomes A solution of tris(2-carboxyethyl)phosphine (TCEP, 0.5 mg) was dissolved in PBS (300 μL) of pH 7.4 and added to the peptide (1 mg, excess to maleimides). The solution was allowed to stand for 15 minutes, after which it was added to 1.5 mL of the polymersomes. The coupling was allowed to proceed for three hours, after which the solution was transferred into a dialysis bag (Spectrapore MWCO 12-14 kDa) and dialysed against PBS buffer for 12 hours.

Conjugation of RI7217 to polymersomes RI7217 antibody was coupled to maleimide polymersomes by a sulfhydryl-maleimide coupling technique as described previously[9] with minor modifications. Free sulfhydryl groups were introduced into the antibody using *N*-succinimidyl-*S*-acetylthioacetate, (SATA. Free SATA was separated from the antibody by centrifugation over a filter with a 30 kDa cut-off (MWCO). SATA groups were deacetylated for 90 min at room temperature by addition of 100 μl of deacetylation solution (0.1M PBS, 0.5M hydroxylamine and 0.02 mM TCEP, pH 7.4) per millilitre of antibody to generate sulfhydryl groups. This resulted in an SH/protein (mol/mol) ratio of 3.1 as determined by Ellman's reagent assay. After deacetylation, the RI7217 antibody was allowed to react with ^{111}In-labelled maleimide polymersomes overnight at 4°C.

Radio TLC Quality control of the coupling of ^{111}In to the polymersomes was performed by spotting 5 μL of the polymersome preparation on an ITLC-SG strip. TLC strips were developed with 0.1 M ammonium acetate (pH 5.5)/0.1 M EDTA (1:1, v/v) as the eluent. After development, the strips were air-dried and read in a VCS-103 radiochromatograph scanner (AmRay Medical, Drogheda, Co.Louth, Ireland). Regions of interest were drawn for ^{111}In-labelled polymersomes (Rf value: 0) and unbound ^{111}In (Rf value: 0.8-0.9), and the relative amounts of these compounds for each sample were

measured. Efficiency of ^{111}In-labelling of polymersomes was >95% and ^{111}In-labelled polymerisomes were stable at room temperature for more than 10 days. Nevertheless, ^{111}In-labelled polymersomes were freshly prepared for each set of *in vivo* experiments.

Tissue biodistribution of functionalized polymersomes Male Balb/c mice were obtained from Harlan (Horst, The Netherland). The mice were kept in standard macrolon cages under controlled conditions (23 ± 1°C, 12-h light, 12-h dark cycle, chow (Arie Blok, Woerden, The Netherlands) and water ad libidum). All experiments were approved by the Animal Ethics Committee of the University of Groningen, The Netherlands and performed by licensed investigators in accordance with the Law on Animal Experiments of The Netherlands. Mice (n = 4) were injected with 200 µl of radio-labelled polymersomes (ca. 180 ug polymer per mouse = 38 nmol polymer / mouse; ca. 0.5 MBq) in PBS by penile vein injection using a 3 / 10 cc Terumo Insulin Syringe U-100 attached to a 29 G needle. At 4 and 24 h after injection, the mice were sacrificed by cervical dislocation. At each time point the kidney, brain, liver, lung, muscle, spleen, and femur (containing bone marrow) were collected, and a blood sample was drawn. The brain was divided into the cerebrum and cerebellum. The cerebrum was subdivided into cerebral cortex and brain rest. The samples were weighed and the radioactivity was measured using a Compugamma CS 1282 gamma counter (LKB-Wallac, Turku, Finland). The radioactivity levels in the injected polymersome solutions served as internal standards. The results were expressed as percentage injected dose per gram of tissue (%ID/g). Where indicated, tissue levels were corrected for capillary blood content[12] using the formula: corrected tissue concentration = [organ concentration – (capillary blood content x blood concentration)] / (1 – capillary blood content), where the tissue capillary blood content is expressed as a fraction of the organ volume, which approximates for bone, brain, kidney, liver, lung, muscle and spleen to 0.11, 0.03, 0.24, 0.31, 0.50, 0.04 and 0.17, respectively)[13].

Statistical analysis Results are presented as mean + standard deviation. The statistical analysis was conducted using SPSS 16.0 for Windows. Due to inhomogeneity of variance the biodistribution data were analyzed by the nonparametric Kruskal-Wallis test, followed by the Mann-Whitney U test to compare the groups for which the Kruskall-Wallis test was significant. P values < 0.05 were considered statistically significant.

5.6 Notes and references

(1) Cecchelli, R.; Berezowski, V.; Lundquist, S.; Culot, M.; Renftel, M.; Dehouck, M. P.; Fenart, L. *Nat Rev Drug Discov* 2007, *6*, 650.

(2) Pardridge, W. M. *Drug Discov Today* 2007, *12*, 54.

(3) Duncan, R. *Nat Rev Drug Discov* 2003, *2*, 347.

(4) van Rooy, I.; Cakir-Tascioglu, S.; Hennink, W. E.; Storm, G.; Schiffelers, R. M.; Mastrobattista, E. *Pharm Res-Dordr* 2011, *28*, 456.

(5) van Rooy, I.; Mastrobattista, E.; Storm, G.; Hennink, W. E.; Schiffelers, R. M. *J Control Release* 2011, *150*, 30.

(6) Pang, Z. Q.; Lu, W.; Gao, H. L.; Hu, K. L.; Chen, J.; Zhang, C. L.; Gao, X. L.; Jiang, X. G.; Zhu, C. Q. *J Control Release* 2008, *128*, 120.
(7) Pang, Z. Q.; Gao, H. L.; Yu, Y.; Guo, L. R.; Chen, J.; Pan, S. Q.; Ren, J. F.; Wen, Z. Y.; Jiang, X. G. *Bioconjugate Chem* 2011, *22*, 1171.
(8) Merrifield, R. B. *J Am Chem Soc* 1963, *85*, 2149.
(9) Derksen, J. T. P.; Scherphof, G. L. *Biochim Biophys Acta* 1985, *814*, 151.
(10) Rao, K. S.; Reddy, M. K.; Horning, J. L.; Labhasetwar, V. *Biomaterials* 2008, *29*, 4429.
(11) Zhang, X. B.; Xie, Y.; Jin, Y. G.; Hou, X. P.; Ye, L. Y.; Lou, J. N. *Drug Deliv* 2004, *11*, 301.
(12) Khor, S. P.; Bozigian, H.; Mayersohn, M. *Drug Metab Dispos* 1991, *19*, 486.
(13) Brown, R. P.; Delp, M. D.; Lindstedt, S. L.; Rhomberg, L. R.; Beliles, R. P. *Toxicol Ind Health* 1997, *13*, 407.

6

Shedding the Hydrophilic Mantle of Polymersomes

Block copolymers of polybutadiene-b-poly(ethylene glycol) were prepared in which both segments were coupled via an acid sensitive hydrazone moiety. Polymersomes that were subsequently formed showed a strong pH-dependent colloidal stability as a result of the pH sensitive removal of the PEG block. By mixing this stimulus responsive block polymer with an inert analogue it was possible to systematically remove percentages of PEG from the polymersome mantle. The minimum amount of surface PEGylation needed to retain stable polymersomes was found to be as low as five percent.

René P. Brinkhuis, Taco R. Visser, Floris P.J.T. Rutjes and Jan C. M. van Hest, *Polymer Chemistry*, **2011**, 2, 550-552

6.1 Introduction

Polymeric vesicles, or polymersomes, can be regarded as the polymeric analogues of liposomes. They are formed by the self-assembly of amphiphilic block copolymers in aqueous media[1-2]. Compared to liposomes, polymersomes are characterized by an increased membrane stability and the ability to enclose larger quantities of hydrophobic compounds[2]. This makes them highly interesting for usage as nanocarriers in biomedical applications such as drug delivery and *in vivo* imaging[3]. Nowadays researchers have gained a high degree of control over polymersome composition, size and peripheral functionalities which are all important elements in the design of drug delivery vehicles[4]. An important challenge however remains the triggered release of compounds from the interior of the polymersomes, which requires a controlled destabilization of the membrane.

Destabilization of the particles is often realized by degradation or a triggered change in solubility of one of the blocks[5], but it can in principle also be realized by removal of the stabilizing hydrophilic segment of the amphiphilic block copolymer. This hydrophilic block is in most cases the biocompatible polymer poly(ethylene glycol) (PEG) which introduces stealth-like properties to the nanocarriers when they circulate through the body. Basically it is the shielding of the hydrophobic domain by highly stretched peripheral PEG chains[6] which gives rise to the stability of polymersomes in water. Until now it is however unclear how much PEG is required to maintain a stable colloidal polymeric capsule. To investigate this, a systematic removal of different percentages of PEG from the polymersome surface should be accomplished. This requires the introduction of a triggerable cleavage site between the hydrophobic and hydrophilic parts of the block copolymer that constitutes the polymersome membrane.

Different block copolymer cleavage methods have already been reported, based on UV light[7-8], reduction[9-14] or oxidative and enzymatic pathways[15]. Site selective acidic cleavable block copolymers reported today make use of a triphenyl ether linker[16], a cyclic ortho ester[17] or cis aconitic acid[18]. All other acid labile systems are based on random hydrolysis[19-22]. An interesting pH cleavable moiety for block copolymer cleavage is the hydrazone linkage. This functionality is well known for its strong acid dependent stability in the physiological pH range[23-25]. Hydrazones have been used in the field of liposomal delivery systems as cleavable linkers between PEG chains and

surface peptides in order to hide the peptides up to the moment of cellular uptake[26]. In another example Kataoka *et al.* showed the efficient release of drugs, conjugated via hydrazone bonds, from polymeric micelles upon lowering the pH to endosomal levels[27]. Amphiphilic block copolymers of which the hydrophobic and hydrophilic parts are connected by the pH sensitive hydrazone linkage have very recently been reported to form pH responsive aggregates in aqueous solution[28].

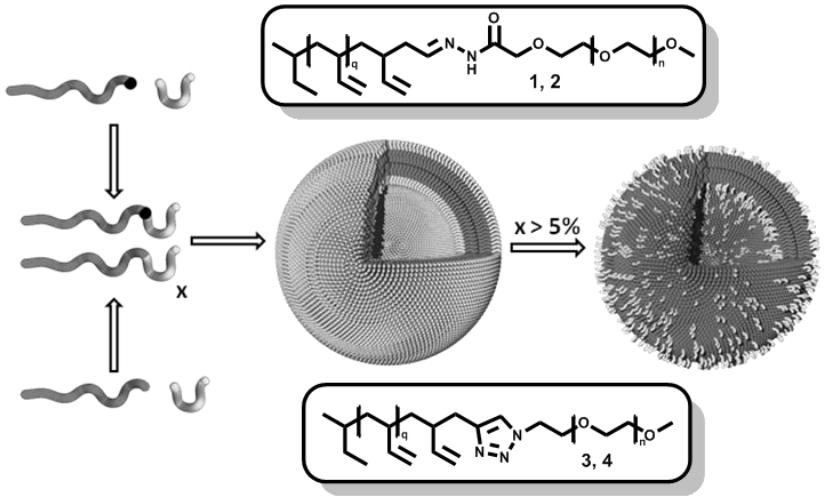

Figure 1. Formation of an inert and an acid labile amphiphilic block copolymer via hydrazone formation (**1**, **2**) and click chemistry (**3**, **4**), respectively. These polymers readily form polymersomes. Lowering the pH will hydrolyse the hydrazones, shedding the poly(ethylene glycol) shell. This will either result in fully disrupting the vesicle or reducing the degree of polymersome PEGylation.

In this chapter the controlled colloidal destabilization of polymersomes formed by the self assembly of amphiphilic block copolymers of polybutadiene-b-poly(ethylene glycol) (PBd-b-PEG) is investigated. By using different combinations of an inert amphiphilic block copolymer and PBd-b-PEG of which both parts are connected by a hydrazone linker, the minimum amount of PEG needed for stabilization is determined. We show that it is possible to take away 95 percent of peripheral PEG chains by lowering the pH, without disrupting the colloidal stability of polymersomes. Furthermore, we can tune the speed of polymersome degradation by adjusting the PEG chain length. This research therefore adds a new element to the methods available to control polymersome stability and gives new insights in the stabilizing power of PEG chains on the polymersome surface. An overview of the procedure followed is depicted schematically in Figure 1.

6.2 Results and Discussion

Hydrazone coupled block copolymers **1** and **2** were synthesized as depicted in Scheme 1. Polybutadiene was synthesized by means of anionic polymerisation and terminated with a protected aldehyde, diethyl chloroacetal[29]. PEG with a molecular weight of 1 and 2 kg/mol was modified into a hydrazide to obtain **8** and coupled to aldehyde end-capped polybutadiene **6** by hydrazone formation. Stable block copolymers **3** and **4** were prepared as described in Chapter 2. In figure 2 the size exclusion chromatograpy (SEC) results of the coupling via hydrazone formation are depicted as analyzed for polymer **1**. This reaction proceeded readily in dichloromethane without the addition of a catalyst. The desired block copolymers were in all cases obtained with a polydispersity index well below 1.2 as determined by SEC.

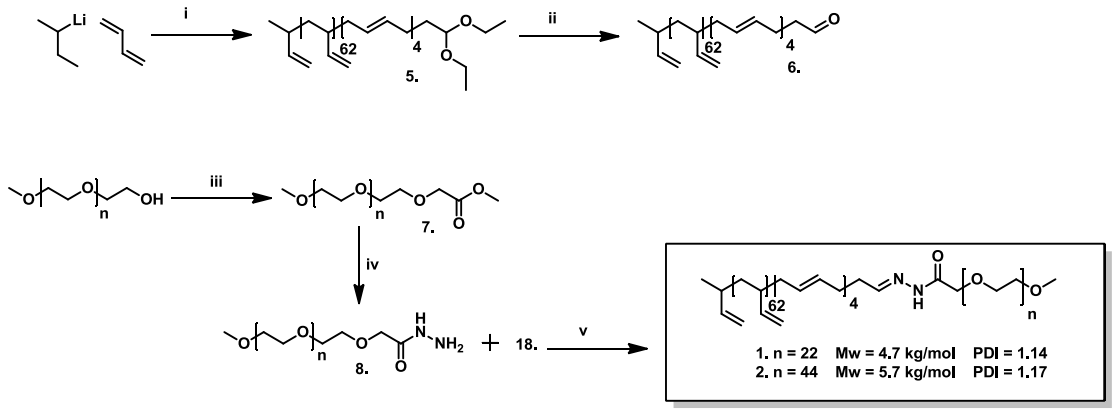

Scheme 1. Synthetic route to hydrazone coupled block copolymers **1** and **2**. i) anionic polymerisation of 1,3 butadiene and endcapping ii) deprotection of aldehyde. iii) PEG methyl ester formation and iv) PEG hydrazine formation v) coupling of polybutadiene and poly(ethylene glycol) by hydrazone formation.

To determine the pH sensitivity it was investigated whether the obtained hydrazone-functional polymers could be fully cleaved at low pH, or whether an equilibrium between polymer **1/2** and their cleaved products was obtained. For this purpose polymers **1** and **2** were assembled into polymersomes, after which the pH was lowered to 4.4. Subsequent TLC analysis showed no traces of the block copolymer, only the free PEG and polybutadiene blocks were observed. These results were confirmed by SEC analysis. As can be observed from Figure 2 no significant amount of block copolymer was present after one hour incubation at pH 4.4.

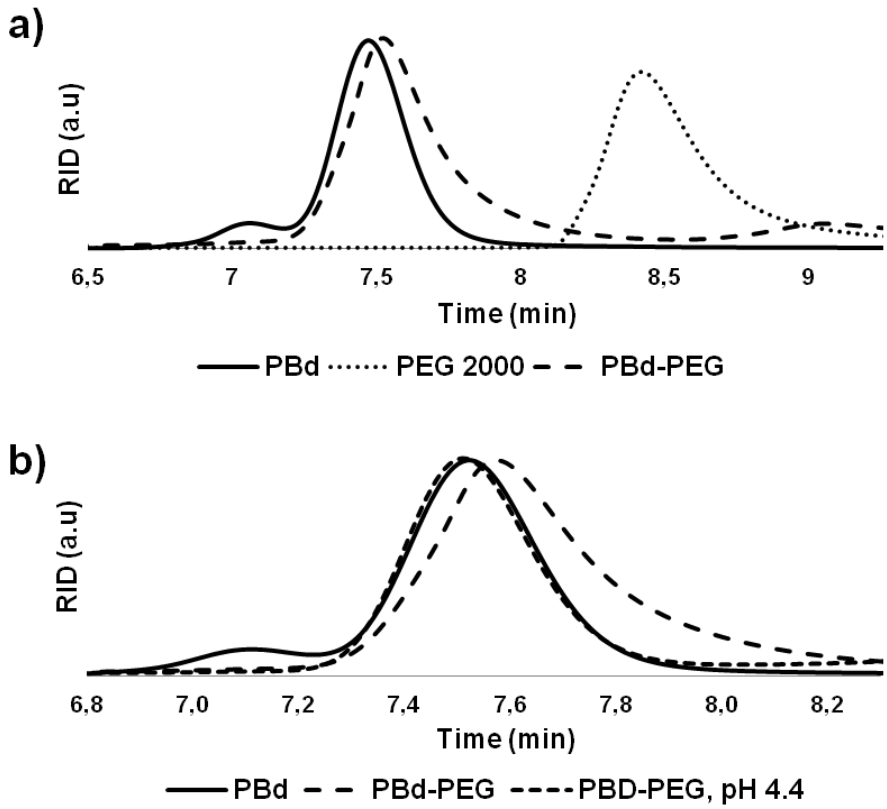

Figure 2. SEC traces of a) Coupling of polybutadiene and PEG via hydrazone formation. b) After incubation of 2 at pH 4.4 the original polybutadiene chain is obtained back.

The pH dependent stability of polymersomes, assembled fully from cleavable polymers **1** or **2**, was evaluated next. A standard solution of extruded polymersomes with an average diameter of around 200 nm was prepared. The pH of this solution was 7.5, so no significant hydrolysis could take place in the time frame of sample preparation (see Figure 3a). After injection of a polymersome sample in buffers ranging in pH, the size distribution was monitored over time by dynamic light scattering (DLS). This method was useful to study destabilization of the polymersomes, since we envisioned that whenever enough PEG was cleaved off, the bare polybutadiene would start to aggregate and form larger, more polydisperse aggregates which eventually would phase separate with water. The DLS results as depicted in Figure 3 show two trends. First of all Figure 3a shows how below pH 5.4 polymersomes assembled from **1** lost their stability within one hour and started to aggregate, whereas at physiological pH (7.4) the vesicles were stable in solution for more than three days. Secondly, the DLS curves plotted in Figure 3b show a marked difference in destabilization rate between PBd-b-PEG **1** and **2** while incubating in the same buffer, pH 6.4. Whereas polymersomes composed of **1**, with the shorter PEG block of 1 kg/mol, started to aggregate after three hours, the time

needed to induce aggregation of polymersomes composed of **2**, with a PEG length of 2 kg/mol was more than doubled. These results suggest that the time dependent stability of these polymeric vesicles can be tuned by adjusting the block copolymer composition. Furthermore, these polymersomes are stable at physiological pH but readily aggregate under slightly acidic conditions. What is not clear from these results is whether the gain in stability is a result of slower hydrolysis or better shielding, if longer peripheral PEG chains are applied.

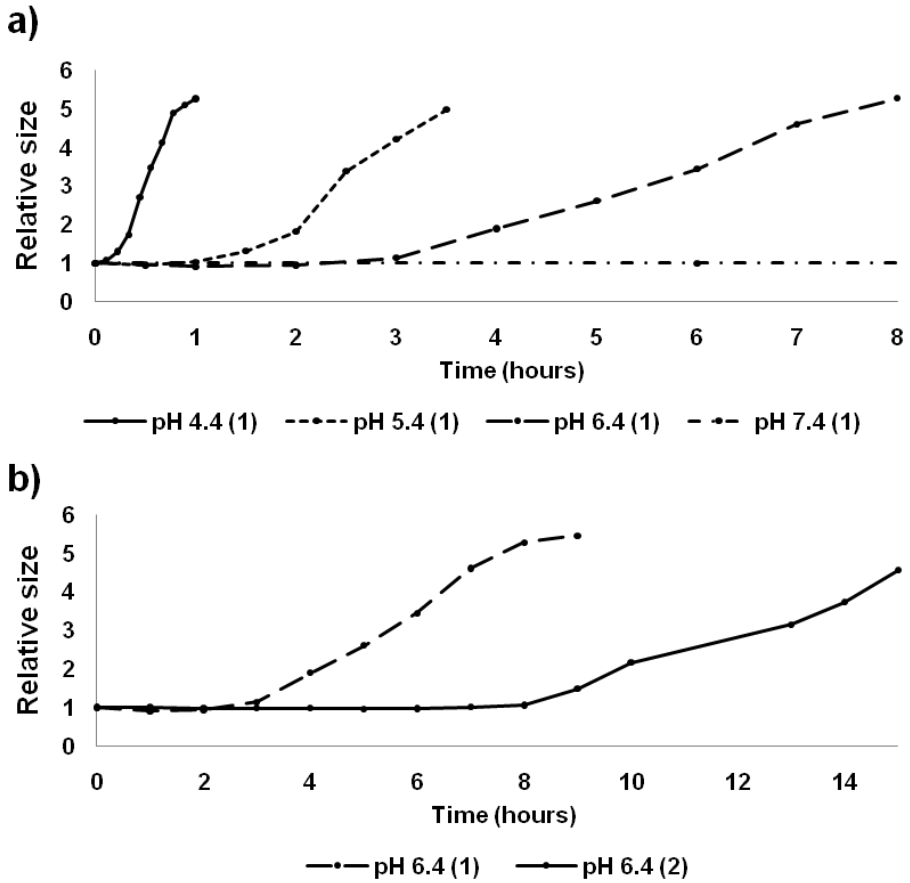

Figure 3. a) Relative size distribution of polymersomes composed of 1 as a function of time in hours upon incubation in buffers of different pH. **b)** Relative size distribution of polymersomes composed of 1 and 2 at pH6.4 as a function of time in hours.

Via this experiment it is also not possible to determine the composition of the vesicles at the point where aggregation starts to occur. It is actually the bending point in the graph which is interesting because this reflects the composition in which there is just enough PEGylation left to stabilize the polybutadiene sphere. To estimate the polymersome composition at the bending points we decided to prepare mixed polymersomes composed of an inert amphiphilic block copolymer (**3** or **4**) and

a pH sensitive one (**1** and **2**). Furthermore, in the previous section we showed that at pH 4.4 block copolymers **1** and **2** are fully cleaved and there is no sign of an equilibrium.

We therefore exposed the mixed polymersomes to a medium with a pH of 4.4. At this point all cleavable PEG chains were removed, leaving a polybutadiene bilayer displaying only the non cleavable PEG chains as drawn in Figure 1. After three days all samples were re-measured with DLS to check whether the particle size remained the same or aggregation had occurred. These measurements were performed for both the 1 kg/mol PEG and 2 kg/mol PEG analogues for which the results are depicted in Table 2. All samples were stable even after cleaving off 90 percent of the PEG chains. The first sample to become unstable consisted of polymersomes that had a ratio of 95 percent **1** to 5 percent of **3**. This actually means that a little more than 5 percent PEGylation with PEG of 1 kg/mol is enough to stabilize the polybutadiene sphere. Upon doubling the chain length to PEG of 2 kg/mol we were able to remove more than 95 percent of the periphery without disrupting the system. This means that when longer PEG chains are employed even less than 5 percent PEGylation will efficiently stabilize these polymersomes.

Table 2. Average size of mixed vesicles **1** with **3** and **2** with **4**. In all cases the DLS revealed a polydispersity well below 0.1 and a derived count rate of ±6000 kcps, except for the unstable ones printed in bold, for which the polydispersity becomes large (>0.6) and the derived count-rate small (<500 kcps).

	Time(h)	**0%**	**85%**	**90%**	**95%**	**100%**
PEGylation 1kg/mol	0	227	230	239	226	208
	72	234	220	247	**2000+**	**2000+**
PEGylation 2kg/mol	0	208	212	251	223	201
	72	208	215	244	242	**2000+**

Although this low amount of PEGylation needed to stabilize polymersomes surprised us at first, it can easily be rationalized by considering generally known systems. In liposomal formulation it is common to introduce five to ten percent PEGylation to induce longer blood circulation times by blocking all interactions with the environment. Furthermore it has been shown for cationic lipid vesicles that ten percent of PEGylation is enough to block all cell interactions, basically shielding a

positively charged bilayer from its surrounding[30]. Finally a theoretical study by Smart *et al* showed how only a very limited amount PEG chains can cover a surface by either adopting a mushroom or a fully stretched shape depending on the PEG density[6].

6.3 Conclusion

We have constructed polymersomes composed of a mixture of stable and pH sensitive, cleavable PBd-b-PEG amphiphilic block copolymers. With these mixed polymersomes we were able to determine the minimum amount of poly(ethylene glycol) needed for stabilization. At physiological pH these polymersomes retained their colloidal stability for at least three days. Under slightly acidic conditions polymersome stability was only lost when the degree of PEGylation was lowered to 5%. This percentage could be even further decreased by doubling the poly(ethylene glycol) molecular weight.

6.4 Acknowledgement

Taco R. Visser is acknowledged for his help in synthesis during his bachelor internship.

6.5 Experimental Procedures

General note All reactions are described for the lower molecular weight analogue, polyethylene glycol with a molecular weight of 1 kg/mol. The procedures for the poly(ethylene glycol) with a molecular weight of 2 kg/mol were identical and performed with equimolar amounts. The synthesis of polymers **3** and **4** is described in Chapter 2.

Materials Sec-butyllithium (ALDRICH 1.4M in hexane), 1,3 butadiene (SIGMA ALDRICH, 99+%), polyethylene glycol 1000 monomethyl ether (FLUKA), polyethylene glycol 2000 monomethyl ether (FLUKA), sodium hydride (ALDRICH, 60% dispersion in mineral oil), hydrazine (ALDRICH, 1M in THF) were used as received. Tetrahydrofuran (THF) (ACROS ORGANICS, 99+% extra pure, stabilized with BHT) was distilled under argon from sodium/benzophenone and triethyl amine (TEA) (BAKER) was distilled from calcium hydride under an argon atmosphere prior to use. Polymersome extrusions were performed using 200 nm filters (Acrodisc 13 mm Syringe Filter, 0.2 µm Nylon membrane) and dialysis was performed using Spectra/Por molecular porous membrane tubing (Spectrum Laboratories, Inc, 12-14.000 MWCO)

Instrumentation MilliQ water was obtained from a Labconco water pro PS system. Thin layer chromatography (TLC) was performed on Merck precoated silica gel 60 F-254 plates (layer thickness 0.25 mm). Compounds were visualized by UV, ninhydrin or permanganate reagent. Column chromatography (CC) was carried out using silica gel, Acros (0.035-0.070 mm, pore diameter ca. 6 nm). Infrared (IR) spectra were obtained using a Thermo Matson IR 300 FTIR spectrometer. Data are presented as the frequency of absorption (cm^{-1}). Proton nuclear magnetic resonance (^1H NMR) spectra were recorded on a Varian Unity Inova 400 FTNMR spectrometer. Chemical shifts are expressed in parts per million (δ scale) relative to the internal standard tetramethylsilane (δ=0.00 ppm). Molecular weight distributions were measured using size exclusion chromatography (SEC) on a Shimadzu (CTO-20A) system equipped with a guard column and a PL gel 5 μm mixed D column (Polymer Laboratories) with differential refractive index and UV (λ=254 nm and λ=345nm) detection, using tetrahydrofuran (SIGMA ALDRICH chromasolv 99.9%) as an eluent at 1 mL/min and T = 30 °C. Particle size distributions were measured on a Malvern instruments Zetasizer Nano-S .

Polybutadiene-hydrazone-poly(ethylene glycol) (1) Polymers **8** (80 mg) and **6** (800 mg , 2 equiv.) were dissolved in dry dichloromethane (2 mL). The mixture was allowed to react for 24 hours while gently stirring after which the mixture was poured on a short silica column, which was eluted with dichloromethane. After all non reacted **6** was flushed off the product was eluted with 8 percent methanol in dichloromethane. After removal of all solvents 300 mg of the product was obtained in 60 percent yield. ^{1}HNMR ($CDCl_3$): δ 5.45 (m, 67H, C*H*CH_2), 4.94 (m, 134H, CHC*H*$_2$), 3.65 (m, 90H, C*H*$_2$C*H*$_2$O), 3.38 (s, 3H, C*H*$_3$O), 2.11 (m, 67H, CH_2C*H*), 1.16 (m, 134H, C*H*$_2$CH). SEC (THF): M_w/M_n = 1.14, see Figure 4. M_n: 4.7 kg/mol.

Polybutadiene-hydrazone-poly(ethylene glycol) (2) ^{1}HNMR ($CDCl_3$): δ 5.45 (m, 67H, C*H*CH_2), 4.94 (m, 134H, CHC*H*$_2$), 3.65 (m, 180H, C*H*$_2$C*H*$_2$O), 3.38 (s, 3H, C*H*$_3$O), 2.11 (m, 67H, CH_2C*H*), 1.16 (m, 134H, C*H*$_2$CH). SEC (THF): M_w/M_n = 1.17, M_n: 5.7 kg/mol.

Aldehyde endcapped Polybutadiene (6) All glassware was extensively cleaned, flushed with 1.6 M butyllithium, rinsed again and flame dried. Then 1,3 butadiene (10.6 gram, 0.19 mol) was condensed into a Schlenk tube and freshly distilled THF (10 mL) was added. The solution was stirred and cooled to -78 °C after which sec-butyllithium (2 mL, 1.4M in hexane, 2.8 mmol) was added at once. The deep orange reaction mixture was allowed to warm to -35 °C and stirred until the colour changed to pale yellow. Another aliquot of THF (10 mL) was added and the temperature was fixed at -35 °C. The reaction was terminated by the addition of 3-chloroacetaldehyde diethyl acetal (2 equiv.) via a syringe and the reaction was allowed to warm to room temperature. After the yellow colour had disappeared MilliQ (10 mL) and TFA (5 mL) were added. The mixture was heated to reflux overnight, after which all THF was removed. Then NaOH solution (65 mL, 1M) was added and the product was extracted with DCM (3x 50 mL). DCM was removed and the product was purified over a silica column (1:1 hexane:DCM, R_f = 0.9) to remove the excess of acetaldehyde. The product was obtained quantitatively as a colourless viscous oil. ^{1}HNMR

($CDCl_3$): δ 9.72 (d, 1H, CH_2CHO), 5.45 (m, 67H, $CHCH_2$), 4.94 (m, 134H, $CHCH_2$), 2.11 (m, 67H, CH_2CH), 1.16 (m, 134H, CH_2CH). SEC (THF): M_w/M_n = 1.14, see Figure 4, M_n: 3.7 kg/mol

α- methoxy ω-methyl ester poly(ethylene glycol) (7) Poly(ethylene glycol) monomethyl ether, (5 g, 1kg/mol, 5 mmol), was coevaporated with benzene three times and dissolved in freshly distilled THF (250 mL). Next, sodium hydride (350 mg, 60% on mineral oil, 1.75 equiv.) was added while an argon atmosphere was applied. While stirring, hydrogen gas was allowed to escape for three hours. The temperature was raised to 60 °C and methyl bromoacetate (3 g, 3.8 equiv.) was added via a syringe. The reaction was allowed to proceed for 12 hours after which all THF was removed and the products were dissolved in 25 mL dichloromethane. The solution was poured on a slab of silica gel and flushed with dichloromethane (250 mL). The product was eluted with 10 percent methanol in dichloromethane, yielding 4.5 gram (90%) product. TLC was run in 14 % MeOH in DCM. Staining was performed with $KMNO_4$, and with ninhydrin as a control (no staining); R_f = 0,60. ^{1}HNMR ($CDCl_3$): δ 3.38 (s, 3H, CH_3O), 3.65 (m, 90H, CH_2CH_2O), 3.75 (s, 3H, $COOCH_3$), 4.17 (s, 2H, OCH_2COO). FT- IR: 2876 cm^{-1} (C-H sat.), 1748 cm^{-1} (C=O). SEC (THF): M_w/M_n = 1.22

α- methoxy ω-hydrazide poly(ethylene glycol) (8) 1.5 gram of **7** (1.5 mmol) was coevaporated with benzene three times and dissolved in 50 mL methanol under an argon atmosphere. While stirring, 1hydrazine solution (5 mL, 1M in THF, 10 equiv.) was added at once. The reaction was refluxed overnight after which the mixture was concentrated. The crude product was dissolved in dichloromethane (50 mL) and washed with 1M HCl solution (50 mL). The organic layer was dried over $MgSO_4$ and all solvents were removed, yielding 1.2 gram (80%) of product. TLC was performed with 14 % MeOH in DCM as eluent; ninhydrin was used as staining agent ; R_f = 0,55. ^{1}HNMR ($CDCl_3$) : δ 3.38 (s, 3H, CH_3O), 3.65 (m, 90H, CH_2CH_2O), δ 4.14 (s, 2H, OCH_2CON). FT-IR: 3400 cm^{-1} (NH), 1683 cm^{-1} (C=O). SEC (THF): M_w/M_n = 1.22, see Figure 4

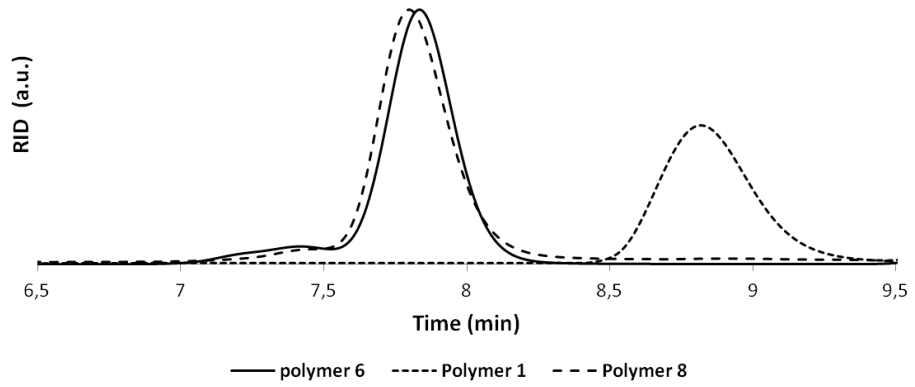

Figure 4. SEC traces of PBd-b-PEG (**1**) and its constituents PBd (**6**) and PEG 1000 derivative (**8**).

Full hydrolysis experiments Vesicles were prepared by dissolving polymer **1** or **2** (40 mg) in THF (0.5 mL). While gently stirring, milliQ (2 mL) was added drop wise. The opaque solution was extruded twice through a 200 nm syringe filter and purified over a Sephadex G200 column. To 900 μL of this vesicle solution, 88 μL of a 2 M Na_2HPO_4 solution and 12 μL of a 1M citric acid solution was added (10x concentrated McIlvain buffer)[31]. After three hours THF (3 mL) was added and the solutions were spotted on TLC eluting with 10% methanol in dichloromethane, as were their constituents and the untreated polymers **1** and **2**. staining was performed with MNO_4. The acid treated samples showed no trace of polymer **1** or **2** but instead showed spot on the position of PEG and PBd. The untreated samples showed a single spot in between PEG and PBd. Finally under these conditions none of the buffering components were eluted on TLC. The remainder of the solution was analyzed by GPC as depicted in Figure 2b. Because of the addition of the buffering components, eluting right after PEG, it was not possible to obtain an undisturbed signal of the free PEG.

Polymersome preparation In general polymeric vesicles were prepared by dissolving 10 mg block copolymer (**1**, **2**, **3**, **4** or the desired combination) in THF (0.5 mL). While gently stirring, MilliQ (2 mL) was added drop wise. The opaque solution was extruded twice through a 200 nm syringe filter and purified over a Sephadex G200 column and all vesicle containing fractions were combined (DLS). The combined vesicle size distribution was measured by DLS.

Stability studies All buffers were prepared according the method of McIlvaine[31] which combines a 0.2 M Na_2HPO_4 and 0.1 citric acid solution to the desired pH in milliQ water. Vesicles were prepared as described above in MilliQ. For each measurement, 200 μL of vesicle solution was added to 800 μL of buffer. The pH was checked and the size distribution was monitored in time by dynamic light scattering.

6.6. Notes and references

(1) Discher, D. E.; Eisenberg, A. *Science* **2002**, *297*, 967.
(2) Discher, B. M.; Won, Y. Y.; Ege, D. S.; Lee, J. C. M.; Bates, F. S.; Discher, D. E.; Hammer, D. A. *Science* **1999**, *284*, 1143.
(3) Ghoroghchian, P. P.; Frail, P. R.; Susumu, K.; Blessington, D.; Brannan, A. K.; Bates, F. S.; Chance, B.; Hammer, D. A.; Therien, M. J. *P Natl Acad Sci USA* **2005**, *102*, 2922.
(4) Du, J. Z.; O'Reilly, R. K. *Soft Matter* **2009**, *5*, 3544.
(5) Meng, F. H.; Zhong, Z. Y.; Feijen, J. *Biomacromolecules* **2009**, *10*, 197.
(6) Smart, T. P.; Mykhaylyk, O. O.; Ryan, A. J.; Battaglia, G. *Soft Matter* **2009**, *5*, 3607.
(7) Schumers, J.-M.; Gohy, J.-F.; Fustin, C.-A. *Polymer Chemistry* **2010**, *1*, 161.
(8) Katz, J., S; Zhuong, S.; Ricart, B. G.; Pochan, D. J.; Hammer, D. A.; Burdick, J. A. *Journal of the American Chemical Society* **2010**, *132*, 3654.
(9) Ma, N.; Li, Y.; Xu, H. P.; Wang, Z. Q.; Zhang, X. *Journal of the American Chemical Society* **2010**, *132*, 442.
(10) Sun, H. L.; Guo, B. N.; Cheng, R.; Meng, F. H.; Liu, H. Y.; Zhong, Z. Y. *Biomaterials* **2009**, *30*, 6358.
(11) Ryu, J. H.; Park, S.; Kim, B.; Klaikherd, A.; Russell, T. P.; Thayumanavan, S. *Journal of the American Chemical Society* **2009**, *131*, 9870.
(12) Klaikherd, A.; Ghosh, S.; Thayumanavan, S. *Macromolecules* **2007**, *40*, 8518.

(13) Cerritelli, S.; Velluto, D.; Hubbell, J. A. *Biomacromolecules* **2007**, *8*, 1966.
(14) Li, Y. T.; Lokitz, B. S.; Armes, S. P.; McCormick, C. L. *Macromolecules* **2006**, *39*, 2726.
(15) Napoli, A.; Boerakker, M. J.; Tirelli, N.; Nolte, R. J. M.; Sommerdijk, N. A. J. M.; Hubbell, J. A. *Langmuir* **2004**, *20*, 3487.
(16) Yurt, S.; Anyanwu, U. K.; Scheintaub, J. R.; Coughlin, E. B.; Venkataraman, D. *Macromolecules* **2006**, *39*, 1670.
(17) Lin, S.; Du, F. S.; Wang, Y.; Ji, S. P.; Liang, D. H.; Yu, L.; Li, Z. C. *Biomacromolecules* **2008**, *9*, 109.
(18) Ulbrich, K.; Etrych, T.; Chytil, P.; Jelinkova, M.; Rihova, B. *J Control Release* **2003**, *87*, 33.
(19) Chen, W.; Meng, F. H.; Cheng, R.; Zhong, Z. Y. *J Control Release* **2010**, *142*, 40.
(20) Jain, R.; Standley, S. M.; Frechet, J. M. J. *Macromolecules* **2007**, *40*, 452.
(21) Ahmed, F.; Discher, D. E. *J Control Release* **2004**, *96*, 37.
(22) Meng, F. H.; Hiemstra, C.; Engbers, G. H. M.; Feijen, J. *Macromolecules* **2003**, *36*, 3004.
(23) Dirksen, A.; Dirksen, S.; Hackeng, T. M.; Dawson, P. E. *Journal of the American Chemical Society* **2006**, *128*, 15602.
(24) King, T. P.; Zhao, S. W.; Lam, T. *Biochemistry-Us* **1986**, *25*, 5774.
(25) Cordes, E. H.; Jencks, W. P. *Journal of the American Chemical Society* **1962**, *84*, 832.
(26) Sawant, R. M.; Hurley, J. P.; Salmaso, S.; Kale, A.; Tolcheva, E.; Levchenko, T. S.; Torchilin, V. P. *Bioconjugate Chem* **2006**, *17*, 943.
(27) Bae, Y.; Fukushima, S.; Harada, A.; Kataoka, K. *Angew Chem Int Edit* **2003**, *42*, 4640.
(28) He, L.; Jiang, Y.; Tu, C.; Li, G.; Zhu, B.; Jin, C.; Zhu, Q.; Yan, D.; Zhu, X. *Chemical Communications* **2010**, 7569.
(29) Hirao, A.; Hayashi, M. *Acta Polym* **1999**, *50*, 219.
(30) Shi, F. X.; Wasungu, L.; Nomden, A.; Stuart, M. C. A.; Polushkin, E.; Engberts, J. B. F. N.; Hoekstra, D. *Biochem J* **2002**, *366*, 333.
(31) Mc Ilvaine, T. C. *Journal of Biological Chemistry* **1921**, *49*, 183.

7

Dynamically Functionalized Polymersomes via Hydrazone Exchange

Polymersomes composed of block copolymers that are coupled via a hydrazone moiety (Chapter 6) are shown to exchange surface PEG chains with the environment via an aniline catalyzed transiminiation under equilibrium conditions. We show that the transimination equilibrium can be used to functionalize polymersomes with a different inner and outer moiety in a dynamic covalent way. Secondly, we show that addition of aniline as catalyst allows to exchange surface properties between polymersomes. These results therefore open new routes to the design of complex vesicular surfaces.

René P. Brinkhuis, Frank de Graaf, Morten Borre Hansen, Taco R. Visser, Floris P. J. T. Rutjes and Jan C. M. van Hest, Polymer Chemistry, accepted

7.1 Introduction

Polymersomes, or polymeric vesicles, can be regarded as the polymeric analogue of liposomes. Due to the higher molecular weight of the building blocks, polymersomes are considerably tougher and less permeable than their low molecular weight counterparts[1]. As a result, polymersomes have an interesting potential for a range of applications such as drug delivery[2-3] and *in vivo* imaging[4-5]. For *in vivo* applications excellent control over stability and release properties is required, as well as the possibility to functionalize the carrier with specific targeting moieties, e.g. ligands. An appreciable amount of research has focused on the functionalization of polymersome surfaces[6] with enzymes, peptides[7] and antibodies[2,8]. However, all these reported functionalization strategies are irreversible or make use of non-covalent interactions[6,9]. In contrast, one can also imagine that polymeric vesicles can be functionalized via covalent bonds that are reversible in nature.

Reversible covalent bonds are (or can be brought) in an equilibrium state, meaning that the bond is reversibly formed and broken as exploited in dynamic combinatorial chemistry[10]. In a recent example, Minkenberg *et al*.[11] used reversible chemistry to spontaneously form amphiphiles that evolved to the thermodynamically most favourable supramolecular composition. If this chemistry is also applicable to preformed polymeric vesicles, it would allow the functionalization of polymersomes in a dynamic and modular way, in which one sample can be (re)-functionalized with a variety of different compounds, while keeping control over vesicle size and stability. Covalent bonds that have the potential to be brought into equilibrium have also been built in polymersomes. However, the reversibility has only been used for (triggered) disruption[12-14], unidirectional surface functionalization[15] or drug release[16-17].

In Chapter 6 we showed that the colloidal stability of polymersomes can be controlled by the introduction of a hydrazone bond. Block copolymers of which both blocks are coupled via a hydrazone moiety can form polymeric vesicles which are stable at physiological pH. However, upon lowering the pH they lose their colloidal stability due to hydrolysis of the hydrazone[18]. Simultaneously, a similar system was independently reported by He *et al*.[19] In both studies, lowering of the pH was used as a trigger to fully hydrolyze the hydrazone bond in the block copolymer, thus removing the PEG periphery.

At neutral pH, hydrazone bonds are equilibrium structures which favour bond formation as depicted in Figure 1a. However, bond formation and dissociation are very

slow. A method to induce faster dynamics in this equilibrium, without shifting the position, proceeds by the addition of a catalyst, aniline[20]. Following this methodology, Dirksen *et al.*[21-23] showed that aniline-catalyzed hydrazone exchange between peptide fragments is 70 fold faster than the non-catalyzed reaction.

In this chapter, we report the use of the aniline catalyzed hydrazone equilibrium in the design of polymersomes with dynamic covalent surfaces. We form polymersomes of a hydrazone coupled amphiphilic block copolymer and make use of the aniline catalyzed hydrazone equilibrium to exchange surface functionalities with the surrounding solution as illustrated in Figures 1b-c. In this way, polymeric vesicles with a different inner and outer functionality can be formed. Finally, we show that exchange of surface properties between polymersomes is possible, following the same approach. This methodology therefore opens new routes in the design of complex polymeric membranes, starting from simple polymersome scaffolds.

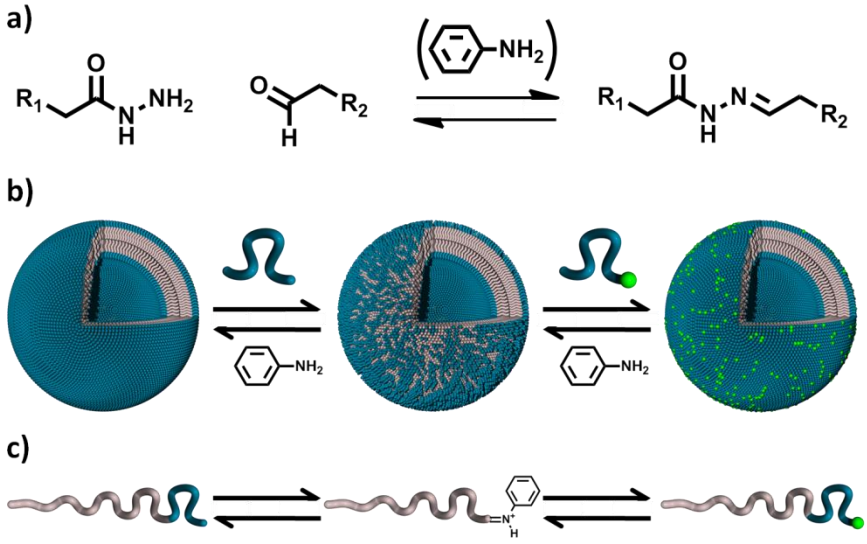

Figure 1. a) Equilibrium between hydrazide, aldehyde and hydrazone. The rate constant can be enhanced by the addition of aniline. **b)** After removing a PEG chain from the polymersome surface, either a PEG chain from solution or the original PEG chain can attack. **c)** Presentation of the exchange on the block copolymer level, expressing the role of aniline.

7.2 Results and Discussion

In Scheme 1 the basic building blocks for the self-assembly of polymersomes and the exchange reactions are depicted. Details on the synthetic procedures can be found in Section 7.5. We chose to work with the amphiphilic block copolymer polybutadiene-

block-poly(ethylene glycol) for two reasons. First of all, this block copolymer is generally considered to be biocompatible and secondly the low glass transition temperature of polybutadiene allows for extrusion and therefore resizing of the polymersomes. This allowed us to prepare well-defined monodisperse samples making comparison of their properties relatively straightforward. PEG derivatives **1** and **2** contained a hydrazide moiety and were partially labelled with fluorescent dansyl and fluorescein (DY_{495}) markers, respectively. Amphiphilic block copolymer **3** contained a hydrazone bond between both blocks and no functional end group. Block copolymer **4** was partially functionalized with rhodamine (DY_{549}) and **5** was functionalized with a maleimide end-group. Finally, as a negative control the stable amphiphilic block copolymers **6** and **7** were employed. These polymers are direct analogues of **3** and **4**, differing only in the connection between both blocks.

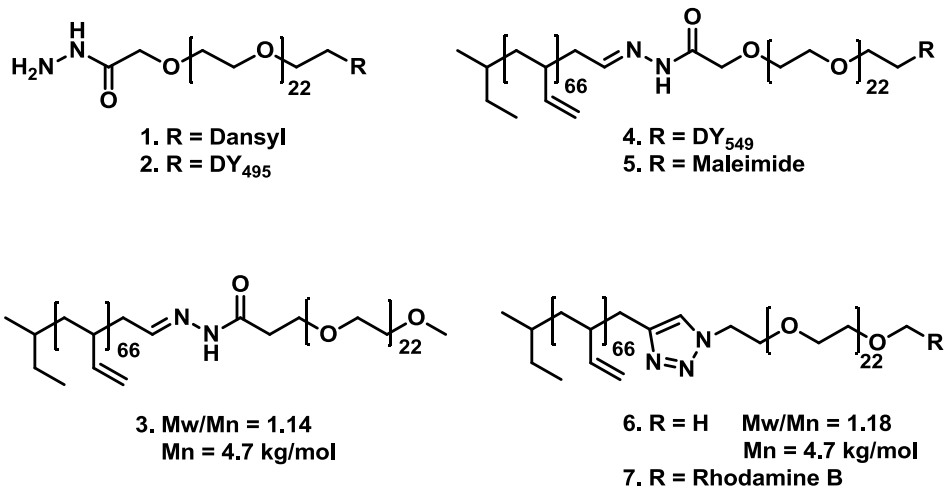

Scheme 1. Overview of polymers used in this study. Polymers **1** and **2** are PEG derivatives, both containing a hydrazide moiety and labelled with dansyl or fluorescein (DY_{495}), respectively. Polymers **3**, **4** and **5** are amphiphilic block copolymers of polybutadiene-b-poly(ethylene glycol), containing a hydrazone linker between both blocks. Polymers **4** and **5** are functionalized with a rhodamine dye (DY_{549}) and a maleimide end group, respectively. Finally, block copolymers **6** and **7** do not contain a hydrazone moiety. Polymer **6** contains no functional end group and **7** is partially labelled with rhodamine B. Both are included as negative controls.

We prepared polymersomes derived from **3** and **6** with a diameter of 220 nm. Thus, polymersomes from **3** contained a hydrazone moiety, while polymersomes from **6** did not and therefore served as a negative control. After the polymersomes were formed, the fluorescent PEG derivative **1** was added to all samples. To initiate the exchange of surface PEG for the dansyl-functionalized PEG (**1**) in solution, aniline (12 equiv) was added as

catalyst to the polymersomes formed from **6** and half of the polymersomes formed from **3**. To the other half of this sample no catalyst was added to serve as second negative control. For each time point a fraction of the samples was withdrawn and purified by size exclusion chromatography (SEC) to separate aniline and unbound PEG from the polymersomes. Next, the fluorescence intensity of the polymersome fraction was measured in a plate reader as plotted in Figure 2a (340 nm (excitation), 560 nm (emission)).

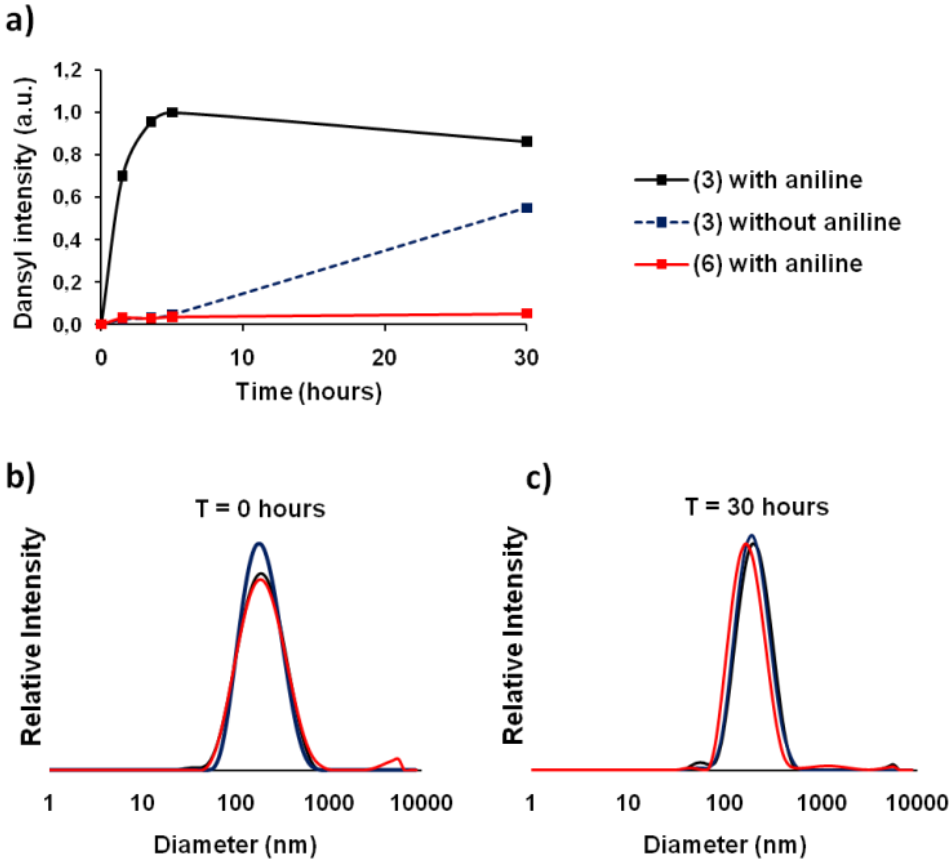

Figure 2. Dynamic functionalization of polymeric vesicles. **a)** Aniline-catalyzed hydrazone surface exchange on polymeric vesicles (black) is faster than non-catalyzed exchange (blue). If no hydrazone is present in the block copolymer, surface exchange is not possible (red). Vesicles were stable and did not change in size during the exchange experiment: 0 hours **b)** and 30 hours **c)** as determined by DLS.

In principle, both samples prepared from polymer **3** should be able to exchange PEG chains with the environment by breaking and forming the hydrazone bonds. However, in the presence of aniline this equilibrium was set much faster, as is clearly visible from Figure 2a. The aniline containing sample reached its maximum fluorescence after 4.5 hours, while the non catalyzed sample had not yet reached its equilibrium position after 30 hours. The negative control, prepared from polymer **6**, does not contain a hydrazone

bond and therefore was unable to exchange surface chains with its surroundings, therefore no increase in fluorescence was observed.

As these experiments were performed at neutral pH, it was expected that these polymeric vesicles kept their colloidal stability[18-19]. To confirm this, we analyzed the size distribution of the polymeric vesicles at each time interval by dynamic light scattering (DLS). As shown in Figures 2b-c no significant change in particle distribution was observed between 0 and 30 hours and moreover the derived count rate at a fixed measurement position appeared nearly equal for all data points, indicating identical concentration and size. This led us to conclude that indeed the surface of these polymersomes was in a dynamic equilibrium with its environment.

To take this concept one step further, we prepared polymeric vesicles of a combination of **3** and **4** in a ratio of 95:5. These polymeric vesicles thus exhibited hydrazone bonds and were partially fluorescently labelled at both the inner and outer surface. As can be derived from the absence of fluorescence in the negative control in Figure 2a (**6** with aniline), free PEG is not able to cross the membrane of these polymeric vesicles on this timescale. Therefore PEG exchange is expected only to proceed on the polymersome outer surface, creating a vesicle with a different inner and outer functionalization. We repeated the aniline-catalyzed experiment with the abovementioned rhodamine prefunctionalized vesicles. Again at each time point any free PEG chains and aniline were separated from the polymersomes by size exclusion chromatography. The size and concentration of all samples was checked by DLS and found to be equal. Next we analyzed the fluorescence intensity of both fluorophores separately in a 96 well plate reader (dansyl excitation 340 nm, emission 540 nm; rhodamine excitation 540 nm, emission 592 nm). Within five hours, the rhodamine intensity decreased to 0.5 (Figure 3a), which is consistent with our hypothesis that only the outer membrane is susceptible to dynamic exchange. Furthermore, the emission of dansyl reached its maximum following an opposite trend compared to the decrease of rhodamine (Figure 3b).

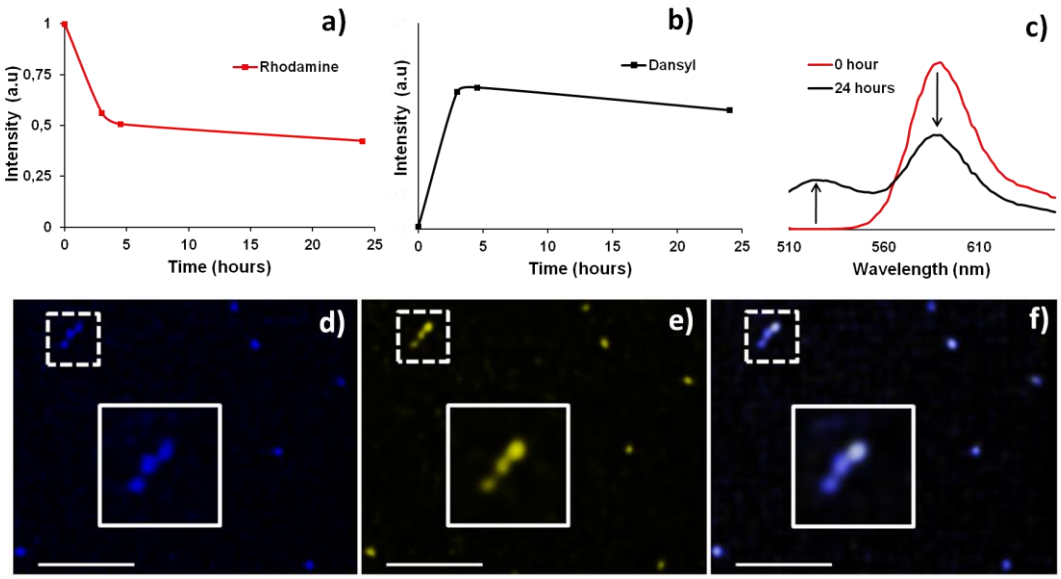

Figure 3. a-b) Starting from rhodamine-functionalized polymersomes the outer rhodamine is replaced by a dansyl-functionalized surface. **c)** Emission spectra of polymersomes before and after surface exchange of rhodamine-functionalized PEG chains by their fluorescein analogue. **d)** CLSM visualization of rhodamine and **e)** CLSM visualization of fluorescein on the same polymersomes and **f)** CLSM overlay image of **d** and **e**. The white bar represents 20 µm.

To visualize the double functionalization of vesicles, we applied confocal laser scanning microscopy (CLSM). For this purpose, we replaced dansyl-PEG for a fluorescein-PEG derivative (**2**) and repeated the experiment. As depicted in Figure 3c (red) at time zero, after mixing and purification by SEC, the emission spectrum of the polymersomes only contained rhodamine emission (480 nm, for excitation of both fluorophores). However, when after 24 hours a sample was purified by size exclusion chromatography, the emission spectrum contained both rhodamine and fluorescein emission. Furthermore, Figure 3d-f show CLSM pictures obtained after 24 hours. Both fluorophores were excited at the same time (476 nm) and selectively captured as described in Section 7.5. As can be seen from Figures 3d-f, a good overlay between both fluorophores exists, indicating that both moieties are present on the same polymeric vesicle. The full and unfiltered pictures are shown in Section 7.5.

In the described experiments, it is not possible to visualize separately the functionalization of the in inner and outer surface. This might be possible on giant unilamellar vesicles[24] in combination with high resolution CLMS. However, together these experiments clearly indicate that a different inner and outer membrane functionalization is obtained. The first experiment proved that free PEG chains in solution cannot cross the polymersome membrane on this time scale. The double

functionalization experiment clearly shows a decrease of 0.5 in rhodamine intensity and finally CLSM shows the colocalization of both fluorophores. Therefore we can conclude that the method as described herein allows for the substitution of the outer PEG surface of polymersomes for a new PEG surface containing a different functionality.

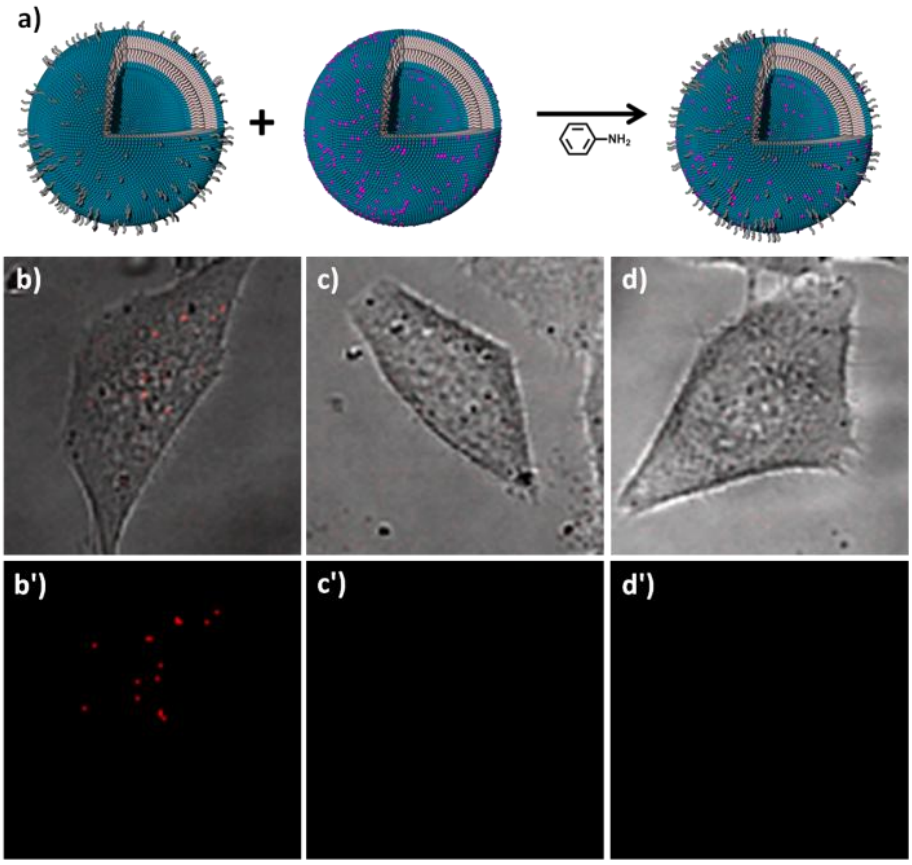

Figure 4. a) Dynamic hydrazone exchange between vesicles functionalized with rhodamine and vesicles functionalized with cell penetrating Tat-peptides will result in a single set of doubly functionalized vesicles. **b**) After exchange polymersomes are both visible by CLSM (coloured in red) and associated with Hela cells **c**) Exchange in absence of Tat-vesicles will not yield vesicles that are both fluorescent and cell adhering. **d**) If rhodamine labelled vesicles are prepared from block copolymers lacking the hydrazone moiety (**6** and **7**), the experiment will not yield vesicles that are both fluorescent and cell adhering. The top images of **b**, **c** and **d** show CLSM and bright field overlay images and the bottom CLSM images of 45 x 45 µm selections. The full unfiltered images are shown in Section 7.5.

In the preceding experiments we have shown that hydrazone-functionalized polymeric vesicles are able to exchange moieties with the surrounding solution. We next investigated whether this exchange would also take place between polymeric vesicles. For this purpose we synthesized a block copolymer analogue with a maleimide end group and a hydrazone unit between both blocks (**5**). We formed polymersomes of a combination of **3** and **5** in a ratio of 8:2. The maleimide functionalities were reacted with

a cysteine residue connected to the cell penetrating Tat-peptide[25-26], resulting in Tat-functional polymersomes.

Rhodamine-functional polymersomes of **3** and **4** (9:1) were also formed as used in the previous experiments. Both types of polymersomes thus contained the hydrazone moiety between both blocks. Rhodamine polymersomes can be visualized by CLSM, but will not adhere to Hela cells, whereas Tat-polymersomes can adhere to cells[7], but are invisible in CLSM. If dynamic exchange between these vesicles should take place, the resulting set of polymersomes should be both fluorescent and have cell-adhesion capacity as depicted schematically in Figure 4a.

After both the rhodamine and the Tat-polymersomes were formed, they were mixed in a 1:1 ratio and aniline was added. The exchange was allowed to proceed overnight, after which aniline and possible free PEG chains were removed by SEC. The sample was added to a Hela cell culture and after washing the cells, CLSM indeed confirmed the presence of cell adhering, fluorescent polymersomes as shown in Figure 4b. This clearly shows that both the cell adhesion and fluorescent properties are contained in a single polymersome. To exclude false positive results we included two negative controls in this study. When rhodamine polymersomes were reacted with aniline without the presence of Tat-polymersomes, no polymersomes were visibly associated with Hela cells (Figure 4c). Secondly, if rhodamine polymersomes were formed lacking the hydrazone moiety (**6** and **7**) and were reacted overnight in the presence of both aniline and Tat-polymersomes, also no vesicles were *visible* in the Hela cells culture (Figure 4d).

7.3 Conclusion

In conclusion, we have introduced a new concept to functionalize polymeric vesicles in a dynamic fashion. We have shown that polymersomes formed from a hydrazone-coupled block copolymer exchange their surface functionality both with dissolved species and with other vesicles via the hydrazone equilibrium. Via this method polymeric vesicles can be conveniently formed with different inner and outer functionalities. Furthermore, multiple functional surfaces can be obtained via one single exchange experiment by mixing the appropriate sets of polymersomes.

7.4 Acknowledgement

Prof. Dr. K.T Kim is thanked for pointing me to the aniline catalyzed hydrazone equilibrium. Taco R. Visser is acknowledged for his help in the synthesis and Frank de Graaf is acknowledged for his help in the exchange experiments and analysis.

7.5 Experimental Procedures

General notes The full synthetic route, including reaction steps and compounds reported in previous chapters is depicted in Scheme 1. Details of the synthesis of compounds **6**, **7, 8, 10** and **12** can be found in Section 2.5. Details of the synthesis of compounds **3** and **11** can be found in Section 6.5. Details of the synthesis of compound **15** were reported by Karlèn *et al.*[27] Details of the synthesis of compound **16** were reported by Deiters *et al.*[28]

Materials BCN dyes SX-1030 and SX-1031 were purchased from Synaffix and copper bromide was washed in ethyl acetate and dried under vacuum prior to use. All other reagents were at least 98% pure and used without further purification. Tetrahydrofuran (THF) (ACROS ORGANICS, 99+% extra pure, stabilized with BHT) was distilled under argon from sodium/benzophenone and triethylamine (TEA) (BAKER) was distilled from calcium hydride under an argon atmosphere prior to use. Polymersome extrusions were performed using 200 nm filters (Acrodisc 13 mm Syringe Filter, 0.2 μm Nylon membrane).

Instrumentation MilliQ water was obtained from a Labconco water pro PS system. Thin layer chromatography (TLC) was performed on Merck precoated silica gel 60 F-254 plates (layer thickness 0.25 mm). Compounds were visualized by UV, ninhydrin and/or permanganate reagents. Column chromatography (CC) was carried out using silica gel, Acros (0.035-0.070 mm, pore diameter ca. 6 nm). Infrared (IR) spectra were obtained using a Thermo Matson IR 300 FTIR spectrometer. Data are presented as the frequency of absorption (cm^{-1}). Proton nuclear magnetic resonance (^{1}HNMR) spectra were recorded on a Varian Unity Inova 400 FTNMR spectrometer. Chemical shifts are expressed in parts per million (δ scale) relative to the internal standard tetramethylsilane (δ=0.00 ppm). Molecular weight distributions were measured using size exclusion chromatography (SEC) on a Shimadzu (CTO-20A) system equipped with a guard column and a PL gel 5 μm mixed D column (Polymer Laboratories) with differential refractive index and UV (λ=254 nm and λ=340nm) detection, using tetrahydrofuran (SIGMA ALDRICH chromasolv 99.9%) as an eluent at 1 mL/min and T = 30 ^{o}C. Particle size distributions were measured on a Malvern instruments Zetasizer Nano-S. A TECAN Infinite 200 PRO plate reader was used to perform fluorescence intensity measurements. Confocal Laser Scanning Microscopy (CLSM) images were recorded on a Leica DM IRE2 TCS SP2 AOBS inverted microscope. An Argon laser and a Vioflame diode laser were used to excite the different fluorophores.

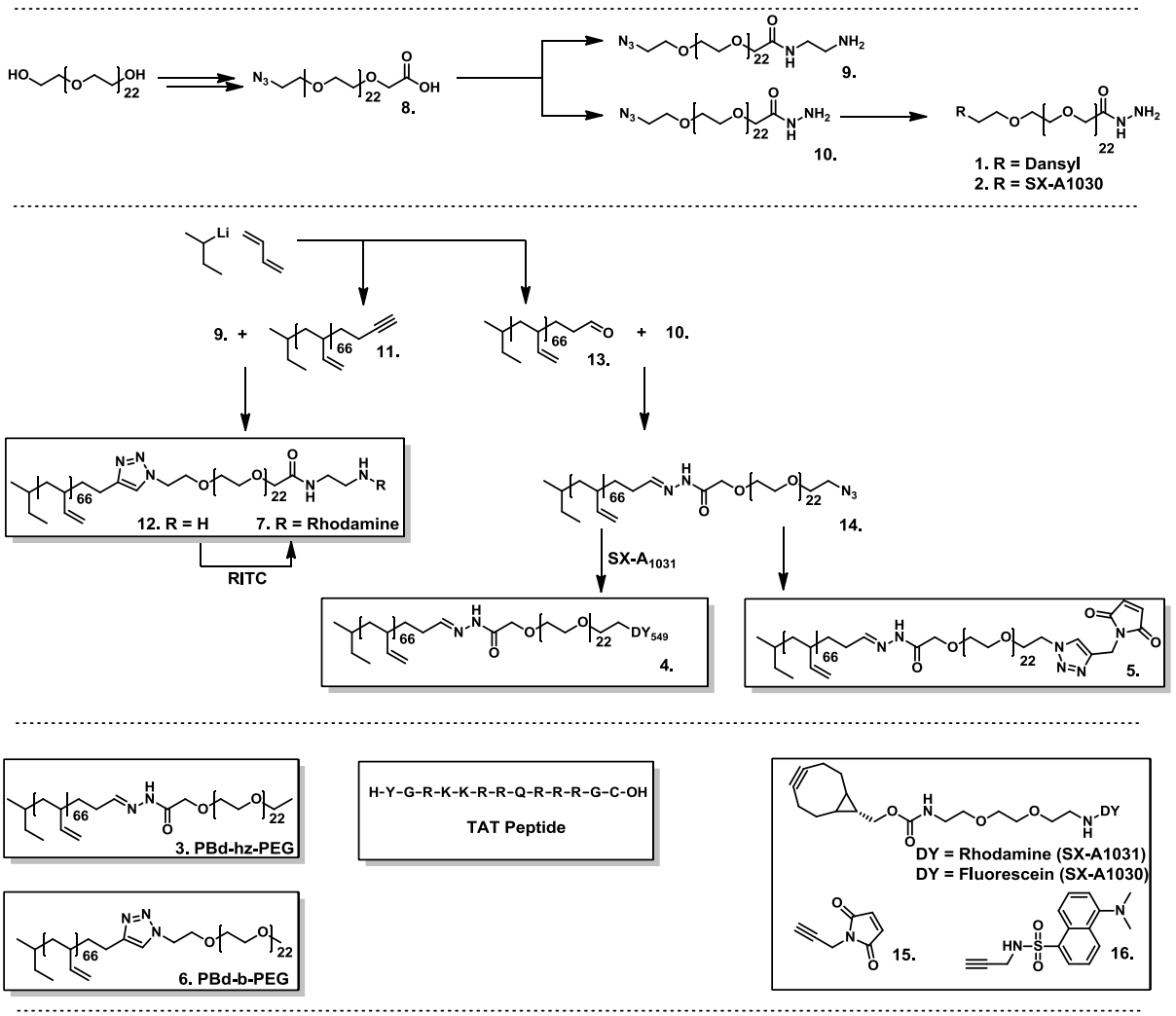

Scheme 1. Overview of the synthetic route to all structures employed in this chapter. Details on the synthetic procedures are described below.

α-Dansyl ω-hydrazine poly(ethylene glycol) (1) Compound **10** (100 mg, 0.1 mmol) was dissolved in THF (10 mL) under an argon atmosphere. CuBr (5 mg), PMDETA (1 drop) and dansyl probe **16** (26 mg, 0.95 equiv.) were added and heated to reflux overnight. Probe **16** was consumed as determined by TLC, after which all solvents were removed and the products were dissolved in DCM (1 mL). The product was purified on a silica column, eluting with DCM to remove any traces of **16**. The product (70 mg, 60%) was obtained by eluting with 8% methanol in dichloromethane (Rf = 0.55 as a bright single fluorescent spot). ^{1}H-NMR ($CDCl_3$): δ 9.33 (s, 1H, CON*H*NH_2), 8.55 (d, 1H), 8.27 (t, 2H), 7.62 (s, 1H, CCH_2N), 7.54 (q, 2H), 7.19 (d, 1H), 4.42 (t, 1H, SNHC*H*$_2$), 4.06 (s, 2H, OCH_2CO), 3.79 (m, 2H, CH_2N), 3.64 (m, 90H, C*H*$_2$C*H*$_2$O), 2.89 (s, 6H, $N(CH_3)_2$), 1.70 (s, 2H, NHN*H*$_2$). SEC (THF): Mn = 1.1 kg/mol, Mw/Mn = 1.26 (detection at 340 nm, while the starting material **10** does not absorb at 340 nm).

Partial fluorescein labelling of α-azido ω-hydrazine poly(ethylene glycol) (2) Polymer **10** (100 mg, 0.1 mmol) was dissolved in methanol (10 mL) and fluorescein probe SX-A1030 (5 mg, 0.06 equiv.) was added. The reaction was allowed to proceed overnight, after which all solvents were removed. TLC, eluting with acetonitrile:MilliQ (9:1) showed full consumption of dye SX-A1030 (RF = 0.75) and a new bright

fluorescent product (RF = 0.05) at the same height as **10** was formed (note that mixing of PEG and SX-A1030 results in a clear separation under these conditions). The product was dissolved in ice-cold dichloromethane (1mL) and filtered over a 0.1 µm syringe filter. The product (85 mg, 80%) was obtained by removing all dichloromethane. SEC (THF): Mn = 1.4 kg/mol, Mw/Mn = 1.31 (detection at 340 nm, whereas the starting material, **10**, does not absorb at 340 nm). ^{1}HNMR ($CDCl_3$): no significant deviation from **10**, due to labelling with only 0.06 equiv. of dye.

Partial Rhodamine labelled Polybutadiene-hydrazone-poly(ethylene glycol) (4) Compound **14** (100 mg, 0.021 mmol) was dissolved in THF (10 mL) and Rhodamine probe SX-A1031 (5 mg, 0.02 equiv.) was added. The reaction was allowed to proceed overnight. Solvents were removed and product **4** was purified by preparative GPC (THF) to yield 70 mg product. The product was highly fluorescent and in contrast to **14** showed absorption in the GPC detector at 340 nm (see Figure 5). Mw/Mn = 1.22, Mn: 4.7 kg/mol. ^{1}HNMR ($CDCl_3$) no significant deviation from **14**, due to the low concentration of dye.

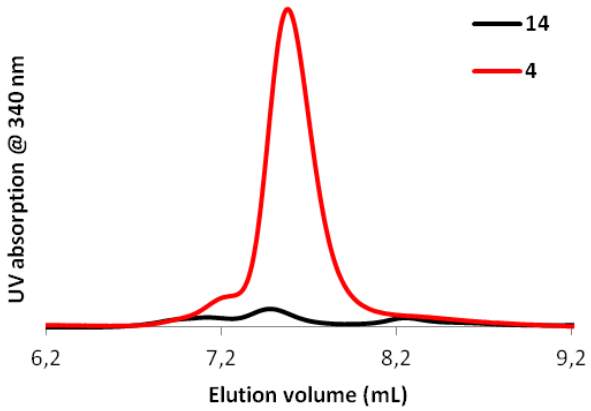

Figure 5. Using equal polymer concentrations for SEC (THF) analysis. UV absorption at 340 nm can be detected for polymer **4**, due to the presence of SX-1031, whereas only limited absorption is observed before the coupling (**14**).

Maleimide end-functional Polybutadiene-hydrazone-poly(ethylene glycol) (5) Compound **14** (100 mg, 21 µmol) was dissolved in THF (10 mL) under an argon atmosphere. Next, CuBr (5 mg, 34 µmol), 1 drop of PMDETA (ca 50 mg, 0.28 mmol) and maleimide **15** (5 mg, 1.6 equiv.) were added and heated to reflux overnight. All solvents were removed and the products were dissolved in dichloromethane (1mL). The product was purified on a silica column, eluting with a gradient of 0 % to 8% methanol in dichloromethane to obtain 55 mg product (Rf in 8% methanol/DCM = 0.65). The product showed, in contrast to **14,** good UV (254 nm) absorption in SEC analysis. SEC (THF): Mw/Mn = 1.26, Mn: 4.7 kg/mol (see Figure 6). ^{1}HNMR ($CDCl_3$): δ 6.96 (s, 2H, maleimide), 5.45 (m, 67H, C*H*CH_2), 4.94 (m, 134H, CHC*H*$_2$), 3.65 (m, 90H, CH_2CH_2O), 2.11 (m, 67H, CH_2CH), 1.16 (m, 134H, C*H*$_2$CH).

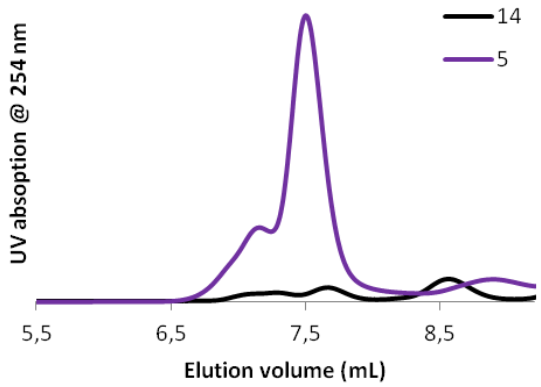

Figure 6. Using equal polymer concentrations for SEC (THF) analysis. UV absorption at 254 nm can be detected for polymer **5**, due to the presence of triazoles and a maleimide, whereas only limited absorption is observed before the introduction of a maleimide (**14**).

Rhodamine labelled Polybutadiene-triazole-poly(ethylene glycol) (7) 50 mg **12** (10 µmol) was dissolved in THF (10 mL) and Et_3N (1 mL) was added. Next. Rhodamine B isothiocyanate (7.5 mg, 1.5 equiv) was added and allowed to react for 48 hours. Solvents were removed and product **7** was purified by preparative SEC (THF) to yield the product product (25 mg, 45%). The product was a single spot on TLC (8 percent methanol in DCM; UV and permanganate stain) which appeared brightly fluorescent. Note that the isothiocyanate coupling of rhodamine B proceeded slowly and the reaction did not go to completion as can be seen from the SEC traces (absorption @ 340 nm) in Figure 7. The elution volume that was collected in preparative SEC (THF) is depicted in the box (6.7 to 8.1 mL)

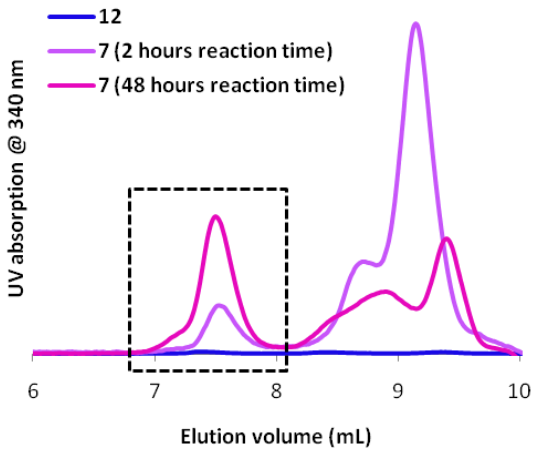

Figure 7. SEC (THF) analysis of block copolymer **12**, which does not absorb at 340 nm before the addition of rhodamine B isothiocyanate. After 2 hours the labelled polymer (top~7.5 mL) does absorb at 340 nm, which increases over the next 46 hours. The dashed box indicates the volume, containing product **7**, that was collected by preparative SEC in THF.

α-azido ω-hydrazine poly(ethylene glycol) (10) Compound **8** (1g, 1 mmol) was dissolved in methanol (50 mL) and 5 drops of concentrated sulfuric acid were added. The mixture was heated under reflux overnight, after which methanol was removed. The product was dissolved in water (50 mL) and extracted with dichloromethane (5x 50 mL). The organic layer was dried over $MgSO_4$ and all solvents were removed. TLC: Rf = 0.65, permanganate staining, running in DCM:MeOH = 92:8. Indicative ^{1}H-NMR ($CDCl_3$) shifts: δ 4.17 (s, 2H, OCH_2COOMe), 3.75 (s, 3H, COOCH_3) and IR: 1748 cm^{-1} (carbonyl/ester)

The product was dissolved in methanol (50 mL) and hydrazine (15 mL, 1M in THF) was added. The mixture was heated under reflux for 48 hours, after which ***almost*** all solvents were removed. The product

was dissolved in dichloromethane (50 mL) and washed with 1M hydrochloric acid (50 mL). The aqueous layer was extracted with dichloromethane (5x 50 mL). The combined organic layers were dried over $MgSO_4$ and all solvents were removed to yield 800 mg product (80%). TLC: Rf = 0.55, permanganate and ninhydrin staining, eluent DCM:MeOH = 92:8. ^{1}HNMR ($CDCL_3$): 3.39 (t, 2H, CH_2N_3), 3.64 (m, 90H, CH_2CH_2O), 4.01 (s, 2H, OCH_2CONH). FTIR: 2098 cm^{-1} (azide), 1696 cm^{-1} (C=O). SEC (THF): Mn = 1 kg/mol, Mw/Mn = 1.22.

ω-azido-Polybutadiene-hydrazone-poly(ethylene glycol) (14) Polymer **10** (80 mg) and **13** (800 mg , 2.5 equiv. 3.7 kg/mol) were dissolved in dry dichloromethane (2 mL). The mixture was allowed to react for 24 hours while gently stirring after which the mixture was poured on a short silica column, which was eluted with dichloromethane. After all non-reacted **13** was flushed off the product was eluted with 8 percent methanol in dichloromethane. After removal of all solvents 240 mg of the product was obtained in 65 percent yield. ^{1}HNMR ($CDCl_3$): δ 5.45 (m, 67H, $CHCH_2$), 4.94 (m, 134H, $CHCH_2$), 3.65 (m, 90H, CH_2CH_2O), 2.11 (m, 67H, CH_2CH), 1.16 (m, 134H, CH_2CH). SEC (THF): Mw/Mn = 1.18, Mn: 4.7 kg/mol (see Figure 8).

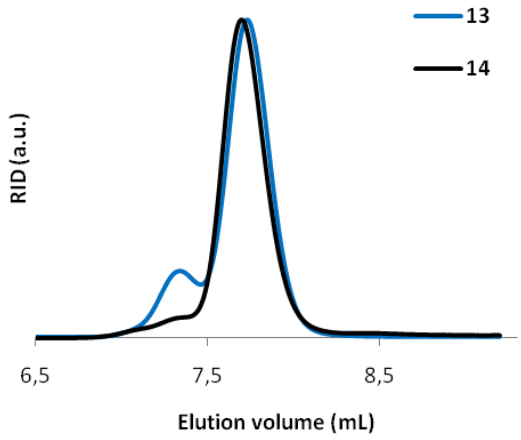

Figure 8. Synthesis of ω-azido-polybutadiene-*hydrazone*-poly(ethylene glycol) (**14**) from polymers **10** and **13**. Due to an increase in molecular weight the GPC trace shifts to shorter elution time.

Tat-peptide Tat-peptide was synthesized by means of standard Fmoc chemistry. The purity was more than 95 percent as analyzed by means of HPLC eluting in water/acetonitrile both containing 0.1% v/v trifluoroacetic acid. The volume fraction of acetonitrile was increased from zero to hundred percent over 30 minutes. Maldi-TOF (cyano-4-hydroxycinnamic acid): [M+H] calc: 1719.0 g/mol and [M+H] found: 1718.7 g/mol.

Polymersome formation (general procedure) 20 mg of the desired (ratio) of block copolymer(s) was dissolved in THF (2 mL) and slowly diluted with MilliQ water (6 mL) to obtain an opaque solution. The solution was extruded three times through a 200 nm syringe filter. THF was removed by purification over a Sephadex G200 column, eluting with demineralised water, after which the polymersome fractions were combined. If needed the pH was adjusted to neutral (NaOH) and the total volume was adjusted to 10 mL

(2 mg/mL, 0.4 mM). The average size was determined by dynamic light scattering and was in all cases around 200 nm with a PDI below 0.2.

Dansyl-PEG solution exchange Three sample solutions were prepared containing: A) 3 mL polymersomes formed from **3** (0.4 mM), 0.8 mg of **1** (0.26 mM) and 1.7 mg aniline (6 mM) B) 3 mL polymersomes formed from **3** (0.4 mM) and 0.8 mg of **1** (0.26 mM) and C) 3 mL polymersomes formed from **6** (0.4 mM), 0.8 mg of **1** (0.26 mM) and 1.7 mg aniline (6 mM) At different time points a 600 µL sample of A, B and C was withdrawn and purified over a Sephadex G200 column, eluting with milliQ. The average size at a fixed attenuator and measurement position was determined by DLS and if necessary the samples were diluted to equally derived count rates. No significant change in size and polydispersity in time was observed. samples were prepared in a 96 well plate (200 µL/well) and measured in a plate reader, 340 nm excitation and 560 nm emission.

Dansyl-PEG/Rhodamine-PEG solution exchange Polymersomes were formed of **3** and **4** in a ratio of 95:5 as described above. The experiment was started by mixing 3 mL of polymersomes (0.4 mM), 3 mg of **1** (1.0 mM) and 1.7 mg aniline (6.0 mM). At different time points a 600 µL sample was withdrawn and purified over a Sephadex G200 column, eluting with MilliQ. The average size at a fixed attenuator and measurement position was determined by DLS and if necessary the samples were diluted. No significant changes in size and polydispersity in time were observed. samples were prepared in a 96 well plate (200 µL/well) and measured in a plate reader. Only the dansyl probe was observed upon excitation at 355 nm and the emission was measured at 540 nm. The rhodamine probe was selectively analyzed with an excitation of 540 nm and emission at 592 nm. Note that these excitations and emissions are not the spectral maxima of the probes, but allow the selective determination of both fluorophores.

Fluorescein-PEG/Rhodamine-PEG solution exchange This experiment was performed to visualize the co localization of two fluorophores at polymersomes. As dansyl was not a suitable probe for CLSM due to fast quenching, it was replaced by fluorescein (compound **2**). Polymersomes were formed of **3** and **4** in a ratio of 95:5 as described above. The experiment was started by mixing 600 µL of polymersomes (0.4 mM), 0.5 mg **2** (0.56 mM) and 3 mg aniline (50 mM). After 24 hours a sample was purified over a Sephadex G200 column eluting with MilliQ water. The average size at a fixed attenuator and measurement position was determined by DLS and no significant change in size and polydispersity was observed. The emission spectrum of both fluorophores was determined simultaneously in the plate reader by excitation at 480 nm. For the CLSM experiment the sample was excited with a 476 nm laser. Rhodamine was selectively visualized by recording emission between 580-610 nm and fluorescein was recorded between 500-530 nm (Figure 9).

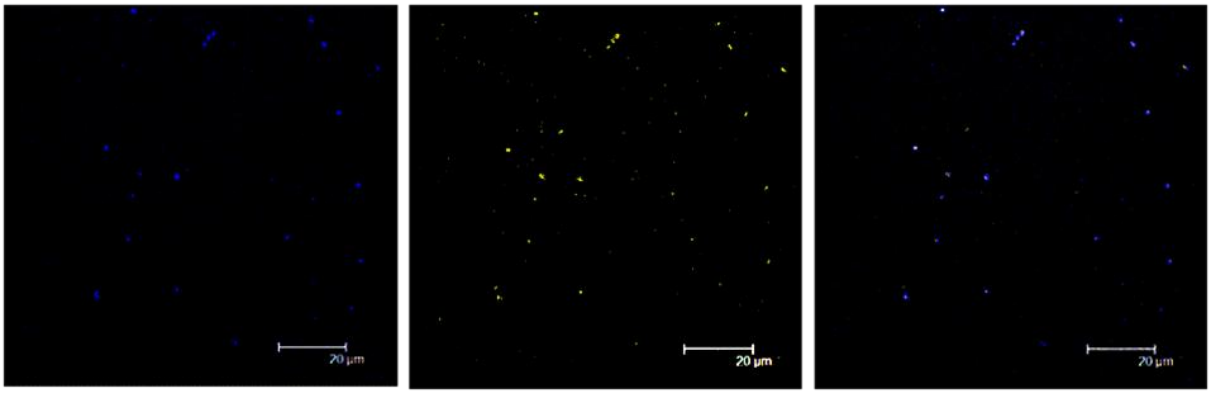

Figure 9. Left, selective detection of rhodamine emission after 24 hours of catalyzed exchange. Middle, selective detection of fluorescein emission and right, the overlay of both images showing the presence of both fluorophores at the same polymeric vesicles after 24 hours of equilibration.

Tat-PEG/Rhodamine-PEG surface exchange Three sets (P1, P2 and P3) of polymersomes were formed as described above. P1 was formed from **3** and **4** in a ratio of 9:1 (rhodamine-labelled) (10 mL, 0.4 mM), P2 was formed from **6** and **7** in a ratio of 9:1 (same as P1 but no hydrazone bonds) (10 mL, 0.4 mM) and P3 was formed from **3** and **5** in a ratio of 8:2 (Maleimide, but no fluorescent label) (10 mL, 0.4 mM)

P3 polymersomes were functionalized with Tat-peptide: 1.1 mg Tat (~0.5 equiv towards maleimides) was dissolved in 1 mL MilliQ and 5 mg tris(2-carboxyethyl)phosphine(TCEP) gel (Piercenet) was added. The mixture was incubated for 30 minutes after which the solution was filtered and added to the full 10 mL of maleimide-functional polymersomes P3. Possible residual Tat-peptide was removed by spin column (4000 rpm, 0.1 nm pores) until the eluate showed negative on Kaiser test (ninhydrin for free amines). The total volume was adjusted to 10 mL to have equal concentrations compared to P1 and P2 (0.4 mM).
Three samples to test polymersome-polymersome surface exchange were prepared as follows: **A**) 600 µL P1 + 600 µL P3 + 1 mg aniline (1.2 mL sample; 0.4 mM in polymer and 9 mM in aniline); **B**) 600 µL P2 + 600 µL P3 + 1 mg aniline (negative control, 1.2 mL sample; 0.4 mM in polymer and 9 mM in aniline) and **C**) 600 µL P1 and 0.5 mg aniline (negative control, 0.6 mL sample; 0.4 mM in polymer and 9 mM in aniline) After 16 hours all samples were purified over a Sephadex G200 column eluting with milliQ water.

Hela Cell Studies The cellular adhesion experiments were performed with HeLa cells, which were seeded one day before the experiment in 8-well microscopy chambers (Nunc, Wiesbaden, Germany) at a density of 40,000 cells/well. At the time of the experiment, cells had grown to approximately 50% confluence. The polymersome samples (20 µL) were diluted with Dulbecco's Modified Eagle Medium DMEM (380 µL) and added to the cells, which were incubated for 1.5 h at 37 °C. The cells were washed with DMEM (3 × 400 µL) and imaged immediately. Confocal laser scanning microscopy was performed using a Leica Microsystems TCS SP2 AOBS system (Mannheim, Germany). Excitation of rhodamine was achieved with an argon laser [488 nm (47%), 514 nm (39%) and 561 nm (36%)] and the resulting emission was acquired between 575 and 725 nm as an average of four scans. The full images are depicted in Figures 10-12

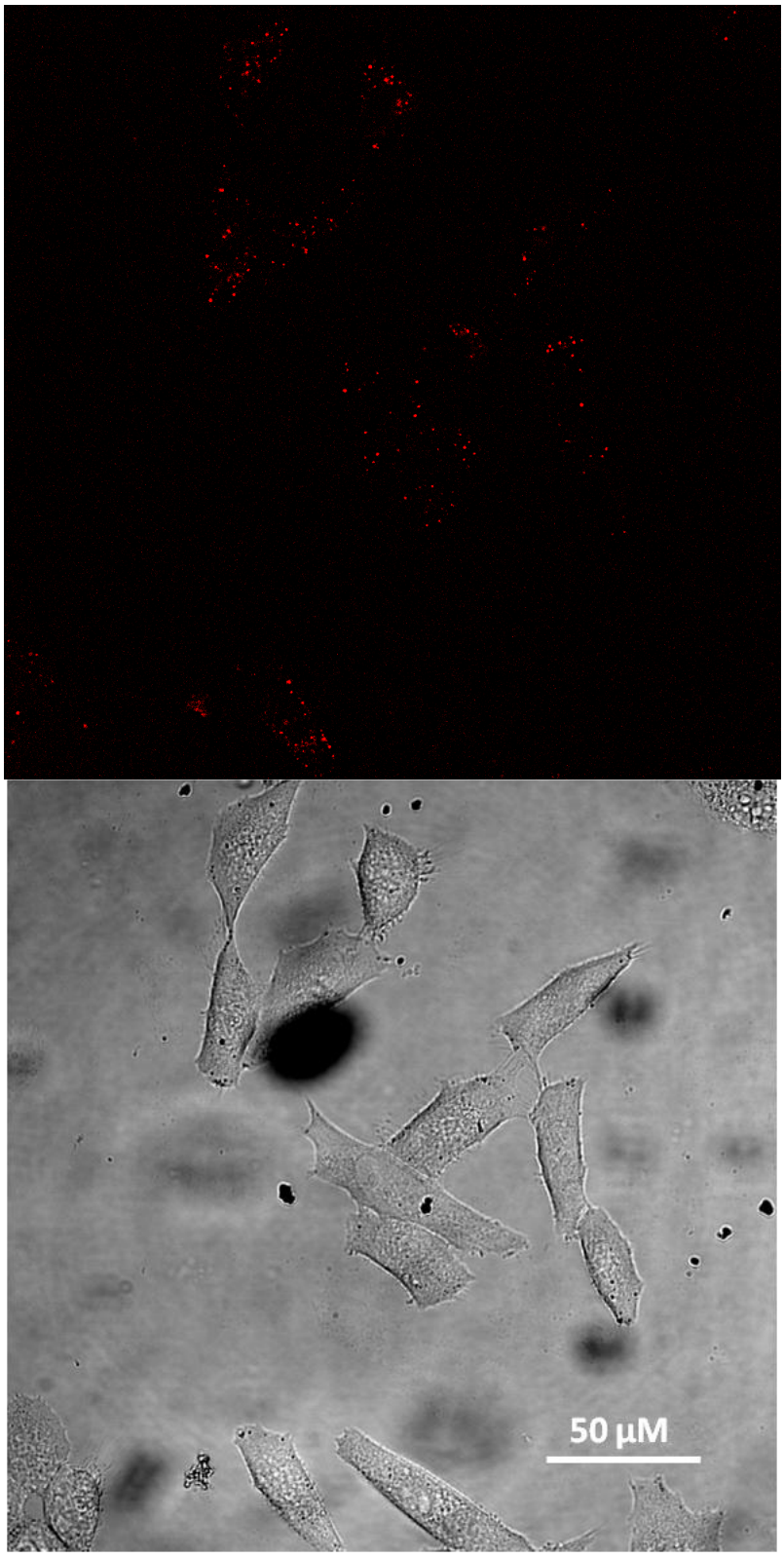

Figure 10. Aniline catalyzed dynamic exchange between a set of Tat-functional polymersomes and a set of rhodamine functional polymersomes results in a new set of polymersomes that are both cell penetrating (Tat, Hela cells) and visible under CLSM. Top) Confocal fluorescent image, polymersomes are coloured as red dots; bottom) corresponding bright field image of the Hela cells.

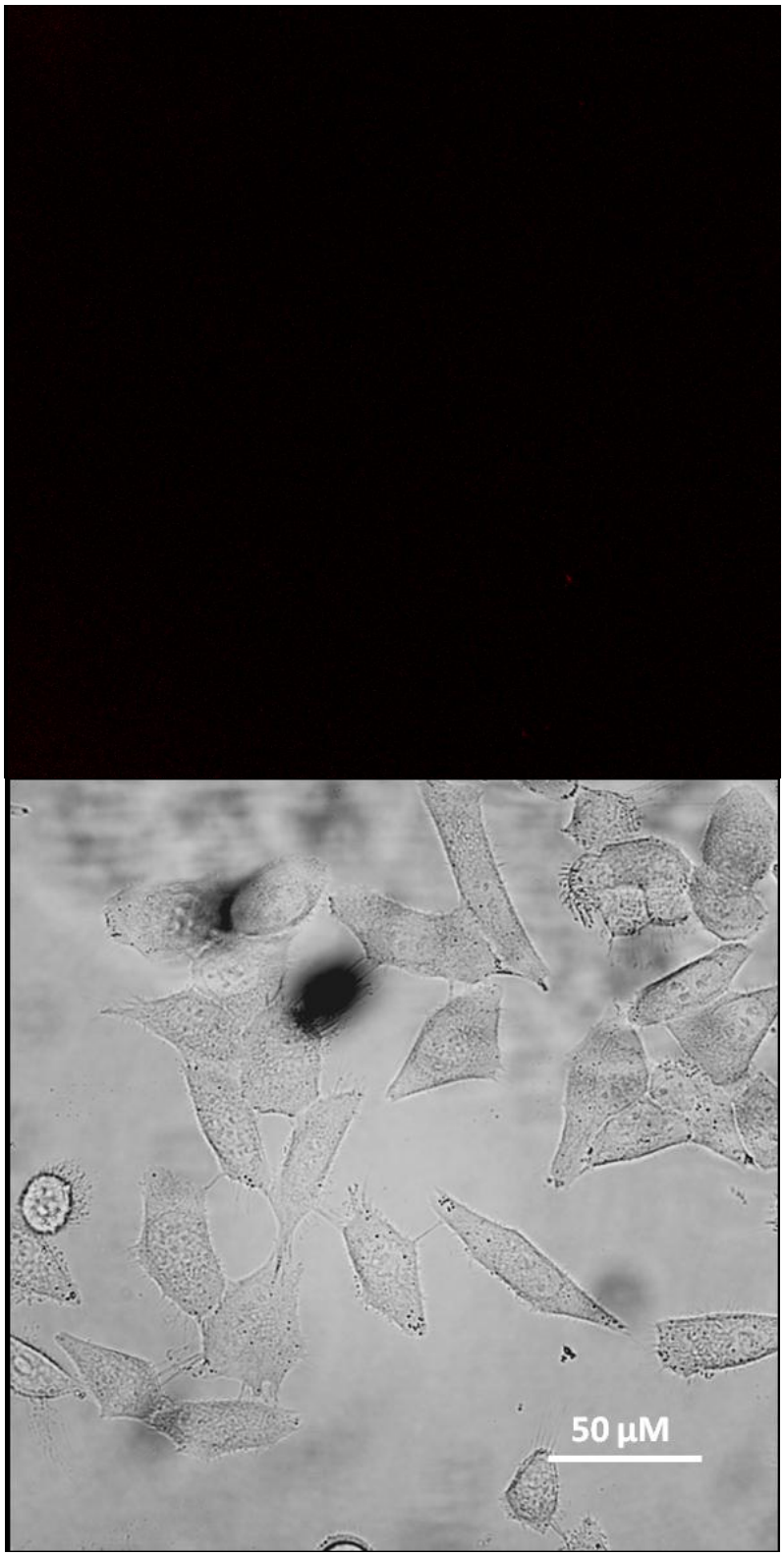

Figure 11. Negative control: Aniline-catalyzed dynamic exchange between a set of Tat-functional polymersomes and a set of irreversibly functionalized (no hydrazone bond) rhodamine-polymersomes does not result in polymersomes that are both cell penetrating (Tat, Hela cells) and visible under CLSM. Top) Confocal fluorescent image, fluorescent-cell penetrating polymersomes would appear as red coloured dots. The absence of polymersomes indicated that indeed no polymersomes adhered or penetrate the Hela cells. Bottom) corresponding bright field image.

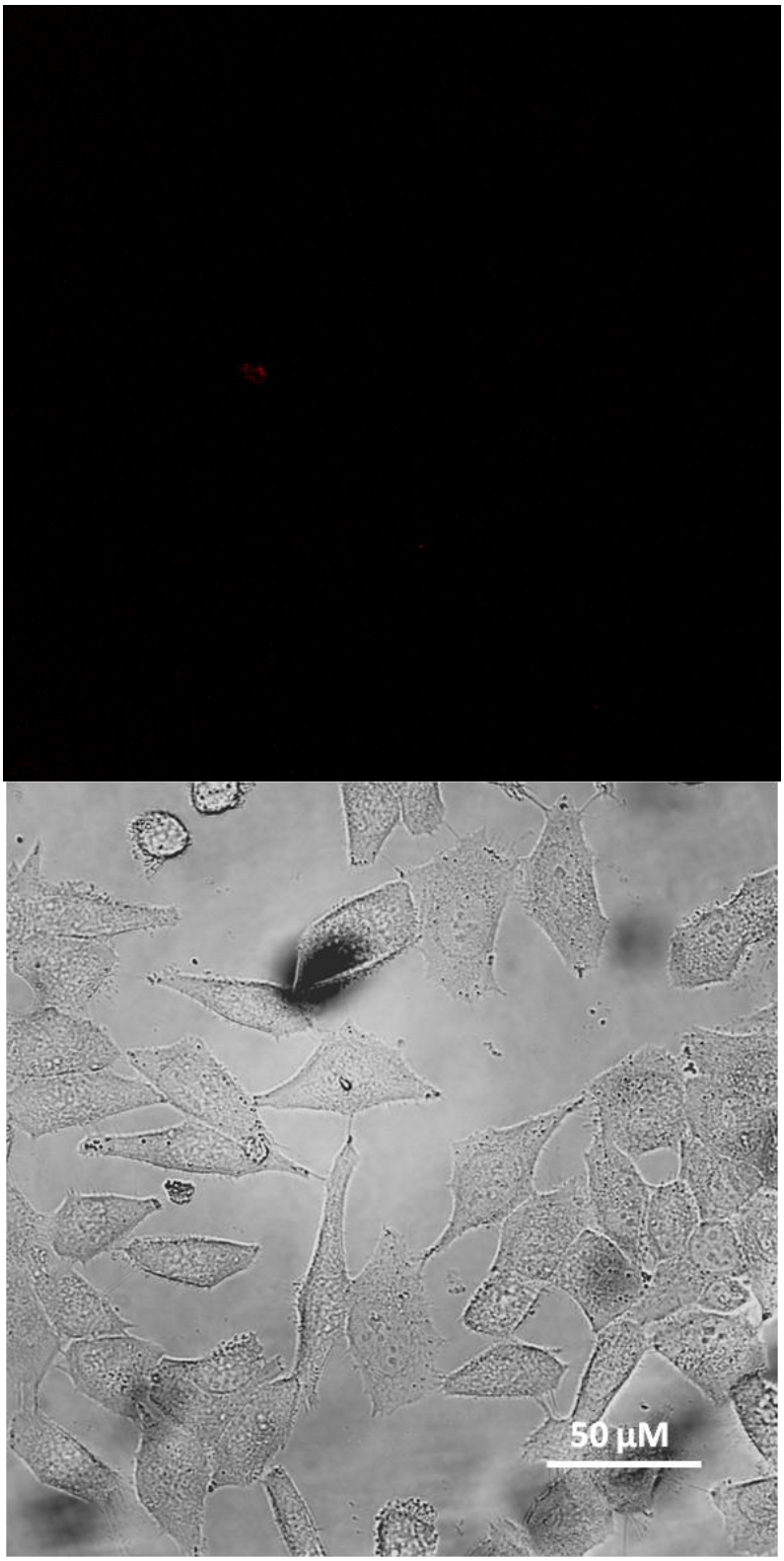

Figure S10. Negative control: Aniline-catalyzed dynamic exchange involving rhodamine-functionalized polymersomes in ***absence*** of Tat-polymersomes does not result in a new set of polymersomes that are both cell penetrating (Hela cells) and visible under CLSM. Top) Confocal fluorescent image, polymersomes would appear as red coloured dots. The absence of polymersomes indicated that indeed no polymersomes adhered or penetrate the Hela cells. Bottom) corresponding bright field image.

7.6 References

(1) Discher, B. M.; Won, Y. Y.; Ege, D. S.; Lee, J. C. M.; Bates, F. S.; Discher, D. E.; Hammer, D. A. *Science* **1999**, *284*, 1143.

(2)Pang, Z. Q.; Lu, W.; Gao, H. L.; Hu, K. L.; Chen, J.; Zhang, C. L.; Gao, X. L.; Jiang, X. G.; Zhu, C. Q. *J Control Release* **2008**, *128*, 120.

(3) Ahmed, F.; Pakunlu, R. I.; Brannan, A.; Bates, F.; Minko, T.; Discher, D. E. *J Control Release* **2006**, *116*, 150.

(4) Cheng, Z. L.; Tsourkas, A. *Langmuir* **2008**, *24*, 8169.

(5) Christian, D. A.; Garbuzenko, O. B.; Minko, T.; Discher, D. E. *Macromol Rapid Comm* **2010**, *31*, 135.

(6) Egli, S.; Schlaad, H.; Bruns, N.; Meier, W. *Polymers* **2011**, *3*, 252.

(7) Christian, N. A.; Milone, M. C.; Ranka, S. S.; Li, G. Z.; Frail, P. R.; Davis, K. P.; Bates, F. S.; Therien, M. J.; Ghoroghchian, P. P.; June, C. H.; Hammer, D. A. *Bioconjugate Chem* **2007**, *18*, 31.

(8) Meng, F. H.; Engbers, G. H. M.; Feijen, J. *J Control Release* **2005**, *101*, 187.

(9) Nehring, R.; Palivan, C. G.; Moreno-Flores, S.; Mantion, A.; Tanner, P.; Toca-Herrera, J. L.; Thunemann, A.; Meier, W. *Soft Matter* **2010**, *6*, 2815.

(10) Lehn, J. M.; Eliseev, A. V. *Science* **2001**, *291*, 2331.

(11) Minkenberg, C. B.; Li, F.; van Rijn, P.; Florusse, L.; Boekhoven, J.; Stuart, M. C. A.; Koper, G. J. M.; Eelkema, R.; van Esch, J. H. *Angew Chem Int Edit* **2011**, *50*, 3421.

(12) Cerritelli, S.; Velluto, D.; Hubbell, J. A. *Biomacromolecules* **2007**, *8*, 1966.

(13) Sourkohi, B. K.; Cunningham, A.; Zhang, Q.; Oh, J. K. *Biomacromolecules* **2011**, *12*, 3819.

(14) Sourkohi, B. K.; Schmidt, R.; Oh, J. K. *Macromol Rapid Comm* **2011**, *32*, 1652.

(15) Egli, S.; Nussbaumer, M. G.; Balasubramanian, V.; Chami, M.; Bruns, N.; Palivan, C.; Meier, W. *J Am Chem Soc* **2011**, *133*, 4476.

(16) Ryu, J. H.; Chacko, R. T.; Jiwpanich, S.; Bickerton, S.; Babu, R. P.; Thayumanavan, S. *J Am Chem Soc* **2010**, *132*, 17227.

(17) Bae, Y.; Fukushima, S.; Harada, A.; Kataoka, K. *Angew Chem Int Edit* **2003**, *42*, 4640.

(18) Brinkhuis, R. P.; Visser, T. R.; Rutjes, F. P. J. T.; van Hest, J. C. M. *Polym Chem-Uk* **2011**, *2*, 550.

(19) He, L.; Jiang, Y.; Tu, C. L.; Li, G. L.; Zhu, B. S.; Jin, C. Y.; Zhu, Q.; Yan, D. Y.; Zhu, X. Y. *Chem Commun* **2010**, *46*, 7569.

(20) Cordes, E. H.; Jencks, W. P. *J Am Chem Soc* **1962**, *84*, 826.

(21) Dirksen, A.; Dirksen, S.; Hackeng, T. M.; Dawson, P. E. *J Am Chem Soc* **2006**, *128*, 15602.

(22) Dirksen, A.; Yegneswaran, S.; Dawson, P. E. *Angew Chem Int Edit* **2010**, *49*, 2023.

(23) Dirksen, A.; Dawson, P. E. *Bioconjugate Chem* **2008**, *19*, 2543.

(24) Zhou, Y. F.; Yan, D. Y. *J Am Chem Soc* **2005**, *127*, 10468.

(25) Green, M.; Loewenstein, P. M. *Cell* **1988**, *55*, 1179.

(26) Frankel, A. D.; Pabo, C. O. *Cell* **1988**, *55*, 1189.

(27) Karlen, B.; Lindeke, B.; Lindgren, S.; Svensson, K. G.; Dahlbom, R.; Jenden, D. J.; Giering, J. E. *J Med Chem* **1970**, *13*, 651.

(28) Deiters, A.; Cropp, T. A.; Mukherji, M.; Chin, J. W.; Anderson, J. C.; Schultz, P. G. *J Am Chem Soc* **2003**, *125*, 11782.

8

Summary & Perspective

Manny potent drugs are hampered by a low bioavailability and never reach the desired tissue, which therefore renders them useless in a clinical environment. Additionally, organisms are equipped with impermeable physiological barriers, among them the blood-brain barrier. One strategy to overcome these obstacles is by chemical modification of the drugs to increase their bioavailability. However, this strategy involves alteration of the chemical structure which in many cases reduces the potency of the drug. Nanotechnology might overcome these obstacles by providing carriers that transport the unmodified drug to the desired place in the body. This thesis describes the design of such a polymeric nanocarrier system based on the block copolymer polybutadiene-block-poly(ethylene glycol) which has the ability to target and cross the blood-brain barrier and allows for in vivo SPECT imaging.

8.1 Summary

In the first chapter an overview of the recent literature on polymeric vesicles, also known as polymersomes, in biomedical applications is given. From this chapter it becomes clear that the possibilities to tailor and optimize polymeric vesicles for a given application are only limited by the creativity of the researchers. The design flexibility makes polymersomes interesting candidates for nanomedicine, but also introduces a high degree of complexity. The rational design of a vesicle starts on the level of the choice of monomers to form amphiphilic block copolymers of predefined molecular weight, and reaches all the way up to the supramolecular level where shape, size, porosity and surface functionality become important.

To tackle this complexity, while retaining the flexibility in design, we have developed in chapter 2 a chemical platform based on the amphiphilic block copolymer polybutadiene-*block*-poly(ethylene glycol) which has the property to self assemble into polymersomes. This platform allows to construct vesicles functionalized with multiple proteins, peptides and imaging probes; furthermore, control over the polymersome size is easily obtained. This chemical platform forms the basis of the research as described in chapters 3-7.

In chapter 3, size was demonstrated to be an important factor influencing the blood circulation of polymersomes. Vesicles of the amphiphilic block copolymer polybutadiene-*block*-poly(ethylene glycol) with an average size of 250, 120 and 90 nm were formed and labelled with a radioisotope, ^{111}In. The biodistribution in mice over all main organs was analyzed and showed a similar trend as found for liposomes. However, for polymersomes the transition from long blood circulation to fast clearance by the liver and spleen was more abrupt, leading to the conclusion that long circulating polymersomes should be formulated well below a size of 100 nm. This sharp transition from long blood circulation (90 nm) to fast liver and spleen accumulation (≥ 120 nm) was also visualized by the non invasive technique of SPECT/CT imaging.

In chapters 4 and 5 we designed a G23-peptide functionalized polymeric vesicle that is able to efficiently cross the blood brain barrier by recognition of the gangliosides GM1 and GT1b. These chapters also nicely illustrate that the design of polymersomes for biomedical (and other) applications is not only dependent on a good control over the chemistry and supramolecular assembly. To identify potent targets and ligands and test

them both *in vitro* and *in vivo* an in dept knowledge over the function and physiology of (in this case) the blood-brain barrier is needed. These kinds of potential drug delivery systems therefore can only be developed by a tight interplay between groups of different expertise such as (polymer) chemistry, nuclear medicine and cell membrane biology.

The resulting G23- tagged polymeric vesicles were additionally labelled with fluorescent or radioisotope labels for *in vitro* and *in vivo* analysis. *In vitro* studies showed a high and selective transcytosis potential for the G23-polymersomes which was confirmed by *in vivo* experiments in mice. An in dept *in vivo* analysis (chapter 5) revealed that G23-polymersomes were able to cross the blood-brain barrier with an efficiency comparable with antitransferrin-tagged polymersomes, which can be regarded as a golden standard. However, an unexpected result was the high accumulation of G23-polymersomes in lung tissue, which might either be circumvented by smart drug administration or be used to its advantage for targeted drug delivery to lung tissue (e.g. tuberculosis).

The final two experimental chapters (6 and 7) describe a more fundamental line of investigation into the design and functionalization of polymersomes. Again, a block copolymer based on polybutadiene-*block*-poly(ethylene glycol) was designed. However, this time both blocks were coupled via a hydrazone moiety, which is a dynamic bond and pH sensitive within the physiological relevant window.

In chapter six we explore the pH dependent stability of polymersomes assembled from hydrazone-coupled block copolymers. It was shown that these polymersomes of predefined size lost their colloidal stability upon lowering the pH from 7.4 to 6.4 and less. When a pH stable block copolymer, as developed in chapter 2, was mixed in structural control was regained. It was demonstrated that the presence of less than 5% of surface PEGylation was sufficient to maintain colloidal stability.

Finally, chapter 7 explores the (catalyzed) dynamic nature of polymersomes assembled from hydrazone-coupled block copolymers. It was shown that the introduction of a hydrazone moiety in polymersomes allows for the construction of more complex, asymmetrical and multifunctional polymeric vesicles. The dynamic nature of the hydrazone bond allowed the exchange of surface functionality both with polymers which were molecularly dissolved and between polymersomes. This opens up

new routes toward more complex multi-functionalized polymeric vesicles with control over size and colloidal stability.

8.2 Perspective

In this thesis a line of research is described, which involves the successful design of a polymersome drug delivery system that can cross the blood-brain barrier *in vivo*. Although several research questions have been appropriately answered, such as targetability, and optimal size for biodistribution, in order to move toward actual applications of these polymeric vesicles in the clinic, important challenges still have to be dealt with in a future line of research.

Throughout this thesis the amphiphilic block copolymer polybutadiene-*block*-poly(ethylene glycol) was used because of its low glass transition temperature and biocompatibility. Although this polymer is not biodegradable on a timescale of days this polymer was chosen since it allowed us to control the overall polymersome structure in a relatively “simple” model. The lack of biodegradability rules out the complicating factor of decomposition, but seriously hampers the applicability in a clinical setting and therefore the biodegradability needs to be addressed in the future research.

In many cases there can be important, and sometimes unpredictable discrepancies between model systems and the actual drug delivery vehicles. For example, in chapter 3 size was subject to research with respect to biodistribution in mice. Although studies with the empty polybutadiene-*block*-poly(ethylene glycol) polymersomes give important insights, they may not reflect the full complexity of a targeted drug delivery vesicle. In chapter 2 it was briefly mentioned that 1 weight percent of a drug could be encapsulated in the vesicle membrane. At this moment it is under investigation whether membrane stiffening, due to drug encapsulation, will influence the blood circulation of 90 nm polymersomes. The effect of size and membrane stiffness are only two parameters that have to be simultaneously considered to understand blood circulation.

The results as discussed chapter 4 and 5 are highly promising for the development of a real biomedical application. In fact, both the *in vitro* and *in vivo* efficiency of transport for G23-tagged polymersomes over the BBB is high compared to most other delivery systems. Moreover, the design of this G23-vesicle, along with the identification of

G23/GM1 as tag and target, was accomplished within four years. However, also in this case many questions still have to be answered. Would a differently sized polymersome perform better, how much of a certain drug can be maximally encapsulated, how can a release mechanism be effectively introduced when the carrier reaches the brain parenchyma and is there an enhanced therapeutic effect? Furthermore, it should be noted that although the brain delivery of G23-polymersomes is high compared to other delivery systems, it is still less than one percent of the injected dose that reaches the brain.

In 1999 Discher et al. published the first in dept study into polymeric vesicles which he coined polymersomes. One feature that was immediately noted is the resemblance with liposomes. Upon extending this comparison, it should be noted that liposomes have been studied for more than 50 years and are nowadays found in approved drug formulations. In this perspective liposomes have a head-start of more than 40 years. However, after a decade of research into polymeric vesicles one can say that basically anything which can be done with liposomes has been published with polymeric vesicles. Furthermore, in many (but not all) cases polymeric vesicles outperform liposomes, making biomedical applications feasible and just a matter of time.

In the near future, a gain in therapeutic effect by replacing existing therapeutics based on e.g. liposomes may be foreseen. But probably the biggest potential for polymersomes lies in the huge diversity of polymers that can and have been used to meet specific criteria for a given application. Chemists can use their full creativity to adjust polymeric vesicles after receiving new input from different fields of science. And it is this adjustability and flexibility in design which elevates polymeric therapeutics above conventional approaches. *Polymer therapeutics* will continue to solve biomedical problems, where the possibilities for conventional medicine end.

8

Samenvatting & Visie

Veel potentiële medicijnen zijn kansloos in een klinische toepassing, omdat ze leiden onder een te lage biologische beschikbaarheid en dus nooit in het juiste weefsel aankomen. Daarnaast kent het lichaam een aantal vrijwel onneembare barrières, waaronder de bloed-hersenbarrière. Een manier om de biologische beschikbaarheid van medicijnen te verbeteren is door ze chemisch aan te passen, maar dit resulteert vaak in een verminderde werking. Een relatief nieuwe manier om dit opstakel te nemen wordt gevonden in de nanotechnologie. Nanotechnologie maakt het mogelijk om deeltjes ter grootte van 1/1000 tot 1/50 haardikte te vormen waar een medicijn ingesloten wordt. Door vervolgens specifieke liganden op deze deeltjes te zetten kan het naar de juiste plek gebracht worden om het medicijn af geven. In dit proefschrift wordt de ontwikkeling van zo'n polymeer nanodeeltje beschreven dat in staat is de bloed-hersenbarrière over te steken en door middel van SPECT/CT scan gevisualiseerd kan worden.

8.1 Samenvatting

In het eerste hoofdstuk wordt een overzicht gegeven van de meest recente literatuur op het gebied van polymeer nanodeeltjes (polymersomen) in biomedische toepassingen. Uit deze literatuurstudie komt naar voren dat de enige beperkende factor in de optimalisatie en toepassing van polymersomen de creativiteit van de onderzoeker is. De flexibiliteit in het design maakt van polymersomen een interessante klasse van deeltjes voor medicijn afgifte, maar maakt ook dat het formuleren erg complex wordt. Rationeel design begint daarom bij de keuze van monomeren om polymeren te maken van een goed gekozen lengte en gaat door tot de supramoleculaire chemie, waar keuzes als vorm, deeltjes grootte en oppervlakte chemie centraal komen te staan.

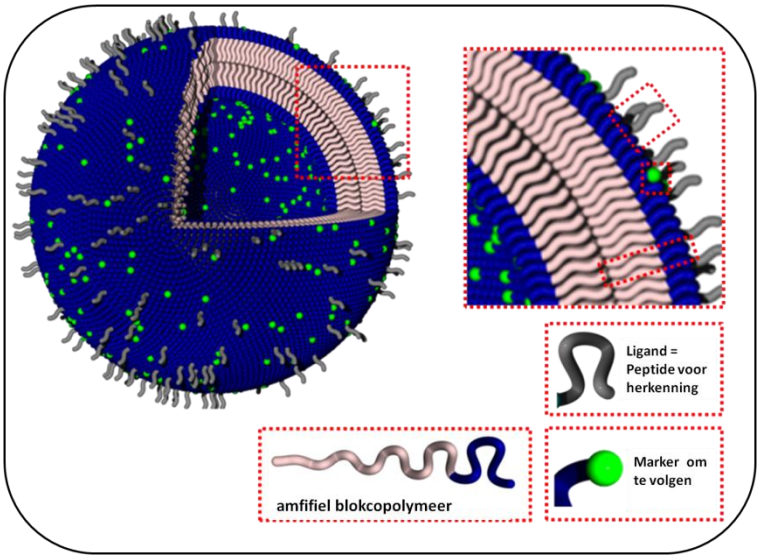

Om een weg te vinden in deze complexe chemische ruimte hebben wij in hoofdstuk 2 een chemisch platform ontwikkeld gebaseerd op het amfifiele blok copolymeer polybutadiene-poly(ethylene oxide). Dit polymeer is in staat om zichzelf te assembleren in een dubbel membraan dat de buitenkant van een sferisch deeltje vormt, een polymersoom. Tevens wordt een methode beschreven om deze deeltjes in grootte te variëren van 1/1000 tot 1/50 van een haardikte en ze te functionaliseren met eiwitten, peptiden en fluorescente/radioactieve labels. Dit chemische platform vormt dan ook het uitgangspunt voor het onderzoek als beschreven in hoofdstukken 3-7.

In hoofdstuk 3 wordt aangetoond dat deeltjes grootte een belangrijke factor is als het gaat om bloedcirculatie. Polymersomen met een gemiddelde grootte van 250, 120 en 90 nm zijn gelabeld met een radioactief isotoop van indium (^{111}In). De biodistributie na 4 en 24 uur over de belangrijkste organen en het bloed is vervolgens bepaald in muizen. De algemene trend was gelijk aan die van liposomen (de fosfolipiden analoog van polymersomen). Echter, de overgang van lange bloed circulatie naar snelle lever- en

mildopname was veel abrupter. Dit leidt tot de conclusie dat voor lange bloedcirculatie de polymersomen kleiner dan 100 nm moeten zijn. Daarnaast is het effect van lange bloedcirculatie voor 90 nm deeltjes en snelle lever- en mildopname voor deeltjes van 120 nm gevisualiseerd d.m.v. SPECT/CT scans, een veel gebruikte techniek in de nucleaire geneeskunde.

In hoofdstukken 4 en 5 wordt de ontwikkeling van een peptide (G23) gefunctionaliseerde polymersome dat de bloed-hersenbarrière kan oversteken beschreven. Dit gebeurd door herkenning van de gangliosiden GM1 en GT1b. Deze hoofdstukken illustreren tevens dat de ontwikkeling van polymersomen voor biomedische (en andere) toepassingen een multidisciplinair onderzoek is, waarvoor onderzoekers uit verschillende velden intensief met elkaar samen moeten werken. In dit geval was naast chemische kennis ook gedegen kennis over de fysiologie van de bloed-hersenbarrière en nucleaire geneeskunde nodig om liganden te identificeren en die zowel *in vitro* als *in vivo* te testen.

Deze samenwerking resulteerde in de ontwikkeling van G23-gefunctionaliseerde polymersomen met een fluorescente en/of radioactieve (^{111}In) label voor *in vitro* en *in vivo* studies. *In vitro* cel studies laten zien dat G23-gefunctionaliseerde polymersomen in staat zijn om selectief over een bloed-hersenbarrière model transporteren (hCMEC/D3, transcytose). Dit wordt ook bevestigd door een eerste kleinschalige muis studie.

In hoofdstuk 5 is de *in vivo* bioditributie van G23-polymersomen in de hersenen en overige organen in detail bestudeerd (muis studies). Deze resultaten zijn in een directe studie vergeleken met transferrin antilichaam gefunctionaliseerde polymersomen. Transferrin antilichaam, met een molecuul gewicht van ~90.000 Dalton, wordt momenteel gezien als de gouden standaard. Onze resultaten laten zien dat het G23-peptide, met een molecuulgewicht van slechts 1.640 Dalton, vergelijkbare resultaten geeft. Echter, we zagen ook een grootte specifieke toename van G23-polymersomen in het longweefsel. Dit zou onderdrukt kunnen worden door aangpaste toediening van de polymersomen, of in het voordeel gebruikt kunnen worden voor medicijn afgifte in de longen.

De laatste twee hoofdstukken (6 en 7) laten een meer fundamentele studie naar design en functionalisering van polymersomen zien. Wederom is het polymeer polybutadiene-

poly(ethylene glycol) gesynthetiseerd, maar dit maal zijn beide delen door een hydrazon binding met elkaar verbonden. Hydrazon bindingen zijn dynamische bindingen met een pH gevoeligheid in een fysiologisch relevante range (pH 5-8).

In hoofdstuk 6 wordt de pH gevoeligheid van deze binding in polymersomen bestudeerd. We tonen aan dat deze polymersomen stabiel zijn bij een pH van 7.4 (bloed) en hun colloïdale stabiliteit verliezen wanneer de pH verlaagd wordt naar 6.4 en lager (endosoom). Door het inmengen van verschillende hoeveelheden van het stabiele polymeer uit hoofdstuk 2 konden polymersomen met verschillende PEGyleringsgraden worden verkregen. De minimum hoeveelheid poly(ethyleen glycol) die nodig is om de colloïdale stabiliteit van polymersomen te behouden is 5 procent.

Tot slot wordt in hoofdstuk 7 een studie gepresenteerd waarin polymersomen met een hydrazon binding stabiel gehouden worden bij pH 7.4. Dit maal werden de aniline gekatalyseerde dynamische eigenschappen van de hydrazon binding gebruikt om functionele groepen te introduceren door middel van oppervlakte uitwisseling. Dit resulteerde in asymmetrische membranen met verschillende functionele groepen aan de binnen- en buitenzijde van de polymersomen. Daarnaast werd aangetoond dat uitwisseling van functionele groepen *tussen* polymersomen mogelijk is. Deze resultaten openen nieuwe mogelijkheden voor de constructie van complexe multifunctionele polymersomen met controle over hun grootte *en* colloïdale stabiliteit.

8.2 Visie

Dit gehele proefschrift is gebaseerd op het polymeer polybutadiene-poly(ethylene glycol). Dit polymeer werd gekozen vanwege zijn lage glastransitie temperatuur (vervormbaar bij kamertemperatuur) en biologische tolerantie. Echter, dit polymeer is niet biologisch degradeerbaar op een tijdschaal van dagen. Toch hebben we voor dit polymeer gekozen, omdat het ons in staat stelt om een relatief simpel polymersome model te bestuderen met goede controle over de structuur. Daarnaast zou biodegradeerbaarheid een extra complexiteit met zich mee brengen, namelijk het uit elkaar vallen van de structuur tijdens de studies. Echter, het is juist de robuustheid van ons model dat in een klinische toepassing zeer ongewenst is. Daarom moet de factor degradeerbaarheid in vervolgstudies zeker geïntroduceerd worden.

Daarnaast zijn alle *in vitro* en *in vivo* studies zijn uitgevoerd met lege polymersomen om belangrijke inzichten te krijgen in bijvoorbeeld de bloedcirculatie en biodistributie

van polymersomen. Echter, ook dit is een versimpelde weergave van een polymersome medicijn-afgifte systeem. In hoofdstuk 2 werden kort enkele experimenten beschreven die aantonen dat polymersomen beladen kunnen worden met 1 procent van een model drug. Deze belading veranderd de stijfheid van het membraan en zal wellicht een invloed op de bloedcirculatie en biodistributie hebben. Een mogelijke verandering als gevolg van medicijn belading wordt momenteel dan ook onderzocht.

Het onderzoek als beschreven in hoofdstuk 4 en 5 zijn zeer veel belovend voor toekomstige biomedische toepassingen. De muizen leken niet te leiden onder de polymersome injecties en zowel de *in vitro* als *in vivo* resultaten laten een zeer hoog transport van polymersomen over de bloed-hersenbarrière zien. Zeker in vergelijking tot de meeste reeds bekende systemen. Hierbij moet ook aangemerkt worden dat het ontwikkelen van de polymersomen, het identificeren van G23-peptiden en het *in vitro/in vivo* testen binnen vier jaar is uitgevoerd. Een extra optimalisatie itteratie zou zeker tot nog betere resultaten leiden, want ook deze hoofdstukken laten vragen onbeantwoord. Zou een andere grootte polymersomen in deze setting andere resultaten geven (combinatie van de factoren grootte en functionalisatie), hoe kunnen we een medicijn vrijgeven als de polymersome in het hersenweefsel is aangekomen en is er een therapeutisch effect in een ziektemodel? Daarnaast moeten we aantekenen dat, hoewel ons systeem nu al efficiënt is vergeleken met andere onderzoeken, er nog altijd minder dan 1 procent van de geïnjecteerde dosis in het hersenweefsel terecht komt. Er is dus nog veel ruimte voor verbetering en het ontwikkelen van betere inzichten ten aanzien van het gebruik van polymersomen in biomedische toepassingen en in het gebied van "polymer therapeutic" in het algemeen.

In 1999 werd door Discher een eerste systematische studie naar de structuur van holle sferische polymeer structuren uitgevoerd. In deze publicatie noemt hij deze structuren polymersomen, naar analogie van liposomen die reeds meer dan 50 jaar bekend en bestudeerd werden. Tegenwoordig worden liposomen gevonden in medicijnen die goedgekeurd zijn voor gebruik in de kliniek. In dat opzichte hebben studies naar liposomen in biomedische toepassingen een voorsprong van meer dan 40 jaar. Echter als je de literatuur vandaag de dag bestudeerd wordt duidelijk dat in ruim tien jaar alles wat ooit gedaan is met liposomen ook met polymersomen is gedaan. Daarnaast blijkt steeds weer dat in veel (maar niet alle) toepassingen polymersomen beter presteren dan

liposomen omdat er veel meer design vrijheid is. Daarom is de introductie van de eerste medische toepassingen van polymersomen in mijn optiek voor de hand liggend en slechts een kwestie van tijd. Ik ben er dan ook van overtuigd dat in de nabije toekomst bestaande therapieën gebaseerd o.a. liposomen vervangen worden door polymersome analoge, maar de grootse potentie ligt in enorme diversiteit van polymeren en structuren die mogelijk zijn voor polymersomen en "polymer therapeutics" in het algemeen om aan specifieke criteria te voldoen. De creativiteit van de chemici is slechts de beperkende factor om formuleringen te verbeteren nadat wetenschappers uit andere disciplines hun input terug hebben gegeven. Het is deze flexibiliteit die "polymeric therapeutics" ver boven conventionele methoden uit tilt. *Polymeric therapeutics* zal biomedische oplossingen blijven bieden waar conventionele therapieën geen antwoord hebben.

Dankwoord

Mij is niets gebeurd
en hij komt er boven op
hij oefent om te praten
en ik, ik hou eindelijk m'n kop

kijk ons zitten bij het water
zoals elk weekend weer
de wereld aan onze gympies
maar we hoeven 't niet meer

we zijn gewoon twee vrienden
en we kijken naar de zee
en we zwijgen van hetzelfde
je hoeft niet elke keer mmmm
met elk circus mee

Mij is niets gebeurd
en hij komt er boven op
hij oefent om te praten
en ik, ik hou eindelijk m'n kop

hij zegt ola hij zegt allah
een lach ontsnapt aan het schavot
ola allah ola Allah

en ik denk
een Spaanse Moslim groet z'n God
een Spaanse Moslim groet z'n God

(Acda & de Munnik)

Doorlopend in dit proefschrift heb ik geprobeerd steeds in de wij-vorm te schrijven, want het moge duidelijk zijn dat ik dit werk zeker niet alleen heb gedaan. Op de werkvloer kon ik rekenen op de steun van mijn collega's, de vaste staf en natuurlijk een klein legertje studenten die veel werk voor mij hebben uitgevoerd. Thuis kon ik op de steun van familie en vrienden rekenen. Helaas kan ik niet iedereen persoonlijk noemen, toch zijn een aantal mensen die ik hieronder kort wil benoemen.

Allereerst natuurlijk mijn promotores Jan van Hest en Floris Rutjes. Ik wil jullie bedanken voor het vertrouwen dat jullie in mij hadden op het moment dat jullie mij een promotieplek aanboden. Jan, met jou heb ik meer de chemie focus op het project besproken en kon altijd op je hulp rekenen. Floris, bij jou kwam ik altijd met de saaiere zakelijke vragen terecht, maar ook de meer organisch chemische vragen werden door jou beantwoord. Ik ben jullie beide zeer dankbaar voor de goede begeleiding en denk met warme gevoelens terug aan de vier jaar die ik in jullie labs heb mogen doorbrengen.

Veel van het werk beschreven in hoofdstukken 4 en 5 is in samenwerking met Julia, Katica, Inge en Dick Hoekstra van de UMC Groningen uitgevoerd. Julia en Katica, I really enjoyed working with the two of you. I think our joined efforts lifted the level of our research. Julia, I like your straight forward and efficient approach. Next time we meet we should have a cup of hot chocolate! Katica, you are one of the strongest women I have ever met and yet you are so warm hearted. A nice combination which I admire in you. Inge, als begeleider van Julia en Katica wil ik ook jou bedanken voor onze geslaagde samenwerking. Dick Hoekstra, niet alleen hebben wij in het beschreven onderzoek samengewerkt, maar je bent ook lid van de manuscriptcommissie. Ik wil je hartelijk bedanken voor deze dubbele rol, maar ook voor de interesse die je altijd in mijn werk hebt getoond.

Iets dichter bij huis in het UMC Nijmegen hebben Peter Laverman en Otto Boerman mij geholpen met de experimenten als in hoofdstuk 3 beschreven. Peter, samenwerken met jou is ontspannen en doelgericht. We hebben een mooie publicatie geproduceerd en zullen elkaar in de toekomst nog vaker zien. Otto Boerman, jou wil ik bedanken voor het steunen van deze samenwerking en natuurlijk voor het plaatsnemen in de manuscriptcommissie.

Ik heb het genoegen gehad om met een groot aantal collega's samen te mogen werken in zowel de Bio- Organische als Synthetisch- Organische groep. Een persoon die er dan meteen uitspringt is Hans Adams, de "peptide master". Hans, jij bent niet weg te denken uit de dankwoorden in Nijmeegse chemie proefschriften. Dat is niet voor niets, want ook in dit proefschrift heb jij een behoorlijke peptide afdruk achter gelaten. Hans, ik zeg altijd maar zo, dat op een gegeven moment iedereen jouw verhalen echt zal gaan missen. Daarom wil ik je bij deze bedanken voor je hulp en gezelschap. Ook gaat er een woord van dank uit naar de vaste staf en in het bijzonder de secretaresses Jacky, Marieke, Paula en Desiree. In het lab heb ik samen mogen werken met vele collega promovendi en postdocs. Jullie hebben er allen voor gezorgd dat ik iedere dag weer met plezier naar Nijmegen ben gereisd om in een goede sfeer aan het werk te gaan. In het bijzonder wil ik Jorgen, Henri en Ferdi bedanken. Regelmatig denk ik nog terug aan de fantastische transdolomiti die wij hebben gefietst, een prestatie en ervaring die ik niet snel zal vergeten.

Wellicht is de grootste bijdrage aan dit proefschrift geleverd door de studenten die ik heb mogen begeleiden. Hoewel niet al hun werk in de publicaties of dit proefschrift terecht is gekomen zijn het hun resultaten die geleid hebben tot de experimenten die uiteindelijk in dit boekje zijn opgenomen. Kelly, Berry, Sander, Jos, Sanne, Taco, Frank en Ruoyu ik heb veel van jullie mogen leren.

Kelly en Berry, jullie hebben een grote bijdrage geleverd in het begin van mijn onderzoek. Dankzij jullie inspanningen is de chemie, zoals beschreven in hoofdstuk 2, tot stand gekomen. Kelly, ik kan ik me de beelden van een meisje van ~1.5 meter dat staand op een krukje een bijna even zo grote kolom tot een goed einde brengt nog levendig voor me halen. Berry, jij was mijn eerste en meest eigenwijze student ooit. Echter, jouw werk aan de anionische polymerisatie van polyethyleen glycol was zeker niet makkelijk. Een deelonderzoek waarin je eigenwijze karakter goed van pas is gekomen.

Sander en Jos, ook jullie hebben tegelijk stage gelopen en hoewel ik soms helemaal gek werd van jullie drukte was dit een topjaar. Sander, als jij je mond opent volgt er een spraakwaterval die geen einde lijkt te krijgen. Je enthousiasme is enorm en uit zich dan ook in een brede interesse van synthetische chemie via stijldansen tot biologie. Jos, jij was verreweg de meest speelse student die ik heb gehad. Hoewel het daardoor soms moeilijk was om je op je werk te laten focussen heb je de basis weten te leggen voor een

mooie publicatie. Een co-auteurschap doet recht aan jouw inspanningen waar je trots op mag zijn.

Sanne en Taco, ook tussen jullie stage zat veel overlap en ik denk dat er een mooie vriendschap tussen beide uit is ontstaan. Taco, jij werd als HBO-student in mijn schoot geworpen. In de eerste instantie wilden ik jou “handige moleculen” voor de hele groep laten synthetiseren. Echter, binnen twee weken zag ik dat dit een grove onderschatting van jouw kunnen was. Dat jij ook zeer uitdagende projecten tot een goed einde weet te brengen komt dan ook naar voren in twee co-auteurschappen. Sanne, jouw vrolijke karakter en gedrevenheid om goede resultaten te behalen zijn onophoudelijk. Hoewel dit een van je sterke punten is, merkte ik dat je soms ook te veel hooi op je vork neemt en heb daarom geprobeerd om je ruimte te geven. Tijdens jouw ministage zag ik dat je zelfstandig ideeën ontwikkeld en je inzet en doorzettingsvermogen niet verminderd als het merendeel van de experimenten mislukt. Dit is een unieke eigenschap! Het is dan ook niet voor niets dat ik je heb gevraagd om ook een lange stage bij mij (en Hanneke) te lopen.

Frank, als natuurwetenschapper kwam jij precies op het juiste moment langs voor een ministage. Je hebt heel wat tijd achter de confocal microscoop doorgebracht en hebt perfect uitgezocht hoe de verschillende polymersome samples op fluorescentie geanalyseerd dienen te worden. Ondanks dat je na een week al wist dat dit type onderzoek niet jouw toekomst zal zijn, heb je extra tijd in je stage gestoken om het project volledig af te ronden. Jij staat model voor een geduldige, serieuze, doordachte en resultaat gerichte onderzoeker.

Ruoyu Xing, I thought I would have no more students yet you came to do an internship with me, although you knew I would leave before you would finish. You are a unique student in the sense that you want to learn chemistry while being a biology student. Besides your study you enjoy life and your stay in the Netherlands to the fullest. Not afraid to meet new people you travelled with couch surf friends to Deventer to visit the Charles Dickens festival, where we also had a few drinks.

Dan zijn er nog een aantal mensen/groepen die ik kort wil benoemen, gewoon omdat ze er zijn of zijn geweest. Te beginnen met het hele team van TI pharma project T5-105 met in het bijzonder nog Hanneke. Ook mijn vrienden waar ik regelmatig mee op trek wil ik

bedanken. Mijn vrienden hebben jarenlang saaie scheikunde verhalen moeten aanhoren, daarom heb ik speciaal voor jullie een Nederlandse samenvatting geschreven.

De liefde voor scheikunde en zin om een studie chemie te studeren is ontstaan in de scheikunde lessen op het voortgezet onderwijs. Jan Legebeke (alias LEGObeke), hoewel u niet mijn eerste scheikunde docent was, was u wel de docent die mijn liefde voor chemie heeft aangewakkerd en gevoed. Jouw lessen hebben de basis gelegd voor mijn zeer geslaagde keuze om chemie te studeren en in de chemie te promoveren.

Twee mensen hebben mij altijd en onvoorwaardelijk gesteund in keuze als kind, jong volwassene en zelfs nu nog. Dat zijn mijn ouders! Er wordt wel eens gezegd dat een kind een product van de opvoeding is. Hoewel ik het daar niet altijd mee eens ben weet ik zeker dat ouders die alle “tools” aanreiken om iets van je leven te maken het maximale hebben gegeven. Papa en mama, ik ben zeer blij met alle mogelijkheden die jullie mij hebben gegeven en zie steeds vaker in wat jullie jezelf daar voor ontzegd hebben. Ik wil jullie, maar ook mijn beide zussen Ingrid en Ester dan ook speciaal benoemen.

Sinds kort heb ik er officieel een tweede familie bij, de familie Bosch. Zij hebben mij het mooiste geven wat zij in huis hadden; Lisette. Na exact 10 jaar mag ik je nu mijn vrouw noemen. Vrijwel mijn hele studie en promotie heb jij meegemaakt en gesteund. Het is fijn om bij jou thuis te komen en te merken dat je naar mijn verhalen luistert. Liesje, ik hou van jou.

About the author

René Brinkhuis (11 April 1981) was born in Deventer and raised in Raalte, the Netherlands, where he attended elementary school and secondary school. In 2001 he started his study chemistry at the Radboud University in Nijmegen. His major was in Bio-Organic Chemistry where he worked on the use of “click chemistry” to functionalize polymeric vesicles. Thereafter he performed a minor in solid state chemistry where he studied the solution growth of quinacridone polymorphs from ionic liquids both experimentally and theoretically. In 2008 he received his master’s (doctoraal) degree in chemistry and started his PhD research in a joined project between the group of Bio-Organic Chemistry (Prof. van Hest) and Synthetic Organic Chemistry (Prof. Rutjes). He studied the use of polymeric vesicles in transport over the blood-brain barrier and SPECT imaging. After finishing his thesis in 2012 he went to work for a spinoff company, 20MED therapeutics, of the department of Bio-Medical Chemistry at Twente University (Prof. Engbersen), where he is currently working on siRNA delivery by poly(amido amine) nanogels.

List of publications

Papers:

1) René P. Brinkhuis, Frank de Graaf, Morten Borre Hanssen, Taco R. Visser, Floris P. J. T. Rutjes and Jan C. M. van Hest, *submitted*

2) Julia V. Georgieva,† René P. Brinkhuis,† Katica Stojanov, Carel A. G. M. Weijers, Han Zuilhof, Floris P.J.T. Rutjes, Dick Hoekstra Jan C.M. van Hest, and Inge S. Zuhorn, *Angewandte Chemie* **2012**, 51, 8339-8342;

3) Katica Stojanov, Julia V. Georgieva,† René P. Brinkhuis,† Jan C. M. van Hest, Floris P. J. T. Rutjes, Rudi A. J. O. Dierckx, Erik F. J. de Vries and Inge S. Zuhorn, *Molecular Pharmaceutics* **2012**, 9, 1620-1627.

4) René P. Brinkhuis,† Katica Stojanov,† Peter Laverman, Jos Eilander, Inge S. Zuhorn, Floris P. J. T. Zuhorn and Jan C. M. van Hest, Bioconjugate Chemistry, *Bioconjugate Chemistry* **2012**, 23, 958-965

5) Britta E. I. Ramakers, Maaike van den Heuvel, Nearchos Tsichlid i Spithas, René P. Brinkhuis, Dennis W. P. M. Löwik and Jan C. M. van Hest, *Langmuir* **2012**, 28, 2049-2055

6) René P. Brinkhuis, Floris P. J. T. Rutjes and Jan C. M. van Hest, *Polymer Chemistry* **2011**, 2, 1449-1462

7) René P. Brinkhuis, Taco R. Visser, Floris P. J. T. Rutjes and Jan C. M. van Hest, P*olymer Chemistry* **2011**, 2, 550-552

8) Joost A. Opsteen, René P. Brinkhuis, Rosalie L. M. Teeuwen, Dennis W. P. M. Löwik and Jan C. M. van Hest, *Chem Comm* **2007**, 3136-3138

† Equal contributions

Poster awards:

Poster award 2011	American Chemical Society – Division of polymer chemistry (POLY)
Denver (CO)	Poster Title: "Dynamic polymersome surfaces"
Poster award 2011	Europian Science Foundation – Polymers to Materials (P2M)
Obernai (France)	Poster Title: "Polymeric Vesicles with Dynamically Controlled Surfaces"